JHR 83: 1–19 (2021)
doi: 10.3897/jhr.83.66400
https://jhr.pensoft.net

RESEARCH ARTICLE

JOURNAL OF Hymenoptera RESEARCH
A peer-reviewed open-access journal
The International Society of Hymenopterists

Two new species of *Drepanoctonus* Pfankuch, 1911 (Hymenoptera, Ichneumonidae) from the Oriental region

Xin-Fang Zheng[1], Alexey Reshchikov[2,3,4], Jing-Xian Liu[1]

1 *Department of Entomology, College of Plant Protection, South China Agricultural University, Guangzhou, China* **2** *Institute of Eastern-Himalaya Biodiversity Research, Dali University, Yunnan, China* **3** *International Centre of Biodiversity and Primates Conservation, Dali, Yunnan 671003, China* **4** *The provincial innovation team of biodiversity conservation and utility of the three parallel rivers region from Dali University, Dali, Yunnan 671003, China*

Corresponding authors: Alexey Reshchikov (alexey.reshchikov@eastern-himalaya.cn); Jing-Xian Liu (liujingxian@scau.edu.cn)

Academic editor: Gavin Broad | Received 24 March 2021 | Accepted 20 May 2021 | Published 28 June 2021

http://zoobank.org/B2D3D417-0E0B-473B-B8E4-E48CCA81CFEA

Citation: Zheng X-F, Reshchikov A, Liu J-X (2021) Two new species of *Drepanoctonus* Pfankuch, 1911 (Hymenoptera, Ichneumonidae) from the Oriental region. Journal of Hymenoptera Research 83: 1–19. https://doi.org/10.3897/jhr.83.66400

Abstract

Two new species of the genus *Drepanoctonus* Pfankuch, 1911 collected in natural habitats with Wild Tea (*Camellia sinensis* var. *assamica*) are described and illustrated: *D. rimdahli* Liu & Reshchikov, **sp. nov.** from Chiang Mai Province, Thailand and *D. chamagudao* Liu & Zheng, **sp. nov.** from Yunnan Province, China. *Drepanoctonus bicolor* Kusigemati, 1971 is recorded from China for the first time. An identification key to the species of the genus is provided.

Keywords

Camellia sinensis assamica, Darwin wasps, Metopiinae, new species, parasitoids, Tea Fauna, Wild Tea

Introduction

Drepanoctonus Pfankuch, 1911 is a small genus in the subfamily Metopiinae (Hymenoptera, Ichneumonidae), comprising six known species. Three species are known from the Palaearctic region (*D. bicolor* Kusigemati, 1971, *D. tibialis* Pfankuch, 1911 and *D. tricoloratus* (Šedivý, 1971)), one from the Oriental region (*D. auritus* Chiu, 1962), one from the Afrotropical region (*D. bicinctus* (Benoit, 1961)), and one from the Australian region (*D. bifasciatus* (Brullé, 1846)) (Yu et al 2016; GBIF 2019) (Fig. 1A). The genus name derives from one of the earliest known host, *Watsonalla binaria* (Hufnagel, 1767) (Lepidoptera, Drepanidae), formerly named *Drepana binaria*, and literally means "the killer of *Drepana*" (Pfankuch 1911). To date, *Watsonalla binaria* (Hufnagel, 1767) is the only reliable host records for the European species *D. tibialis* (Pfankuch 1911, pers. comm. Bauer) (Fig. 1C). The other host records of the genus are only literally reported by some authors (Aubert 1965; Capek et al. 1982), but without any reliable evidence.

In the present study, two species are described as new to science: *Drepanoctonus chamagudao* Liu & Zheng, sp. nov. from Southwest China, and *Drepanoctonus rimdahli* Liu & Reshchikov, sp. nov. from Northern Thailand (Fig. 1B). They represent the first record of *Drepanoctonus* in continental China and Thailand respectively. In addition, *Drepanoctonus bicolor* Kusigemati, 1971 is recorded from China for the first time.

Materials and methods

The specimens examined are deposited in the following institutions (curators in parenthesis):

NHRS Swedish Museum of Natural History, Stockholm (Hege Vårdal);
QSBG Queen Sirikit Botanic Garden, Chiang Mai (Wichai Srisuka);
SCAU Hymenopteran Collection of South China Agricultural University (Jing-Xian Liu);
TARI Taiwan Agricultural Research Institute (Chi-Feng Lee).

The specimens of *Drepanoctonus rimdahli* Liu & Reshchikov, sp. nov. were collected in Northern Thailand by Malaise trap during the "Tea Fauna" project (http://teafauna.com) in the understory of an old secondary forest with *Camellia sinensis* var. *assamica* (Masters) Kitamura (Fig. 1B). The Tea Fauna Project is focused on biodiversity associated with tea plants across their native range in the Eastern Himalaya Region, including Northern Thailand and Yunnan Province of China (Reshchikov et al. 2019). A single specimen of *D. chamagudao* Liu & Zheng, sp. nov. was collected using a sweep net in a shrub plant community (mainly *Ageratina adenophora* (Spreng.) R.M. King and H. Rob.) in Ailao Mountain (Ancient Tea Horse Road, Yunnan Province, China).

Specimens were examined using the Zeiss Stemi 508 stereomicroscope. Images were acquired digitally using the KEYENCE VHX-5000 Digital Microscope

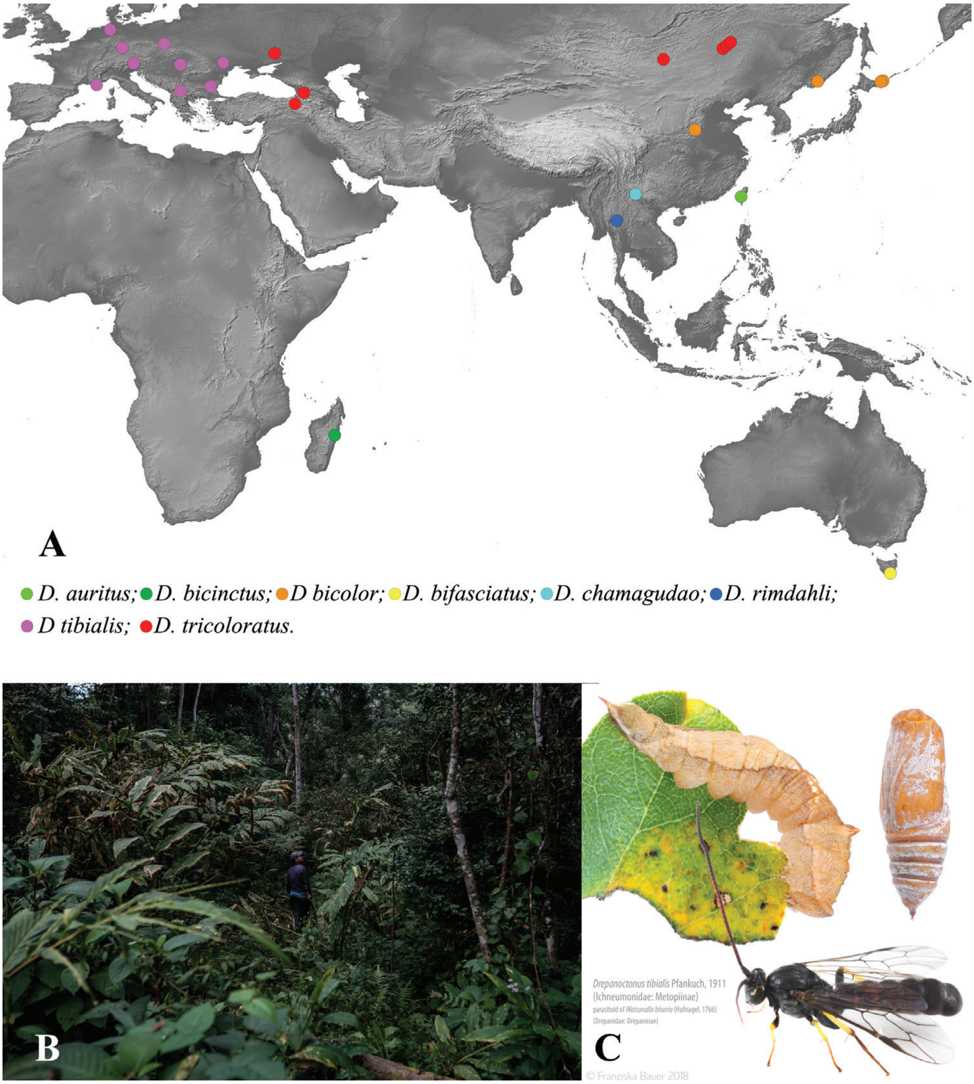

Figure 1. A distribution of the genus *Drepanoctonus* Pfankuch, 1911 **B** type habitat of *D. rimdahli* Liu & Reshchikov, sp. nov. **C** *D. tibialis* Pfankuch, 1911 with its host, *Watsonalla binaria* (Hufnagel, 1767), Germany, Saxony, Radeburg-Berbisdorf, 18 Oct. 2016, ex. 25 May 2017, Franziska Bauer leg. (pers. comm. Bauer)

Imaging System, Leica S8APO Digital Microscope System and processed with Adobe Photoshop.

Morphological terminology and nomenclature of wing venation follows Broad et al. (2018). Abbreviations and morphological terms used in the text: T1–T7, refers to the metasomal tergites 1–7. POL = the shortest distance between the posterior lateral ocelli; OD = the longest diameter of a posterior lateral ocellus; OOL = the shortest distance between a posterior lateral ocellus and a compound eye.

Molecular analysis

Genomic DNA of the new species was extracted from two females and one male using DNeasy Blood and Tissue Kit (Qiagen, Hilden, Germany), following a non-destructive DNA extraction protocol as described in Taekul et al. (2014). The LCO 1490 and HCO2198 primers (Folmer et al. 1994) were used to amplify the barcode region of the mitochondrial cytochrome oxidase subunit I (*COI*). PCRs were carried out using Tks Gflex DNA Polymerase (Takara) and amplified in a T100 Thermal Cycler (Bio-rad). Amplicons were sequenced on an Applied Biosystems (ABI) 3730XL by Sangon Biotech (Shanghai, China). Preliminary alignment was carried out by Geneious 11.0.3 and analyzed using MEGA X software. Following extraction voucher specimens were washed in 100% alcohol and deposited in NHRS, QSBG and SCAU. All the amplified sequences were deposited in GenBank.

Results

Following the non-destructive extraction of DNA, the three specimens were identified as two new species: *Drepanoctonus chamagudao* sp. nov. (MW528531) and *Drepanoctonus rimdahli* sp. nov. (MW528532; MW528533; MW528534), as described below. These two distinct species are also supported by the *COI* sequences, pairwise percentage identify of the sequences was 84.4%–84.6% (interspecies distance between *D. chamagudao* sp. nov. and *D. rimdahli* sp. nov), and 99.9%–100% (intraspecies distance of *D. rimdahli* sp. nov.).

Taxonomy

Order Hymenoptera
Family Ichneumonidae
Subfamily Metopiinae

Genus *Drepanoctonus* Pfankuch, 1911

Drepanoctonus Pfankuch, 1911: 688. Type species: *Drepanoctonus tibialis* Pfankuch. Designated by Horstmann, 1986. Monobasic.

Zonopius Benoit, 1961, 63: 305. Type species: *Zonopius bicinctus* Benoit. Original designation. Synonymized by Townes 1971.

Generic diagnosis. Fore wing length 6.0–9.0 mm. Body with punctures rather sharp and dense. Combined face and clypeus weakly convex; upper margin of face produced medially as an acute triangle between bases of antennae (except *D. rimdahli* sp. nov.). Pronotum posteriorly with a swelling just below its upper margin. Epicnemial carina with upper end far from the front edge of mesopleuron. Mesopleuron moderately convex.

Propodeum rather short, latero-median longitudinal carinae complete, anterior transverse carina absent, area superomedia confluent with area basalis; posterior transverse carina complete or interrupted in the middle. Propodeal spiracle elongate. Spurs of middle tibia elongate, approximately equal in length. Fore wing with 1cu-a opposite or distad to M&RS, and 2rs-m nearly opposite to 2m-cu. T1 with an oblique baso-dorsal edge, with latero-median longitudinal carinae strong and sharp to apex. T2 usually with a pair of latero-median longitudinal carinae, either shortly present on base or reaching to posterior margin of tergite. T3 and T4 with or without a single weak, incomplete median longitudinal carina. Laterotergite of T2 vestigial, that of T3 narrowly wedge shaped, and that of T4 to T6 moderately wide and separated from their tergites by a crease (Townes 1971).

Distribution. Palaearctic, Oriental, Australian and Afrotropical regions (Fig. 1C).

Biology. Parasitoids of Drepanidae (Lepidoptera) (Pfankuch 1911; Yu et al. 2016).

Key to species of *Drepanoctonus* (modified from Tolkanitz, 1987)

1 Latero-median longitudinal carinae of T2 either absent, only present on anterior 0.3 of the tergite, or present as foveolate lines (Fig. A) **2**

– Latero-median longitudinal carinae of T2 strong and reaching the posterior margin of the tergite (Fig. B) **4**

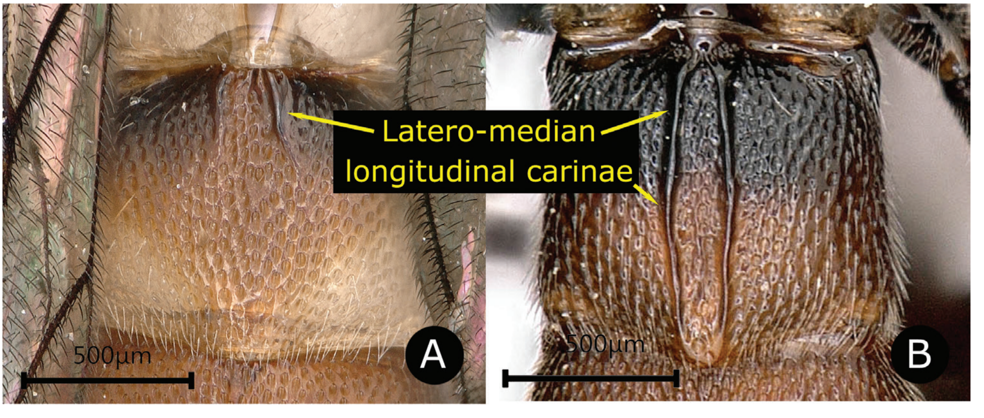

2 T2 medially with a pair of foveolate lines at base; T3 to T5 medially with a depressed triangular area at base; fore wing with 1cu-a oblique and almost opposite to M&RS; hind tibia entirely reddish brown without white or yellow band; upper margin of pronotum yellow; T4 with a yellow band posteriorly (Fig. A) .... ***D. bicinctus* (Benoit, 1961)**

– T2 medially either without foveolate lines or carinae, or anteriorly with a pair of short latero-median longitudinal carinae; T3 to T5 without depressed triangular area at base; fore wing with 1cu-a distinctly distad of M&RS; hind tibia reddish brown with a sub-basal white or yellow band; upper margin of pronotum reddish brown or entirely black; T4 without a yellow band (Fig. B) **3**

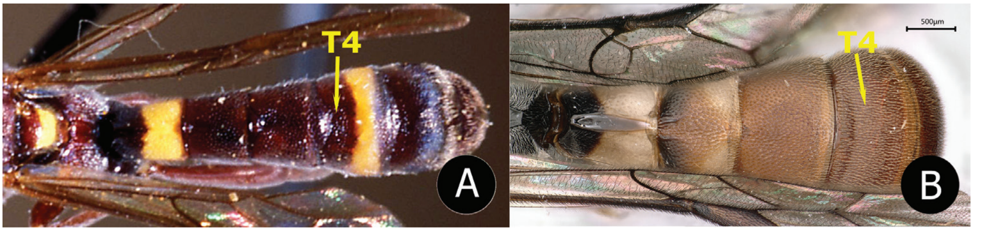

3 Upper margin of face not produced backward as inter-antennal projection; area superomedia of propodeum polished and glabrous; T2 with a pair of short latero-median longitudinal carinae on anterior 0.3 of tergite (Fig. A); T3 evenly reddish brown .... ***D. rimdahli* sp. nov.**

– Upper margin of face produced backward forming an inter-antennal projection; area superomedia of propodeum with several transverse wrinkles; T2 without a pair of short latero-median longitudinal carinae (Fig. B); T3 posteriorly with a wide yellow band .... ***D. bifasciatus* (Brullé, 1846)**

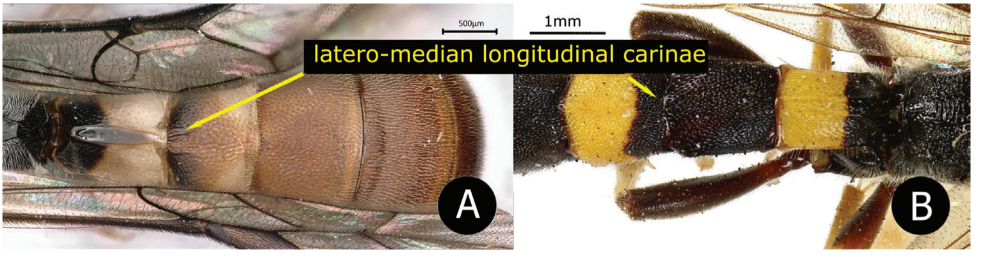

4 T3 without latero-median longitudinal carinae (Fig. A) **5**

– T3 with latero-median longitudinal carinae (Fig. B) **6**

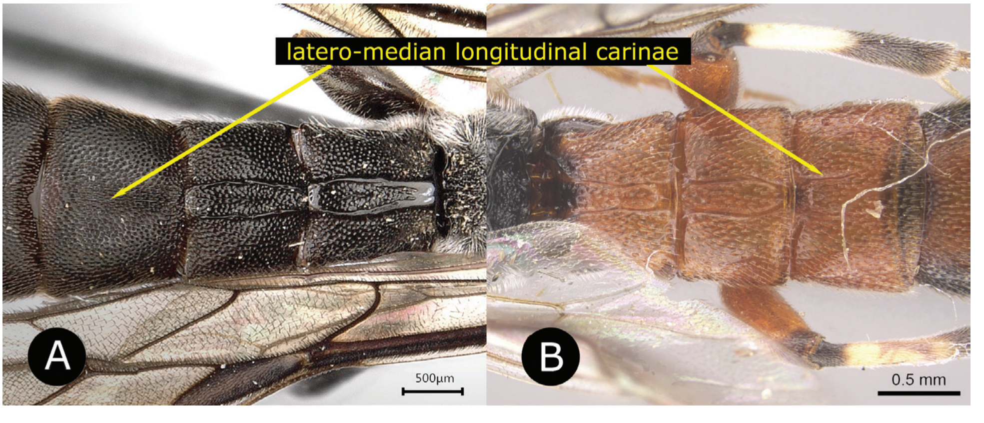

5 T2 to T6 transverse, roughly wrinkled and punctate; metasoma black, T1 to T6 with their apical margins reddish–brown; femora black with apex yellow; all tibiae yellow .... ***D. tibialis* Pfankuch, 1911**

– T2 to T6 not transverse, punctate; metasoma with T1 and T2 black, T3 to T6 reddish; femora entirely black, fore tibia reddish-brown, mid and hind tibia black .... ***D. bicolor* Kusigemati, 1971**

6 Posterior transverse carina of propodeum complete (Fig. A); fore wing with 1cu-a opposite to M&RS; T3 with a pair of latero-median longitudinal carinae on anterior half (Fig. A), T4 without carina; T1–T3 usually red, T5 posteriorly with round white spot .... ***D. tricolorata* (Šedivý, 1971)**

– Posterior transverse carina of propodeum incomplete, dorso-medially absent (Fig. B); fore-wing with 1cu-a distinctly distad of M&RS; both T3 and T4 with a single median longitudinal carina (Fig. B) 7

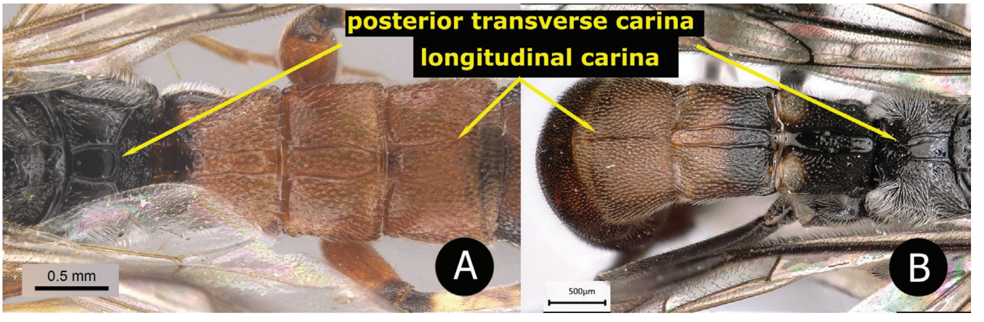

7 Metasoma mainly blackish–brown, T1 with a pair of triangular yellow spots on latero-posterior corners; T2 with a yellow band on posterior 0.2–0.4 which is interrupted by latero-median longitudinal carinae (Fig. A).............. ....***D. auritus* Chiu, 1962**

– Metasoma mainly reddish, T1 black with a pair of yellow spots on latero-posterior corners, T2 with anterior half black and posterior half reddish (Fig. B) ....***D. chamagudao* sp. nov.**

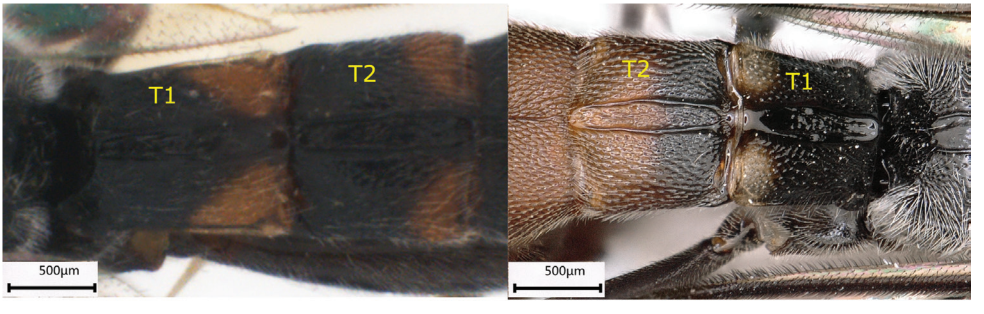

***Drepanoctonus bicolor* Kusigemati, 1971**
Fig. 2

Drepanoctonus bicolor Kusigemati, 1971, 250.

Materials examined. China: 1 male, Shanxi province, Mt. Lishan, Xiahe Protection Area, 35°20.40'N, 112°32.41'E, 780 m, 22–25 Aug. 2012, Ren Ya-Jun leg. (SCAU). **New to China.**

Figure 2. *Drepanoctonus bicolor* Kusigemati, 1971, female **A** habitus, lateral view.

Comments. The specimen from China is slightly different from the holotype in having the third metasomal tergite blackish–brown and medially longitudinally convex, and the fourth tergite light reddish-brown (Fig. 2A).

Distribution. China (Shanxi Province), Russia, Japan.

Drepanoctonus chamagudao **Liu & Zheng, sp. nov.**
http://zoobank.org/49362125-03C8-440B-82F5-9C145BE214C9
Figs 3, 4

Materials examined. ***Holotype***, female. China: Yunnan Province, Yuxi City, Xinping County, Mt. Ailao, Cha Ma Gu Dao, 98°53'43.38"N, 28°18'56.4984"E, 2538 m, 8. Aug. 2018, Zheng Xin-Fang leg., DNA voucher, SCAU 3013943, GenBank number: MW528531, (**SCAU**).

Descriptions. Female. Fore wing length 7.5 mm, body length 8.0 mm (Fig. 3).

Head. Combined face and clypeus densely and strongly punctate, densely setose, 0.7× as wide as high (Fig. 4A). Clypeus with transverse wrinkles. Mandible bidentate, with lower tooth as long as the upper one. Inner eye orbit weakly curved above antennal sockets. Vertex strongly vertical behind posterior ocelli, with minute punctures, densely setose. POL:OD:OOL=2:1.2:1. Temple strongly narrowed behind eyes in dorsal view (Fig. 4F), densely setose. Occipital carina complete and sharp. Antenna with 41 flagellomeres, first flagellomere 2.6× as long as its posterior width, 1.4× as long as the second, antenna weakly flattened from 9th flagellomere to apex.

Mesosoma. Pronotum strongly punctate and setose on upper half, more or less shiny and glabrous on lower half, with a row of short and transverse wrinkles along posterior margin. Epomia strong, reaching upper 0.8 of pronotum. Mesoscutum

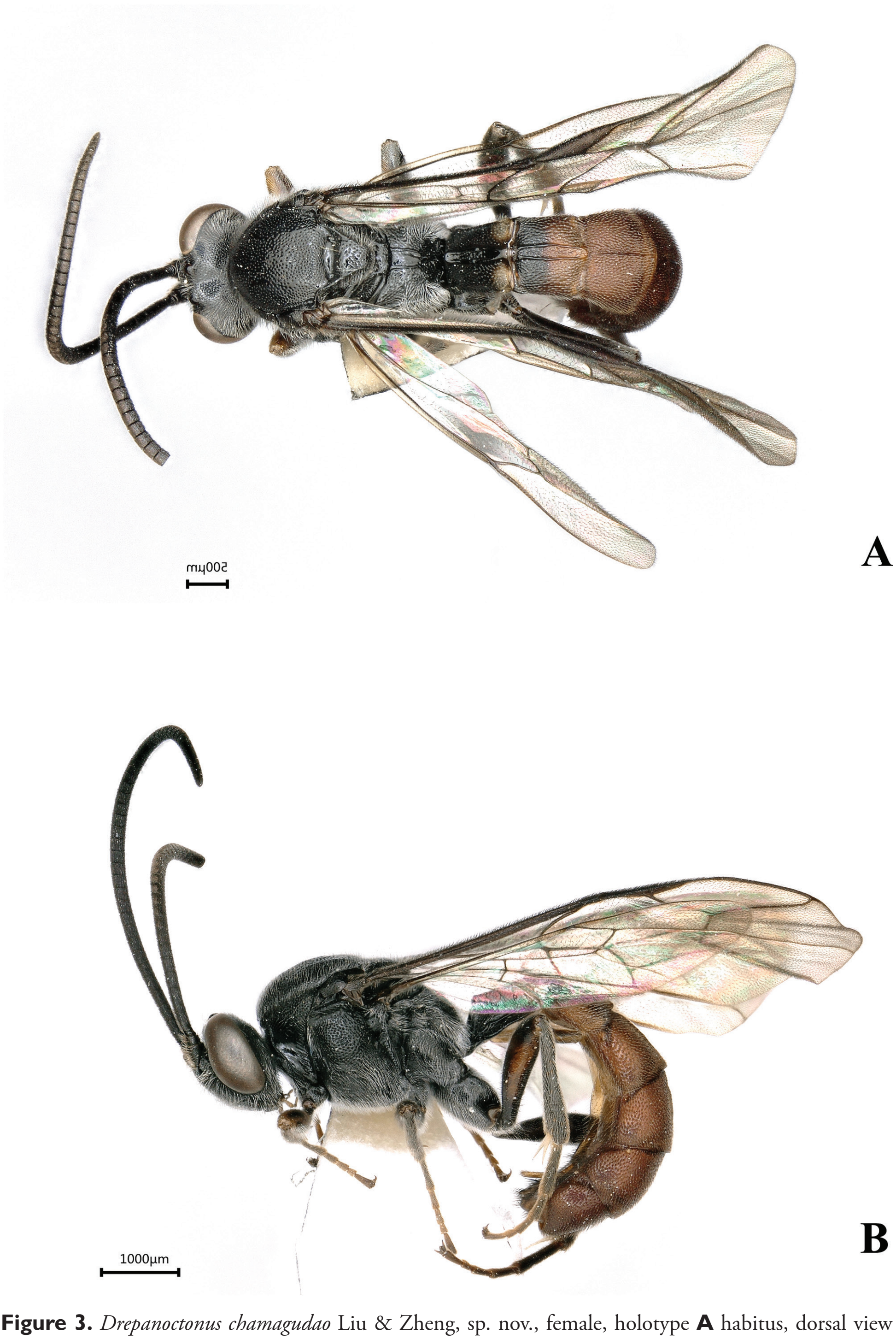

Figure 3. *Drepanoctonus chamagudao* Liu & Zheng, sp. nov., female, holotype **A** habitus, dorsal view **B** habitus, lateral view.

strongly punctate and setose (Fig. 4C). Notaulus absent. Scutellum flattened, sparsely punctate, with lateral carinae present at base (Fig. 4C). Mesopleuron (Fig. 4D) strongly roundly convex, densely punctate, sternaulus weakly impressed; epicnemial carina with dorsal end distant from the front edge of mesopleuron, speculum very small and polished. Mesopleural suture weakly foveolate. Metapleuron sparsely punctate, lower part of metapleuron with several transverse wrinkles, juxtacoxal carina present, submetapleural carina complete. Propodeum short, dorsal lateral areas strongly punctate and setose, area superomedia polished and nearly impunctate, latero-median longitudinal carinae complete and parallel, dorsomedial section of posterior transverse carina absent (Fig. 4B); lateral longitudinal carina strong and complete; pleural area rugose-punctate, with dense and long setae, pleural carina strong and complete. Spiracle elongate, 2.0× as long as its median width, connected to pleural carina by a short carina.

Wings. Fore wing with 1cu-a distad of M&RS, separated from M&RS by 0.67× its own length, 2m-cu almost opposite to 2rs-m, 3rs-m absent. Hind wing with Cu & cu-a interrupted above the middle, distal abscissa of Cu weakly pigmented.

Legs. Fore and mid claws with 1–2 pectinate teeth at base. Mid tibial spurs nearly equal in length. Hind femur 4.8× as long as its maximum width, hind tibia 5.8× as long as its maximum width, hind tibial spurs equal in length, 0.57× as long as 1st segment of tarsus (Fig. 4G). Ratio of segments of hind tarsus as follows: 36: 18:12:7:12.

Metasoma. T1 1.0× as long as its apical width, punctate, latero-median longitudinal carinae strong, anterior base of T1 strongly oblique in lateral view, dorsolateral carina sharp and complete, spiracle located on anterior 0.3 of the tergite (Fig. 4E). T2 weakly transverse, 0.9× as long as its apical width, strongly punctate with a pair of latero-median longitudinal carinae reaching to posterior margin of tergite (Fig. 4E). T3 strongly punctate, 0.78× as long as apical width, with median longitudinal carina reaching to apical 0.8 of tergite (Fig. 4E). T4 transverse, strongly punctate, centrally with a median longitudinal carina, both ends of the carina distant from the margins of tergite. T5 strongly punctate, punctures of central area close to each other. T6 shallowly punctate. T7 very short. Ovipositor short, 0.88× as long as 1st segment of hind tarsus.

Colour. Head and mesosoma black, covered with whitish setae (Fig. 4A, F). Antenna black, 9th segment to the apex ventrally blackish–brown (Fig. 3A, B). Palpi blackish–brown. All coxae and trochanters black (Fig. 3B), fore leg dark brown with anterior sides of femur and tibia light brown; mid leg blackish–brown, anterior side of femur and ventral side of tarsus brown; hind leg black, anterior side of femur reddish–brown (excluding basal 0.3 which is black), tibial spurs whitish, ventral side of tarsus slightly tinged with reddish brown. First tergite black, with two yellowish white spots on posterior lateral corners, second tergite with anterior 0.4 black and posterior 0.6 reddish brown, the remaining tergites reddish brown (Fig. 3A). Wings hyaline, veins and pterostigma black (Fig. 3A).

Male. Unknown.

Distribution. China (Yunnan province).

Comments. This species is similar to *D. bicolor* (Fig. 2), but it differs from the latter in the presence of median longitudinal carina on T3 and T4 (Fig. 4E), the col-

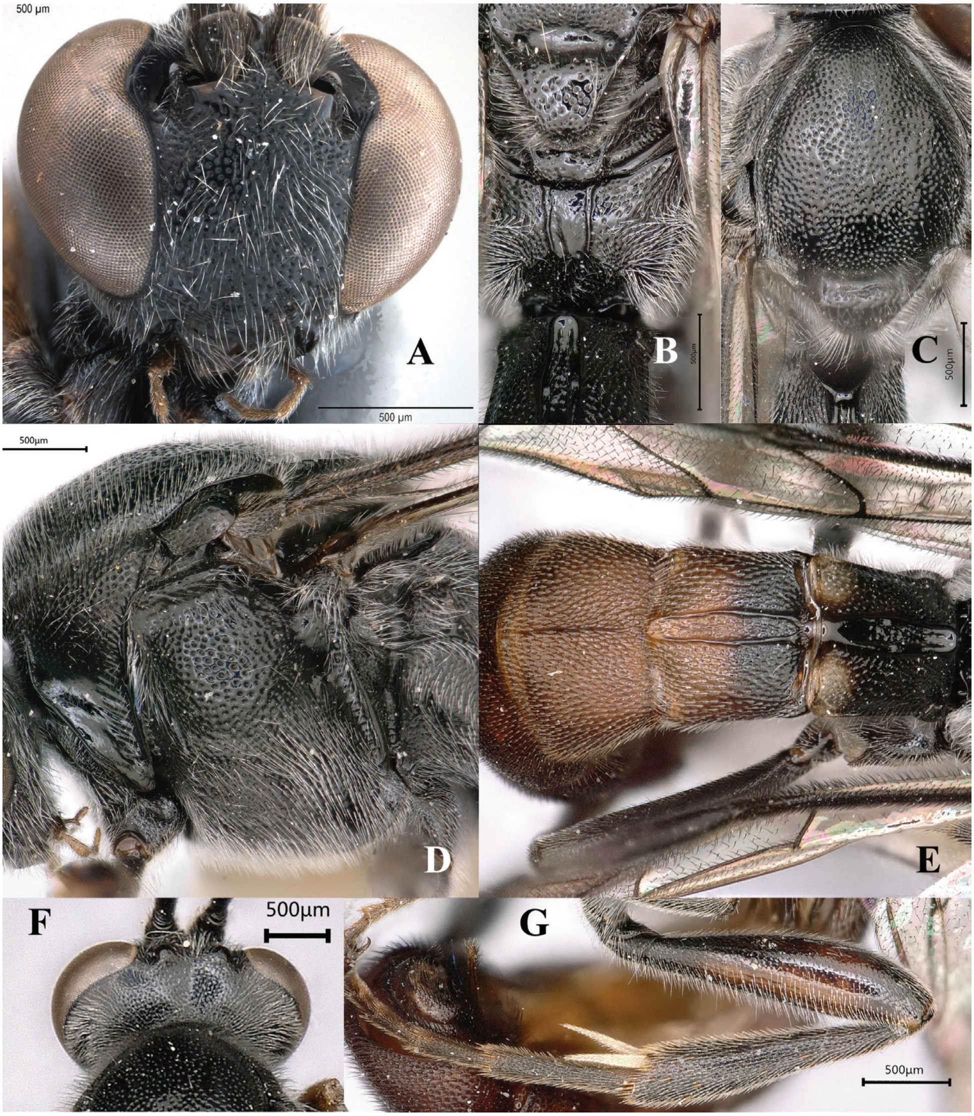

Figure 4. *Drepanoctonus chamagudao* Liu & Zheng, sp. nov., female, holotype **A** face **B** propodeum, dorsally **C** mesonotum **D** mesopleuron **E** T1–T3, dorsally **F** head, dorsally **G** hind leg, laterally.

ouration of the second tergite which is black on anterior half and reddish brown on posterior half, the colouration of the first tergite which has yellow spots on its posterior lateral corners (Fig. 3B).

It also very resembles *Drepanoctonus auritus* Chiu, 1962 (Fig. 5A, B), but can be separated from the latter by the colour pattern of its metasoma (Fig. 4E), T1 black with a pair of yellowish white spots on its posterior lateral corners, and the posterior half of T2 and following tergites reddish, hind femora with anterior sides reddish–brown (Fig. 4E).

Etymology. The species is named after the type locality, Chamagudao, which means the Ancient Tea Horse Road of Yunnan province.

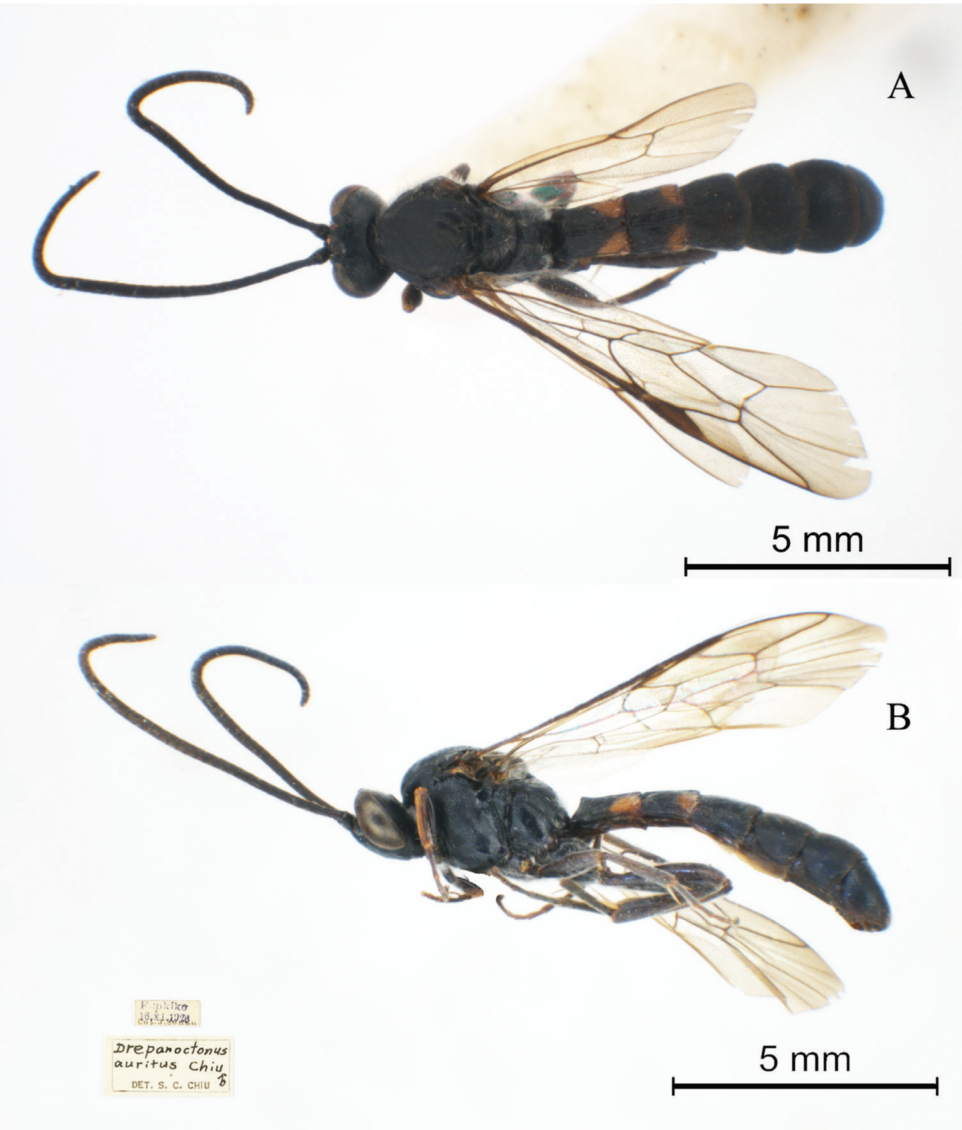

Figure 5. *Drepanoctonus auritus* Chiu, 1962, female, holotype **A** habitus, dorsal view **B** habitus, lateral view.

Drepanoctonus rimdahli **Liu & Reshchikov, sp. nov.**
http://zoobank.org/442B0121-963C-49F1-8FAC-CEA1D81C3E60
Figs 6, 7

Materials examined. ***Holotype***, female, Thailand: Chiang Mai, Mae Taeng, Pa Pae, 19°14'30.6"N, 98°30'14.1"E, old forest with *C. sinensis assamica*, Malaise trap (Dara#1), 04.V-25.V.2017, Monsoon Tea leg. (NHRS), DNA voucher, SCAU3013719, GenBank number: MW528534; ***Paratypes,*** 1 female, the same locality as holotype, Malaise trap (Dara#1), 12 Apr. – 03 May 2017, Monsoon Tea leg., DNA voucher, SCAU 3013713, GenBank number: MW528533, (QSBG); 1 male, the same locality as holotype, Malaise trap (Dara#1), 12 Apr. – 03 May 2017, Monsoon Tea leg., DNA voucher, SCAU 3013712, GenBank number: MW528532(QSBG).

Description. Holotype. Female, fore wing length 7.5 mm, body length 9.0 mm (Fig. 6A, B).

Head. Combined face and clypeus weakly convex, 0.80–0.90× as wide as high, densely and evenly punctate, lateral corner of clypeus weakly wrinkled (Fig. 7A); upper margin of face not produced medially as an acute triangle between bases of antennae. Lateral and posterior margins of antennal sockets developed into a low flange with weak earlike dorsolateral projections. Inner orbits of eye weakly concave above antennal sockets. Vertex strongly vertical behind posterior ocelli, with minute punctures, densely setose. POL:OD:OOL=2:1.2:1. Temple strongly narrowed behind eyes in dorsal view (Fig. 7C), densely setose. Occipital carina complete and sharp. Antenna with 37 flagellomeres, first flagellomere 2.9× as long as its posterior width, 1.5× as long as the second flagellomere, ventral side of 9th flagellomere to apex flattened, with sensilla plates.

Mesosoma. Pronotum with upper lateral corner finely punctate and densely setose, lower part polished with a row of transverse depressions. Epomia strong, reaching to upper 0.8 of pronotum. Mesoscutum with minute punctures, distance between punctures 0.5–1.0× the diameter of a puncture (Fig. 7D). Notaulus absent. Scutellum scattered with sparse punctures, lateral carina sharp, reaching to 0.6 of scutellum (Fig. 7B). Mesopleuron (Fig. 7E) strongly convex, with moderately dense minute punctures, separated from each other by 1.0–2.0× the diameter of a puncture; epicnemial carina with dorsal end far from the front edge of mesopleuron; speculum very small; mesopleural furrow weakly foveolate. Metapleuron (Fig. 7E) moderately convex, upper 2/3 with sparse minute punctures, anterior lower 1/3 with scattered, weak wrinkles, juxtacoxal carina incomplete, with only basal 0.6 present; submetapleural carina complete. Propodeum short, latero-median longitudinal carinae complete and gradually convergent from base to middle; area superomedia polished and glabrous, closed posteriorly; posterior transverse carina complete (Fig. 7B); dorsal lateral areas of propodeum densely setose, with minute punctures; pleural carina strong and complete; pleural area weakly rugose-punctate, densely setose. Spiracle elongate, 2.0× as long as its median width, connected with pleural carina by a short carina.

Wings. Fore wing with 1cu-a distad of M&Rs by 0.5× the length of 1cu-a, 2rs-m slightly reclivous, very slightly anterior of 2m-cu. Hind wing with Cu & cu-a interrupted on lower 0.4, distal abscissa of Cu distinct.

Legs. Mid tibial spurs equal in length and 0.63× the length of 1st segment of hind tarsus. Hind femur 4.0× as long as its maximum width (Fig. 7G); hind tibia 0.53× as long as its maximum width, with several bristles on posterior half, longest tibial spur 0.88× the length of 1st segment of hind tarsus. Ratio of segments of hind tarsus: 38:20:14:8:14.

Metasoma. T1 1.25× as long as its posterior width, latero-median longitudinal carinae weak but forming a longitudinal convex area, lateral area of T1 subpolished, with sparse minute punctures, dorsolateral carina complete and sharp (Fig. 7F). T2

Figure 6. *Drepanoctonus rimdahli* Liu & Reshchikov, sp. nov., female, holotype **A** habitus, dorsal view **B** habitus, lateral view **C** male paratype, lateral view.

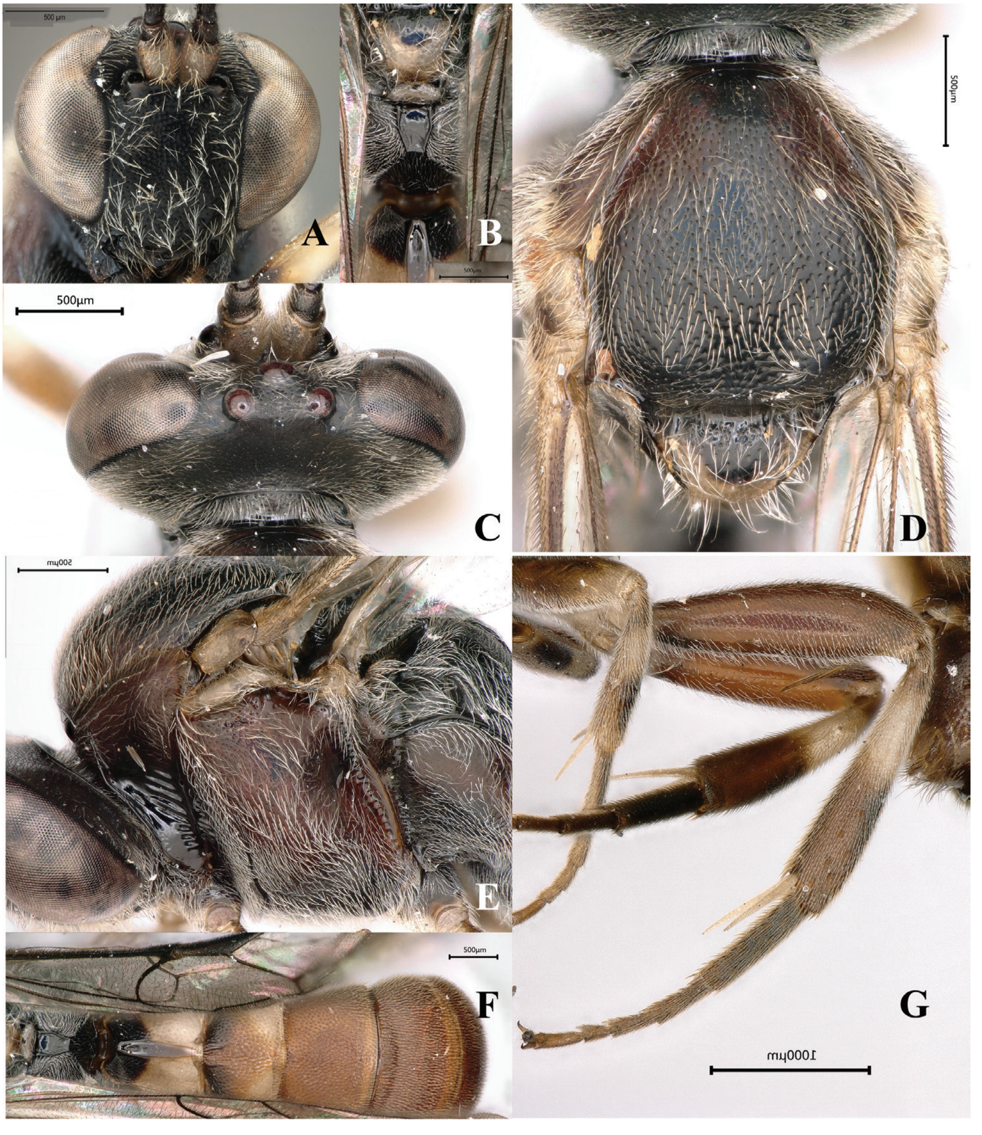

Figure 7. *Drepanoctonus rimdahli* Liu & Reshchikov, sp. nov., female, holotype **A** face **B** propodeum, dorsally **C** head, dorsally **D** mesoscutum **E** mesopleuron **F** T1–T4, dorsally **G** hind leg, laterally.

moderately densely punctate, 0.83× as long as its apical width, without distinct carinae, but anteriorly and centrally with a pair of short stubs (Fig. 7F). T3 strongly punctate without any carinae (Fig. 7F). T4 with dense minute punctures, anterior 0.3 centrally with some short longitudinal wrinkles. T5 finely punctate. T6 polished, with sparse and minute punctures. Ovipositor 1.2× as long as 1st segment of hind tarsus, ventral valve with its anterior 0.3 weakly swollen.

Colour. Body with whitish setae. Head black (Fig. 7A, C). Antenna blackish–brown, scape whitish with lateral black marks. Pronotum with upper part dark reddish–brown, lower part black; mesoscutum black with anterior lateral corners dark reddish-brown; scutellum yellowish–white with a round black spot in anterior half; mesopleuron with upper 2/3 dark reddish-brown and lower 1/3 black, epicnemium black with upper 0.2 dark reddish-brown; subtegular ridge yellowish–white; metapleuron with upper half dark reddish-brown and lower half black; propodeum black. Metasoma reddish-brown, T1 yellowish–white with anterior 0.3 black and a longitudinal black stripe between mediodorsal carinae. T2 reddish brown with anterior corners black and posterior lateral corners yellowish–brown. Fore coxa and trochanter black with anterior side yellowish–white, fore femur brown with anterior side and apex yellowish–white, fore tibia yellowish–white, fore tarsus yellowish-brown; mid coxa black with anterior side yellowish-white, mid trochanter brown with anterior side white, mid femur brown, ventrally blackish–brown, apex of femur yellowish–white, mid tibia brown, with a sub-basal yellowish-white band, posterior 0.5 with outer margin blackish–brown, mid tarsus dark brown; hind coxa black with apex reddish-brown, hind trochanter yellowish-brown, hind femur reddish–brown, hind tibia brown with a sub-basal whitish band, hind tarsus blackish brown, hind tibial spur yellowish–white. Wings hyaline, tegula yellowish–white.

Male. (Fig. 6C) Similar to female. Fore wing length 6.5 mm, body length 8.5 mm. Combined face and clypeus moderately densely punctate, 3/4 as wide as high; POL:OD:OOL=3.5:2.25:1. Antenna with 38 flagellomeres, first flagellomere 2.6× as long as its posterior width, 1.5× as long as the second flagellomere. Hind femur 3.9× as long as its maximum width, longer spur of hind tibia 2/3 as long as 1st segment of hind tarsus. Ratio of segments of hind tarsus: 30:15:10:5:10. Head and mesosoma black. Antenna blackish–brown, scape yellowish–white with lateral blackish–brown marks. Metasoma reddish–brown, first tergite yellowish–brown, anterior 0.2 black, centrally with a longitudinal blackish–brown band between the latero-median longitudinal carinae. Tegula and subtegular ridge yellowish brown. All coxae black; fore trochanter blackish–brown, fore femur dark brown, fore tibia and tarsus yellowish–white. Mid trochanter brown with posterior half yellowish–white, mid femur brown, mid tibia brown with a sub-basal white band, mid tarsus yellowish–white. Hind leg brown, hind trochanter yellowish–white, hind tibia with a sub-basal whitish band, 1st segment of hind tarsus blackish brown. Wings hyaline, veins and pterostigma blackish–brown.

Variation. T2 of a female paratype, with a pair of short carinae on anterior 0.4 of tergite. Pronotum largely black with upper margin tinged with indistinct dark reddish-brown. Mesopleuron weakly marked with dark reddish-brown.

Distribution. Thailand (Chiang Mai).

Comments. This species can be separated from other species of the genus by the following combined characters: the upper margin of face not produced medially as an acute triangle between bases of antennae (Fig. 7A), T2 centrally with a pair of short stubs anteriorly, T3 and following tergites without carina (Fig. 7F).

Etymology. The species is named after Mr. Kenneth Rimdahl, the founder of Monsoon Tea, in recognition of his efforts in saving Thai forests.

Discussion

In most species of *Drepanoctonus* the upper margin of the face is distinctly produced medially as an acute triangle between bases of antennae, and the upper side of the triangle is deeply grooved. This character is absent in *D. rimdahli* sp. nov., but we place this species in the genus *Drepanoctonus* because all other diagnostic characters match the generic description. Two species, *D. rimdahli* sp. nov. and *D. bicinctus*, have a pair of short stubs or incomplete latero-median longitudinal carinae on their second metasomal tergite (Fig. 7F), while the remaining species have a pair of strong and complete latero-median longitudinal carinae (Fig. 4E); this carina is completely absent in *D. bifasciatus*. Two species *D. chamagudao* sp. nov. and *D. auritus* have a single weak, incomplete, median longitudinal carina on T3 and T4 (Figs 3A, 4E, 5A, B), but these two species can be easily distinguished from each other by the colour pattern of metasoma.

Because of the lack of fresh material for the known species of *Drepanoctonus*, only the *COI* sequences of the two new species is available as an additional evidence for identification and future molecular analysis.

The scattered worldwide distribution of the genus *Drepanoctonus* (Fig. 1), is probably due to the lack of sampling (Yu et al. 2016; GBIF 2019).

Acknowledgements

The authors are deeply grateful to the team of Monsoon Tea and its founder Kenneth Rimdahl for assistance in sampling in Northern Thailand; William Persson for type locality photography, Wang Peng for his kind help in field work in Yunnan; Ren Ya-Jun (South China Agricultural University) for collecting the specimens from Shanxi; Chi-Feng Lee (TARI), Simon van Noort (Iziko South African Museum), Agnièle Touret-Alby (MNHN) for their kind help and providing images of *Drepanoctonus* specimens; Franziska Bauer for the illustration of *D. tibialis* with its host and collecting information; Tony Hunter (World Museum, Liverpool, UK) for linguistic review of the manuscript; two reviewers, Filippo Di Giovanni (University of Pisa, Italy) and Mabel Alvarado (National University of San Marcos, Peru) for useful suggestions and review of our manuscript. This project was supported by the Natural Science Foundation of Guangdong Province (No.2021A1515010730, LJX), the Second Tibetan Plateau Scientific Expedition and Research Program (STEP), Grant No. 2019QZKK0402(AR), and Collaborative Innovation Center for Biodiversity and Conservation in the Three Parallel Rivers Region of China (AR).

References

Aubert JF (1965) Les Ichneumonides du rivage méditerranéen français (8e serie, Region Cotiere entre La Ciotat et Saint-Tropez). Vie et Milieu 16: 549–573.

Benoit PLG (1961) Nouveaux Metopiinae de Madagascar (Hym. Ichneumonidae). Revue de Zoologie et de Botanique Africaines 63: 299–308.

Broad GR, Shaw MR, Fitton MG (2018) Ichneumonid wasps (Hymenoptera: Ichneumonidae): their classification and biology. Handbooks for the Identification of British Insects 7(12): 1–418.

Capek M, Hladil J, Šedivý J (1982) Verzeichnis der aus verschiedenen Insekten erzogenen parasitschen Hymenopteren – Teil VI. Entomological Problems (Bratislava) 17: 325–371.

Folmer O, Black M, Hoeh W, Lutz R, Vrijenhoek R (1994) DNA primers for amplification of mitochondrial cytochrome c oxidase subunit from diverse metazoan invertebrates. Molecular Marine Biology and Biotechnology 3(5): 294–299.

GBIF Secretariat (2019) GBIF Backbone Taxonomy. Checklist dataset. https://doi.org/10.15468/39omei [accessed via https://www.gbif.org/species/1285027 on 2020-08-27]

Horstmann K (1986) Typenrevision der von Karl Pfankuch beschriebenen Arten und Formen der Familie Ichneumonidae (Hymenoptera). Entomologische Mitteilungen aus dem Zoologischen Museum Hamburg 8: 251–264.

Kusigemati K (1971) Taxonomic studies on the subfamily Metopiinae of Japan (Hymenoptera: Ichneumonidae). Memoirs of the Faculty of Agriculture, Kagoshima University 8(1): 205–298.

Pfankuch K (1911) Die Ichneumonidengattung *Drepanoctonus* Kriechb. (Hym.). Deutsche Entomologische Zeitschrift 1911: 687–689. https://doi.org/10.1002/mmnd.48019110613

Pfankuch K (1935) Verzeichnis der Ichneumoniden von Bremen und Umgegend. Mitteilungen aus dem Entomologischen Verein in Bremen 22(1934): 6–30.

Reshchikov A, Santos BF, Liu JX, Barthélémy C (2019) Review of *Palpostilpnus* Aubert (Hymenoptera, Ichneumonidae, Phygadeuontinae), with the description of ten new species. European Journal of Taxonomy 582: 1–63. https://doi.org/10.5852/ejt.2019.582

Taekul C, Valerio AA, Austin AD, Klompen H, Johnson NF (2014) Molecular phylogeny of telenmine egg parasitoids (Hymenoptera: Platygastridae s.l: Telenominae): evolution of host shifts and implications for classification. Systematic Entomology 39: 24–35. https://doi.org/10.1111/syen.12032

Tolkanitz VI (1987) Parasitic Hymenoptera. Ichneumonidae- Metopiinae. Fauna Ukraina 11(2): 1–212. [In Russian]

Townes HK (1971) The genera of Ichneumonidae, Part 4. Memoirs of the American Entomological Institute 17: 1–372.

Yu DS, van Achterberg C, Horstmann K (2016) Taxapad 2016, Ichneumonoidea. Database on flash-drive, Nepean.

Supplementary material 1

fasta file of COI sequences of some species

Authors: Xin-Fang Zheng, Alexey Reshchikov, Jing-Xian Liu

Data type: sequence of COI

Explanation note: COI sequences of different individual speciemns from the two new species.

Link: https://doi.org/10.3897/jhr.83.66400.suppl1

JHR 83: 21–72 (2021)
doi: 10.3897/jhr.83.63353
https://jhr.pensoft.net

RESEARCH ARTICLE

JOURNAL OF Hymenoptera RESEARCH
A peer-reviewed open-access journal
The International Society of Hymenopterists

New records of Braconinae (Hymenoptera, Braconidae) from South Korea

Konstantin Samartsev[1], Deok-Seo Ku[2]

1 *Zoological Institute, Russian Academy of Sciences, St. Petersburg 199034, Russia* **2** *The Science Museum of Natural Enemies, Geochang, 50147, South Korea*

Corresponding author: Konstantin Samartsev (k.samartsev@gmail.com)

Academic editor: J. Fernandez-Triana | Received 19 January 2021 | Accepted 19 March 2021 | Published 28 June 2021

http://zoobank.org/3F3A83D4-9079-476E-AE59-FCE2E7EFEABF

Citation: Samartsev K, Ku D-S (2021) New records of Braconinae (Hymenoptera, Braconidae) from South Korea. Journal of Hymenoptera Research 83: 21–72. https://doi.org/10.3897/jhr.83.63353

Abstract

Two genera (*Campyloneurus* Szépligeti and *Craspedolcus* Enderlein) and 31 species of Braconinae are recorded for the first time from South Korea, including one new subspecies (*Bracon albion continentalis* **ssp. nov.**). Two new synonyms are proposed: *Bracon leptotes* Li, He & Chen, 2020, **syn. nov.** (= *B.* (*Bracon*) *semitergalis* Tobias, 2000) and *B. megaventris* Li, He & Chen, 2020, **syn. nov.** (= *B.* (*B.*) *terebralis* Tobias, 2000). For all species with problematic identification descriptions, diagnoses and illustrations are provided.

Keywords

New record, new subspecies, new synonym, Palaearctic

Introduction

Braconinae are the largest subfamily of the braconid wasps (Yu et al. 2016). The large number of revealed taxa and the lack of adequate literature for identification of most of its species and even genera are complicating the faunistic and taxonomic investigations in the subfamily. The absence of large-scale reviews and revisions of the most common taxa of Braconinae presents a particular difficulty for the study of the East Asian part of the Palaearctic region. The current paper provides a contribution to the fauna of the Korean Peninsula.

First-time records of the species of Braconinae from the Korean Peninsula are found in 14 publications. Except for five recent articles (Lee et al. 2018; Papp 2018; Kang et al. 2019; Samartsev and Ku 2020; Yu et al. 2020), most of the significant literature on the fauna of Korea is cited in the Taxapad catalogue (Cushman 1931; Matsumura 1931; Watanabe 1932, 1935; Papp 1996, 1998, 2012; Belokobylskij and Tobias 2000; Ku et al. 2001; all cited by Yu et al. 2016). A total of 93 currently valid species from 17 genera of braconines have been indicated for the Korean Peninsula. It is notable that 70 species were added by Jenő Papp, mostly on the basis of the material from North Korea. The fauna of South Korea has been less explored.

The present study is based on an extensive collection of Braconinae of South Korea accumulated by the second author. Involving the type material on the species described from the Russian Far East and information on braconines recently described from China and Japan, we add 31 species and 2 genera (*Campyloneurus* Szépligeti and *Craspedolcus* Enderlein) to the known fauna of the region. One of the reported species previously known from Europe differs enough to be described as a new subspecies (*Bracon albion continentalis* ssp. nov.).

In recent years, knowledge about the Braconinae of China develops rapidly (for example, Li et al. 2016, 2020a, b, c). Due to incompleteness or inaccessibility of information about most of the known species of the subfamily and lack of reliable keys, the risks of misidentification or description of synonymous species during this work are high. For example, two recently described species from China are found to be junior synonyms of species presented in the current article. We provide illustrated descriptions for the species of Braconinae from the East Palaearctic region originally briefly described in Russian (Tobias and Belokobylskij 2000) and for some widely distributed, but complicated in identification species.

Material and methods

Terminology

Morphological nomenclature follows Quicke (1987) and van Achterberg (1993); the transverse pronotal sulcus is included after Karlsson and Ronquist (2012). The length of fifth segment of hind tarsus is measured without its pretarsus; first metasomal tergite is measured from its articulating condyle [term applied after Vilhelmsen et al. (2010)].

Abbreviations of morphological terms:

Od maximum diameter of lateral ocellus;
OOL ocular-ocellar distance;
POL postocellar distance.

Museum acronyms:

HNHM Hungarian Natural History Museum (Budapest, Hungary);

IRSNB Royal Belgian Institute of Natural Sciences (Brussels, Belgium);
NIBR National Institute of Biological Resources (Incheon, South Korea);
RMNH Naturalis Biodiversity Centre (Leiden, Netherlands);
SMNE Science Museum of Natural Enemies (Geochang, South Korea);
ZISP Zoological Institute of the Russian Academy of Sciences (Saint Petersburg, Russia);
ZMLU Lund Museum of Zoology, Lund University (Lund, Sweden).

List of collection localities in South Korea (numbers in brackets correspond to the numbers of points on the map in Fig. 1)

Gangwon-do • Goseong-gun: [1] Hyeonnae-myeon, Baebong-ri; [2] Ganseong-eup: [4] Jinbu-ri; [3] Geojin-eup, Naengcheon-ri, Geonbongsa Temple; [5] Toseong-myeon, Sinpyeong-ri, Seoraksan Mountain (Sinseonbong, or Sinseon-Peaks) • Sokcho-si: [6] Nohak-dong; [7] Seorak-dong • Yanggu-gun, [8] Bangsan-myeon, Omi-ri • Inje-gun, [9] Inje-eup, Hapgang-ri • Yangyang-gun, [10] Seo-myeon, Galcheon-ri, Yaksusan Mountain • Chuncheon-si, [11] Dongsan-myeon, Joyang-ri, Joyang bridge • Hongcheon-gun: [12] Duchon-myeon; [13] Naechon-myeon, Waya-ri, Baegamsan Mountain • Pyeongchang-gun, [14] Jinbu-myeon, Dongsan-ri, Odaesan Mountain • Donghae-si, [15] Bukpyeong-dong • Hoengseong-gun, [16] Gonggeun-myeon, Hakdam-ri • Yeongwol-gun: [17] Nam-myeon; [18] Hanbando-myeon, Ssangyong-ri; [19] Kimsatgat-myeon, Nae-ri, Town Daeyachi • Taebaek-si: [21] Cheoram-dong; [20] Cheoram-dong, Geumganggol (Geumgang valley); [22] Taebaeksan Mountain.

Seoul-si • Gwanak-gu, [23] Shinrim-dong.

Gyeonggi-do • Pocheon-si: [24] Idong-myeon, Dopyeong-ri, Valley Baekun; [25] Yeongbuk-myeon, Sanjeong-ri, Lake Sanjeong; [26] Hwahyeon-myeon, Hwahyeon-ri, Unaksan Mountain • Paju-si: [27] Gunnae-myeon, Jeomwon-ri; [28] Munsan-eup, Majeong-ri, Freedom Bridge (pond) • Yangju-si, [29] Nam-myeon • Gapyeong-gun: [30] Buk-myeon, Dodae-ri, Myeongjisan Mountain; Cheongpyeong-myeon: [31] Cheongpyeong-ri, Cheongpyeong Amusement Park; [32] Homyeong-ri, Cheongpyeong Dam; [33] Seorak-myeon, Gail-ri • Yangpyeong-gun, [34] Okcheon-myeon, Yongcheon-ri, Yongmunsan Mountain • Gunpo-si, [35] Sokdal-dong, Surisan Mountain • Suwon-si: [36] Jangan-gu, Pajang-dong, Gwanggyosan Mountain; Gwonseon-gu: [38] Seodun-dong: [37] Yeogisan Mountain • Hwaseong-si, [39] Bibong-myeon.

Gyeongsangbuk-do • Bonghwa-gun: [40] Seokpo-myeon, Seokpo-ri; [41] Mulya-myeon, Ojeon-ri, Seondalsan Mountain; [42] Beopjeon-myeon, Eoji-ri, Norujae mountain pass; [43] Myeongho-myeon • Gimcheon-si: [44] Eomo-myeon, Gurye-ri; [45] Daedeok-myeon, Churyang-ri Sudosan Mountain • Yeongcheon-si, [46] Hwabuk-myeon, Sangsong-ri, Nogwijae ridge • Seongju-gun, [47] Suryun-myeon, Bongyang-ri • Gyeongju-si, [48] Hyeongok-myeon, Geumjang-ri, Bridge Geumjang • Gyeongsan-si: [50] Yeongnam University: [49] Department of Biology.

Chungcheongnam-do • Yesan-gun, [51] Deoksan-myeon, Sudeoksa Temple • Gongju-si, [52] Banpo-myeon, Hakbong-ri • Geumsan-gun: [53] Chubu-myeon, Seongdang-ri, Gaedeoksa Temple; [54] Nami-myeon, Boseok Temple.

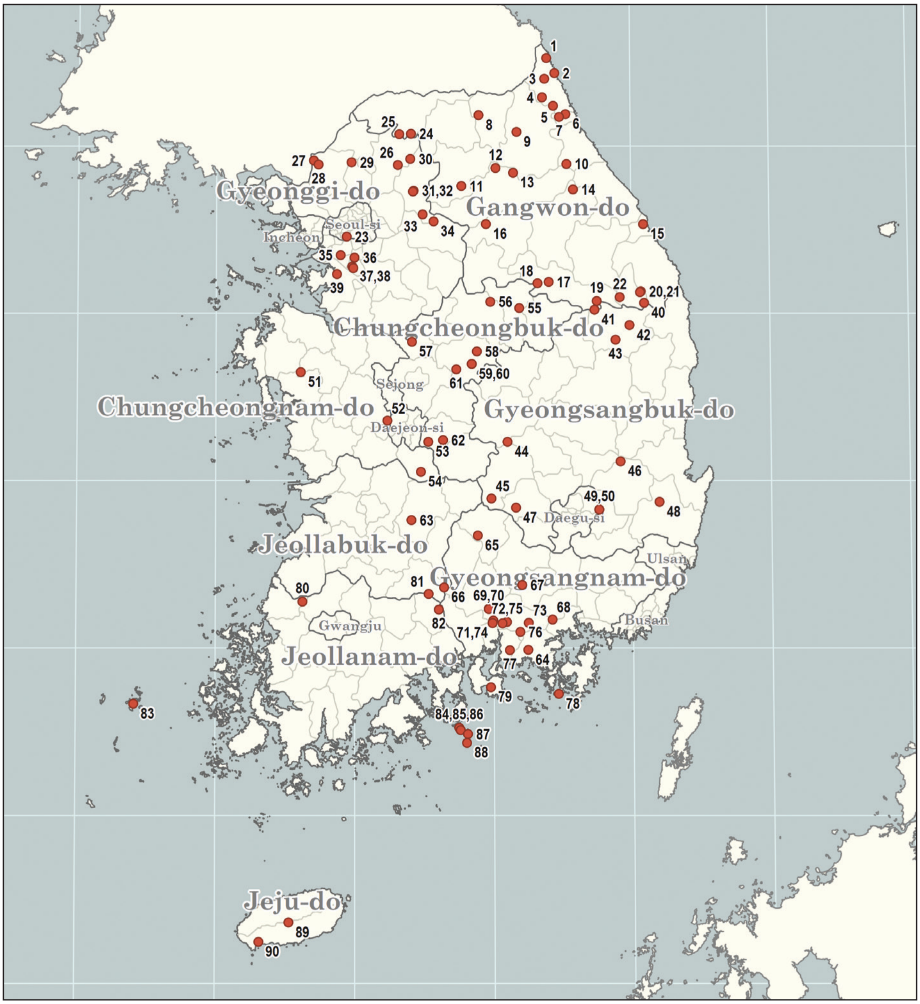

Figure 1. Collecting localities of the material on the listed species. Point numbers correspond with numbers in brackets in text.

Chungcheongbuk-do • Jecheon-si, [55] Geumseong-myeon, Seongnae-ri • Chungju-si, [56] Sancheok-myeon, Yeongdeok-ri • Jincheon-gun, [57] Jincheon-eup, Saseong-ri • Goesan-gun, [58] Chilseong-myeon, Ssanggok-ri; Cheongcheon-myeon: [59] Sagimak-ri; [60] Sagimak-ri, Mindung Mountain; [61] Cheongcheon-ri • Okcheon-gun, [62] Iwon-myeon, Iwon-ri.

Jeollabuk-do • Jinan-gun, [63] Jinan-eup, Danyang-ri, Maisan Mountain.

Gyeongsangnam-do • Goseong-gun: [64] Sangni-myeon, Bupo-ri; [65] Geochang-eup, Songjeong-ri • Hamyang-gun, [66] Macheon-myeon • Uiryeong-gun, [67] Garye-myeon, Gapeul-ri, Jagulsan Mountain • Changwon-si, [68] Masanhappo-gu, Jinbuk-myeon, Yeonghak-ri, Seobuk Mountain • Jinju-si: [69] Daepyeong-myeon: [70] Daepyeong-ri; [71] Naechon-ri; [72] Gajwa-dong; [73] Jinseong-myeon, Daesa-ri; Naedong-myeon: [74] Naepyeong-ri; [75] Doksan-ri (around the forest road); [76] Geumgok-myeon • Sacheon-si, [77] Baekcheon-dong, Waryongsan Mountain • Tongyeong-si, [78] Hansan-myeon, Bijin Island, Bijin-ri • Namhae-gun, [79] Idong-myeon, Sinjeon-ri, Geumsan Mountain.

Jeollanam-do • Jangseong-gun, [80] Samgye-myeon, Singi-ri, Taecheongsan Mountain, Bongjeongsa Temple • Gurye-gun: [81] Sandong-myeon, Jwasa-ri, Jirisan Mountain (Simwon); [82] Toji-myeon, Oegok-ri, Jirisan Mountain (Piagol) • Sinan-gun, [83] Heuksan-myeon, Heuksando Island • Yeosu-si, Nam-myeon: [84], Dumo-ri, Town Moha; [85] Yuseong-ri, Geumodo Island, Daedaesan Mountain; [86] Geumodo Island, Uhak-ri; [87] Ando Island, Ando-ri; [88] Yeondo Island, Yeondo-ri.

Jeju-do • Jeju-si, [89] Odeung-dong, Hanlla Mountain • Seogwipo-si, [90] Andeok-myeon, Sanbangsan Mountain.

The distribution map is generated in R using the packages *sf*, *ggplot2* and *shadowtext* based on the data from the Database of Global Administrative Areas (gadm.org). Distribution by countries is listed mainly according to Yu et al. (2016), other references are indicated in the text.

Material of related species used in diagnoses of taxa and illustrations

***Bracon* (*Osculobracon*) *subcingillus* Tobias, 2000**

Type material. ***Holotype.*** Russia – **Primorskiy Territory** • female; Partizansky District, 15 km NW of Partizansk; 13 Jul. 1979; S.A. Belokobylskij leg.; forest; ZISP.

***Iphiaulax impeditor* (Kokujev, 1898)**

Type material. ***Lectotype.*** Uzbekistan/Tajikistan • female; "from Yavan to Guzar"; 28 May 1888; A.P. Semenov leg.; ZISP.

Other material. Russia – **Saratov Province** • 1 female; Krasnokutsky District, Dyakovka, Yeruslan River bank; 26 Jun. 2012; D.M. Astakhov leg.; ZISP B0081 • 1 female; Krasnokutsky District, 5 km W of Dyakovka; 27 Jun. 2012; K. Samartsev leg.; burnt area; ZISP B0082.

Results

Genus *Atanycolus* Foerster, 1862

***Atanycolus ivanowi* (Kokujev, 1898)**
Figs 2–5, A1

Material. South Korea (1 female, 1 male). – **Gangwon-do** • 1 female; Yanggu-gun, [8] Bangsan-myeon, Omi-ri; 13 Jun. 1992; D.-S. Ku leg.; NIBR 510 • 1 male; same data as for preceding; SMNE 511.

Additional material. ?Italy • 1 male (lectotype of *Bracon sculpturatus* Thomson, 1892); ZMLU • 1 female (paralectotype of *B. sculpturatus* Thomson); ZMLU.

Romania • 1 female (lectotype of *Atanycolus signatus* Szépligeti, 1901); Transylvania, Domogled Mountains; 15–27 Jun. 1876; A. Moczáry leg.; HNHM 153261.

Russia – **Orenburg Province** • 1 female; Saraktashskiy District, Saraktashskiy forestry, quarter 33; 16 Jul. 2007; T.S. Kostromina and V.A. Kozlov leg.; on fallen poplars; ZISP B0094.

Slovakia • 1 female (paralectotype of *A. signatus* Szépligeti); Zádiel; HNHM 153262.

Ukraine • 1 female (lectotype of *Vipio ivanowi* Kokujev, 1898); vicinity of Kharkiv, Vodyanoye; 26 Jun. 1886; I.Ya. Shevyrev leg.; ZISP.

Turkmenistan – **Ahal Region** • 1 female; "sovkhoz Sovet Azerbaydzhany"; 1 Oct. 1988; Pashaev leg.; apricot; from "*Sph*. *kam*. and *chr*." [*Sphenoptera* spp.]; ZISP B0095.

Distribution. Caucasus: Armenia, Azerbaijan. Central Asia: Tajikistan, Turkmenistan, Uzbekistan. China: Xinjiang (Li et al. 2020a). Europe: Eastern, Southern, and Western Europe. Iran. Japan: Hokkaido. Kazakhstan. Russia: Eastern Siberia, European part, Far East: Jewish Autonomous Province, Primorskiy Territory, Sakhalin Island; Ural (Kostromina 2010). South Korea (new record). Turkey.

Diagnosis. The species is easily recognisable by the following character states: the median area of third metasomal tergite strongly elevated and transverse, with rounded sides and strongly narrowed posteriorly (Fig. 5); third and fourth tergites longitudinally rugose, their apical margins with incomplete, weak and weakly crenulate transverse subapical grooves. See also Li et al. (2020a: 15) for taxonomic literature and additional illustrations.

Genus *Bracon* Fabricius, 1804

Remarks. The subgeneric classification of the genus requires revision. Most of the Palaearctic species of *Bracon* are arranged in three subgenera, *Bracon* s. str., *Glabrobracon* Fahringer, and *Lucobracon* Fahringer (Tobias 1986). The species that may be unambiguously attributed to one of the discussed subgenera are more common in the West Palaearctic, but classification of a big part of species is difficult, because they frequently combine diagnostic characters of different subgenera. For example, some of otherwise obvious members of *Glabrobracon* have the wide hypostomal depression (one of the main characters of the subgenus *Lucobracon*, e.g. *B. brevis* Telenga and *B. otiosus* Marshall), others have the enlarged basitarsi (characterising the section *Orthobracon* Fahringer of the subgenus *Bracon*; e.g. *B. pauris* Beyarslan and *B. rozneri* Papp). This ambiguity of subgeneric diagnoses caused instability of composition of the main subgenera in interpretation by different authors. For example, the type species of the genus, *B. minutator* (Fabricius), in violation of the Principle of Coordination has been placed in the section *Orthobracon* of the subgenus *Bracon* by Tobias (1986) and together with the most part of the latter section has been transferred to the subgenus *Glabrobracon* by Papp (2008). These problems are most noticeable in the Far Eastern species which morphological peculiarity has rendered the diagnoses of

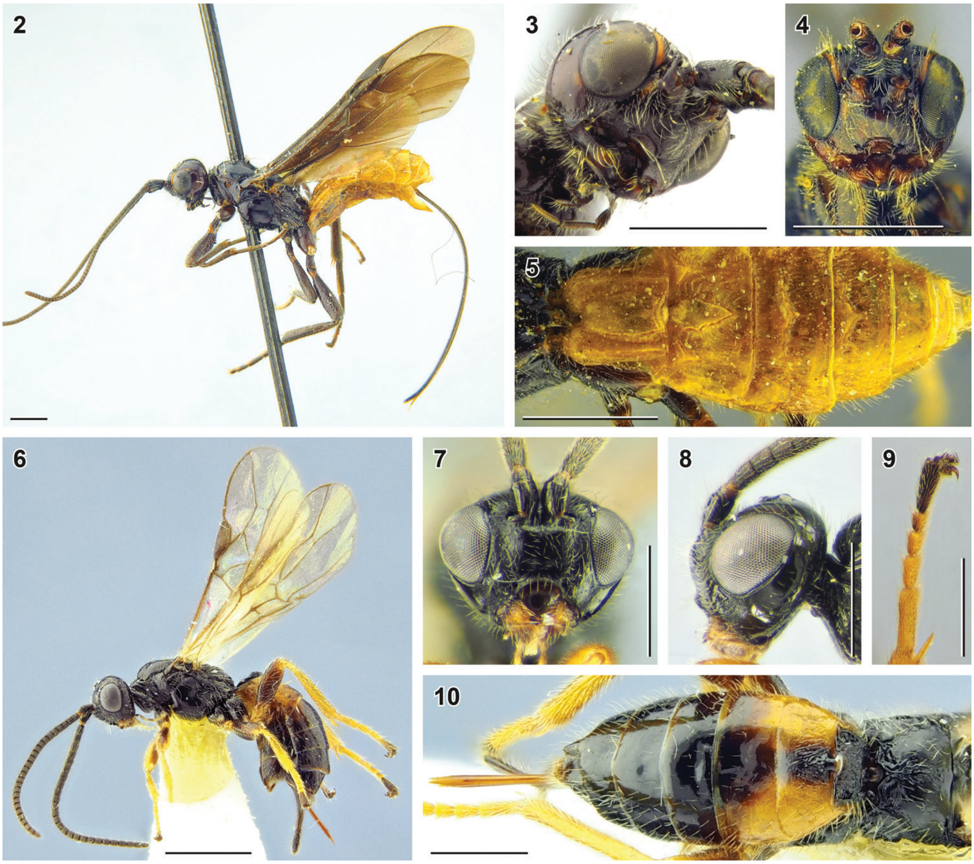

Figures 2–10. *Atanycolus ivanowi* (Kokujev, 1898) (**2, 3** lectotype, female, ZISP **4, 5** paralectotype of *A. signatus* Szépligeti, 1901, female, HNHM) and *Bracon* (*Bracon*) *albion albion* Papp, 1999 (**6–10** paratype, female, HNHM) **2, 6** habitus, lateral view **3** head, ventrolateral view **4, 7** head, anterior view **5, 10** metasoma, dorsal view **8** head, lateral view **9** hind tarsus. Scale bars: 0.5 mm (**7–10**); 1 mm (**2–6**).

the main subgenera very diffused and almost inapplicable (Tobias and Belokobylskij 2000). Thus, until reliable criteria of the subgeneric division of *Bracon* are established, we consider the species of *Glabrobracon* and *Lucobracon* in the nominative subgenus.

***Bracon* (*Bracon*) *albion albion* Papp, 1999**
Figs 6–10

Bracon (*Glabrobracon*) *albion* Papp, 1999: 146.

Material examined. United Kingdom – **Scotland** • 4 females (paratypes); Dunbartonshire, Caldarvan; 27 Jun. 1983–7 Jul. 1983; I.C. Christie leg.; bog with *Betula* and *Myrica*, Malaise trap; HNHM 153307–153310 • 4 males (paratypes); same data as for preceding;

HNHM 153316–153319 • 2 females (paratypes); Dunbartonshire, Caldarvan; 7–18 Jul. 1983; I.C. Christie leg.; bog with *Betula* and *Myrica*, Malaise trap; HNHM 153311, 153312 • 2 males (paratypes); same data as for preceding; HNHM 153320, 153321 • 1 female (paratype); same data as for preceding; 19 Jul. – 18 Aug. 1983; 153313; HNHM • 1 female (paratype); Perthshire, vicinity of Crianlarich, Coire Choille Chuilc; Jul. 1985; I. MacGowan and R.M. Lyszkowski leg.; pine forest; HNHM 153314.

Distribution. Europe: United Kingdom.

Diagnosis. The species belongs to the section *Orthobracon* Fahringer sec. Tobias (1986) of the subgenus *Bracon* and may be compared with *B. exhilarator* Nees, 1834, *B. longigenis* Tobias, 1957, *B. munki* Papp, 2011, *B. pertinax* Papp, 1984, and *B. terebralis* Tobias, 2000. *B. albion* differs from all above mentioned species by a combination of strongly enlarged fifth tarsal segment (Fig. 9) and thickened antenna (especially in Europe; Fig. 6).

Remarks. A single female paratype of *B. albion albion* Papp from Denmark belongs to *B. albion continentalis* ssp. nov. Thus, the nominative subspecies is considered to be endemic of the British Isles.

Bracon (*Bracon*) *albion continentalis* ssp. nov.

http://zoobank.org/7133D622-79D7-46C2-BF09-1589BCB23B05
Figs 11–21, A1

Type material. ***Holotype.*** South Korea – **Gyeongsangbuk-do** • female; Seongju-gun, [47] Suryun-myeon, Bongyang-ri; 9 Jun. 1992; D.-S. Ku leg.; NIBR 344.

Paratypes. (2 females). South Korea – **Chungcheongbuk-do** • 1 female; Jecheon-si, [55] Geumseong-myeon, Seongnae-ri; 10 Jun. 1992; D.-S. Ku leg.; SMNE 331. – **Gyeongsangnam-do** • 1 female; Geochang-gun, [65] Geochang-eup, Songjeong-ri; 35.6712, 127.8850; 3 Jun. 2019; K. Samartsev leg.; forest on a mountain, sweeping; ZISP B0058.

Additional material. Denmark • 1 female (paratype of *B. albion albion* Papp, 1999); Jutland, NE of Ribe, Haslund Krat; 13 Jul. 1987; T. Munk leg.; HNHM 153315.

Russia – **Novgorod Province** • 1 female; Pestovskiy District, 20 km NW of Pestovo, Tychkino; 6 Jul. 1986; V.I. Tobias leg.; ZISP • 2 females; same data as for preceding; 29 Jul. 1990; ZISP B0078, B0079.

Etymology. The name *continentalis* is formed from Latin noun *continens* indicating the wide distribution of the subspecies across the continental part of Palaearctic in contrast with the island distribution of the nominative subspecies.

Description. Female. Body length 3.5–3.8 mm (Russian non-type specimens: 2.8–3.2 mm); fore wing length 3.2–3.6 mm (2.9–3.2 mm).

Head. Width of head (dorsal view) 1.6–1.8× (1.8–1.9×) its median length. Transverse diameter of eye (dorsal view) 1.8–1.9× (1.9–2.0×) longer than temple. Eyes with sparse, short setae. OOL 2.4–2.6× (2.2×) Od; POL 1.1–1.2× (1.2–1.4×) Od; OOL

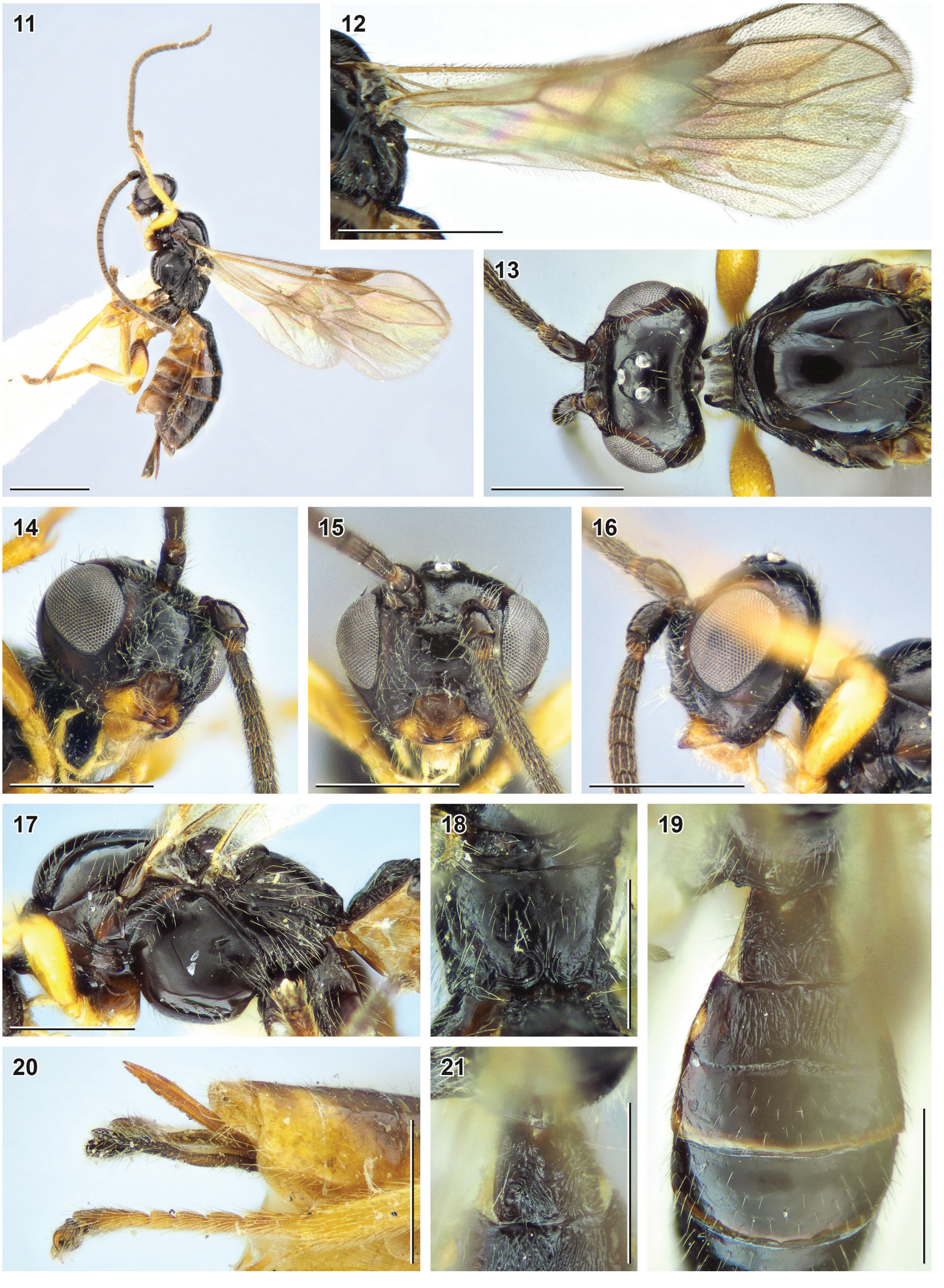

Figures 11–21. *Bracon* (*Bracon*) *albion continentalis* ssp. nov. (holotype, female, NIBR) **11** habitus, lateral view **12** wings **13** head and mesoscutum, dorsal view **14** head, ventrolateral view **15** head, anterior view **16** head, lateral view **17** mesosoma, lateral view **18** propodeum, dorsal view **19** metasoma, dorsal view **20** hind tarsus and ovipositor **21** first metasomal tergite, dorsal view. Scale bars: 0.5 mm (**13–21**); 1 mm (**11, 12**).

2.0–2.3× (1.6–1.7×) POL. Frons with deep medio-longitudinal groove. Longitudinal diameter of eye (lateral view) 1.4–1.5× its transverse diameter. Transverse diameter of eye (lateral view) 2.0–2.2× (2.3–2.4×) longer than minimum width of temple, hind margins of eye and temple subparallel to broadened downwards. Face width 1.7–1.9× combined height of face and clypeus; 2.2–2.3× width of hypoclypeal depression. Longitudinal diameter of eye 2.4–2.7× (2.3–2.4×) longer than malar space (anterior view); malar space 0.75–0.90× basal width of mandible. Malar suture absent. Width of hypoclypeal depression 1.3× distance from depression to eye. Clypeus prominent, its height about 0.33× (0.25×) width of hypoclypeal depression. Maxillary palp longer than eye, but shorter than head.

Antenna 0.75–0.90× as long as fore wing, with 29 antennomeres. First, middle, and penultimate flagellomeres 1.4–1.7× (1.5–1.8×), 1.3–1.5× (1.2–1.3×), and 1.5–1.7× longer than wide, respectively.

Mesosoma 1.6× (1.6–1.7×) longer than its maximum height. Transverse pronotal sulcus deep, smooth or weakly crenulate. Notauli impressed anteriorly, shallow and not united posteriorly. Mesoscutum with setae only on notaulic area. Scutellar sulcus crenulate. Mesepimeral sulcus smooth (weakly crenulate), mesopleural pit deep, separated from mesepimeral sulcus. Metapleural sulcus smooth or weakly crenulate (crenulate). Propodeal spiracle round, located in middle of propodeum. Propodeum with branching medio-longitudinal keel in apical half (complete).

Wings. Fore wing 0.92–0.95× as long as body. Pterostigma 2.8–3.3× longer than wide. Vein r arising from basal 0.50–0.55× (0.45–0.50×) of pterostigma. Vein 1-R1 1.4–1.5× (1.6–1.7×) longer than pterostigma. Marginal cell 8–10× longer than distance from its apex to apex of wing. Vein 3-SR 2.1–2.7× vein r, 0.55–0.65× vein SR1, 1.2–1.5× vein 2-SR. Vein 1-M 0.67–0.70× vein 1-SR+M, 1.5–1.8× vein m-cu, 2.0–2.2× vein cu-a. Vein 2-SR+M 0.10–0.25× vein 2-SR, 0.2–0.4× vein m-cu. Vein 1-CU1 (posterior margin of discal cell) 2.4–2.7× (2.7–3.6×) vein cu-a. Vein cu-a antefurcal or interstitial. Vein 2-1A of hind wing absent or very short.

Legs. Fore tibia with longitudinal and transverse apical rows of thick setae. Hind femur 2.4–2.5× longer than wide. Hind tibia 1.5–1.6× longer than hind femur, without subapical row of thick setae, its inner spur about 0.6× (0.65–0.75×) as long as hind basitarsus. Hind tarsus 0.85–0.90× as long as hind tibia. Fifth segment (without pretarsus) of hind tarsus 1.9–2.1× (1.8–1.9×) longer than second segment and 1.2–1.3× longer than hind basitarsus. Claws with rectangular (acute angularly protruding) basal lobe.

Metasoma 1.2–1.5× longer than mesosoma. First metasomal tergite with more or less developed dorsolateral carinae composed of multiple rugae and with lateral carinae, its median length 0.80–0.85× its apical width; median area separated by rugate furrow. Second tergite with weak, very short, and narrow triangular median area and weakly impressed dorsolateral impressions, medially 0.75–0.95× as long as third tergite and 0.70–0.75× (0.75–0.85×) as large as apical width of first tergite. Basal width of second metasomal tergite 1.8–2.1× (1.6–1.7×) its median length. Suture between second and third tergites weak laterally, medially deep, weakly curved and crenulate. Apical margins of third to sixth tergites thin, without transverse subapical grooves.

Ovipositor sheath 0.75–0.85× as long as hind tibia and 0.20–0.25× as long as fore wing. Apex of ovipositor with weak nodus and developed ventral serration.

Sculpture. Face (almost) smooth (weakly granulate); malar space granulate; frons weakly granulate. Mesosoma mostly smooth; metanotum smooth with rugae on margins; propodeum smooth (granulate-rugulose posteriorly) with tree-like rugosity in apical half. First tergite laterally rugulose, its median area posteriorly obliquely rugulose to rugose; second metasomal tergite longitudinally rugose medially, laterally granulate-rugulose; third and posterior tergites (almost) smooth.

Colour. Body mostly black; legs rusty brown, coxae black, middle and hind femora basally dark brown, or all legs entirely, except for brownish coxae and tarsi, brownish yellow; ventral side of metasoma anteriorly yellowish brown, or metasoma mostly brownish yellow, medio-longitudinally brown; maxillary palps brownish yellow or pale yellow; wing membrane weakly brownish darkened, pterostigma and wing veins brown.

Male. Unknown.

Distribution. Europe: Northern Europe (Denmark: Papp 1999, as *B. albion*). South Korea. Russia: European part: Novgorod Province, Saratov Province (Samartsev 2013, as *B. albion*).

Diagnosis. The new subspecies differs from *B. albion albion* Papp by the extremely short basitarsus and enlarged fifth segment of the hind leg (Fig. 20). In addition, the Korean specimens of *B. albion continentalis* ssp. nov. have less thickened antennae (Fig. 11), more coarsely (with distinct longitudinal rugae) sculptured second metasomal tergite (Fig. 19), and almost smooth face (Fig. 14; weakly granulate in the European specimens).

***Bracon* (*Bracon*) *imbricatellus* Tobias, 2000**
Figs 22–28, A1

Material. South Korea (4 females). – **Gyeonggi-do** • 1 female; Suwon-si, [36] Jangan-gu, Pajang-dong, Gwanggyosan Mountain; 22 Jul. 1998; D.-S. Ku leg.; light trap; SMNE 943 • 1 female; Suwon-si, [37] Gwonseon-gu, Seodun-dong, Yeogisan Mountain; 31 Jul. 1995; June-Yeol Choi leg.; Malaise trap; SMNE 944 • 1 female; same data as for preceding; 14 Aug. 1995; ZISP 937 • 1 female; same data as for preceding; NIBR 938.

Additional material. Japan – **Fukushima Prefecture** • 1 female (holotype); Hinoemata; 16–18 Aug. 1999; S.A. Belokobylskij leg.; ZISP.

Distribution. Japan: Honshu. South Korea (new record).

Description. Female. Fore wing length 2.6–3.0 mm. Width of head (dorsal view) 1.7–1.8× its median length. Transverse diameter of eye (dorsal view) 1.6–2.0× longer than temple. OOL 2.0–2.8× Od; POL 1.2–1.8× Od; OOL 1.6–1.7× POL. Longitudinal diameter of eye (lateral view) 1.3–1.6× its transverse diameter; hind margins of eye and temple subparallel. Face width 1.4–1.5× combined height of face and clypeus. Longitudinal diameter of eye 3.1–3.3× longer than malar space (anterior view). Malar suture weak under eye, smoothed near mandible. Width of hypoclypeal depression

1.2–1.4× distance from depression to eye. Antenna 0.90–0.95× as long as fore wing, with 24–25 antennomeres. First, middle and penultimate flagellomeres 2.0–2.1×, 1.7–2.0, and 1.8–2.2× longer than wide, respectively. Mesosoma 1.7–1.8× longer than its maximum height. Mesoscutum evenly, but sparsely setose. Notauli deep anteriorly, shallow and not united posteriorly. Mesepimeral and metapleural sulci smooth. Medio-longitudinal keel developed in apical third of propodeum, branching. Fore wing vein r arising from basal 0.40–0.45 of pterostigma; vein 1-R1 1.5–1.7× longer than pterostigma; marginal cell 12–16× longer than distance from its apex to apex of wing; vein 3-SR 2.0–2.5× vein r, 0.55–0.65× vein SR1, 1.3–1.4× vein 2-SR. Hind femur 3.0–3.4× longer than wide. Hind tibia without subapical row of thick setae. Fifth segment of hind tarsus 0.50–0.55× and 0.95–1.00× as long as hind basitarsus and second segment, respectively. Claws with acute angularly protruding basal lobe. First metasomal tergite with incomplete dorsal carina and developed dorsolateral carinae, its median length 0.70–0.85× its apical width. Second tergite with weak, narrow, longitudinal median area, weak anterolateral areas with smooth sculpture, and with deep s-shaped crenulate dorsolateral impressions bordered by long carinae; medially 1.1–1.5× longer than third tergite; its basal width 1.3–1.8× its median length. Second metasomal suture deep, curved and crenulate. Apical margins of third–sixth tergites thick, with weakly foveate transverse subapical grooves. Ovipositor sheath 0.85–1.00× as long as hind tibia and 0.23–0.25× as long as fore wing. Apex of ovipositor with weak nodus and ventral serration. Body mainly smooth; face medially and malar space granulate, face laterally and frons weakly granulate; propodeum posteriorly hardly coriaceous, with tree-like rugosity medially in posterior half; first metasomal tergite smooth to weakly foveate; second tergite areolate-rugose to foveate; third–sixth tergites smoothed foveate, or metasoma entirely areolate-rugose to foveate-rugose. Head and mesosoma mostly reddish brown with yellowish brown pattern, legs and lateral and ventral parts of metasoma reddish yellow; antenna basally reddish yellow, flagellum darkening apically; maxillary palps yellow; tegulae brownish yellow; propodeum and most of metasoma dorsally dark brown; wing membrane weakly darkened, pterostigma and veins brown.

Remarks. Relationships of the species are given below, in the diagnosis of *B. virgatus* Marshall.

Bracon (*Bracon*) *kasparyani* Samartsev, 2018

Fig. A2

Material. South Korea (23 females, 7 males). – **Gangwon-do** • 2 females; Goseong-gun, [3] Geojin-eup, Naengcheon-ri, Geonbongsa Temple; 25 May 1993; D.-S. Ku leg.; SMNE 572, 573 • 1 female; Donghae-si, [15] Bukpyeong-dong; 28 May 1993; D.-S. Ku leg.; NIBR 582 • 1 male; Yeongwol-gun, [17] Nam-myeon; 24 May 1993; D.-S. Ku leg.; SMNE 577 • 2 females; Yeongwol-gun, [18] Hanbando-myeon, Ssangyong-ri; 24 May 1993; D.-S. Ku leg.; SMNE 578, 579 • 1 female; Taebaek-si, [20] Cheoram-dong, Geumganggol; 8 Jul. 1991; D.-S. Ku leg.; SMNE 592 • 1 female;

Taebaek-si, [21] Cheoram-dong; 22 Jun. 1991; D.-S. Ku leg.; SMNE 575 • 1 male; same data as for preceding; 6 Jul. 1991; SMNE 593. – **Gyeonggi-do** • 1 female; Pocheon-si, [26] Hwahyeon-myeon, Hwahyeon-ri, Unaksan Mountain; 14 Jun. 1992; D.-S. Ku leg.; SMNE 596 • 1 female; Suwon-si, [37] Gwonseon-gu, Seodun-dong, Yeogisan Mountain; 19–26 May 1994; D.-S. Ku leg.; Malaise trap; SMNE 590. – **Gyeongsangbuk-do** • 2 females; Bonghwa-gun, [40] Seokpo-myeon, Seokpo-ri; 28 May 1993; D.-S. Ku leg.; SMNE 580, 581 • 1 male; same data as for preceding; SMNE 583 • 1 female; Gimcheon-si, [44] Eomo-myeon, Gurye-ri; 9 Jun. 1992; D.-S. Ku leg.; SMNE 589 • 2 males; Yeongcheon-si, [46] Hwabuk-myeon, Sangsong-ri, Nogwijae ridge; 29 May 1993; D.-S. Ku leg.; SMNE 586, 587. – **Chungcheongnam-do** • 1 female; Geumsan-gun, [53] Chubu-myeon, Seongdang-ri, Gaedeoksa Temple; 22 May 1993; D.-S. Ku leg.; ZISP 574. – **Chungcheongbuk-do** • 1 female; Jincheon-gun, [57] Jincheon-eup, Saseong-ri; 15 Jun. 1992; D.-S. Ku leg.; SMNE 600 • 1 male; same data as for preceding; SMNE 601 • 1 female; Goesan-gun, [58] Chilseong-myeon, Ssanggok-ri; 23 May 1993; D.-S. Ku leg.; SMNE 594 • 1 female; Goesan-gun, [59] Cheongcheon-myeon, Sagimak-ri; 23 May 1993; D.-S. Ku leg.; SMNE 576. – **Jeollabuk-do** • 1 female; Jinan-gun, [63] Jinan-eup, Danyang-ri, Maisan Mountain; 16 Jun. 1996; D.-S. Ku leg.; SMNE 599. – **Gyeongsangnam-do** • 1 female; Jinju-si, [69] Daepyeong-myeon; 12 Jun. 1992; D.-S. Ku leg.; SMNE 591 • 1 male; Jinju-si, [70] Daepyeong-myeon, Daepyeong-ri; 23 Jun. 1992; D.-S. Ku leg.; SMNE 597 • 1 female; Jinju-si, [72] Gajwa-dong; 9 Jun. 1993; D.-S. Ku leg.; ZISP 588 • 2 females; same data as for preceding; 14 Jul. 1993; SMNE 584, 585 • 1 female; Sacheon-si, [77] Baekcheon-dong, Waryongsan Mountain; 5 Jun. 1993; J.-S. Cheon leg.; ZISP 595. – **Jeollanam-do** • 1 female; Gurye-gun, [81] Sandong-myeon, Jwasa-ri, Jirisan Mountain (Simwon); 30–31 Jun. 1992; D.-S. Ku leg.; light trap; SMNE 598.

Distribution. Japan: Hokkaido (Samartsev 2018). Russia: Far East (Samartsev 2018): Amur Province, Kuril Islands, Primorskiy Territory, Sakhalin Island. South Korea (new record).

Remarks. The diagnosis of the species is presented in Samartsev (2018) and Samartsev and Ku (2020).

***Bracon* (*Bracon*) *kotenkoi* Samartsev, 2018**
Fig. A3

Material. South Korea (2 females). – **Jeollanam-do** • 1 female; Sinan-gun, [83] Heuksan-myeon, Heuksando Island; 26 Aug. 1993; D.-S. Ku leg.; NIBR 404 • 1 female; Yeosu-si, [88] Nam-myeon, Yeondo Island, Yeondo-ri; 5 Aug. 1993; D.-S. Ku leg.; SMNE 405.

Distribution. Russia: Far East: Primorskiy Territory (Samartsev 2018). South Korea (new record).

Remarks. The diagnosis of the species is presented in Samartsev (2018) and Samartsev and Ku (2020).

***Bracon* (*Bracon*) *longigenis* Tobias, 1957**
Figs 29–36, A3

Material. South Korea (4 females). – **Gyeongsangbuk-do** • 1 female; Gyeongsan-si, [50] Yeongnam University; 4 May 1988; D.-S. Ku leg.; SMNE 676. – **Chungcheong-nam-do** • 1 female; Geumsan-gun, [53] Chubu-myeon, Seongdang-ri, Gaedeoksa Temple; 22 May 1993; D.-S. Ku leg.; NIBR 673 • 1 female; same data as for preceding; SMNE 674 • 1 female; same data as for preceding; ZISP 675.

Additional material. Russia – **Crimea Republic** • female (holotype); Simferopol; 17 May 1927; V. and E. Kusnetzovs leg.; ZISP • 1 female (paratype); same data as for holotype; ZISP. – **Saratov Province** • 1 female; Krasnoarmeysky District, 4 km NW of Melovoye; 29 May 2011; K. Samartsev leg.; sparse oak forest; ZISP B0088.

Distribution. Israel. Russia: European part. South Korea (new record). Turkey.

Description. Female. Fore wing length 2.9–3.2 mm. Width of head (dorsal view) 1.8–1.9× its median length. Transverse diameter of eye (dorsal view) 1.8–2.0× longer than temple. OOL 1.9–2.9× Od; POL 1.3–1.7× Od; OOL 1.3–2.1× POL. Longitudinal diameter of eye (lateral view) 1.3× its transverse diameter; hind margins of eye and temple subparallel. Face width 1.4–1.7× combined height of face and clypeus. Longitudinal diameter of eye 1.7–1.8× longer than malar space (anterior view). Malar suture absent. Width of hypoclypeal depression 0.85–0.97× distance from depression to eye. Antenna 1.0–1.2× as long as fore wing, with 30–33 antennomeres. First, middle and penultimate flagellomeres 1.7–2.0×, 1.3–1.6×, and 1.8–2.0× longer than wide, respectively. Mesosoma 1.7× longer than its maximum height. Mesoscutum setose only on notaulic area. Notauli impressed anteriorly, shallow and not united posteriorly. Mesepimeral sulcus weakly crenulate; metapleural sulcus crenulate. Medio-longitudinal keel on propodeum complete, branching. Fore wing vein r arising before middle of pterostigma; vein 1-R1 1.5–1.6× longer than pterostigma; marginal cell 10–15× longer than distance from its apex to apex of wing; vein 3-SR 2.0–2.4× vein r, 0.55–0.65× vein SR1, 1.3–1.5× vein 2-SR. Hind femur 2.8–3.5× longer than wide. Hind tibia with subapical transverse row of spiny setae. Fifth segment of hind tarsus 0.6–0.9× and 1.1–1.5× as long as hind basitarsus and second segment, respectively (see also a remark below). Claws with large rectangular basal lobe. First metasomal tergite with complete dorsal carinae and developed dorsolateral carinae, its median length 0.85–0.95× its apical width. Second tergite with indistinct median area and with shallow dorsolateral impressions, medially 0.9–1.0× as long as third tergite; its basal width 1.4–1.8× its median length. Second metasomal suture deep, strongly curved and crenulate. Apical margins of third to sixth tergites thin. Ovipositor sheath 0.70–0.85× as long as hind tibia and 0.20–0.25× as long as fore wing. Apex of ovipositor with weak nodus and distinct ventral serration. Body mostly smooth; face weakly granulate; frons and malar space granulate; propodeum medioposteriorly granulate-rugulose; median area of first tergite posteriorly rugose; second tergite rugose to granulate-rugulose, third–fifth tergites granulate to weakly granulate, sixth tergite almost smooth. Head and

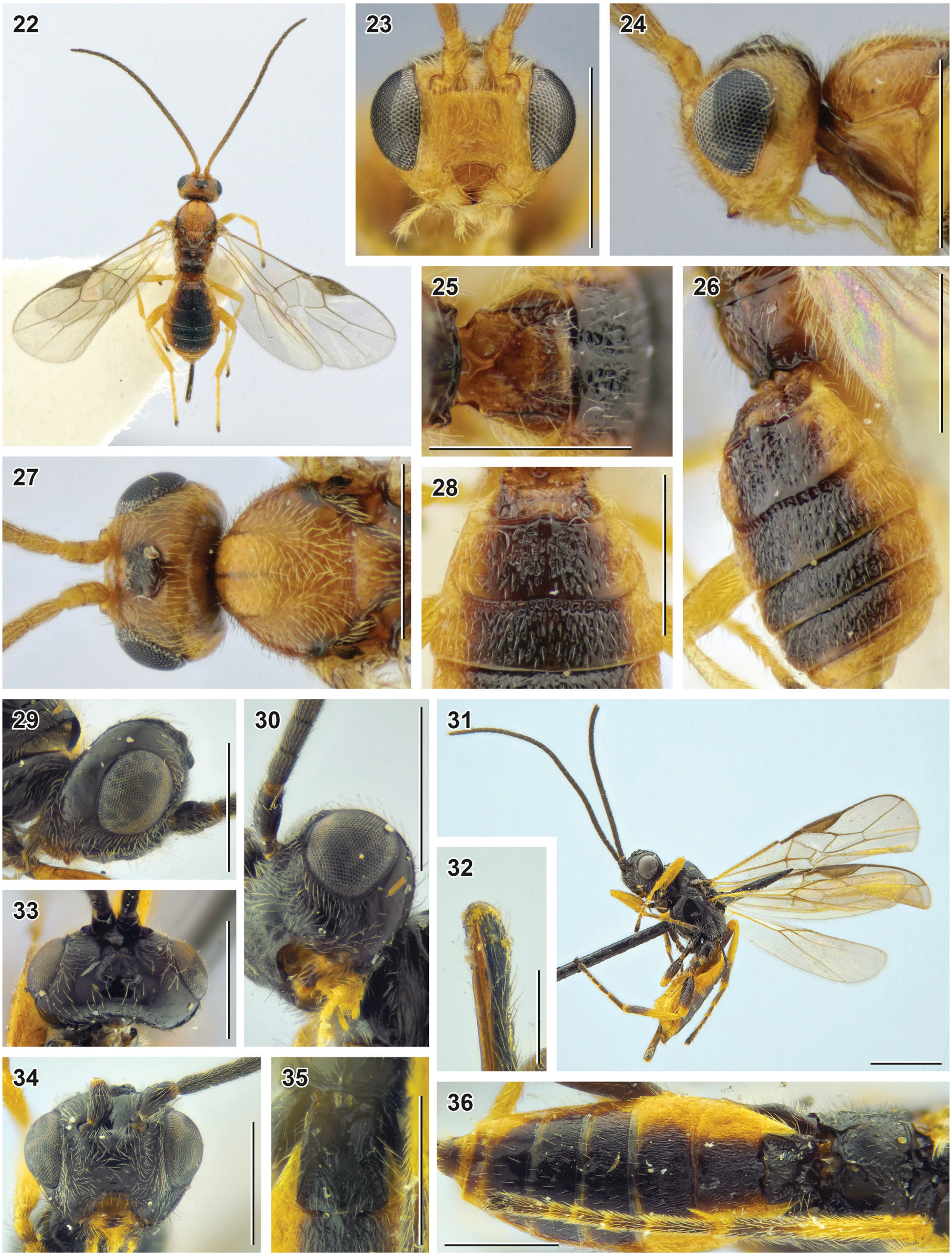

Figures 22–36. *Bracon* (*Bracon*) *imbricatellus* Tobias, 2000 (**22–28** holotype, female, ZISP) and *B.* (*B.*) *longigenis* Tobias, 1957 (**29, 31, 32, 35, 36** holotype **30, 34** paratype, female, ZISP) **22** habitus, dorsal view **23, 34** head, anterior view **24, 29** head, lateral view **25, 35** first metasomal tergite, dorsal view **26** metasoma, dorsolateral view **27, 33** head (and mesoscutum), dorsal view **28** metasoma, dorsal view **30** head, ventrolateral view **31** habitus, lateral view **32** apex of ovipositor **36** metasoma and hind tarsus, dorsal view. Scale bars: 0.25 mm (**32**); 0.5 mm (**23–30, 34–36**); 1 mm (**31**).

mesosoma brownish black, metasoma medio-longitudinally dark brown; lateral parts of metasomal tergites and ventral side of metasoma reddish yellow; legs mostly reddish yellow or middle and hind legs with developed dark brown pattern; maxillary palps yellow; tegulae yellowish brown; wing membrane weakly darkened, pterostigma and veins brown or yellowish brown.

Diagnosis. Within the section *Orthobracon* Fahringer sec. Tobias (1986), *B. longigenis* is remarkable by the very long malar space (Figs 30, 33), entirely sculptured metasoma with elongate first tergite (Figs 35, 36), and dark-coloured body.

Remarks. The specimens from South Korea have the apical tarsomere 1.4–1.5× longer than the second tarsal segment (while in *B. longigenis* from Europe this ratio is 1.15–1.25) and entirely light-coloured legs (except the brownish hind tarsus; middle and hind legs extensively darkened in *B. longigenis* from Europe).

Bracon (*Bracon*) *santachezae* Samartsev, 2018

Fig. A3

Material. South Korea (1 female, 1 male). – **Gyeonggi-do** • 1 female; Paju-si, [27] Gunnae-myeon, Jeomwon-ri; 3 Jun. 1998; Heung-Sik Lee leg.; NIBR 401 • 1 male; Paju-si, [28] Munsan-eup, Majeong-ri, Freedom Bridge (pond); 3 Jun. 1998; Heung-Sik Lee leg.; SMNE 403.

Distribution. Russia: Far East: Primorskiy Territory (Samartsev 2018). South Korea (new record).

Remarks. The diagnosis of the species is presented in Samartsev (2018).

Bracon (*Bracon*) *semitergalis* Tobias, 2000

Figs 37–45, A4

Bracon semitergalis Tobias, 2000 in Belokobylskij and Tobias 2000: 126.
Bracon leptotes Li, He & Chen, 2020b: 222; syn. nov.

Material. South Korea (9 females, 4 males). – **Gangwon-do** • 1 female; Goseong-gun, [5] Toseong-myeon, Sinpyeong-ri, Seoraksan Mountain; 2 Aug. – 19 Oct. 2002; D.-S. Ku leg.; Malaise trap; SMNE 767 • 1 female; Gapyeong-gun, [32] Cheongpyeong-myeon, Homyeong-ri, Cheongpyeong Dam; 14 Jun. 1992; D.-S. Ku leg.; NIBR 1441 • 1 female; Yangpyeong-gun, [34] Okcheon-myeon, Yongcheon-ri, Yongmunsan Mountain; 14 Jun. 1992; D.-S. Ku leg.; SMNE 1489 • 1 male; Suwon-si, [37] Gwonseon-gu, Seodun-dong, Yeogisan Mountain; 11 May 1994; D.-S. Ku leg.; SMNE 763. – **Gyeongsangbuk-do** • 1 male; Bonghwa-gun, [40] Seokpo-myeon, Seokpo-ri; 28 May 1993; D.-S. Ku leg.; SMNE 765. – **Chungcheongbuk-do** • 1 male; Chungju-si, [56] Sancheok-myeon, Yeongdeok-ri; 23 May 1993; D.-S. Ku leg.; SMNE 755 • 1 female; Jincheon-gun, [57] Jincheon-eup, Saseong-ri; 15 Jun.

1992; D.-S. Ku leg.; SMNE 768 • 1 female; Goesan-gun, [61] Cheongcheon-myeon, Cheongcheon-ri; 23 May 1993; D.-S. Ku leg.; SMNE 754 • 1 male; Okcheon-gun, [62] Iwon-myeon, Iwon-ri; 22 May 1993; D.-S. Ku leg.; SMNE 762. – **Gyeongsangnam-do** • 1 female; Jinju-si, [72] Gajwa-dong; 15 May 1993; D.-S. Ku leg.; ZISP 764. – **Jeollanam-do** • 1 female; Gurye-gun, [81] Sandong-myeon, Jwasa-ri, Jirisan Mountain (Simwon); 4 Aug. 1996; K.-J. Hong leg.; SMNE 766 • 1 female; Yeosu-si, [88] Nam-myeon, Yeondo Island, Yeondo-ri; 20 Jul. 1993; D.-S. Ku leg.; SMNE 760 • 1 female; same data as for preceding; ZISP 761.

Additional material. Russia – **Primorskiy Territory** • 1 female (holotype); Shkotovskiy District, Anisimovka; 5–7 Jun. 1993; S.A. Belokobylskij leg.; forest, meadow; ZISP.

Distribution. Russia: Far East: Primorskiy Territory; South Korea (new record).

Description. Female. Fore wing length 2.7–3.4 mm. Width of head (dorsal view) 1.7× its median length. Transverse diameter of eye (dorsal view) 2.3–2.5× longer than temple. OOL 2.6–2.8× Od; POL 1.3–1.5× Od; OOL 1.8–2.2× POL. Longitudinal diameter of eye (lateral view) 1.3–1.4× its transverse diameter; hind margins of eye and temple subparallel. Face width 1.3–1.5× combined height of face and clypeus. Longitudinal diameter of eye 3.2–3.6× longer than malar space (anterior view). Malar suture absent. Width of hypoclypeal depression 1.5–1.8× distance from depression to eye. Antenna 1.0–1.1× as long as fore wing, with 27–32 antennomeres. First, middle and penultimate flagellomeres 2.2–2.5×, 1.5–1.9, and 1.9–2.5× longer than wide, respectively. Mesosoma 1.6× longer than its maximum height. Mesoscutum setose on notaulic area and with sparse setae medio-longitudinally. Notauli very deep anteriorly, impressed and almost united posteriorly. Mesepimeral and metapleural sulci smooth. Medio-longitudinal keel developed in apical third of propodeum, branching. Fore wing vein r arising from basal 0.45–0.50 of pterostigma; vein 1-R1 1.4–1.8× longer than pterostigma; marginal cell 9–13× longer than distance from its apex to apex of wing; vein 3-SR 2.3–2.6× vein r (Li et al. 2020b: 3×), 0.5–0.6× vein SR1, 1.2–1.4× vein 2-SR (Li et al. 2020b: 1.7×). Hind femur 3.6–3.8× longer than wide. Hind tibia with without subapical row of thick setae. Fifth segment of hind tarsus 0.45–0.50× and 0.88–0.90× as long as hind basitarsusas and second segment, respectively. Fifth segment of hind tarsus as long as second segment. Claws with shortly protruding and blunt basal lobe. First metasomal tergite with incomplete dorsal carinae strongly curved towards apex of tergite and with developed dorsolateral carinae, its median length 0.95–1.20× its apical width. Second tergite with weak elongate-triangulate median area and with more or less deep s-shaped crenulated dorsolateral impressions; medially 0.90–1.15× as long as third tergite; its basal width 1.3–1.6× its median length. Second metasomal suture deep, curved and crenulate. Apical margins of third to sixth tergites thin. Ovipositor sheath 1.2–1.7× longer than hind tibia and 0.35–0.50× as long as fore wing. Apex of ovipositor with developed nodus and ventral serration. Body mainly smooth; face medially weakly granulate under toruli, laterally almost smooth; frons weakly granulate; malar space granulate; first metasomal tergite obliquely rugulose posteriorly, second or second and third tergites striate-rugulose, fourth tergite with rugulose to papillary-like sculpture, fifth and sixth tergites with weakening papillary-like sculpture or almost smooth (Li et al. 2020b: fig. 6e, metasomal sculpture strongly smoothed, second tergite weakly rugulose, third and fourth tergites weakly shagreen to smooth). Body mainly dark brown, most of legs and ventral side of metasoma yellow; head ventrally, scape, pronotum, tegula brownish yellow; maxillary palps pale yellow; wing membrane weakly darkened, pterostigma yellowish brown, veins pale brown.

Diagnosis. Relationships of *Bracon semitergalis* are listed in the diagnosis of *B. tergalis* (see below).

Bracon (*Bracon*) *sergeji* Tobias, 2000

Figs 46–54, A5

Material. South Korea (5 females). – **Gyeonggi-do** • 1 female; Suwon-si, [37] Gwonseon-gu, Seodun-dong, Yeogisan Mountain; 19 Aug. 1983; Y.I. Lee leg.; SMNE 756. – **Gyeongsangnam-do** • 1 female; Namhae-gun, [79] Idong-myeon, Sinjeon-ri, Geumsan Mountain; 21 Aug. 1992; D.-S. Ku leg.; SMNE 758. – **Jeollanam-do** • 1 female; Jangseong-gun, [80] Samgye-myeon, Singi-ri, Taecheongsan Mountain, Bongjeongsa Temple; 11 Jul. 1998; D.-S. Ku leg.; light trap; NIBR 759 • 1 female; Yeosu-si, [84] Nam-myeon, Dumo-ri, Town Moha; 20 Jul. 1993; D.-S. Ku leg.; SMNE 749 • 1 female; Yeosu-si, [85] Nam-myeon, Yuseong-ri, Geumodo Island, Daedaesan Mountain; 3 Aug. 1993; D.-S. Ku leg.; ZISP 750.

Additional material. Japan – **Hokkaido Prefecture** • 1 female (paratype); Sapporo, Maruyama Mountain; 5 Sep. 1999; S.A. Belokobylskij leg.; ZISP A0045. – **Tochigi Prefecture** • 1 female (paratype); Nikko; 2–3 Oct. 1999; S.A. Belokobylskij leg.; ZISP A0046. – **Fukushima Prefecture** • 1 female (paratype); Hinoemata; 16–18 Aug. 1999; S.A. Belokobylskij leg.; ZISP A0047.

Distribution. Japan: Hokkaido, Honshu. South Korea (new record).

Description. Female. Fore wing length 2.7–3.7 mm. Width of head (dorsal view) 1.7–1.9× its median length. Transverse diameter of eye (dorsal view) 1.5–1.7× longer than temple. OOL 2.4–2.8× Od; POL 1.6–2.0× Od; OOL 1.4× POL. Longitudinal diameter of eye (lateral view) 1.4–1.6× its transverse diameter; hind margins of eye and temple subparallel. Face width 1.5–1.6× combined height of face and clypeus. Face width 1.9–2.4× larger than width of hypoclypeal depression. Longitudinal diameter of eye 2.9–3.5× longer than malar space (anterior view). Malar suture absent. Width of hypoclypeal depression 1.2–1.6× larger than distance from depression to eye. Antenna 0.84–0.90× as long as fore wing, with 25–27 antennomeres. First, middle and penultimate flagellomeres 1.9–2.3×, 1.5–2.2 × and 1.7–2.2× longer than wide, respectively. Mesosoma 1.4–1.6× longer than its maximum height. Mesoscutum setose on notaulic area, with sparse setae medio-longitudinally. Notauli very deep anteriorly, impressed and not united posteriorly. Mesepimeral and metapleural sulci smooth. Medio-longitudinal keel developed in apical third of propodeum, branching. Fore wing vein r arising from basal 0.40–0.45 of pterostigma; vein 1-R1 1.5× longer than pterostigma;

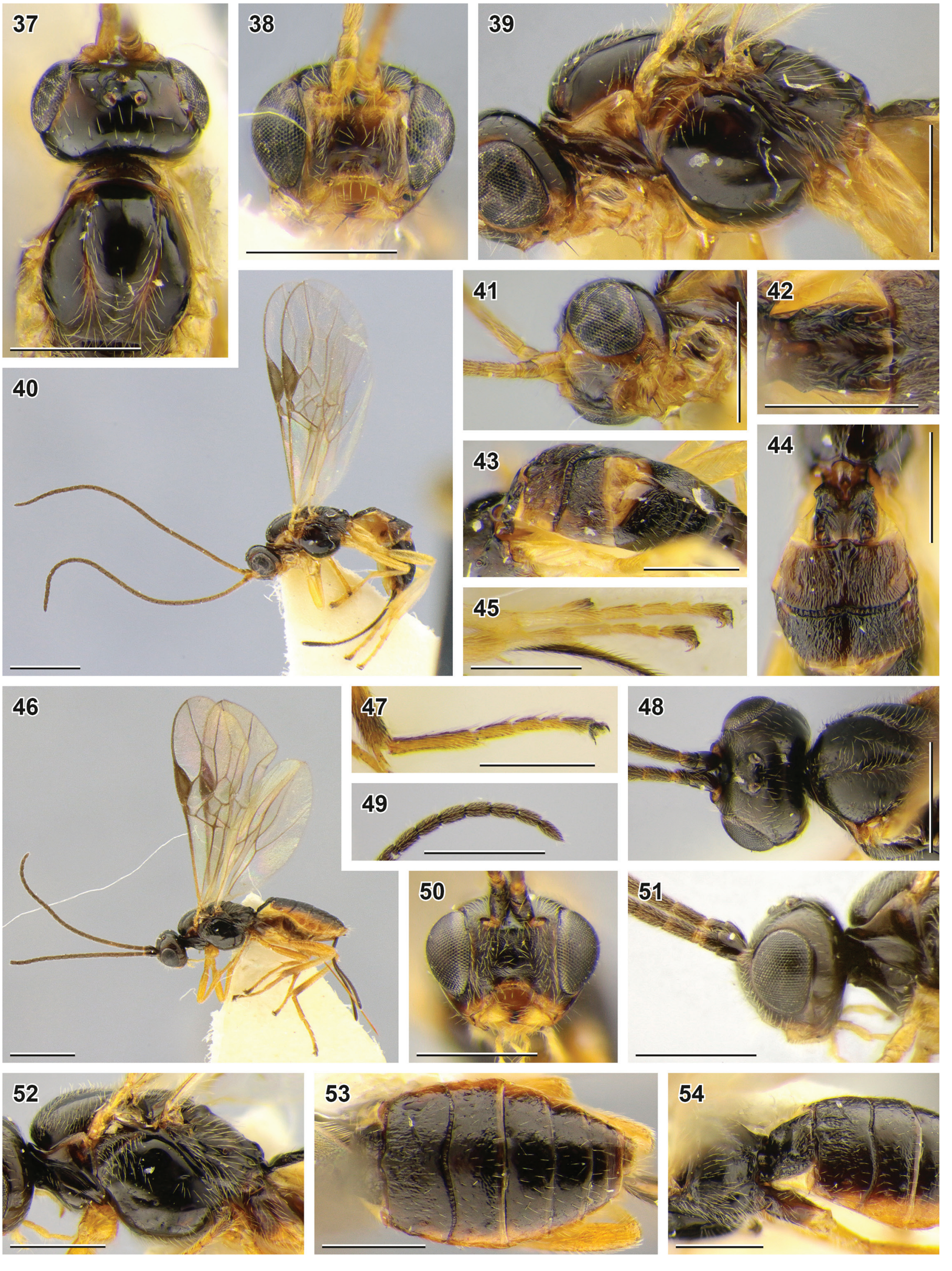

Figures 37–54. *Bracon* (*Bracon*) *semitergalis* Tobias, 2000 (**37–45** holotype, female, ZISP) and *B.* (*B.*) *sergeji* Tobias, 2000 (**46–54** paratype, female, ZISP) **37, 48** head and mesoscutum, dorsal view **38, 50** head, anterior view **39, 52** mesosoma, lateral view **40, 46** habitus, lateral view **41** head, ventrolateral view **42** first metasomal tergite, dorsal view **43** metasoma, dorsolateral view **44, 54** first–third metasomal tergites **45, 47** hind tarsus **49** apex of antenna **51** head, lateral view **53** metasoma, dorsal view. Scale bars: 0.5 mm (**37–40, 41–45, 47–54**); 1 mm (**40, 46**).

marginal cell 7–9× longer than distance from its apex to apex of wing; vein 3-SR 2.5–2.9× vein r, 0.55–0.70× vein SR1, 1.3–1.6× vein 2-SR. Hind femur 3.9–4.4× longer than wide. Hind tibia with 2 thick setae subapically. Fifth segment of hind tarsus 0.45–0.50× as long as hind basitarsus, 0.90–0.97× as long as second segment. Claws with acute angularly protruding basal lobe. First metasomal tergite with incomplete dorsal carina and developed dorsolateral carinae; its median length 0.80–0.93× its apical width. Second tergite without median area and with very shallow s-shaped weakly crenulate dorsolateral impressions not bordered by carinae; medially 1.0–1.2× longer than third tergite; its basal width 1.7–2.0× its median length. Second metasomal suture deep, curved and crenulate. Apical margins of third to sixth tergites thick, with weakly foveate transverse subapical grooves. Ovipositor sheath 1.3–1.4× longer than hind tibia, 0.37–0.41× as long as fore wing. Apex of ovipositor with weak nodus and distinct ventral serration. Body mainly smooth; frons, face, and malar space granulate; first tergite posteriorly rugose; second tergite laterally longitudinally rugulose, anteromedially rugose to rugulose; third tergite granulate-rugulose to weakly granulate; fourth–sixth tergites weakly granulate to smooth. Body mostly brownish black; legs and lateral sides of metasoma reddish brown; maxillary palps, basal half of hind tibia, and metasoma ventrally pale yellow; tegulae brownish yellow; wing membrane weakly darkened, pterostigma and veins brown.

Diagnosis. Relationships of *Bracon sergeji* are listed in the diagnosis of *B. tergalis* (see below).

Bracon (*Bracon*) *subcylindricus* Wesmael, 1838

Figs 55–57, A5

Material. South Korea (3 females, 7 males). – **Gangwon-do** • 1 female; Goseong-gun, [2] Ganseong-eup; 25 May 1993; D.-S. Ku leg.; NIBR 407 • 4 males; same data as for preceding; SMNE 408–411 • 1 female; Goseong-gun, [3] Geojin-eup, Naengcheon-ri, Geonbongsa Temple; 25 May 1993; D.-S. Ku leg.; ZISP 412 • 2 males; Chuncheon-si, [11] Dongsan-myeon, Joyang-ri, Joyang bridge; 24 May 1994; D.-S. Ku leg.; SMNE 414, 415 • 1 male; Pyeongchang-gun, [14] Jinbu-myeon, Dongsan-ri, Odaesan Mountain; 27 May 1993; D.-S. Ku leg.; SMNE 413. – **Chungcheongnam-do** • 1 female; Yesan-gun, [51] Deoksan-myeon, Sudeoksa Temple; 11 Aug. 1991; D.-S. Ku leg.; ZISP 406.

Additional material. Astrakhan Province • 2 females; Kamyzyaksky District, Astrakhan Nature Reserve, Damchiksky section; 19 Jul. 1974; V.V. Kostyukov leg.; Phragmites, Typha, Carex; ZISP A0057, A0058 • 1 female; same locality as for preceding; 21 Jul. 1974; V.V. Kostyukov leg.; Phragmites; ZISP A0059 • 1 female; Astrakhan, Gorodskoy Island; 26 Jun. 2004; S.A. Belokobylskij leg.; wet and dry meadows, forest; ZISP A0056.

Chechen Republic • 2 females (lectotype and paralectotype of *Bracon kiritshenkoi* Telenga, 1936); Kizlyar District, Starogladovskaya; 8 Jul. 1927; A.N. Kiritshenko leg.; ZISP.

Volgograd Province • 1 female; Pallasovskiy District, Lake Elton; 16 Jun. 2004; A.I. Khalaim leg.; Khara River, steppe; ZISP A0055.

Distribution. Caucasus. Europe: Eastern, Northern, Southern, and Western Europe. Iran. Kazakhstan. Russia: European part (Samartsev 2019); Ural. South Korea (new record). Turkey.

Description. Female. Fore wing length 3.0–4.8 mm. Width of head (dorsal view) 1.6–1.8× its median length. Transverse diameter of eye (dorsal view) 1.2–1.7× longer than temple. OOL 2.5–3.3× Od; POL 1.3–1.8× Od; OOL 1.8–2.1× POL. Longitudinal diameter of eye (lateral view) 1.4–1.6× its transverse diameter; hind margins of eye and temple subparallel to broadened downwards. Face width 1.6–1.7× combined height of face and clypeus. Longitudinal diameter of eye 2.4–2.9× longer than malar space (anterior view). Malar suture absent. Width of hypoclypeal depression 1.0–1.5× larger than distance from depression to eye. Antenna 1.1–1.2× longer than fore wing, with 33–43 antennomeres. First, middle and penultimate flagellomeres 1.7–2.1×, 1.3–1.7 ×, and 1.6–2.1× longer than wide, respectively. Mesosoma 1.7–1.9× longer than its maximum height. Mesoscutum setose only on notaulic area. Notauli deep anteriorly, shallow and united posteriorly. Mesepimeral and metapleural sulci (weakly) crenulate. Medio-longitudinal keel on propodeum complete, with transverse rugae. Fore wing 0.8–1.0× as long as body. Pterostigma 2.7–3.7× longer than wide; vein r arising from basal 0.45–0.55× of pterostigma; vein 1-R1 1.4–1.7× longer than pterostigma. Marginal cell 6–12× longer than distance from its apex to apex of wing; vein 3-SR 2.2–3.4× vein r, 0.60–0.85× vein SR1, 1.3–1.6× vein 2-SR. Hind femur 2.9–3.4× longer than wide. Hind tibia with subapical transverse row of thick setae. Fifth segment of hind tarsus 0.5–0.7× as long as hind basitarsus, 0.95–1.15× as long as second segment. Claws with small not protruding ventrally basal lobe. First metasomal tergite with complete or incomplete dorsal carina and developed dorsolateral carinae, its median length 0.7–0.8× its apical width. Metasoma 0.29–1.49× as long as mesosoma. Median length of first tergite. Second tergite without distinct median area and with shallow s-shaped weakly crenulate dorsolateral impressions not bordered by carinae; medially 0.9–1.1× as long as third tergite, its basal width 1.6–1.8× its median length. Second metasomal suture deep, curved and crenulate. Apical margins of third to sixth tergites more or less thick, without transverse subapical grooves. Ovipositor sheath 0.80–1.15× as long as hind tibia, 0.25–0.35× as long as fore wing. Apex of ovipositor with developed nodus and ventral serration. Body mainly smooth; face, frons, and malar space weakly granulate; propodeum posteriorly more or less rugose; first metasomal tergite posteriorly areolate-rugose; second tergite rugose to granulate-rugulose; third–sixth tergites with gradually weakening papillary-like sculpture. Coloration (Korean specimens): head, mesosoma and metasoma medio-longitudinally brownish black; tegula, legs, and lateral and ventral sides of metasoma reddish yellow; wing membrane more or less brownish darkened, pterostigma and wing veins brown.

Remarks. The key to related species and the taxonomic history of *B. subcylindricus* had been published earlier (Samartsev 2018, 2019).

***Bracon* (*Bracon*) *terebralis* Tobias, 2000**
Figs 59–67, A5

Bracon terebralis Tobias, 2000 in Belokobylskij and Tobias 2000: 138.
Bracon megaventris Li, He & Chen, 2020b: 227; syn. nov.

Material. South Korea (13 females, 1 male). – **Gangwon-do** • 1 female; Sokcho-si, [7] Seorak-dong; 11 Jun. 1992; D.-S. Ku leg.; SMNE 961. – **Gyeonggi-do** • 4 females; Gapyeong-gun, [31] Cheongpyeong-myeon, Cheongpyeong-ri, Cheongpyeong Amusement Park; 14 Jun. 1992; D.-S. Ku leg.; SMNE 193, 423–425 • 1 male; same data as for preceding; SMNE 426 • 1 female; Suwon-si, [37] Gwonseon-gu, Seodun-dong, Yeogisan Mountain; 11 May 1994; D.-S. Ku leg.; SMNE 427 • 1 female; same data as for preceding; 26 May 1994; SMNE 428 • 2 females; same data as for preceding; 8 Jun. 1994; ZISP 430, 431 • 1 female; same data as for preceding; NIBR 432 • 2 females; same data as for preceding; SMNE 865, 913. – **Gyeongsangbuk-do** • 1 female; Bonghwa-gun, [41] Mulya-myeon, Ojeon-ri, Seondalsan Mountain; 28 May 1998; Jeong-Gyu Kim leg.; SMNE 429.

Additional material. Russia – **Primorskiy Territory** • 1 female (holotype); Partizansky District, 10 km SE of Partizansk, Novitskoe; 20 Jul. 1984; S.A. Belokobylskij leg.; oak forest; ZISP.

Distribution. Russia: Far East: Primorskiy Territory. South Korea (new record).

Description. Female. Fore wing length 2.7–2.9 mm (Li et al. 2020b: 3.6 mm). Width of head (dorsal view) 1.7–1.8× its median length. Transverse diameter of eye (dorsal view) 1.8–2.1× longer than temple. OOL 2.2–2.8× Od; POL 1.3–1.6× Od; OOL 1.6–1.8× POL. Longitudinal diameter of eye (lateral view) 1.4–1.5× its transverse diameter; hind margins of eye and temple parallel to broadened downwards. Face width 1.5–1.6× combined height of face and clypeus. Longitudinal diameter of eye 2.4–3.2× longer than malar space (anterior view). Malar suture absent. Width of hypoclypeal depression 1.2–1.5× distance from depression to eye. Antenna 1.1–1.2× longer than fore wing, with 29–32 (Li et al. 2020b: 35) antennomeres. First, middle and penultimate flagellomeres 2.1–2.3×, 1.8–2.3× and 2.1–2.4× longer than wide, respectively. Mesosoma 1.8–2.0× longer than its maximum height. Mesoscutum setose on notaulic area and medioposteriorly. Notauli deep anteriorly, shallow and not united posteriorly. Mesepimeral and metapleural sulci smooth. Propodeum with short medio-longitudinal keel apically, branching. Fore wing vein r arising from basal 0.45–0.50 of pterostigma; vein 1-R1 1.4× longer than pterostigma; marginal cell 11–16× distance from its apex to apex of wing; vein 3-SR 2.7–3.5× vein r, 0.5–0.6× vein SR1, 1.2–1.5× vein 2-SR. Hind femur 2.7–3.1× longer than wide. Hind tibia without subapical row of thick setae. Fifth segment of hind tarsus 0.6–0.7× as long as hind basitarsus, 1.0–1.3× longer than second segment. Claws with large, more or less angularly protruding basal lobe. First metasomal tergite with incomplete dorsal carinae more or less strongly curved towards apex of tergite and with weakly separated dorsolateral carinae, its median length 0.95–1.10× as large as

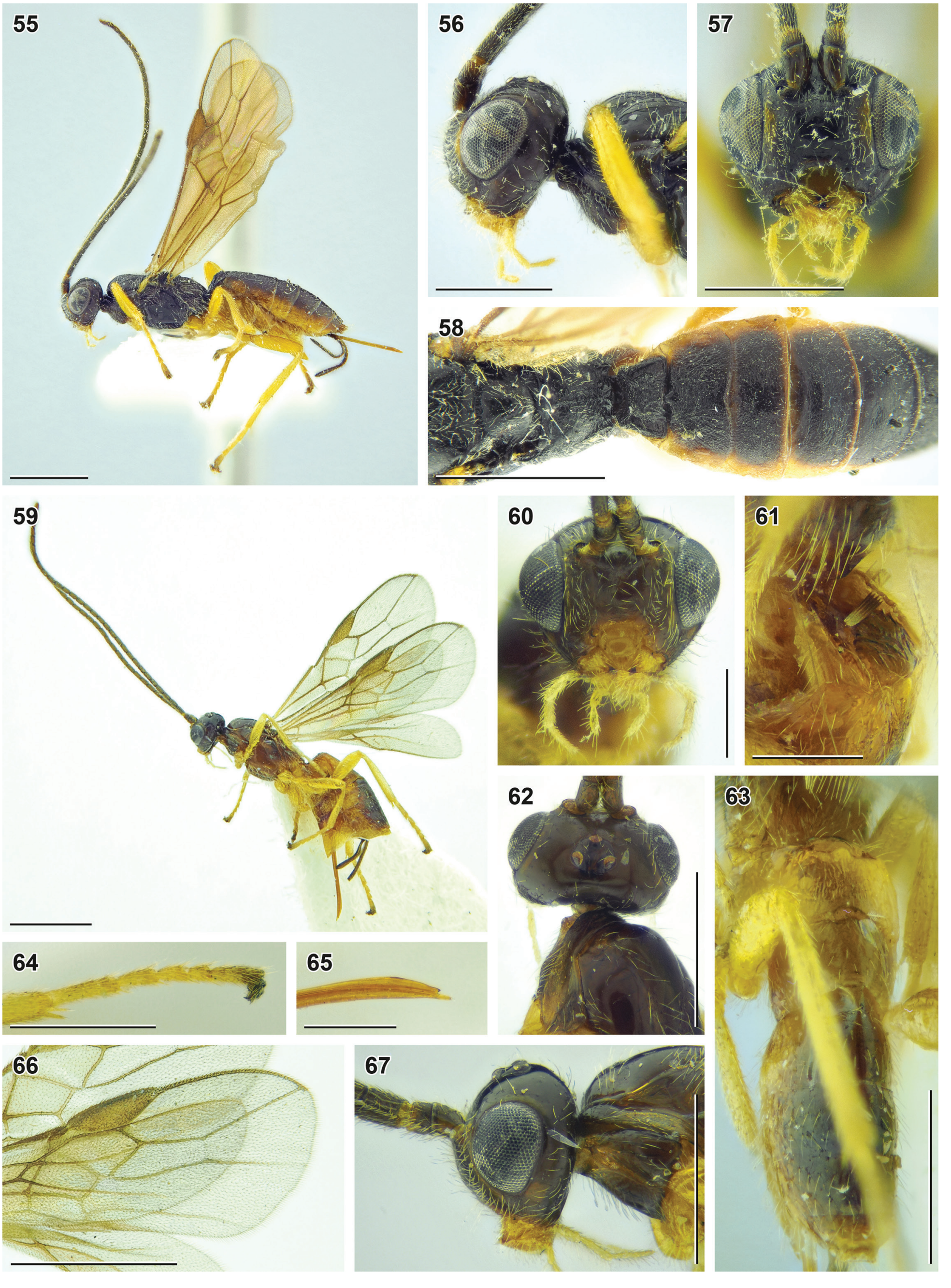

Figures 55–67. *Bracon* (*Bracon*) *subcylindricus* Wesmael, 1838 (**55–57** female, NIBR **58** female, ZISP) and *B.* (*B.*) *terebralis* Tobias, 2000 (**59–63** holotype, female, ZISP) **55, 59** habitus, lateral view **56, 67** head, lateral view **57, 60** head, anterior view **58, 63** metasoma and propodeum, dorsal view **61** first metasomal tergite, dorsolateral view **62** head, dorsal view **64** hind tarsus **65** apex of ovipositor **66** apex of fore wing. Scale bars: 0.25 mm (**60, 61, 65**); 0.5 mm (**56, 57, 62–64, 67**); 1 mm (**55, 59, 66**).

its apical width. Second tergite with very short triangle weakly elevated median area and without dorsolateral impressions; medially 0.86–0.97× as long as third tergite; its basal width 1.4–1.6× its median length. Apical margins of third–sixth tergites thin. Ovipositor sheath 0.75–0.90× as long as hind tibia, 0.20–0.25× as long as fore wing. Apex of ovipositor with weak nodus and weak ventral serration. Body mostly smooth; face and frons smooth; malar space granulate; propodeum rugulose near its posterior margin; first metasomal tergite laterally weakly rugulose, its median area obliquely rugulose posteriorly; second tergite rugulose to almost smooth; third tergite weakly granulate to smooth; posterior tergites smooth. Body mostly brownish black; legs and desclerotised parts of metasomal sterna yellow; maxillary palps pale yellow; tegulae yellow or brownish yellow; wing membrane weakly brownish darkened, pterostigma brown and wing veins brown.

Diagnosis. *Bracon terebralis* differs from other species of the section *Orthobracon* Fahringer sec. Tobias (1986) by a combination of the short ovipositor, strongly smoothed sculpture on head (Fig. 60), propodeum, and metasoma (Fig. 63), and by the long antenna with ca. 30–35 segments (Fig. 59).

***Bracon* (*Bracon*) *tergalis* Tobias, 2000**

Figs 68–76, A6

Material. South Korea (20 females, 4 males). – **Gangwon-do** • 1 female; Goseong-gun, [3] Geojin-eup, Naengcheon-ri, Geonbongsa Temple; 22 May 1992; D.-S. Ku leg.; SMNE 1537 • 1 female; Goseong-gun, [5] Toseong-myeon, Sinpyeong-ri, Seoraksan Mountain; 2 Aug. – 19 Oct. 2002; D.-S. Ku leg.; Malaise trap; SMNE 778 • 1 female; Yeongwol-gun, [18] Hanbando-myeon, Ssangyong-ri; 24 May 1993; D.-S. Ku leg.; SMNE 752 • 1 female; Taebaek-si, [22] Cheoram-dong, Taebaeksan Mountain; 23 Jun. 1989; D.-S. Ku leg.; SMNE 753 • 1 female; same data as for preceding; 20 Jun. 1991; SMNE 771. – **Gyeonggi-do** • 1 female; Pocheon-si, [24] Idong-myeon, Dopyeong-ri, Valley Baekun; 13 Jun. 1996; H.J. Cheon leg.; SMNE 757 • 1 female; Yangju-si, [29] Nam-myeon; 12 Jun. 1996; H.J. Cheon leg.; SMNE 776 • 1 male; Gapyeong-gun, [30] Buk-myeon, Dodae-ri, Myeongjisan Mountain; 14 Jun. 1992; D.-S. Ku leg.; SMNE 783 • 1 male; same data as for preceding; ZISP 784 • 1 female; Gapyeong-gun, [31] Cheongpyeong-myeon, Cheongpyeong-ri, Cheongpyeong Amusement Park; 14 Jun. 1992; D.-S. Ku leg.; SMNE 781 • 1 female; same data as for preceding; ZISP 782 • 1 male; Suwon-si, [37] Gwonseon-gu, Seodun-dong, Yeogisan Mountain; 8 Jun. 1994; D.-S. Ku leg.; SMNE 1057 • 1 female; Suwon-si, [38] Gwonseon-gu, Seodun-dong; 27–29 Apr. 1994; D.-S. Ku leg.; Malaise trap; ZISP 1153 • 1 female; same data as for preceding; 25 Apr. 1994; SMNE 770 • 1 female; Hwaseong-si, [39] Bibong-myeon; 1 Jun. 1994; D.-S. Ku leg.; SMNE 751. – **Gyeongsangbuk-do** • 1 male; Bonghwa-gun, [40] Seokpo-myeon, Seokpo-ri; 28 May 1993; D.-S. Ku leg.; SMNE 779. – **Chungcheongnam-do** • 1 female; Yesan-gun, [51] Deoksan-myeon, Sudeoksa Temple; 11 Aug. 1991; D.-S. Ku leg.; NIBR 1009 • 1 female; Geumsan-gun, [54] Nami-myeon, Boseok Temple; 5–9 Jun. 1998; Pierre Tripotin leg.; Malaise trap; SMNE 780. – **Chungcheongbuk-**

do • 1 female; Jecheon-si, [55] Geumseong-myeon, Seongnae-ri; 10 Jun. 1992; D.-S. Ku leg.; SMNE 777. – **Gyeongsangnam-do** • 1 female; Goseong-gun, [64] Sangni-myeon, Bupo-ri; 3 May 1993; D.-S. Ku leg.; SMNE 1105 • 1 female; Jinju-si, [72] Gajwa-dong; 25 Oct. 1993; D.-S. Ku leg.; SMNE 773 • 1 female; same data as for preceding; 6 Jun. 1993; SMNE 774 • 1 female; Jinju-si, [74] Naedong-myeon, Naepyeong-ri; 30–31 May 1993; D.-S. Ku leg.; SMNE 772. – **Jeollanam-do** • 1 female; Gurye-gun, [82] Toji-myeon, Oegok-ri, Jirisan Mountain (Piagol); 24 Jan. 1995; S.H. Lee leg.; SMNE 775.

Additional material. Russia – **Primorskiy Territory** • 1 female (holotype); Khasansky District, env. Khasan; 25 May 1979; S.Yu. Storozhenko, V.S. Sidorenko leg.; oak forest; ZISP • 1 female; Lazovsky District, 18 km SE of Lazo, State Reserve of Laso, cordon America; 24–29 Aug. 2006; S.A. Belokobylskij leg.; forest edges, clearings; ZISP A0050 • 1 female; Shkotovsky District, Ussurisky Nature Reserve; 25 Aug. 2001; S.Yu. Storozhenko and V.S. Sidorenko leg.; ZISP A0042.

Distribution. Russia: Far East: Primorskiy Territory; South Korea (new record).

Description. Female. Fore wing length 3.2–4.0 mm. Width of head (dorsal view) 1.7–1.9× its median length. Transverse diameter of eye (dorsal view) 1.7–2.2× longer than temple. OOL 2.1–2.7× Od; POL 0.93–1.83× Od; OOL 1.5–2.3× POL. Longitudinal diameter of eye (lateral view) 1.3–1.5× its transverse diameter; hind margins of eye and temple subparallel. Face width 1.4–1.6× combined height of face and clypeus. Longitudinal diameter of eye 3.1–3.3× longer than malar space (anterior view). Malar suture absent. Width of hypoclypeal depression 1.5–1.6× larger than distance from depression to eye. Antenna 0.75–1.10× as long as fore wing, with 27–34 antennomeres. First, middle and penultimate flagellomeres 1.8–2.5×, 1.4–2.2×, and 1.8–2.2× longer than wide, respectively. Mesosoma 1.5–1.6× longer than its maximum height. Mesoscutum widely setose on notaulic area and posteriorly, often with sparse setae medio-longitudinally. Notauli deep anteriorly, shallow and united posteriorly. Mesepimeral sulcus smooth, metapleural sulcus crenulate. Medio-longitudinal keel more or less developed in apical third of propodeum, branching. Fore wing vein r arising from basal 0.40–0.48 of pterostigma; vein 1-R1 1.5–1.8× as long as pterostigma; marginal cell 8.5–13.5× longer than distance from its apex to apex of wing; vein 3-SR 2.3–2.9× vein r, 0.52–0.64× as long as vein SR1, 1.3–1.5× vein 2-SR. Hind femur 3.4–4.3× longer than wide. Hind tibia without subapical row of thick setae. Fifth segment of hind tarsus 0.4–0.5× as long as hind basitarsus and 0.85–1.00× as long as its second segment. Claws with shortly protruding and blunt basal lobes. First metasomal tergite with incomplete or complete dorsal carina and developed dorsolateral carinae, its median length 0.83–0.96× its apical width. Second tergite with weak, narrow, longitudinal median area and with more or less deep s-shaped crenulate dorsolateral impressions not bordered by carinae; medially 1.0–1.3× longer than third tergite; its basal width 1.6–1.8× its median length. Second metasomal suture deep, curved and crenulate. Apical margins of third–sixth tergites more or less thick. Ovipositor sheath 1.3–1.7× as long as hind tibia and 0.37–0.49× as long as fore wing. Apex of ovipositor with weak nodus and weak ventral serration. Body mainly smooth; face and frons weakly granulate, malar space granulate; mesopleuron smooth or partially with weak coriaceous sculpture; propodeum posteriorly almost smooth or weakly granulate; first metasomal tergite laterally weakly rugulose, posteriorly rugose; second tergite striate-rugulose or rugose to rugulose; posterior tergites with weakening papillary-like sculpture. Head, mesosoma and metasoma dorsally brownish black; head ventrally, pronotum, and mesoscutum along notauli, lateral margins of metasoma rusty brown or reddish yellow; tegula and legs brownish yellow; maxillary palps pale yellow; wing membrane weakly darkened, pterostigma brown, wing veins yellowish brown to brown.

Diagnosis. *Bracon tergalis* may be compared with *B. sergeji* and *B. semitergalis*. The differences between three species are presented in the key below.

1 Face almost smooth, weakly granulate laterally and under toruli (Figs 38, 41). Median area of second metasomal tergite distinct, triangle and elongate (Fig. 44). Scape brownish yellow (Fig. 38). Median length of first tergite 0.95–1.20× its apical width (Fig. 42). Basal width of second metasomal tergite 1.3–1.6× its median length (Fig. 44) .... ***Bracon* (*Bracon*) *semitergalis* Tobias**

– Face mostly granulate (Figs 50, 69, 75). Median area of second metasomal tergite weakly defined, longitudinal (Fig. 73) or triangle, but short (Fig. 54). Scape dark-coloured (Figs 51, 69). Median length of first tergite 0.80–0.95× its apical width (Figs 54, 76). Basal width of second metasomal tergite 1.6–2.0× its median length (Figs 53, 73) **2**

2 Second metasomal tergite with weaker sculpture, rugose to rugulose (Figs 53, 54). Apical margins of third to sixth tergites with shallow weakly crenulate transverse subapical grooves. Transverse pronotal and metapleural sulci smooth (Fig. 52) .... ***Bracon* (*B.*) *sergeji* Tobias**

– Second metasomal tergite with coarser sculpture, distinctly longitudinally striate-rugose (Fig. 73). Apical margins of third to sixth tergites without subapical grooves. Transverse pronotal and metapleural sulci crenulate .... ***Bracon* (*B.*) *tergalis* Tobias**

Remarks. The differences between *B. tergalis* and *B. sergeji* are very weak, but persistent in the series of specimens of similar size. Because it is possible to separate two species using these characters, we treat them as valid species.

***Bracon* (*Bracon*) *virgatus* Marshall, 1897**

Figs 77–83, A7

Material. South Korea (9 females). – **Gyeonggi-do** • 1 female; Suwon-si, [37] Gwonseon-gu, Seodun-dong, Yeogisan Mountain; 29 May – 6 Jul. 1994; D.-S. Ku leg.; Malaise trap; NIBR 942 • 1 female; same data as for preceding; 23–29 Jun. 1994; ZISP 939 • 1 female; same locality as in preceding; 10 Jul. 1995; June-Yeol Choi leg.; Malaise trap; SMNE 935 • 1 female; same data as for preceding; 7 Aug. 1995; SMNE

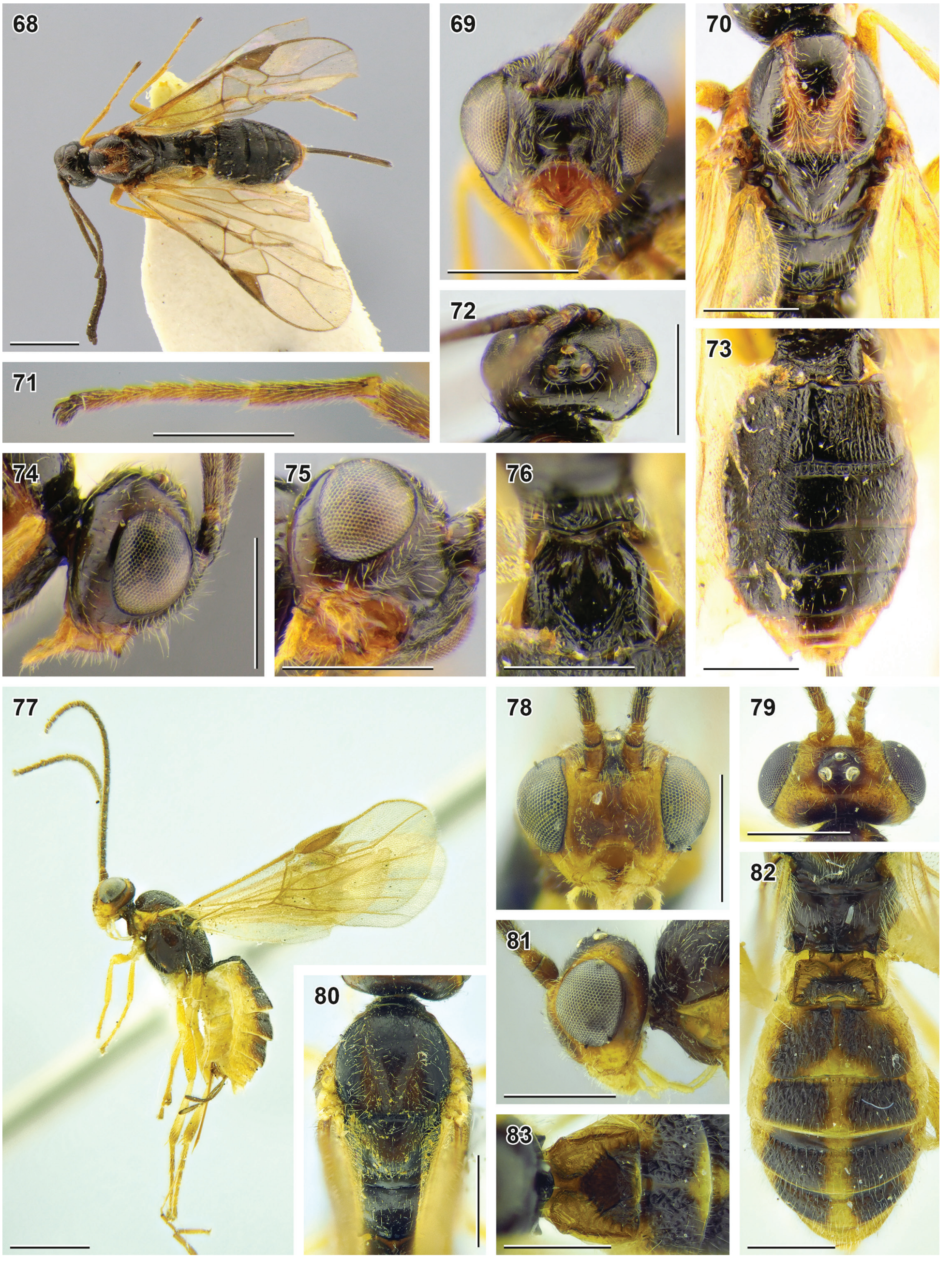

Figures 68–83. *Bracon* (*Bracon*) *tergalis* Tobias, 2000 (**68–76** holotype, female, ZISP) and *B.* (*B.*) *virgatus* Marshall, 1897 (**77, 78, 80, 81** female, SMNE **79, 82, 83** female, ZISP) **68** habitus, dorsal view **69, 78** head, anterior view **70, 80** mesosoma, dorsal view **71** hind tarsus habitus, lateral view **72, 79** head, dorsal view **73, 82** metasoma, dorsal view **74, 83** head, lateral view **75** head, ventrolateral view **76, 83** first metasomal tergite, dorsal view. Scale bars: 0.5 mm (**69–73, 78–83**); 1 mm (**68, 77**).

940 • 1 female; same data as for preceding; 3 Jun. 1996; SMNE 932 • 1 female; same data as for preceding; 30 Jun. 1997; SMNE 933 • 1 female; same locality as in preceding; 5 Aug. 1997; June-Yeol Choi leg.; SMNE 934 • 1 female; same data as for preceding; 25 Aug. 1997; June-Yeol Choi leg.; Malaise trap; ZISP 936. – **Gyeongsangbuk-do** • 1 female; Bonghwa-gun, [43] Myeongho-myeon; 28 May 1993; D.-S. Ku leg.; SMNE 941.

Additional material. Netherlands • 1 female (holotype of *Bracon lineifer* van Achterberg, 1988); Waarder, Oosteinde, 33; 5–7 Aug. 1973; C. van Achterberg leg.; RMNH.

Distribution. Europe: Eastern Europe: Hungary; Western Europe: Great Britain, the Netherlands, Switzerland. South Korea (new record).

Description. Female. Fore wing length 2.9–3.3 mm. Width of head (dorsal view) 2.0–2.1× its median length. Transverse diameter of eye (dorsal view) 2.3–2.5× longer than temple. OOL 1.9–2.0× Od; POL 0.95–1.10× Od; OOL 1.8–2.0× POL. Longitudinal diameter of eye (lateral view) 1.3× larger than its transverse diameter; hind margins of eye and temple subparallel. Face width 1.4–1.5× combined height of face and clypeus. Face width 2.3× larger than width of hypoclypeal depression. Longitudinal diameter of eye 3.1–3.2× longer than malar space (anterior view). Malar suture deep under eye, weak near mandible, smooth. Width of hypoclypeal depression 1.1–1.2× larger than distance from depression to eye. Antenna about 0.9× as long as fore wing, with 26–30 antennomeres. First, middle and penultimate flagellomeres 1.7–1.8×, 1.5–1.9×, and about 2.0× longer than wide, respectively. Mesosoma 1.4–1.5× longer than its maximum height. Mesoscutum evenly, but sparsely setose. Notauli very deep anteriorly, impressed and not united posteriorly. Mesepimeral and metapleural sulci smooth. Medio-longitudinal keel developed in apical half of propodeum, branching. Fore wing vein r arising from basal 0.45–0.50 of pterostigma; vein 1-R1 1.5–1.6× longer than pterostigma; marginal cell 10–11× longer than distance from its apex to apex of wing; vein 3-SR 2.0–2.4× vein r, about 0.55× vein SR1, 1.3–1.5× vein 2-SR. Hind femur 3.5–4.1× longer than wide. Hind tibia with without subapical row of thick setae. Fifth segment of hind tarsus 0.5–0.6× as long as hind basitarsus, 0.9–1.0× as long as second segment. Claws with long triangularly protruding acute basal lobe. First metasomal tergite with complete dorsal carina and developed dorsolateral carinae, its median length 0.76–0.82× its apical width. Second metasomal tergite with weak, narrow, longitudinal median area and with deep s-shaped crenulate dorsolateral impressions bordered by long carinae; medially 1.2× longer than third tergite; its basal width 1.6× its median length. Apical margins of third to sixth tergites thick, without transverse subapical grooves. Ovipositor sheath 0.96–0.98× as long as hind tibia, 0.25–0.27× as long as fore wing. Apex of ovipositor with developed nodus and weak ventral serration. Head and mesosoma almost entirely smooth (only face and frons with vague granulate sculpture); apical two thirds of propodeum with tree-like rugosity; first metasomal tergite rugose posteriorly and laterally; second tergite areolate-rugose, third tergite areolate-rugose to foveate, fourth–fifth tergites irregularly foveate, sixth tergite smooth. Head and mesosoma dark brown with yellowish brown (or rusty) pattern, metasoma dorsally dark brown with yellow medio-longitudinal stripe and lateral and ventral sides; scape and tegula rusty; palps and legs yellow; wing membrane weakly darkened, pterostigma and wing veins brown.

Diagnosis. *Bracon virgatus* Marshall is similar to *B. imbricatellus* Tobias; their differences are listed below. Both species may be also compared with the *B. sculptithorax* species group (see Samartsev and Ku 2020: 18), but differ by the absence of granulate sculpture on gena, vertex, mesopleuron, and mesoscutum.

1 Transverse diameter of eye in dorsal view 1.6–2.0× temple (Fig. 27), in lateral view, 1.5–2.1× minimum width of temple (Fig. 24). Mesosoma 1.7–1.8× longer than its maximum height. Hind femur 3.0–3.4× longer than wide. Anterolateral areas of second metasomal tergite weakly separated by having smoothed sculpture (Figs 25, 26, 28). Apical margins of third to sixth metasomal tergites with weakly foveate transverse subapical grooves (Fig. 26). Spiracle of second metasomal tergite located in middle of tergite (Fig. 28). Propodeal spiracle located in middle of propodeum (lateral view) .... ***Bracon* (*Bracon*) *imbricatellus* Tobias**

– Transverse diameter of eye in dorsal view 2.3–2.5× temple (Fig. 79), in lateral view, 2.7–3.4× minimum width of temple (Fig. 81). Mesosoma 1.4–1.5× longer than its maximum height (Fig. 77). Hind femur 3.5–4.1× longer than wide. Anterolateral areas of second metasomal tergite not separated (Figs 82, 83). Apical margins of third to sixth metasomal tergites without transverse subapical grooves. Spiracle of second metasomal tergite located in anterior part of tergite (Fig. 82). Propodeal spiracle located behind middle of propodeum (lateral view) ....***Bracon* (*B.*) *virgatus* Marshall**

Remarks. The type of *B. virgatus* was not examined for the current study. Our taxon concept of the species is based on the examination of the type of *B. lineifer* van Achterberg, 1988, which was synonymised with *B. virgatus* by Papp (1999), however, without due justification. The specimens from South Korea differ from the type of *B. lineifer* by weakly sculptured, almost smooth face and frons (Fig. 78).

***Bracon* (*Bracon*) *yasudai* Maeto & Uesato, 2007**

Fig. A7

Material. South Korea – **Gangwon-do** • 1 female; Yeongwol-gun, [19] Kimsatgat-myeon, Nae-ri, Daeyachi Town; 28 May 1998; Jeong-Gyu Kim leg.; NIBR 677.

Distribution. Japan: Ryukyu. South Korea (new record).

Remarks. The detailed description of the species (Maeto and Uesato 2007: 56) provides all necessary characters for its identification.

***Bracon* (*Habrobracon*) *nigricans* (Szépligeti, 1901)**
Fig. A7

Material. South Korea (2 females, 1 male). – **Gyeonggi-do** • 1 female; Suwon-si, [38] Gwonseon-gu, Seodun-dong; 12 May 1983; Y.I. Lee leg.; NIBR 568. – **Gyeongsangbuk-do** • 1 female; Gyeongju-si, [48] Hyeongok-myeon, Geumjang-ri, Bridge Geumjang; 20 Jun. 1992; D.-S. Ku leg.; ZISP 567. – **Chungcheongnam-do** • 1 male; Geumsan-gun, [53] Chubu-myeon, Seongdang-ri, Gaedeoksa Temple; 22 May 1993; D.-S. Ku leg.; SMNE 569.

Additional material. China – **Qinghai** • 2 females (lectotype and paralectotype of *Habrobracon mongolicus* Telenga, 1936); Eastern Tsaidam, Keluke Lake, Bayingoule River; 21 May 1895; V.I. Roborovsky and P.K. Kozlov leg.; ZISP • 2 females (paralectotypes of *H. mongolicus* Telenga); same data as for preceding; 28 May 1895; ZISP.

Hungary • 1 male (lectotype of *Habrobracon nigricans* Szépligeti, 1901); Budapest; 5 Jul. 1899; HNHM Hym.Typ.No.995.

Distribution. Caucasus. Central Asia. China: Fujian, Ningxia Hui, Qinghai (Samartsev 2019), Shaanxi, Xinjiang. Europe: Eastern, Northern, Southern, and Western Europe. Iran. Kazakhstan. Mongolia. North Africa: Tunisia. Russia: Eastern Siberia: Tyva Republic (Samartsev 2019); European part; Far East: Chukotka Autonomous Area (Samartsev 2019), Khabarovsk Territory, Primorskiy Territory, Sakhalin Island; Ural (Kostromina 2010). South Korea (new record). Turkey.

Description. Female. Fore wing length 2.5–2.6 mm. Width of head (dorsal view) 1.8–1.9× its median length. Transverse diameter of eye (dorsal view) 1.5–2.0× longer than temple. OOL 3.0–3.6× Od; POL 1.9–2.1× Od; OOL 1.6–1.7× POL. Longitudinal diameter of eye (lateral view) 1.6× larger than its transverse diameter; hind margins of eye and temple broadened downwards. Face width ca. 1.7× combined height of face and clypeus. Longitudinal diameter of eye 2.4–2.7× longer than malar space (anterior view). Malar suture absent. Width of hypoclypeal depression about 1.4× distance from depression to eye. Antenna 0.70–0.85× as long as fore wing, with 21–23 antennomeres. First, middle and penultimate flagellomeres 1.8–2.0×, 1.6–1.8×, and 1.5× longer than wide, respectively. Mesosoma 1.4–1.5× longer than its maximum height. Mesoscutum evenly setose. Notauli not impressed. Fore wing vein r arising from basal 0.47–0.50× of pterostigma; vein 1-R1 1.3× longer than pterostigma; marginal cell 1.5–2.1× longer than distance from its apex to apex of wing; vein 3-SR 0.75–0.90× vein r, 0.25–0.30× vein SR1, 0.73–0.88× vein 2-SR. Hind femur 3.8–3.9× longer than wide. Fifth segment of hind tarsus 0.5× as long as hind basitarsus, about 0.75× as long as second segment. Claws with small rectangular basal lobe. First metasomal tergite without dorsal and dorsolateral carinae, its median length 0.9× its apical width. Second metasomal tergite without median area and dorsolateral impressions; medially 1.1× longer than third tergite; its basal width about 1.8× its median length. Ovipositor sheath about 0.9× as long as hind tibia, about 0.3× as long as fore wing. Apex of ovipositor with developed nodus and ventral serration. Body mostly granulate, second metasomal tergite medially rugulose-punctate. Body mainly brownish black with reddish yellow to yellowish brown maxillary palp, tegula, pattern on legs, patches along eye and on latero-posterior corners of second metasomal tergite; wing membrane weakly darkened, pterostigma and veins yellowish brown.

Diagnosis. The diagnosis of the species and its taxonomic literature were presented by Samartsev (2019: 62).

Bracon (*Habrobracon*) *stabilis* Wesmael, 1838

Figs 84–86, A7

Material. South Korea (1 female, 2 males). – **Gyeonggi-do** • 1 male; Suwon-si, [38] Gwonseon-gu, Seodun-dong; 15 Jun. 1994; D.-S. Ku leg.; SMNE 565. – **Gyeongsangbuk-do** • 1 female; Bonghwa-gun, [42] Beopjeon-myeon, Eoji-ri, Norujae mountain pass; 28 May 1993; D.-S. Ku leg.; ZISP 564. – **Chungcheongbuk-do** • 1 male; Goesan-gun, [60] Cheongcheon-myeon, Sagimak-ri, Mindung Mountain; 23 May 1993; D.-S. Ku leg.; NIBR 566.

Additional material. Belgium • female (lectotype); Brussels; IRSNB • 7 females (paralectotypes); Brussels; IRSNB • 2 males (paralectotypes); Brussels; IRSNB.

Russia – **Samara Province** • 1 female; Bogatovsky District, 6 km NE of Belovka, near Kutuluk storage pond; 31 Jul. 2010; K. Samartsev leg.; steppe, meadow herbs in ravine; ZISP A0120.

Distribution. Caucasus. China: Fujian, Xinjiang. Cyprus. Europe: Eastern, Northern, Southern and Western Europe. Iran. Israel. Kazakhstan. North Africa: Tunisia. North America. Russia: Eastern Siberia: Buryatia Republic, Irkutsk Province, Zabaikalskiy Territory; European part; Far East: Primorskiy Territory, Sakhalin Island; Western Siberia: Kemerovo Province (Tobias 1971). South Korea (new record). Turkey.

Description. Female. Fore wing length 3.1–3.7 mm. Width of head (dorsal view) 1.9–2.0× its median length. Transverse diameter of eye (dorsal view) 1.6–1.8× longer than temple. OOL 2.0–2.9× Od; POL 1.3–2.0× Od; OOL 1.4–1.6× POL. Longitudinal diameter of eye (lateral view) 1.5× larger than its transverse diameter; hind margins of eye and temple subparallel. Face width 1.6–1.7× combined height of face and clypeus. Longitudinal diameter of eye 2.3–2.6× longer than malar space (anterior view). Malar suture absent. Width of hypoclypeal depression 1.0–1.2× distance from depression to eye. Antenna 0.55–0.75× as long as fore wing, with ca. 24 antennomeres. First, middle and penultimate flagellomeres 1.6–2.3×, 1.6–1.9×, and 1.6–1.9× longer than wide, respectively. Mesosoma about 1.4× longer than its maximum height. Mesoscutum evenly, but sparsely setose. Notauli weakly impressed and not united posteriorly. Medio-longitudinal keel developed in apical third of propodeum, simple. Fore wing vein r arising from basal 0.45–0.48× of pterostigma. Vein 1-R1 1.3–1.4× longer than pterostigma. Marginal cell 2.5–4.5× longer than distance from its apex to apex of wing. Vein 3-SR 1.3–1.7× vein r, about 0.35× vein SR1, 0.90–0.95× vein 2-SR. Hind femur 4.2–4.3× longer than wide. Fifth segment of hind tarsus 0.45–0.48× as long as hind basitarsus and about 0.8× as long as second segment. Claws protruding triangular basal lobes. First metasomal tergite without dorsal and dorsolateral carinae, its median length 0.7–0.9× its apical width. Second metasomal tergite without median area and dorsolateral impressions; medially 1.0–1.2× longer than third tergite; its basal width about 1.9–2.0× its median length. Second metasomal suture deep, curved and crenulate. Apex of ovipositor with weak nodus and weak ventral serration. Body mostly granulate; submedian longitudinal stripes on mesoscutum smooth; second tergite anteromedially granulate-rugulose. Body mainly brownish black with reddish yellow pattern on head, mesoscutum and legs; maxillary palp brown; wing membrane brownish darkened, pterostigma brown with yellowish patch basally, wing veins brown.

Diagnosis. *Bracon stabilis* may be identified using the key provided in Loni et al. (2016: 138).

Bracon (*Orientobracon*) *maculaverticalis* Li, He & Chen, 2016

Fig. A8

Material. South Korea (2 males). – **Gangwon-do** • 1 male; Goseong-gun, [4] Ganseong-eup, Jinbu-ri; 12 Jun. 1992; D.-S. Ku leg.; NIBR 16. – **Gyeongsangbuk-do** • 1 male; Gyeongsan-si, [49] Yeongnam University, Department of Biology; 20–26 Jun. 1989; J.S. Park leg.; SMNE 17.

Distribution. China (Li et al. 2016): Guizhou, Zhejiang. South Korea (new record).

Remarks. The detailed description and diagnosis of the species are provided in Li et al. (2016: 463).

Bracon (*Osculobracon*) *cingillus* Tobias, 2000

Figs 87–92, A8

Material. South Korea (3 females). – **Gangwon-do** • 1 female; Hongcheon-gun, [13] Naechon-myeon, Waya-ri, Baegamsan Mountain; 1 Sep. – 18 Oct. 2002; D.-S. Ku leg.; Malaise trap; SMNE 303. – **Chungcheongnam-do** • 1 female; Gongju-si, [52] Banpo-myeon, Hakbong-ri; 15 Jun. 1992; D.-S. Ku leg.; NIBR 310. – **Gyeongsangnam-do** • 1 female; Uiryeong-gun, [67] Garye-myeon, Gapeul-ri, Jagulsan Mountain; 12 Jun. 1990; D.-S. Ku leg.; ZISP 309.

Additional material. Japan – **Tochigi Prefecture** • 1 female (paratype); Nikko; 2–3 Oct. 1999; S.A. Belokobylskij leg.; ZISP.

Russia – **Primorskiy Territory** • 1 female (holotype); Chernigovsky District, 10 km SE of Chernigovka; 28 Aug. 1996; S.A. Belokobylskij leg.; forest; ZISP.

Distribution. Japan: Hokkaido, Honshu. Russia: Far East: Primorskiy Territory. South Korea (new record).

Descrition. Female. Fore wing length 2.5–3.4 mm. Width of head (dorsal view) 1.8–2.0× its median length. Transverse diameter of eye (dorsal view) 1.7–2.1× longer

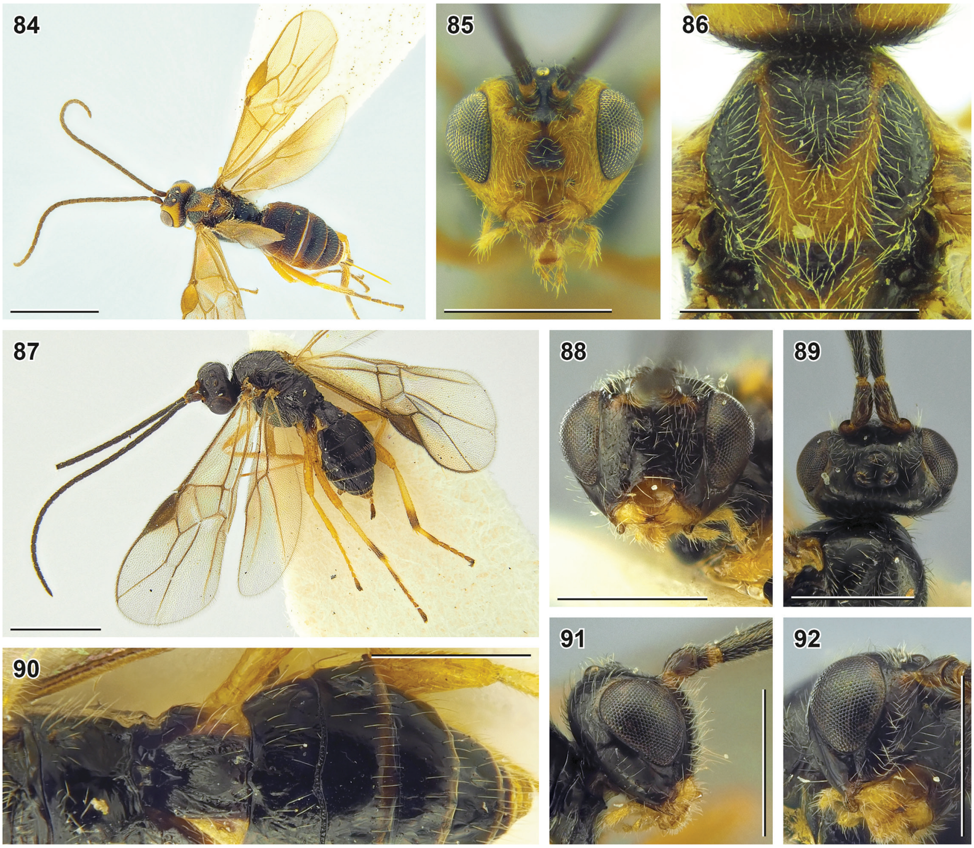

Figures 84–92. *Bracon* (*Habrobracon*) *stabilis* Wesmael, 1838 (**84–86** female, ZISP) and *B.* (*Osculobracon*) *cingillus* Tobias, 2000 (**87–92** holotype, female, ZISP) **84, 87** habitus, dorsal view **95, 88** head, anterior view **86** mesoscutum, dorsal view **89** head, dorsal view **90** metasoma and propodeum, dorsal view **91** head, lateral view **92** head, ventrolateral view. Scale bars: 0.5 mm (**85, 86, 88–92**); 1 mm (**84, 87**).

than temple. OOL 2.3–2.4× Od; POL 1.2–1.4× Od; OOL 1.7–1.9× POL. Longitudinal diameter of eye (lateral view) 1.4–1.5× its transverse diameter; hind margins of eye and temple broadened downwards or subparallel. Face width about 1.4× combined height of face and clypeus. Longitudinal diameter of eye 2.6–3.0× longer than malar space (anterior view). Malar suture deep, smooth. Width of hypoclypeal depression 1.1–1.2× distance from depression to eye. Antenna 1.1–1.2× longer than fore wing, with 29–34 antennomeres. First, middle and penultimate flagellomeres 2.2–2.3×, 2.0–2.1×, and 2.0–2.2× longer than wide, respectively. Mesosoma 1.5–1.6× longer than its maximum height. Mesoscutum setose only on notaulic area. Notauli impressed anteriorly, shallow posteriorly. Mesepimeral and metapleural sulci smooth. Propodeum without medio-longitudinal keel. Fore wing vein r arising from basal 0.4× of pterostigma; vein 1-R1 about 1.3× longer than pterostigma; marginal cell about 5.2× longer than distance from its apex to apex of wing; vein 3-SR 2.3–2.5× vein r, about 0.6×

vein SR1, 1.6–1.7× vein 2-SR. Hind femur 3.8–4.3× longer than wide. Hind tibia with 1–2 thick setae subapically. Fifth segment of hind tarsus 0.35–0.40× as long as hind basitarsus, 0.60–0.65× as long as second segment. Claws with large, protruding and blunt basal lobes. First metasomal tergite without dorsal and dorsolateral carinae, its median length 1.1–1.3× its apical width. Second tergite with weak triangle median area and with very shallow s-shaped smooth dorsolateral impressions not bordered by carinae; medially 0.93–0.97× as long as third tergite; its basal width 1.7–1.8× its median length. Second metasomal suture deep, curved and smooth or weakly crenulate. Anterolateral margin of second metasomal tergite at most shortly desclerotised, apical margins of third to sixth tergites widely desclerotised. Ovipositor sheath about 0.65× as long as hind tibia, about 0.2× as long as fore wing. Apex of ovipositor with weak nodus and ventral serration. Head and mesosoma entirely smooth; first tergite weakly rugulose laterally and posteriorly, second and sometimes also third tergite weakly rugulose, but smooth on sides, fourth–fifth tergites hardly granulate to smooth. Body black or brown, legs and palps yellow, apex of hind tibia and hind tarsus brown; wing membrane weakly darkened, pterostigma and veins brown.

Diagnosis. Within the subgenus *Osculobracon* Papp, *Bracon cingillus* Tobias is most similar to *B. subcingillus* Tobias, 2000 because of the crenulated furrow of the first metasomal tergite, more or less complete absence of desclerotised areas in anterolateral margins of the second metasomal tergite, and development of sculpture on two basal tergites (Fig. 90). The differences between two species are listed below.

1 Median length of first metasomal tergite (measured from spiracle) 0.8–1.0× its apical width (Fig. 90). Claws with large acutely protruding basal lobe. Mesosoma 1.5–1.6× longer than its maximum height .... ***Bracon* (*Osculobracon*) *cingillus* Tobias**

– Median length of first metasomal tergite (measured from spiracle) 1.2× its apical width. Claws with small weakly pointed basal lobe. Mesosoma 1.4× longer than its maximum height .... ***Bracon* (*O.*) *subcingillus* Tobias**

***Bracon* (*Rostrobracon*) *urinator* (Fabricius, 1798)**

Fig. A8

Material. South Korea – **Jeju-do** • 1 female; Jeju-si, [89] Odeung-dong, Hanlla Mountain; 10 Aug. 1995; S.H. Lee leg.; NIBR 13.

Distribution. Afghanistan. Caucasus. Central Asia. China: Liaoning, Shaanxi, Shandong, Zhejiang. Cyprus. Europe: Eastern, Northern, Southern, and Western Europe. Iran. Israel. Kazakhstan. Mongolia. North Africa: Algeria, Canary Islands, Egypt, Tunisia. Russia: Eastern Siberia: Buryatia Republic, Zabaikalskiy Territory; European part; Far East: Primorskiy Territory; Ural (Kostromina 2010). Saudi Arabia. South Korea (new record). Syria. Turkey.

Remarks. *Rostrobracon* Tobias, 1957 is considered here a valid subgenus, because its synonymisation with *Cyanopterobracon* Tobias, 1957 was not justified (Papp 2012). On the contrary, the latter subgenus differs by the less elongate eyes, about 1.5× as long as wide in lateral view (in *Rostrobracon*, ca. 2×), the long malar space, ca. 0.5× longitudinal diameter of eye in anterior view (ca. 0.25×), the elongate, 1.3–1.6× as long as high, mesosoma (robust, 1.1–1.2× as long as high) with evenly convex median lobe of mesoscutum (the median lobe dorsally flattened in anterior part), the deep second metasomal suture (mostly shallow in *Rostrobracon*), and the shorter ovipositor sheath, ca. as long as hind tibia (ca. 2× as long as hind tibia in *Rostrobracon*).

Bracon (*Sculptobracon*) *obsoletus* Li, He & Chen, 2016

Fig. A9

Material. South Korea (23 females, 5 males). – **Gangwon-do** • 1 female; Goseong-gun, [1] Hyeonnae-myeon, Baebong-ri; 26 May 1993; D.-S. Ku leg.; SMNE 237 • 1 female; Goseong-gun, [3] Geojin-eup, Naengcheon-ri, Geonbongsa Temple; 25 May 1993; D.-S. Ku leg.; SMNE 238 • 1 female; Inje-gun, [9] Inje-eup, Hapgang-ri; 27 May 1993; D.-S. Ku leg.; SMNE 233 • 1 female; Donghae-si, [15] Bukpyeong-dong; 28 May 1993; D.-S. Ku leg.; SMNE 231 • 1 female; Yeongwol-gun, [18] Hanbando-myeon, Ssangyong-ri; 24 May 1993; D.-S. Ku leg.; ZISP 258. – **Gyeonggi-do** • 1 female; Paju-si, [28] Munsan-eup, Majeong-ri, Freedom Bridge (pond); 3 Jun. 1998; leg.; NIBR 236 • 1 male; Gapyeong-gun, [32] Cheongpyeong-myeon, Homyeong-ri, Cheongpyeong Dam; 14 Jun. 1992; D.-S. Ku leg.; SMNE 242 • 1 female; Suwon-si, [37] Gwonseon-gu, Seodun-dong, Yeogisan Mountain; 29 May – 6 Jul. 1994; D.-S. Ku leg.; Malaise trap; ZISP 239 • 1 female; same locality as in preceding; 16 Jun. 1994; J.Y. Choi leg.; 249; SMNE • 1 female; Suwon-si, [38] Gwonseon-gu, Seodun-dong; 5 Sep. 1986; Seong-Bok Ahn leg.; apricot; SMNE 248 • 5 females; same data as for preceding; 9 Oct. 1985; SMNE 244–247, 253 • 1 female; same locality as in preceding; 30 Jun. 1995; D.J. Im leg.; SMNE 250 • 1 male; same locality as in preceding; 7 Aug. 1996; Seong-Bok Ahn leg.; ZISP 251 • 3 males; same data as for preceding; SMNE 252, 254, 255 • 2 females; Hwaseong-si, [39] Bibong-myeon; 1 Jun. 1994; D.-S. Ku leg.; SMNE 234, 235. – **Gyeongsangbuk-do** • 1 female; Gimcheon-si, [45] Daedeok-myeon, Churyang-ri Sudosan Mountain; 1 Sep. 1995; June-Yeol Choi leg.; SMNE 243 • 1 female; Yeongcheon-si, [46] Hwabuk-myeon, Sangsong-ri, Nogwijae ridge; 29 May 1993; D.-S. Ku leg.; SMNE 232. – **Gyeongsangnam-do** • 2 females; Jinju-si, [73] Jinseong-myeon, Daesa-ri; 8 May 1993; D.-S. Ku leg.; SMNE 240, 241. – **Jeju-do** • 2 females; Seogwipo-si, [90] Andeok-myeon, Sanbangsan Mountain; 26 Aug. 1997; D.-S. Ku leg.; Tree Colony; SMNE 256, 257.

Distribution. China: Shanxi (Li et al. 2016). South Korea (new record).

Remarks. The detailed description and diagnosis of the species are provided in Li et al. (2016: 471).

Genus *Campyloneurus* Szépligeti, 1900

Remarks. Due to the recent discovery of the species with character states intermediate between *Acampyloneurus* van Achterberg and *Campyloneurus* Szépligeti (Li et al. 2020c) the taxonomic statuses and diagnoses of these genera require special revision. Here we consider the species previously classified as *Acampyloneurus* (Samartsev 2019) as the members of *Campyloneurus*, because they fit in the new range of variability of the latter genus.

Campyloneurus bohayicus (Belokobylskij, 2000), comb. nov.

Fig. A10

Material. South Korea – **Gyeongsangnam-do** • 1 female; Tongyeong-si, [78] Hansan-myeon, Bijin Island, Bijin-ri; 14–16 Sep. 1997; Pierre Tripotin leg.; Malaise trap; NIBR 525.

Distribution. Russia: Far East: Primorskiy Territory. South Korea (new record).

Remarks. The species has been re-described and its taxonomic position has been reviewed recently (Samartsev 2019). The species is very similar to *Campyloneurus pachypus* Li, van Achterberg & Chen, 2020, their differences are listed in diagnosis of the latter species.

Campyloneurus pachypus Li, van Achterberg & Chen, 2020

Figs 93–98, A10

Material. South Korea – **Gangwon-do** • 1 female; Hongcheon-gun, [12] Duchon-myeon; 11 Oct. 1995; J.Y. Choi leg.; NIBR 524.

Distribution. China (Li et al. 2020c): Hubei, Zhejiang. South Korea (new record).

Description. Character states from Li et al. (2020c) are given in parentheses. **Female.** Body length 4.7 mm (6.4–6.6 mm), fore wing length 4.8 mm. Transverse diameter of eye (dorsal view) 1.6× (2.1×) and (lateral view) 1.8× longer than temple. POL 1.4× Od (1×); OOL 2.5× Od (2×); OOL 1.8× POL (2×). Face width 1.2× (1.4×) combined height of face and clypeus, 2.0× width of hypoclypeal depression. Longitudinal diameter of eye 3.1× longer than malar space (anterior view). Malar suture absent. Scape (lateral view) 1.6× longer than maximum wide, longer ventrally, than dorsally, concave laterally. Mesosoma 1.6× (1.8×) longer than its maximum height. Notauli deep anteriorly, absent and not united posteriorly. Fore wing vein 1-R1 1.5× longer than pterostigma. Vein 3-SR 3.2× (3.3×) vein r, 0.63× (0.68×) vein SR1, 2.1× vein 2-SR. Vein 1-SR+M curved forward proximately. Wing membrane evenly setose in base of hind wing. Hind femur 3.7× (3.8×) longer than wide. Claws with moderate large rounded basal lobe. Median length of first metasomal tergite as large as its apical width (1.1× its apical width). Dorsal carinae of first metasomal tergite incomplete, strongly curved towards apex; dorsolateral carinae developed. Second metasomal tergite medially 1.3× longer than third tergite; basal width of second tergite 1.4× larger than its median length; with long weakly converging sublateral carinae; without sublateral posteriorly diverging grooves. Anterolateral areas of second metasomal tergite elongate-triangulate, very long, smooth, with sharp crenulate margins; median area of tergite strongly elevated, short and wide, transverse-triangle, with long narrow "tail" posteriorly; separated by sharp crenulate margin. Transverse subapical grooves absent on third tergite, incomplete on fourth tergite, and complete on fifth tergite, crenulate. Ovipositor sheath 0.95× as long as hind tibia, 0.3× (0.2×) as long as fore wing. Apex of ovipositor with developed nodus and ventral serration. Body mostly smooth; first metasomal tergite laterally weakly rugulose, its median area apically foveate-rugose; second tergite medially rugose, laterally smooth. Coloration mostly as in *Cyanopterus tricolor* (Ivanov), but tegula and fore legs entirely yellow and mesoscutum and scutellum rusty.

Diagnosis. The species is very similar to *Campyloneurus bohayicus* (Belokobylskij, 2000), their differences are listed below.

1 Scape about 2× longer than maximum wide (Samartsev 2019: fig. 24). Head black. Apex of ovipositor without nodus and ventral serration, simple and acute (ibid: fig. 24). Face more or less granulate (ibid: fig. 5). Hind wing membrane proximally with sparse setosity near vein cu-a (ibid: fig. 25). Anterolateral areas of second metasomal tergite elongate-triangulate, but less long (ibid: fig. 14) .... ***Campyloneurus bohayicus* (Belokobylskij)**

– Scape about 1.5× longer than maximum wide (Fig. 96; Li et al. 2020c: fig. 16K). Head rusty. Apex of ovipositor with well-developed nodus and ventral serration (Fig. 97; Li et al. 2020c: fig. 16i). Face smooth (Fig. 94; Li et al. 2020c: 16g). Hind wing membrane proximally evenly setose (Fig. 93; Li et al. 2020c: 16b). Anterolateral areas of second metasomal tergite elongate-triangulate, very long (Fig. 94; Li et al. 2020c: fig. 16e) .... ***Campyloneurus pachypus* Li, van Achterberg & Chen**

Campyloneurus penini (Belokobylskij, 2000), comb. nov.

Fig. A10

Material. South Korea (1 female, 3 males). – **Gangwon-do** • 1 female; Hongcheon-gun, [13] Naechon-myeon, Waya-ri, Baegamsan Mountain; 1 Sep. – 18 Oct. 2002; D.-S. Ku leg.; Malaise trap; SMNE 526 • 1 male; Yeongwol-gun, [18] Hanbando-myeon, Ssangyong-ri; 24 May 1993; D.-S. Ku leg.; NIBR 529 • 1 male; same data as for preceding; ZISP 528. – **Chungcheongbuk-do** • 1 male; Goesan-gun, [59] Cheongcheon-myeon, Sagimak-ri; 23 May 1993; D.-S. Ku leg.; SMNE 527.

Distribution. Russia: Far East: Primorskiy Territory. South Korea (new record).

Remarks. The taxonomic position of the species has been reviewed recently (Samartsev 2019).

Genus *Craspedolcus* Enderlein, 1920

Craspedolcus kurentzovi **(Belokobylskij, 1986)**
Fig. A10

Material. South Korea – **Gyeonggi-do** • 1 female; Gunpo-si, [35] Sokdal-dong, Surisan Mountain; 10 Jun. 1998; Hyong-Kun Lee leg.; light trap; NIBR 817.

Distribution. Japan: Shikoku (Belokobylskij and Tobias 2000). Russia: Far East: Primorskiy Territory. South Korea (new record).

Remarks. The taxonomic position of the species has been reviewed recently (Samartsev 2019).

Genus *Cyanopterus* Haliday, 1835

Cyanopterus tricolor **(Ivanov, 1896)**
Figs 99–104, A10

Material. South Korea (4 females, 2 males). – **Gangwon-do** • 1 female; Yangyang-gun, [10] Seo-myeon, Galcheon-ri, Yaksusan Mountain; 9 Aug. 1989; K.T. Park leg.; NIBR 517 • 1 female; Hongcheon-gun, [13] Naechon-myeon, Waya-ri, Baegamsan Mountain; 31 Jul. 2002; D.-S. Ku leg.; light trap; ZISP 515 • 1 male; Hoengseong-gun, [16] Gonggeun-myeon, Hakdam-ri; 24 May 1993; D.-S. Ku leg.; SMNE 518. – **Gyeongsangbuk-do** • 1 female; Gyeongsan-si, [49] Yeongnam University, Department of Biology; 19 Jun. 199?; S.K. Lee leg.; SMNE 516. – **Chungcheongbuk-do** • 1 male; Goesan-gun, [59] Cheongcheon-myeon, Sagimak-ri; 23 May 1993; D.-S. Ku leg.; ZISP 519. – **Gyeongsangnam-do** • 1 female; Jinju-si, [75] Neadong-myeon, Doksan-ri (Around the forest road); 5–20 May 2003; Tea-Ho Ahn leg.; Malaise trap; SMNE HYM-BRA_ATH_0000150.

Additional material. Ukraine • 1 male (lectotype); Kupyansk; 23 May 1895; P.V. Ivanov leg.; blackthorn; ZISP.

Russia – **Primorskiy Territory** • 1 female; Khasansky District, 30 km S of Slavyanka; 3 Aug. 1985; S.A. Belokobylskij leg.; oak forest, hazel grove; ZISP B0075 • 1 female; Mikhaylovsky District, Tarasovka; 24 Jul. 1972; L. Kulikova leg.; flowers, soybean, wheat; ZISP B0077 • 1 female; Spassky District, Spassk-Dalny; 17 May – 21 Jun. 1996; S.A. Belokobylskij leg.; shrubs, forest; ZISP B0076.

Distribution. China (Cao et al. 2020): Jilin, Liaoning. Eastern Europe. Russia: European part; Far East: Jewish Autonomous Province, Primorskiy Territory; Western Siberia (Belokobylskij and Tobias 2000). South Korea (new record).

Description. Female. Body length 4.1–5.8 mm, fore wing length 4.3–6.2 mm. Transverse diameter of eye (dorsal and lateral view) 1.1–1.4× longer than temple. POL 1.1–1.3× Od. OOL 2.5–2.8× Od. OOL 1.9–2.4× POL. Face width 1.2–1.5× combined height of face and clypeus, 1.9–2.0× width of hypoclypeal depression. Longitudinal diameter of eye 2.2–2.7× longer than malar space (anterior view).

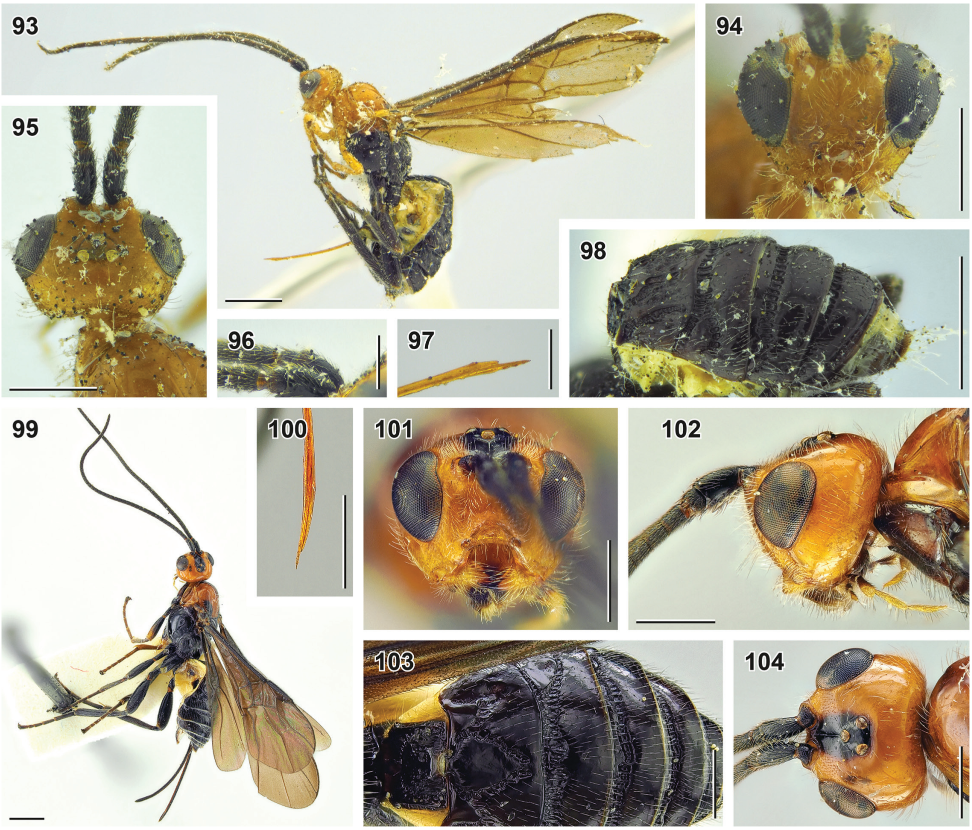

Figures 93–104. *Campyloneurus pachypus* Li, van Achterberg & Chen, 2020 (**99–104** female, NIBR) and *Cyanopterus tricolor* (Ivanov, 1896) (**99–104** female, ZISP) **93, 99** habitus, lateral view **94, 101** head, anterior view **95, 104** head, dorsal view **96** scape, lateral view **97, 100** apex of ovipositor **98** metasoma, dorsolateral view **102** head, lateral view **103** mesosoma, dorsal view. Scale bars: 0.25 mm (**96, 97**); 0.5 mm (**94, 95, 100–104**); 1 mm (**93, 98, 99**).

Malar suture absent. Scape (lateral view) as long dorsally as ventrally, concave laterally. Mesosoma 1.5–1.7× longer than its maximum height. Notauli impressed anteriorly, shallow and not united posteriorly. Fore wing vein 1-R1 1.4–1.8× longer than pterostigma. Marginal cell 5.5–6.6× longer than distance from its apex to apex of wing. Vein 3-SR 3.5–3.9× vein r. Vein 3-SR 0.50–0.70× vein SR1. Vein 3-SR 1.8–2.3× vein 2-SR. Vein 1-SR+M weakly curved forward proximately. Wing membrane evenly setose in base of hind wing. Hind femur 3.2–3.4× longer than wide. Claws with moderately large rounded basal lobe. Median length of first tergite 1.0–1.2× its apical width. Dorsal carinae of first metasomal tergite absent; dorsolateral carinae weakly separated. Second metasomal tergite medially 1.25–1.30× as long as third tergite; with long parallel sublateral carinae and anterolateral, posteriorly diverging sublateral crenulated grooves; basal width of second tergite 1.4–1.6× its median length. Anterolateral areas of second metasomal tergite elongate-triangulate, strongly separated by crenulate furrows and sharp crenulate margins; median area of tergite strongly elevated, triangle, large and wide, rounded on sides, separated by crenulate furrows and complete sharp margin. Apical margins of third to sixth tergites without transverse subapical grooves. Ovipositor sheath about 1.5× longer than hind tibia, 0.41–0.46× as long as fore wing. Apex of ovipositor without distinct nodus, acute; with weak or more or less developed ventral serration. Body entirely smooth, only first metasomal tergite sometimes foveate-rugose apicomedially. Body mostly brownish black; head, prothorax (often also mesoscutum), tegulae and pattern on fore leg reddish yellow; maxillary palps yellow; wing membrane brownish darkened; pterostigma and wing veins brown; membranous areas of metasomal sterna pale yellow.

Diagnosis. *Cyanopterus tricolor* differs from similar species (*C. hinoemataensis*, *C. kusarensis*, and *C. praecinctus*) by the relatively long ovipositor (in related species it is 0.85–1.00× and 0.2–0.3× as long as hind tibia and fore wing, respectively) and absence of transverse subapical grooves on third–fifth metasomal tergites.

Genus *Iphiaulax* Foerster, 1863

Iphiaulax mactator (Klug, 1817)

Fig. A11

Material. South Korea (1 female, 1 male). – **Gangwon-do** • 1 male; Yanggu-gun, [8] Bangsan-myeon, Omi-ri; 13 Jun. 1992; D.-S. Ku leg.; NIBR79. – **Seoul-si** • 1 female; Gwanak-gu, [23] Shinrim-dong; 29 Jun. 1973; H.-M. Kim leg.; SMNE78.

Distribution. Caucasus. China: Henan, Hunan (Li et al. 2020c), Inner Mongolia (Li et al. 2020c), Jilin. Europe: Eastern, Southern, and Western Europe. Iran. Kazakhstan. Mongolia. Russia: Eastern Siberia: Buryatia Republic, Zabaikalskiy Territory; European part; Far East: Amur Province, Jewish Autonomous Province, Primorskiy Territory. South Korea (new record). Turkey.

Remarks. See Li et al. (2020c) for the diagnosis of the species.

Iphiaulax wuhainensis Wang & Chen, 2008

Figs 105–109, A11

Material. South Korea (9 females, 14 males) • 2 females; without explicit locality ["白桥" = 白橋, ("White Bridge")]; 9 Aug. 1957; SMNE 65, 66. – **Gangwon-do** • 1 male; Yanggu-gun, [8] Bangsan-myeon, Omi-ri; 13 Jun. 1992; D.-S. Ku leg.; SMNE 474. – **Chungcheongbuk-do** • 1 male; Okcheon-gun, [62] Iwon-myeon, Iwon-ri; 22 May 1993; D.-S. Ku leg.; SMNE 491. – **Gyeongsangnam-do** • 1 female; Uiryeong-gun, [67] Garye-myeon, Gapeul-ri, Jagulsan Mountain; 21 Jul. 1992; D.-S. Ku leg.; SMNE 473 • 1 male; Changwon-si, [68] Masanhappo-gu, Jinbuk-myeon, Yeonghak-ri, Seobuk Mountain; 20 Jul. 1992; D.-S. Ku leg.; SMNE 475 • 1 male; Jinju-si, [71] Daepyeong-myeon, Naechon-ri; 4 Jul. 1992; D.-S. Ku leg.; SMNE 487 • 2 females; Jinju-si, [72] Gajwa-dong; 16 Jun. 1993; D.-S. Ku leg.; NIBR 476, 477 • 2 females; same data as for preceding; SMNE 478, 479 • 2 males; same data as for preceding; SMNE 480, 481 • 1 male; same data as for preceding; 19 Jun. 1993; SMNE 486 • 1 male; same data as for preceding; 9 Jun. 1993; ZISP 489 • 1 male; same data as for preceding; SMNE 490 • 1 female; same data as for preceding; 22 Aug. 1993; SMNE 488 • 1 male; Jinju-si, [75] Neadong-myeon, Doksan-ri (Around the forest road); 1 Jun. 2003; Tea-Ho Ahn leg.; sweeping; SMNE HYM-BRA_ATH_0000675 • 1 male; Jinju-si, [76] Geumgok-myeon; 26 May 1984; S.J. Choi leg.; SMNE 485 • 1 male; same data as for preceding; 1 Jun. 1984; SMNE 484 • 2 males; same data as for preceding; 21 Jun. 1984; SMNE 482, 483 • 1 female; same locality as in preceding; 16 Jun. 1985; G.J. Jeong leg.; ZISP 472.

Additional material. China – **Liaoning** • 1 female; Shenyang; 1 Jul. 1952; I.A. Rubtsov leg.; ZISP.

Distribution. China: Inner Mongolia, also presumably Beijing, Liaoning, Shaanxi, Shandong, Zhejiang (see remarks). South Korea (new record).

Description. Female. Body length 5–8 mm; fore wing length 5–7 mm. Width of head (dorsal view) 1.5–1.7× its median length. Transverse diameter of eye (dorsal view) 1.3–1.4× and longer than temple. OOL 3.1–3.7× Od; POL 1.5–1.8× Od; OOL 1.9–2.2× POL. Face width 1.5–1.6× combined height of face and clypeus; 2.2–2.5× larger than width of hypoclypeal depression. Longitudinal diameter of eye 1.7–1.8× longer than malar space (anterior view). Malar suture weakly impressed (sometimes more deep under eye), weakly crenulate and densely setose. Antenna with 47–61 antennomeres. Scape (lateral view) longer ventrally than dorsally, somewhat swollen. First, middle and penultimate flagellomeres 1.5–1.8×, about 1.3×, and 1.4–1.6× longer than wide, respectively. Apical flagellomere weakly pointed, apically with flat inclined area. Mesosoma 1.8–1.9× longer than its maximum height. Notauli deep anteriorly, absent and not united posteriorly. Mesoscutum setose only on notaulic area. Mesepimeral and metapleural sulci smooth, mesopleural pit indistinct. Fore wing vein 1-R1 1.2–1.4× longer than pterostigma; marginal cell 2.7–3.6× longer than distance from its apex to apex of wing. Vein 3-SR 2.9–3.3× vein r, 0.53–0.63× vein SR1, 1.7–2.1× vein 2-SR. Wing membrane evenly setose in base of hind wing. Hind femur 3.3–4.0× longer than wide. Claws with moderately large rounded basal lobe. Median length of first tergite 1.1–1.3× its apical width. Dorsolateral carinae of first metasomal tergite absent or weakly separated (sometimes only behind spiracle), dorsal carinae absent. Second tergite medially about 1.2× longer than third tergite; with deeply impressed anteriorly and very shallow posteriorly, smooth s-shaped dorsolateral longitudinal impressions and with anterolateral posteriorly diverging deep smooth furrows; basal width of second metasomal tergite 1.2–1.5× larger than its median length. Apical margins of third to sixth tergites thick, without transverse subapical grooves. Ovipositor sheath

0.80–1.05× as long as hind tibia and 0.24–0.30× as long as fore wing. Apex of ovipositor with weakly widened blunt upper valve and weakly developed or absent ventral serration. Body entirely smooth. Head, mesosoma and legs mainly brownish black, metasoma reddish yellow. Face, anterior and posterior margins of eye, lateral sides of pronotum, mesoscutum along notauli, apex of fore femur, and base of fore tibia reddish yellow. Maxillary palps brownish black, tegulae dark brown. Wing membrane deeply darkened, somewhat lighter apically; pterostigma brown, sometimes with small yellowish patch basally, wing veins dark brown.

Male. Body length 4.0–5.5 mm; fore wing length 4.3–5.5 mm. Antenna with 41–51 antennomeres. First flagellomere 1.8–2.2× longer than its apical width. Mesosoma 1.9–2.1× longer than its maximum height. Vein 3-SR 2.9–3.8× vein r. Hind femur 3.6–4.6× longer than wide. Furrows on metasoma weakly crenulate. Basal width of second metasomal tergite 1.0–1.2× larger than its median length. Second tergite sometimes weakly and sparsely foveate. Apex of metasoma with brownish black patch.

Diagnosis. *Iphiaulax wuhainensis* is very similar to *I. impeditor* (Kokujev, 1898) distributed in Europe, Caucasus, Western and Central Asia (including Kazakhstan), Western Siberia, and Krasnoyarsk Territory in Eastern Siberia. Two taxa may represent two subspecies or geographical varieties of one species. The differences between *I. wuhainensis* and *I. impeditor* are presented below.

1 Pterostigma yellow with brown patch apically (Fig. 110). Anterolateral areas of second–fifth metasomal tergites separated by crenulate furrows (Fig. 116). Second tergite with smoothed foveate sculpture; first tergite laterally weakly rugulose (Fig. 115). Malar suture deep, sparsely setose (Figs 112, 113). Mesopleural pit deep and separated from mesepimeral sulcus. Marginal cell 2.2–2.4× longer than distance from its apex to apex of wing .... ***Iphiaulax impeditor*** **(Kokujev)**

– Pterostigma brown, sometimes with small yellowish patch basally (Fig. 105). Anterolateral areas of second–fifth metasomal tergites separated by smooth furrows (Fig. 109). Second tergite smooth (sometimes only with sparse narrow punctures); first metasomal tergite laterally smooth (Fig. 107). Malar suture weakly impressed, densely setose (Fig. 106). Mesopleural pit indistinct. Marginal cell 2.7–3.6× longer than distance from its apex to apex of wing.... .... ***Iphiaulax wuhainensis*** **Wang & Chen**

Remarks. Two of three works indicating *Iphiaulax impeditor* in China (Wang et al. 2008; Li et al. 2020c) list mostly the same material. Both works do not indicate the most distinct differences between *I. impeditor* and *I. wuhainensis*, the coloration of the pterostigma and sculpture of metasoma. In addition, the pictures of *I. impeditor* in Li et al. (2020c: figs 33, 34) obviously represent a specimen of *I. wuhainensis*. Thus, both indications of *I. impeditor* in China are doubtful and likely belong to *I. wuhainensis*. *I. impeditor* has been also listed for the north-east part of China (Liaoning: Tobias and

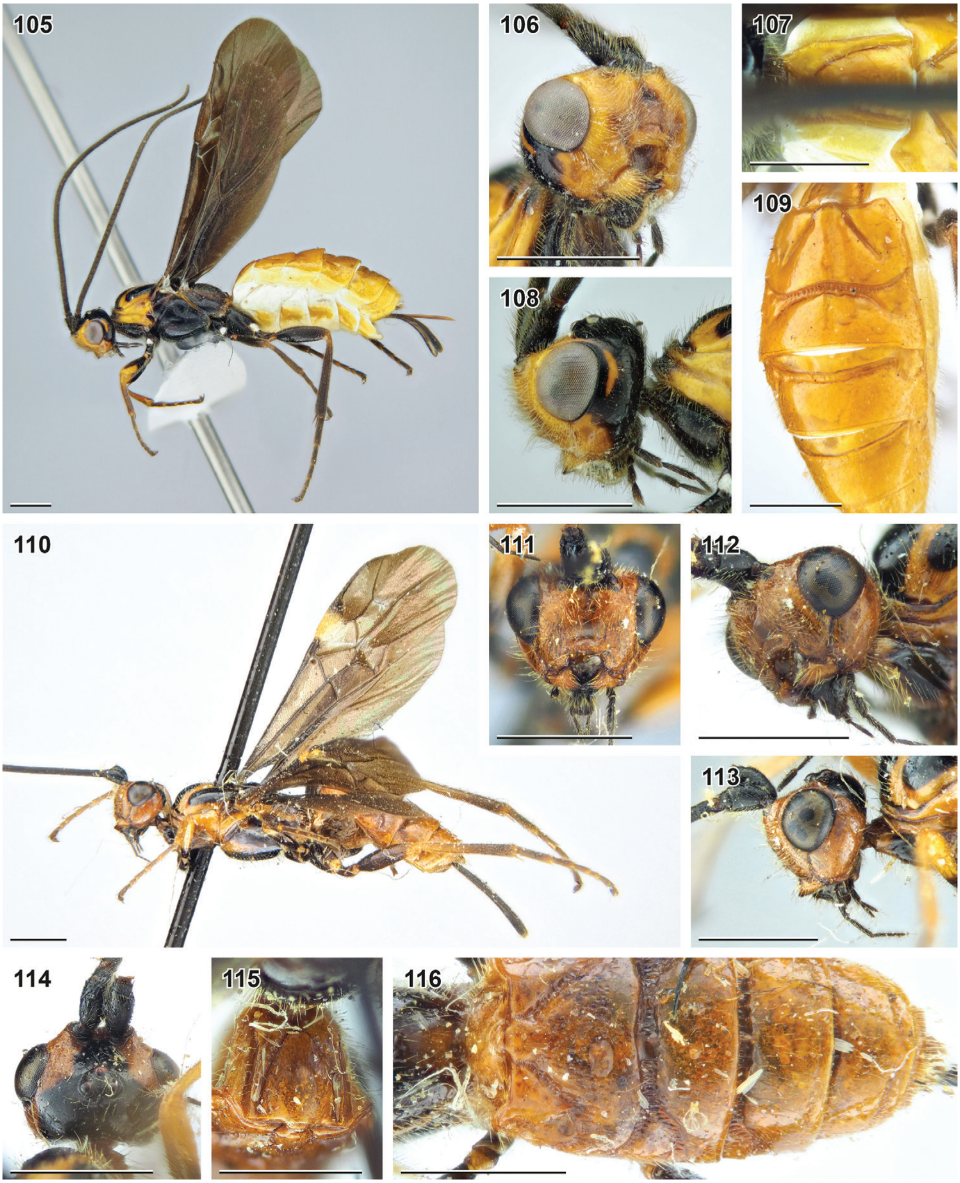

Figures 105–116. *Iphiaulax wuhainensis* Wang & Chen, 2008 (**105–109** female, NIBR) and *Iphiaulax impeditor* (Kokujev, 1898) (**110–116** lectotype, female, ZISP) **105, 110** habitus, lateral view **106, 112** head, ventrolateral view **107, 115** first metasomal tergite, dorsal view **108, 113** head, lateral view **109** metasoma, dorsolateral view **111** head, anterior view **114** head, dorsal view **116** metasoma, dorsal view. Scale bars: 1 mm.

Belokobylskij 2000). This indication is based on a single specimen in the collection of ZISP (the label is cited above in the additional material for the species), which also belongs to *I. wuhainensis*.

Genus *Syntomernus* Enderlein, 1920

Syntomernus asphondyliae (Watanabe, 1940)

Fig. A11

Material. South Korea (4 females, 2 males). – **Gangwon-do** • 1 female; Goseong-gun, [2] Ganseong-eup; 25 May 1993; D.-S. Ku leg.; NIBR 464 • 2 males; same data as for preceding; SMNE 465, 466. – **Gyeongsangnam-do** • 2 females; Hamyang-gun, [66] Macheon-myeon; 1 Sep. 2016; Heung-Yoon Oh leg.; from silver vine (*Actinidia polygama*) gall; NIBR • 1 female; same data as for preceding; ZISP.

Distribution. Japan: Honshu, Kyushu. Russia: Far East: Khabarovsk Territory, Primorskiy Territory. South Korea (new record).

Remarks. *Bracon flaccus* Papp, 1996 described from North Korea used to be considered a synonym of *Syntomernus asphondyliae* (Watanabe) (Tobias and Belokobylskij 2000), but recently has been synonymised with *S. sunosei* (Maeto, 1991) (Samartsev and Ku 2020). The key to the Eastern-Palaearctic species of *Syntomernus* is given in Samartsev and Ku (2020: 34).

Syntomernus tamabae (Maeto, 1991)

Fig. A12

Material. South Korea (1 female, 4 males). – **Gangwon-do** • 2 males; Sokcho-si, [6] Nohak-dong; 11 Jun. 1992; D.-S. Ku leg.; SMNE 470, 471 • 1 male; Inje-gun, [9] Inje-eup, Hapgang-ri; 27 May 1993; D.-S. Ku leg.; NIBR 468. – **Chungcheongnam-do** • 1 female; Geumsan-gun, [53] Chubu-myeon, Seongdang-ri, Gaedeoksa Temple; 22 May 1993; D.-S. Ku leg.; SMNE 467. – **Jeollanam-do** • 1 male; Yeosu-si, [86] Nam-myeon, Geumodo Island, Uhak-ri; 19 Jul. 1993; D.-S. Ku leg.; SMNE 469.

Distribution. Japan: Honshu, Kyushu, Ryukyu, Shikoku. South Korea (new record).

Remarks. The key to the Eastern-Palaearctic species of *Syntomernus* is provided by Samartsev and Ku (2020: 34).

Genus *Uncobracon* Papp, 1996

Remarks. *Uncobracon* has been considered either a separate genus (Papp 1996: 168; Tan et al. 2012: 64) or a subgenus of the genus *Bracon* (Tobias and Belokobylskij 2000: 119; Lee et al 2020b: 242). We follow the first point of view as more justified.

***Uncobracon belokobylskii* Samartsev, 2018**
Fig. A12

Material. South Korea (4 females, 1 male). – **Gyeonggi-do** • 1 female; Pocheon-si, [25] Yeongbuk-myeon, Sanjeong-ri, Lake Sanjeong; 14 Jun. 1992; D.-S. Ku leg.; SMNE 443 • 1 male; Gapyeong-gun, [30] Buk-myeon, Dodae-ri, Myeongjisan Mountain; 14 Jun. 1992; D.-S. Ku leg.; SMNE 1681 • 1 female; Suwon-si, [37] Gwonseon-gu, Seodun-dong, Yeogisan Mountain; 23–29 Jun. 1994; D.-S. Ku leg.; Malaise trap; SMNE 444. – **Gyeongsangnam-do** • 1 female; Jinju-si, [72] Gajwa-dong; 16 Jun. 1993; D.-S. Ku leg.; NIBR 445. – **Jeollanam-do** • 1 female; Yeosu-si, [84] Nam-myeon, Dumo-ri, Town Moha; 20 Jul. 1993; D.-S. Ku leg.; SMNE 442.

Distribution. Russia: Far East: Primorskiy Territory (Samartsev 2018). South Korea (new record).

Remarks. The diagnosis of the species is provided in Samartsev (2018).

***Uncobracon tricoloratus* (Tobias, 2000)**
Fig. A12

Material. South Korea – **Jeollanam-do** • 1 female; Yeosu-si, [87] Nam-myeon, Ando Island, Ando-ri; 4 Aug. 1993; D.-S. Ku leg.; NIBR 930.

Distribution. China: Zhejiang (Li et al. 2020c). Russia: Far East: Primorskiy Territory. South Korea (new record).

Remarks. The keys to the species of *Uncobracon* is presented in Samartsev (2018) and Li et al. (2020c).

Discussion

This article includes 31 species new to the fauna of the Korean Peninsula, most of which (21 species) have relatively narrow distribution restricted to some regions of China, the Russian Far East, and Japan. Almost all (18) of these Eastern-Palaearctic species were described in 2000 or later and known only by the description or by two works. Therefore, it is too early to discuss the patterns of distribution of these taxa. It is worth noticing the finding of *Iphiaulax wuhainensis* (from North, Northeast, and East China and South Korea), that is extremely close to *I. impeditor* distributed from Eastern Europe to Eastern Siberia. Two species are very close and differ mostly by the coloration pattern and development of the body sculpture, but these differences appear to be persistent and the known ranges of the two taxa do not overlap witnessing to the valid status of *I. wuhainensis*.

The minority of indicated species have been known for a long time as widespread taxa, but have not been recorded in the Korean Peninsula. These are the species with wide Transpalaearctic distribution, i.e. *Atanycolus ivanowi*, *Bracon* (*Habrobracon*) *nigricans*, *B.* (*Rostrobracon*) *urinator*, *Cyanopterus tricolor*, and *Iphiaulax mactator*, and the Holarctic *B.* (*H.*) *stabilis*. The rest of the species, *Bracon* (*Bracon*) *albion*, *B.* (*B.*) *longigenis*, *B.* (*B.*) *subcylindricus*, and *B.* (*B.*) *virgatus*, have been known only from the western part of the Palaearctic region, and their occurrence in South Korea is quite unexpected. The latter mentioned species, even though it was described from Europe, has the habitus more characteristic of the Far Eastern members of *Bracon* (the metasoma with areolate sculpture and pale yellow medio-longitudinal stripe and the setose middle lobe of mesoscutum) and shows no related species known in the West Palaearctic.

Current investigation is carried out on the basis of ca. 1800 specimens of Braconinae from the Korean Peninsula stored in the collections of SMNE, NIBR, and ZISP. We have published the results of study of about 35% of this material (in Samartsev and Ku 2020 and current paper). New distributional and taxonomic data added connections between the faunas of East-Asian countries, which seem too disconnected because they for a long time were separately investigated by different scientists and still are understudied. In addition, the conducted work allowed us to provide illustrated diagnoses for 16 complicated in identification species of Braconinae, most of which were described in a scarcely illustrated key in Russian (Tobias and Belokobylskij 2000). Providing relevant diagnostic information on the known East Palaearctic braconines makes them accessible for identification, that is essential in current period, when the fauna of East Asia is becoming intensively investigated.

Most of the unpublished material from South Korea available for us is represented by the taxa similar to widespread species, mostly of the genus *Bracon*. Identification of this material is difficult, because it requires the involvement of many additional taxa from the West Palaearctic. Nevertheless, we are aimed to finish this work by publishing a review of the fauna of the Korean Peninsula with an analysis of its composition and ties with neighboring regions and keys to species.

Acknowledgements

We are deeply thankful to Cornelis van Achterberg (RMNH), Yvonnick Gérard (IRSNB), Christer Hansson (ZMLU), and Zoltán Vas (HNHM) for the opportunities to study the necessary type material, to Yang Li (Chengdu Normal University, Chengdu, China) for the pictures of several types and help with translating the labels in Chinese, and to Kyoungim Kim (SMNE) and Julia Samartseva (ZISP) for the help with arranging data. We also thank C. van Achterberg and two reviewers, Yang Li and Estefany Karen López-Estrada, for the examination of the manuscript and helpful criticism and corrections. This work was supported by a grant from the National Institute of Biological Resources (NIBR) funded by the Ministry of Environment (MOE) of the Republic of Korea (NIBR201902205 and NIBR202102204); participation of KS was partly performed in the frames of the state research project No AAAA-A19-119020690101-6 and supported by the Russian Foundation for Basic Research (grant No 19-04-00027).

References

Cao L-M, van Achterberg C, Tang Y-L, Wang X-Y, Yang Z-Q (2020) Revision of parasitoids of *Massicus raddei* (Blessig & Solsky) (Coleoptera, Cerambycidae) in China, with one new species and genus. Zootaxa 4881(1): 104–130. https://doi.org/10.11646/zootaxa.4881.1.7

Kang G-W, Choi J-K, Ku D-S, Lee J-W (2019) Discovery of two previously unrecorded species of Braconidae (Hymenoptera: Ichneumonoidea) from South Korea. Journal of National Park Research 10(2): 279–282.

Karlsson D, Ronquist F (2012) Skeletal morphology of *Opius dissitus* and *Biosteres carbonarius* (Hymenoptera: Braconidae), with a discussion of terminology. PLoS ONE 7(4): e32573. https://doi.org/10.1371/journal.pone.0032573

Kostromina TS (2010) To the knowledge of the cyclostome braconid wasps (Hymenoptera: Braconidae) of South Urals. Proceedings of the Russian Entomological Society 81(2): 47–50. [In Russian]

Lee H-R, An T-H, Ku D-S, Byun B-K (2018) Nine newly recorded species of the family Braconidae (Hymenoptera) in Korea. Animal Systematics, Evolution & Diversity 34(1): 10–17.

Li Y, He J-H, Chen X-X (2016) Four subgenera of *Bracon* Fabricius (Hymenoptera, Braconidae, Braconinae) newly recorded from China, with description of five new species. Zootaxa 4208(5): 459–473. https://doi.org/10.11646/zootaxa.4208.5.4

Li Y, He J-H, Chen X-X (2020a) Review of six genera of Braconinae Nees (Hymenoptera, Braconidae) in China, with the description of eleven new species. Zootaxa 4818(1): 1–74. https://doi.org/10.11646/zootaxa.4818.1.1

Li Y, He J-H, Chen X-X (2020b) The subgenera *Glabrobracon* Fahringer, *Lucobracon* Fahringer and *Uncobracon* Papp of the genus *Bracon* Fabricius (Hymenoptera, Braconidae, Braconinae) in China, with the description of eleven new species. Deutsche Entomologische Zeitschrift 67(2): 209–252. https://doi.org/10.3897/dez.67.57668

Li Y, van Achterberg C, Chen X-X (2020c) Two genera *Campyloneurus* Szépligeti and *Iphiaulax* Foerster in China, with the descriptions of fourteen new species (Hymenoptera, Braconidae, Braconinae). Zootaxa 4884(1): 1–67. https://doi.org/10.11646/zootaxa.4884.1.1

Loni A, Samartsev KG, Scaramozzino PL, Belokobylskij SA, Lucchi A (2016) Braconinae parasitoids (Hymenoptera, Braconidae) emerged from larvae of *Lobesia botrana* (Denis & Schiffermüller) (Lepidoptera, Tortricidae) feeding on *Daphne gnidium* L. ZooKeys 587: 125–150. https://doi.org/10.3897/zookeys.587.8478

Maeto K, Uesato T (2007) A new species of *Bracon* (Hymenoptera: Braconidae) parasitic on alien sweet potato weevils in the south-west islands of Japan. Entomological Science 10(1): 55–63. https://doi.org/10.1111/j.1479-8298.2006.00198.x

Papp J (1996) Braconidae (Hymenoptera) from Korea, XVIII. Annales Historico-Naturales Musei Nationalis Hungarici 88: 145–170.

Papp J (1999) Two new species of *Bracon* from Britain (Hym., Braconidae, Braconinae). Entomologist's Monthly Magazine 135(1620–1623): 145–152.

Papp J (2008) A revision of the *Bracon* (subgenera *Bracon* s. str., *Cyanopterobracon*, *Glabrobracon*, *Lucobracon*, *Osculobracon* subgen. n., *Pigeria*) species described by Szépligeti from the western Palaearctic Region (Hymenoptera: Braconidae, Braconinae). Linzer Biologische Beiträge, 40(2): 1741–1837.

Papp J (2012) A revision of the *Bracon* Fabricius species in Wesmael's collection deposited in Brussels (Hymenoptera, Braconidae, Braconinae). European Journal of Taxonomy 21: 1–154. https://doi.org/10.5852/ejt.2012.21

Papp J (2018) Braconidae (Hymenoptera) from Korea, XXIV. Species of thirteen subfamilies. Acta Zoologica Hungarica 64(1): 21–50. https://doi.org/10.17109/AZH.64.1.21.2018

Quicke DLJ (1987) The Old World genera of braconine wasps (Hymenoptera: Braconidae). Journal of Natural History 21: 43–157. https://doi.org/10.1080/00222938700770031

Samartsev KG (2013) On the rare species of cyclostome braconid wasps (Hymenoptera: Braconidae) from the Middle and Lower Volga territories of Russia. Caucasian Entomological Bulletin 9(2): 315–328. https://doi.org/10.23885/1814-3326-2013-9-2-315-328

Samartsev KG (2018) New species of the subfamily Braconinae (Hymenoptera: Braconidae) from the Russian Far East. Zootaxa 4388(2): 238–254. https://doi.org/10.11646/zootaxa.4388.2.6

Samartsev KG (2019) To the knowledge of the subfamily Braconinae (Hymenoptera: Braconidae) of Russia. Proceedings of the Russian Entomological Society 90: 54–85. https://doi.org/10.47640/1605-7678_2019_90_54

Samartsev K, Ku D-S (2020) New species of the genera *Bracon* Fabricius and *Syntomernus* Enderlein (Hymenoptera, Braconidae, Braconinae) from South Korea. ZooKeys 999: 1–47. https://doi.org/10.3897/zookeys.999.58747

Tan J-L, Sheng M-L, van Achterberg K, Sun S-P (2012) The first record of the genus *Uncobracon* Papp from China (Hymenoptera: Braconidae). Zootaxa 3323: 64–68. https://doi.org/10.11646/zootaxa.3323.1.5

Tobias VI (1971) Review of the Braconidae (Hymenoptera) of the USSR. Proceedings of the All-Union Entomological Society 54: 156–268. [In Russian]

Tobias VI (1986) Braconinae. In: Medvedev GS (Ed.) Key to Insects of the European Part of the USSR. Hymenoptera. Vol. III, pt 4. Nauka (Leningrad): 94–149. [In Russian]

Tobias VI, Belokobylskij SA (2000) 6. Subfam. Braconinae. In: Lehr PA (Ed.) Key to the Insects of Russian Far East. Vol. IV. Neuropteroidea, Mecoptera, Hymenoptera, part 4. Dal'nauka (Vladivostok): 109–192. [In Russian]

van Achterberg C (1993) Illustrated key to the subfamilies of the Braconidae (Hymenoptera: Ichneumonoidea). Zoologische Verhandelingen 283: 1–189.

Vilhelmsen L, Mikó I, Krogmann L (2010) Beyond the wasp-waist: structural diversity and phylogenetic significance of the mesosoma in apocritan wasps (Insecta: Hymenoptera). Zoological Journal of the Linnean Society 159(1): 22–194. https://doi.org/10.1111/j.1096-3642.2009.00576.x

Wang YP, Shi M, He JH, Chen XX (2008) Taxonomic study of the tribe Iphiaulacini (Hymenoptera: Braconidae: Braconinae) from China with descriptions of two new species. Entomotaxonomia 30(3): 181–195.

Yu DS, van Achterberg C, Horstmann K (2016) Taxapad 2016, Ichneumonoidea 2015. Database on flash-drive. Nepean (Ontario), Canada.

Yu Y, Choi S, Sohn J, Han H-W, Kim H (2020) New records of the two genera of parasitoid wasps (Hymenoptera: Ichneumonoidea) from South Korea. Korean Journal of Applied Entomology 59(4): 311–315. https://doi.org/10.5656/KSAE.2020.09.0.036

Appendix 1

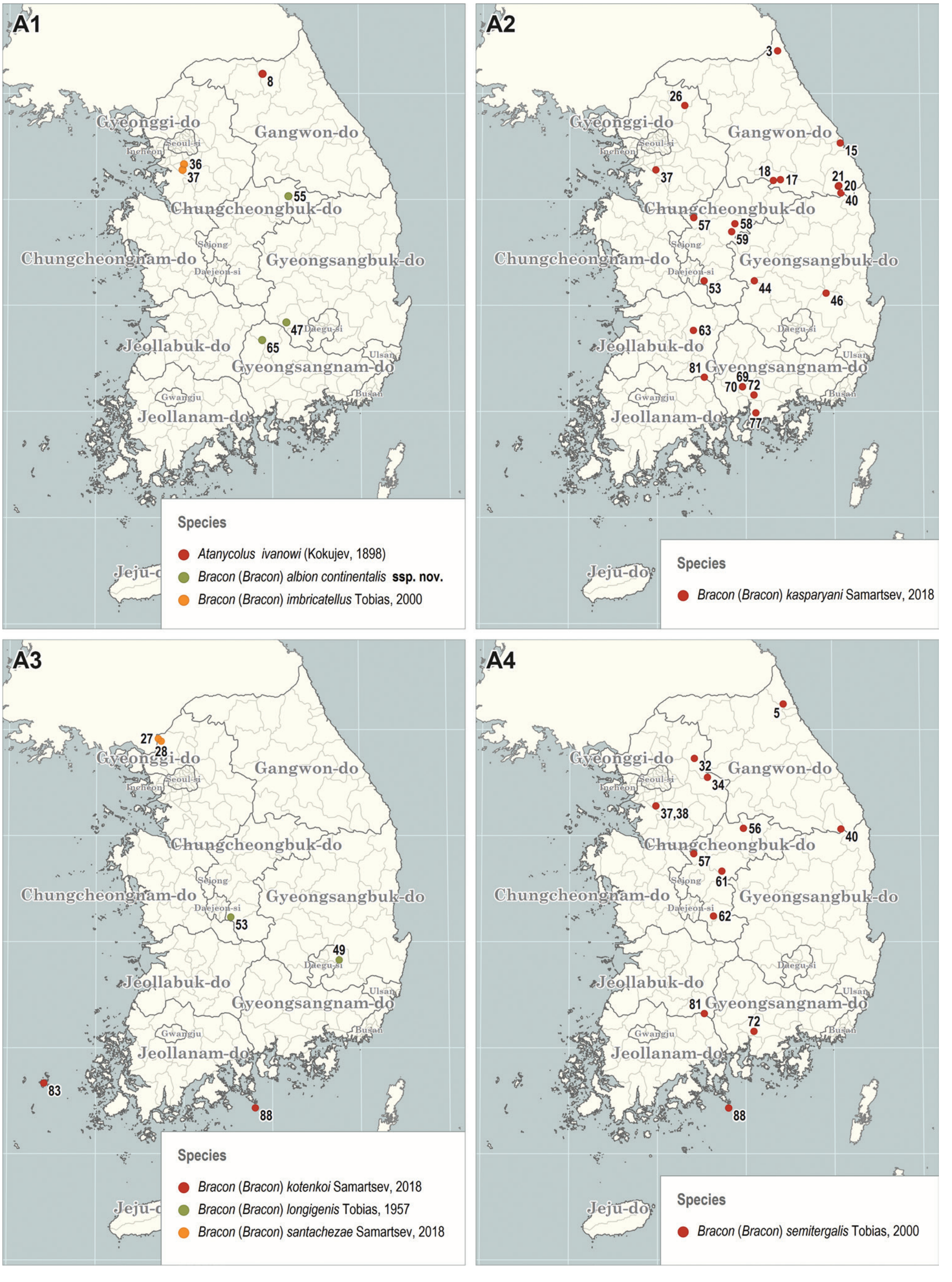

Figures A1–A4. Collecting localities of the material on the species new to South Korea. Point numbers correspond with numbers in brackets in text.

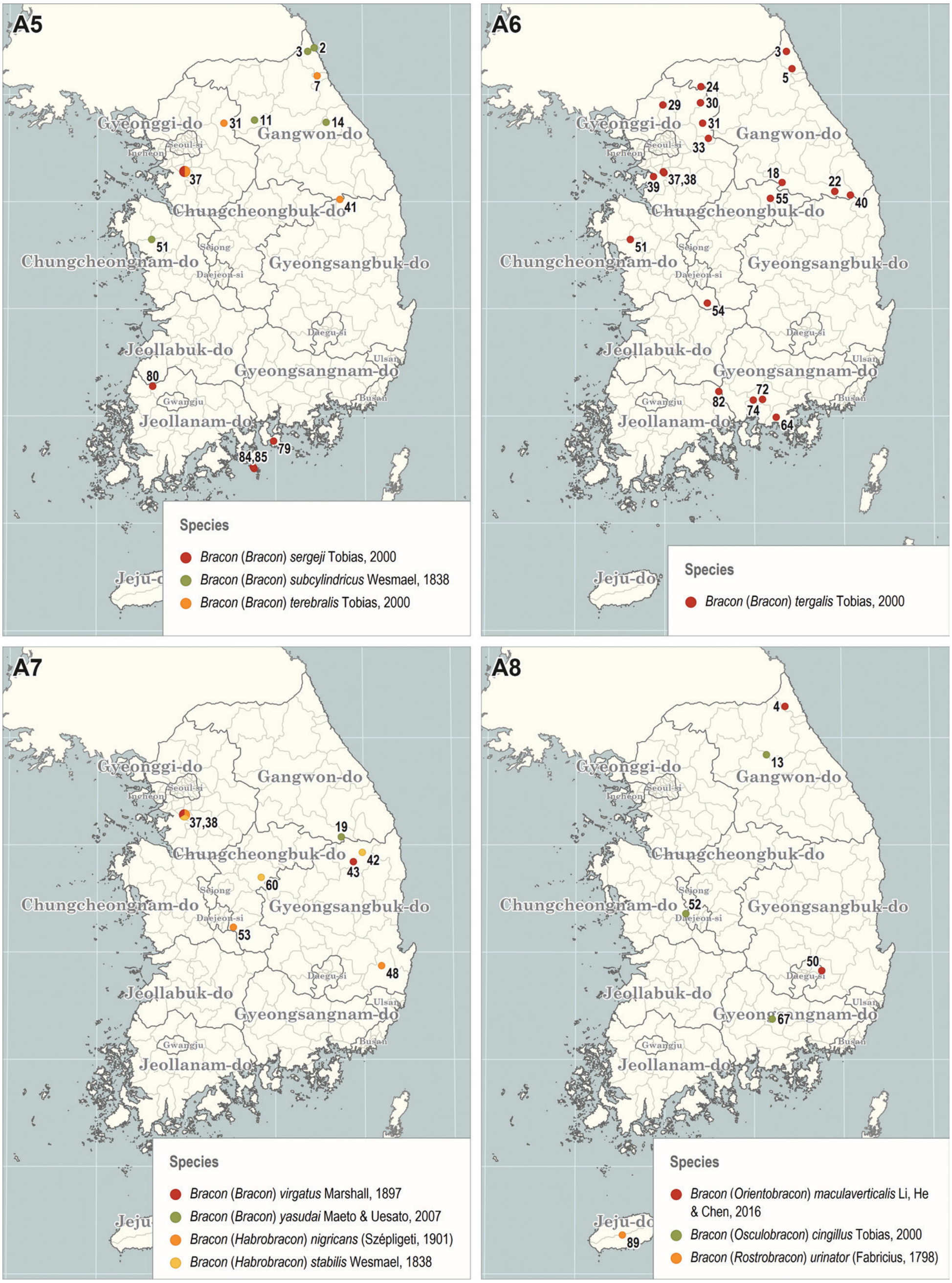

Figures A5–A8. Collecting localities of the material on the species new to South Korea. Point numbers correspond with numbers in brackets in text.

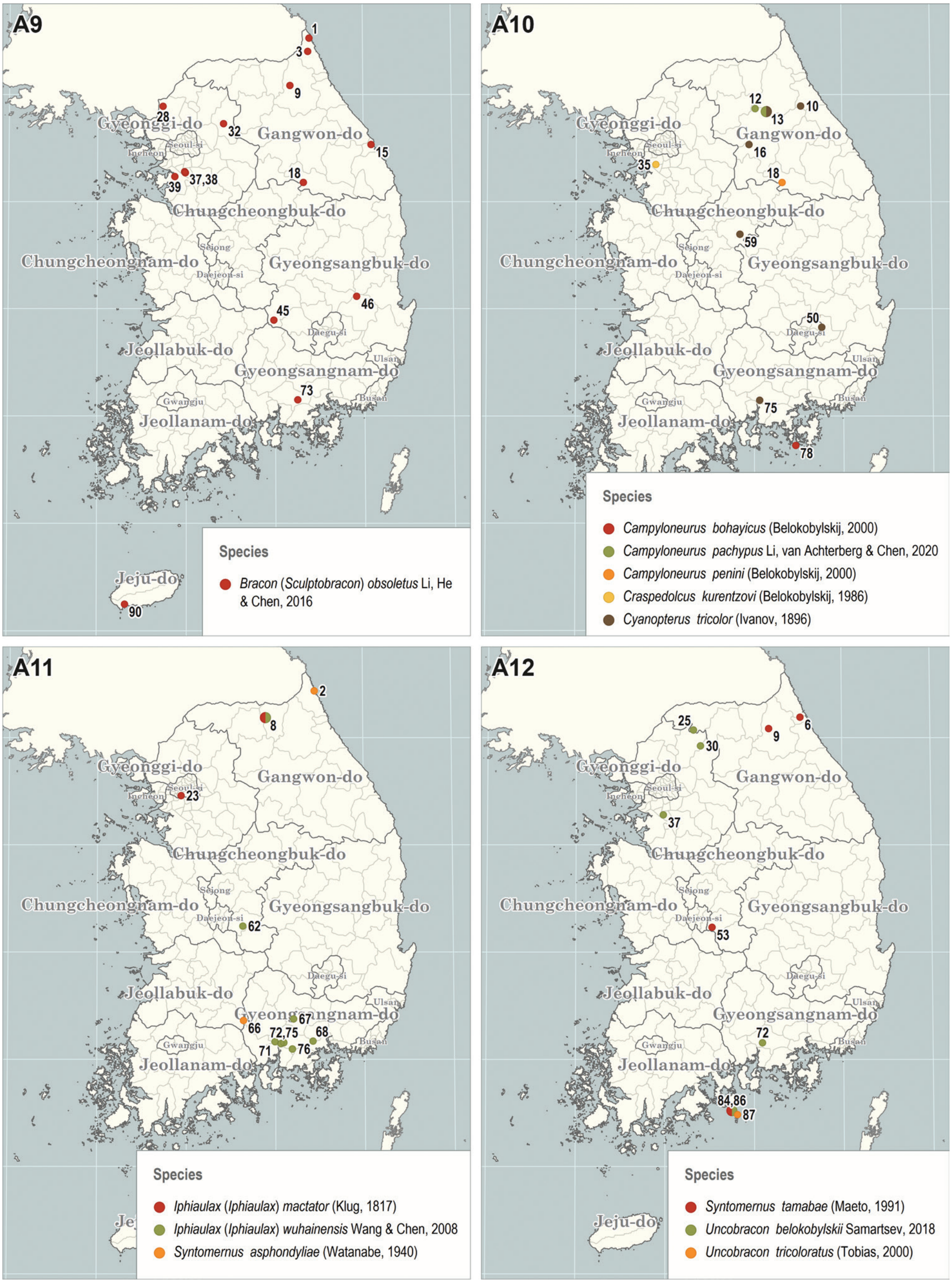

Figures A9–A12. Collecting localities of the material on the species new to South Korea. Point numbers correspond with numbers in brackets in text.

JHR 83: 73–99 (2021)
doi: 10.3897/jhr.83.64018
https://jhr.pensoft.net

RESEARCH ARTICLE

JOURNAL OF Hymenoptera RESEARCH
A peer-reviewed open-access journal
The International Society of Hymenopterists

Ovipositor of the braconid wasp *Habrobracon hebetor*: structural and functional aspects

Michael Csader[1], Karin Mayer[1], Oliver Betz[1], Stefan Fischer[1,2], Benjamin Eggs[1]

1 *Evolutionary Biology of Invertebrates, Institute of Evolution and Ecology, University of Tübingen, Auf der Morgenstelle 28, 72076, Tübingen, Germany* **2** *Tübingen Structural Microscopy Core Facility (TSM), Center for Applied Geosciences, University of Tübingen, Schnarrenbergstrasse 94–96, 72076, Tübingen, Germany*

Corresponding author: Michael Csader (m.csader@web.de)

Academic editor: J. Fernandez-Triana | Received 5 February 2021 | Accepted 22 April 2021 | Published 28 June 2021

http://zoobank.org/FEA676AD-6473-4EA3-8F74-E7F83A572234

Citation: Csader M, Mayer K, Betz O, Fischer S, Eggs B (2021) Ovipositor of the braconid wasp *Habrobracon hebetor*: structural and functional aspects. Journal of Hymenoptera Research 83: 73–99. https://doi.org/10.3897/jhr.83.64018

Abstract

The Braconidae are a megadiverse and ecologically highly important group of insects. The vast majority of braconid wasps are parasitoids of other insects, usually attacking the egg or larval stages of their hosts. The ovipositor plays a crucial role in the assessment of the potential host and precise egg laying. We used light- and electron-microscopic techniques to investigate all inherent cuticular elements of the ovipositor (the female 9th abdominal tergum, two pairs of valvifers, and three pairs of valvulae) of the braconid *Habrobracon hebetor* (Say, 1836) in detail with respect to their morphological structure and microsculpture. Based on serial sections, we reconstructed the terebra in 3D with all its inherent structures and the ligaments connecting it to the 2nd valvifers. We examined the exact position of the paired valvilli, which are bilateral concave structures that protrude into the egg canal. In *H. hebetor*, these structures putatively divert the egg ventrally between the 1st valvulae for oviposition. We discuss further mechanical and functional aspects of the ovipositor in order to increase the understanding of this putative key feature in the evolution of braconids and of parasitoid wasps in general.

Keywords

3D reconstruction, Braconidae, functional morphology, Hymenoptera, parasitoid, SEM, serial sectioning, terebra

Introduction

Most hymenopteran species belong to the guild of parasitoids of other insects (Quicke 1997). The astonishing radiation of the most diverse parasitoid wasp lineages (i.e. Ceraphronoidea, Ichneumonoidea and Proctotrupomorpha; = Parasitoida *sensu* Peters et al. 2017) has been estimated to have occurred 266–195 million years ago. This process was presumably triggered by continuous adaptations of the parasitoid lifestyle including features such as endoparasitism, miniaturization, and/or modifications of the ovipositor (Peters et al. 2017). Adaptations in oviposition behavior and the morphological structure of the ovipositor might not only have increased the reproductive success of the wasps, but have potentially also enabled them to oviposit in a multitude of different substrates, facilitating the acquisition of new hosts and host ranges (Gauld and Bolton 1988; Quicke 1997). The ovipositor of parasitoid wasps serves a set of functions: penetration of the substrate (if the host is concealed) or of the targeted egg/puparium, the location, assessment, and piercing of the host, the injection of venom, the killing of the competitors' eggs or larvae, the finding of a suitable place for egg laying, and oviposition (Quicke et al. 1999).

The hymenopteran ovipositor is an anatomical and functional cluster that consists of the following elements: the paired 1st valvulae (8th gonapophyses), the 2nd valvula (fused 9th gonapophyses), the paired 3rd valvulae (9th gonostyli), the paired 1st valvifers (fusion of the 8th gonocoxites and gonangula (Vilhelmsen 2000)), the paired 2nd valvifers (9th gonocoxites), and the female T9 (9th abdominal tergum) (Snodgrass 1933; Oeser 1961). All the morphological terms are applied according to the Hymenoptera Anatomy Ontology (HAO; Yoder et al. 2010; Hymenoptera Anatomy Consortium 2021; a table of the terms used and of their definitions is given in Table A1 in the Appendix 1). The 1st valvifer is connected to the 2nd valvifer via the intervalvifer articulation and with the female T9 via the tergo-valvifer articulation. Each of the 1st valvulae is attached to the corresponding 1st valvifer via the dorsal ramus of the 1st valvula, whereas the 2nd valvula is connected to the 2nd valvifer via the basal articulation and fine ventral rami of the 2nd valvula (cf. Bender 1943). Both the 1st and the 2nd valvulae are firmly interlocked along almost their entire length via a tongue and groove-like system called the olistheter. They form the terebra (= ovipositor shaft) and accommodate the egg canal (Oeser 1961; Quicke et al. 1994).

Despite many comparative studies on the terebra of hymenopterans (Snodgrass 1933; Oeser 1961; Quicke et al. 1994; LeRalec et al. 1996), the number of publications concerning the entire ovipositor is limited for the vast number of hymenopteran (super-)families. Studies that describe all the inherent cuticular elements and muscles of the ovipositor and (in part) also consider functional aspects include several basal 'symphytan' families (Smith 1970, 1972; Vilhelmsen 2000; Vilhelmsen et al. 2001), some aculeate species (i.e. *Apis melifera* Linnaeus, 1758 (Apidae) (Snodgrass 1933), species belonging to Chrysidoidea (Barbosa et al. 2021), *Sceliphron destillatoruim* (Illiger, 1807) (Sphecidae), *Ampulex compressa* (Fabricius, 1781) (Ampulicidae) (Graf et al. 2021), *Vespa crabro* Linnaeus, 1758 (Vespidae) (Stetsun and Matushkina 2020), and species belonging to the Crabronidae (Matushkina 2011; Matushkina and Stetsun 2016; Stetsun et al. 2019) and Pompilidae (Kumpanenko and Gladun 2018)), and a few parasitoid species belonging to the Cynipoidea (Frühauf 1924; Fergusson 1988), Platygastroidea (Field and Austin 1994), Chalcidoidea (Hanna 1934; King 1962; King and Copland 1969; Copland and King 1972a, 1972b, 1972c, 1973; Copland 1976), and Ceraphronoidea (Ernst et al. 2013). The musculoskeletal ovipositor system and the actuation mechanisms of ichneumonoid wasps have been described recently in the ichneumonid *Venturia canescens* (Gravenhorst, 1829) (Eggs et al. 2018) and the braconid *Diachasmimorpha longicaudata* (Ashmead, 1905) (van Meer et al. 2020), respectively. Furthermore, drawings of the braconid ovipositor including all inherent cuticular elements exist for *Atanycolus rugosiventris* (Ashmead, 1889) (Snodgrass 1933), *Apanteles congestus* (Nees, 1834) (Oeser 1961), and *Stenobracon deesae* (Cameron, 1902) (Alam 1953; Venkatraman and Subba Rao 1954).

However, knowledge about structural and functional aspects of the ovipositor system of the ecologically and morphologically extremely diverse and species-rich Braconidae remains limited.

Habrobracon hebetor (Say, 1836) (Fig. 1a, b) is a gregarious, idiobiont, larval ectoparasitoid of pyralid moths (Lepidoptera) (Paust et al. 2006) and is well known for its use in biological pest control (Paust et al. 2006; Mbata and Shapiro-ilan 2010; Sanower et al. 2018). Dweck et al. (2008) provided the first morphological descriptions of the ovipositor of this species, with a strong focus on the terebra and its sensillar equipment. In the present study, however, we aim to describe thoroughly all the inherent cuticular elements of the ovipositor of *H. hebetor* in order further to discuss their structural, mechanical, and functional aspects. We have therefore combined scanning electron microscopic (SEM) and light-microscopic studies on both complete cuticular structures and histological serial sections. Serial sections of the terebra have been used to provide a 3D reconstruction that has helped us to understand its morphology especially with regard to all its functionally clustered inherent structures. Finally, we present a structural model of the braconid ovipositor and discuss its mode of function.

Materials and methods

Study animals

The *H. hebetor* (Fig. 1a, b) specimens used in this study originated from Sauter & Stepper GmbH (Ammerbuch, Germany), where they were bred on larvae of *Ephestia kuehniella* Zeller, 1879 (Lepidoptera: Pyralidae).

Sample preparation and light microscopy

For whole mount samples, female *H. hebetor* were killed in 70 % ethanol at 45 °C. The metasoma was cut off and macerated in 10% aqueous potassium hydroxide for up

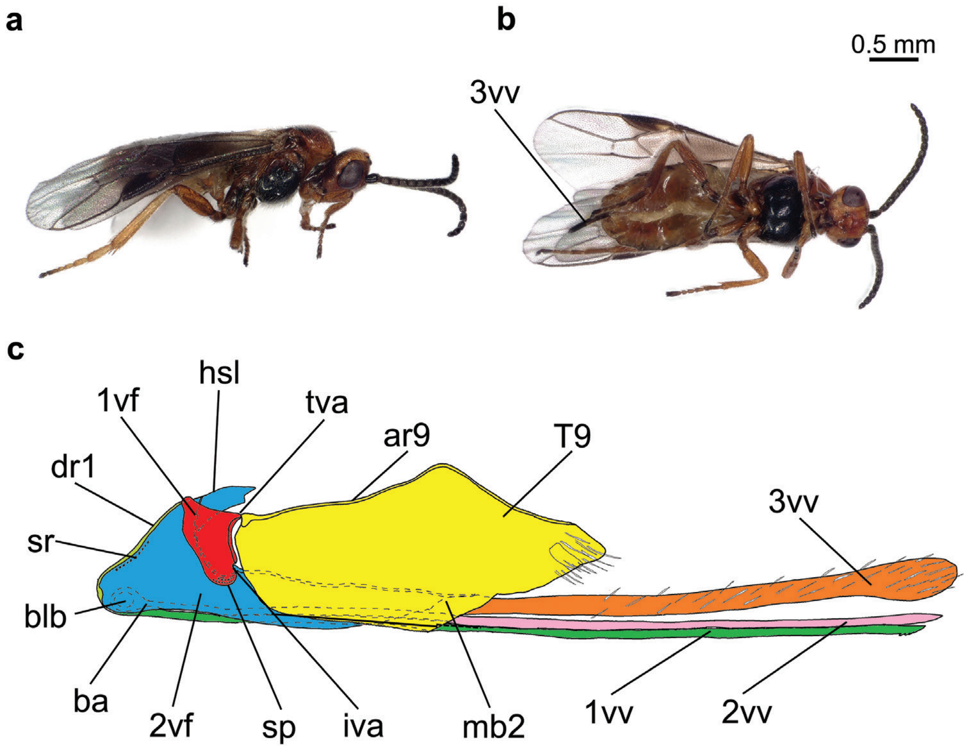

Figure 1. Habitus images of female *Habrobracon hebetor*: lateral (**a**) and ventral (**b**) ascpect. Schematic drawing of the ovipositor of *H. hebetor* (lateral view) based on the light microscopic and SEM images (**c**). Abbreviations: 1vf = 1st valvifer; 1vv = 1st valvula; 2vf = 2nd valvifer; 2vv = 2nd valvula; 3vv = 3rd valvula; ar9 = anterior ridge of T9; ba = basal articulation; blb = bulb; dr1 = dorsal ramus of the 1st valvula; hsl = hook-shaped lobe of the 2nd valvifer; iva = intervalvifer articulation; mb2 = median bridge of 2nd valvifers; sr = sensillar row of the 2nd valvifer, sp = sensillar patch of the 2nd valvifer; T9 = female T9; tva = tergo-valvifer articulation.

to 24 h at room temperature to remove tissues, cleaned in distilled water on a mini-shaker, and dehydrated stepwise in ethanol. We then dissected the ovipositor out of the metasoma by using thin tungsten needles, mounted the specimen onto a microscope slide, and embedded it in Entellan® (Merck KGaA, Darmstadt, Deutschland).

For semithin serial sections, we anaesthetized female *H. hebetor* with carbon dioxide. The metasomas were removed and, in order to avoid autolysis, immediately submersed in a primary fixative containing 2.5% glutaraldehyde and 5% sucrose, buffered with 0.1 M cacodylate to pH 7.4. During this fixation, the samples were held in an ice bath at approximately 4 °C for 4 h. Samples were rinsed three times for 10 min in pre-chilled 0.1 M cacodylate buffer (pH 7.4) and post-fixed by using a solution of 1% osmium tetroxide in 0.1 M cacodylate buffer at 4 °C for 4 h. After being further rinsed in the same buffer, the samples were dehydrated through a graded series of ethanol with steps of 30% for 15 min and 50% for 10 min at 4 °C, three times per step, and of 70%

for 10 min, three times at room temperature. The following steps were performed at room temperature. *En bloc* staining was conducted using a saturated solution of 70% ethanolic uranyl acetate for 12 h on a rotatory shaker. Afterwards, dehydration was continued in 5% steps, three times for 10 min each. The fully dehydrated samples were washed in 100% propylene oxide twice for 1 h , and subsequently infiltrated in Spurr low-viscosity embedding resin (Polysciences Inc., Warrington, PA, USA) via a propylene oxide:resin mixture at ratios of 1:1, 1:3, and 1:7 for 1 h per step and then in pure resin for 17 h on a rotatory shaker. As a last incubation step, the samples were placed in fresh pure resin, embedded in silicon molds, and polymerized at 70 °C for 8 h.

Semithin sections of 600 nm were cut perpendicularly to the terebra of *H. hebetor* by using an ultramicrotome Leica Ultracut UTC (Leica Microsystems GmbH, Wetzlar, Germany) equipped with a diamond knife (45° knife angle; DuPont Instruments, Wilmington, DE, USA); a series was obtained with 1920 sections. Semithin sections were then mounted on a microscopic slide by using a 'Perfect Loop for Light Microscopy' (Electron Microscopy Sciences, Hatfield, PA, USA), stained with Stevenel's blue (del Cerro et al. 1980) for 40 min at 60 °C, and subsequently washed in distilled water twice for 5 min each. After being dried, the stained sections were embedded in 'Xylolfreies Eindeckmittel' (Engelbrecht Medizin- und Labortechnik GmbH, Edermüde, Germany).

The image stack for the 3D reconstruction was generated using a Zeiss Axioplan (Carl Zeiss Microscopy GmbH, Jena, Deutschland) light microscope, equipped with a Nikon D7100 single-lens reflex digital camera (Nikon K.K., Tokio, Japan) and Helicon Remote software version 3.6.2.w (Helicon Soft Ltd, Kharkiv, Ukraine). Flawed images (missing or folded structures and staining problems) were replaced by a copy of the previous or the following image (this was the case for fewer than 3% of the images) for reconstruction purposes. Adobe Photoshop Lightroom version 6.0 (Adobe Systems, San José, CA, USA) was used for initial image processing (white balancing, color contrasting, black and white conversion), whereas Fiji (Schindelin et al. 2012; available online at https://imagej.net/Fiji) was employed for cropping, CLAHE filtering, and image stack calibration by using the plugin TrakEM2 (Cardona et al. 2012). A preliminary least square rigid alignment followed by an elastic alignment of the image stack was performed using the 'Elastic Stack Alignment' plugin (Saalfeld et al. 2012). The aligned image stack was then imported into Amira version 6.0 (FEI Company, Hillsboro, OR, USA). We pre-segmented the 1st and 2nd valvulae, the duct of the venom gland and the ligaments that connect the terebra and the 2nd valvifer in the software's segmentation editor by manually labeling approximately every 15th virtual slice along the terebra and every 4th virtual slice in the proximal bulbous region and assigned them to different 'materials'. The labels served as an input for automated segmentation by using the Biomedical Image Segmentation App Biomedisa (available online at https://biomedisa.de) (Lösel et al. 2020). The output of Biomedisa was then partially corrected manually in Amira, and a final surface model was generated.

Schematic drawings of the cross-sections of the terebra were generated in Inkscape version 0.92.4 (Inkscape Community; available online at http://www.inkscape.org/) based on the original light-microscopic images of the semithin sections.

For lateral and ventral habitus images, female wasps were imaged with a Keyence VHX-7000 Digital Microscope (Keyence Corporation, Osaka, Japan) using focus stacking.

Scanning electron microscopy (SEM)

For scanning electron microscopy (SEM), the specimens were air-dried in a desiccator with Silica gel blue (Carl Roth GmbH & Co. KG, Karlsruhe, Deutschland) for at least four days before being mounted with double-sided adhesive tabs onto stubs and sputter-coated with 19 nm pure gold by using an Emitech K550X (Quorum Technologies Ltd, West Sussex, UK). Images were taken with a scanning electron microscope of the type EVO LS 10 (Carl Zeiss Microscopy GmbH, Jena, Germany) and SmartSEM version V05.04.05.00 software (Carl Zeiss Microscopy GmbH, Jena Germany).

Results and discussion

As in all hymenopterans, the ovipositor of *H. hebetor* consists of three pairs of valvulae, two pairs of valvifers, and the female T9 (Fig. 1c).

Overall structure of the terebra

The 1st and 2nd valvulae form the terebra and enclose the egg canal (cf. Figs 2c–g, 3; Suppl. material 1). The terebra of *H. hebetor* extends far beyond the posterior tip of the metasoma. They are interconnected by a tongue and groove-like system, called the olistheter (oth; Fig. 2a–h). The olistheter comprises two longitudinal ridges that are called the rhachises (rh; Figs 2a, 5c, d) on both sides at the ventral surface of the 2nd valvula and that fit into corresponding T-shaped grooves termed the aulaxes (au; Figs 2a, 4b, f, h)

Figure 2. (next page) Cross sections through the terebra of *Habrobracon hebetor* (from proximal to distal); schematic drawings of the 1st and 2nd valvula (**a–i**) based on the light microscopic images of the presented semithin sections (**a'–i'** 600 nm; stained with Stevenel's blue). The drawings are of the same size ratio. The 2nd valvulae possesses, in the proximal region, two lumina that merge into one in the most distal region (**h–i**). The bulbs (**b**) and the valvilli (**g**) are visible. The orange lines (in **e, f**) mark the position of the distally pointing ctenoid structures on the dorsal surfaces of the 1st valvulae, which are in close contact with the ventral surface of the 2nd valvula. The genital membrane connects the dorsal margins of the 2nd valvifers (**b'–h'**) **c** fine cuticular structures arise from the dorsal and ventral parts of the 2nd valvula and define the lumina of the bulbs (arrow) **h I** olistheter-like interlocking system connecting the medial surfaces of the apices of the paired 1st valvulae (arrow). Final segmented 3D reconstruction based on a semithin section series (600 nm thickness) **a*–i*** position of each single section marked on the final 3D reconstruction of the terebra. Abbreviations: 1vv = 1st valvula; 2vv = 2nd valvula; 3vv = 3rd valvula; au = aulax; blb = bulb; cr = longitudinal crack of 2nd valvula; ec = egg canal; fl1 = longitudinal flap of the 1st valvula; gm = genital membrane; igs = internal guiding structure; l1 = lumen of 1st valvula; l2 = lumen of 2nd valvula; lb = lumen of the bulb; lg = ligament; oth = olistheter; rh = rhachis; vd = duct of the venom gland; vl = valvillus.

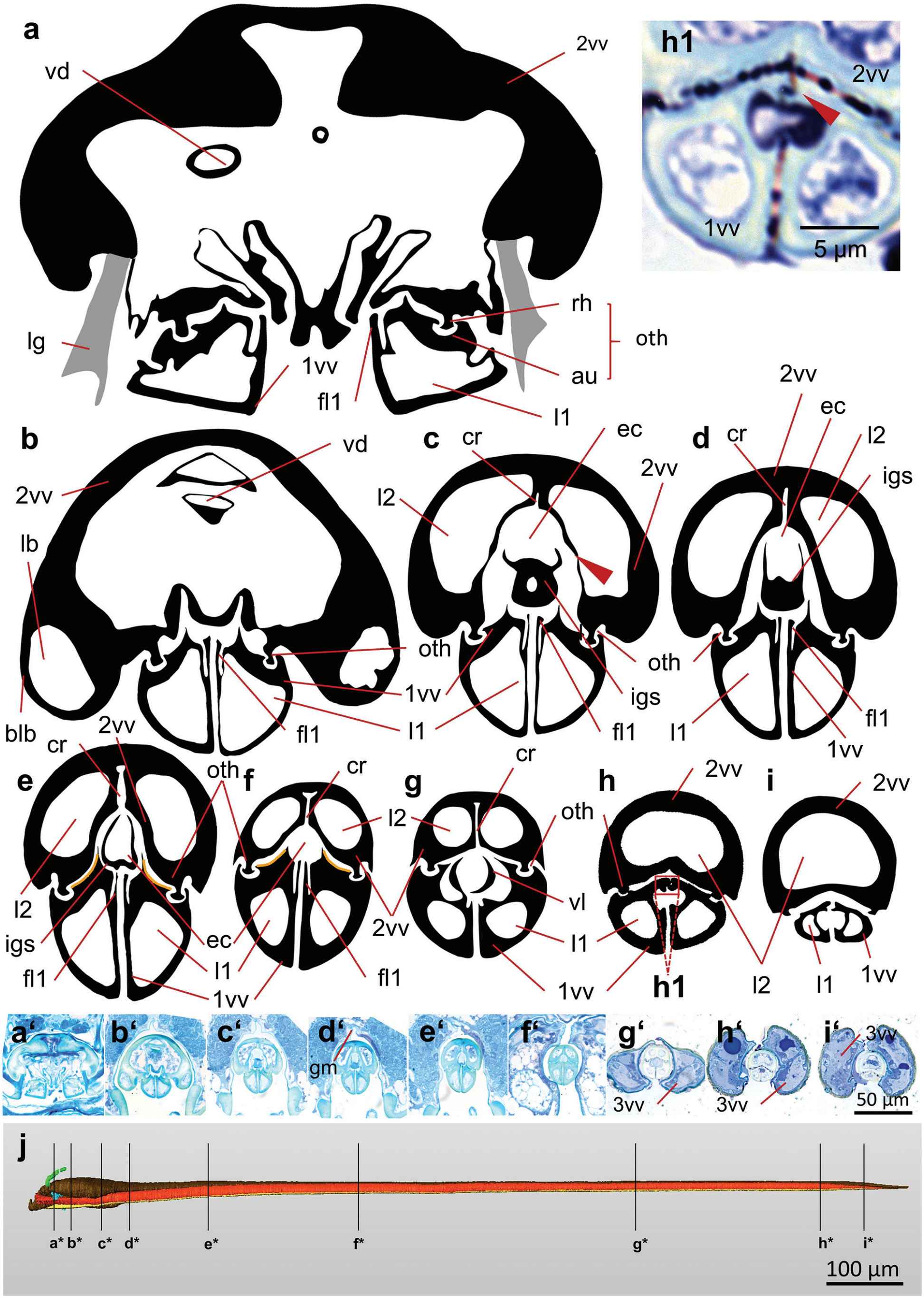
a
vd
2vv
lg
1vv
fl1
rh
au
oth
l1
h1
2vv
1vv
5 µm
b
vd
2vv
lb
blb
oth
1vv
fl1
l1
c
cr
ec
l2
2vv
oth
igs
fl1
l1
1vv
d
cr
ec
2vv
l2
igs
fl1
1vv
l1
e
cr
2vv
oth
l2
igs
fl1
ec
l1
1vv
f
cr
l2
2vv
fl1
g
cr
oth
vl
l1
1vv
h
2vv
h1
l2
i
2vv
l1
1vv
a'
b'
c'
d'
gm
e'
f'
g'
3vv
h'
3vv
i'
3vv
50 µm
j
a* b* c* d* e* f* g* h* i*
100 µm

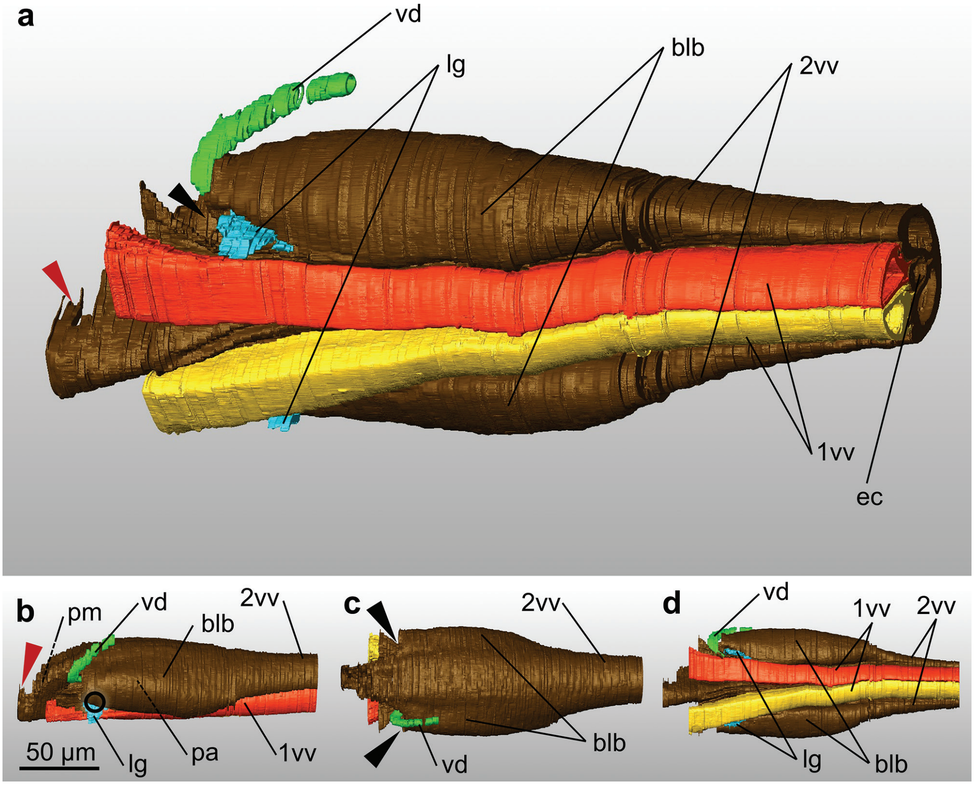

Figure 3. 3D reconstruction of the basal part of the terebra of *Habrobracon hebetor* composed of the 2nd valvulae and the paired 1st valvulae, based on a semithin section series (600 nm thickness **a** lateroventral aspect **b** lateral aspect **c** dorsal aspect **d** ventral aspect). The duct of the venom gland enters dorsoproximally on the left side only. The two ligaments connect the 2nd valvula to the anterior parts of the 2nd valvifers (not visible in these images). The black circle (**b**) indicates the rotation axis of the basal articulation. The lines of the processus articularis and processus musculares (**b**) point to their presumed position according to the results of van Meer et al. (2020). The peak-like structure at the anterior end of the 2nd valvula (red arrow in **a, b**) is part of the processus musculares. There are two openings (black arrows in **a, c**) at the proximal side of the bulbs. The duct of the venom gland enters on the left side only. Abbreviations: 1vv = 1st valvula; 2vv = 2nd valvula; blb = bulb; ec = egg canal; lg = ligament; pa = processus articularis; pm = processus musculares; vd = duct of the venom gland.

along the dorsal surface of each of the 1st valvulae. This system allows the 1st valvulae to slide longitudinally relative to each other when actuated by the corresponding operating muscles (Oeser 1961; Quicke et al. 1994). Distally pointing scale-like structures are found on both the olistheter elements and might reduce the friction forces by reducing the contact surface between the 1st valvulae and the 2nd valvula (sc; Fig. 4f) (Rahman et al. 1998).

In *H. hebetor*, the cross sections of the terebra differ notably along its length (Fig. 2a–i). A common oviduct enters the proximal bulbous part of the terebra (Bender

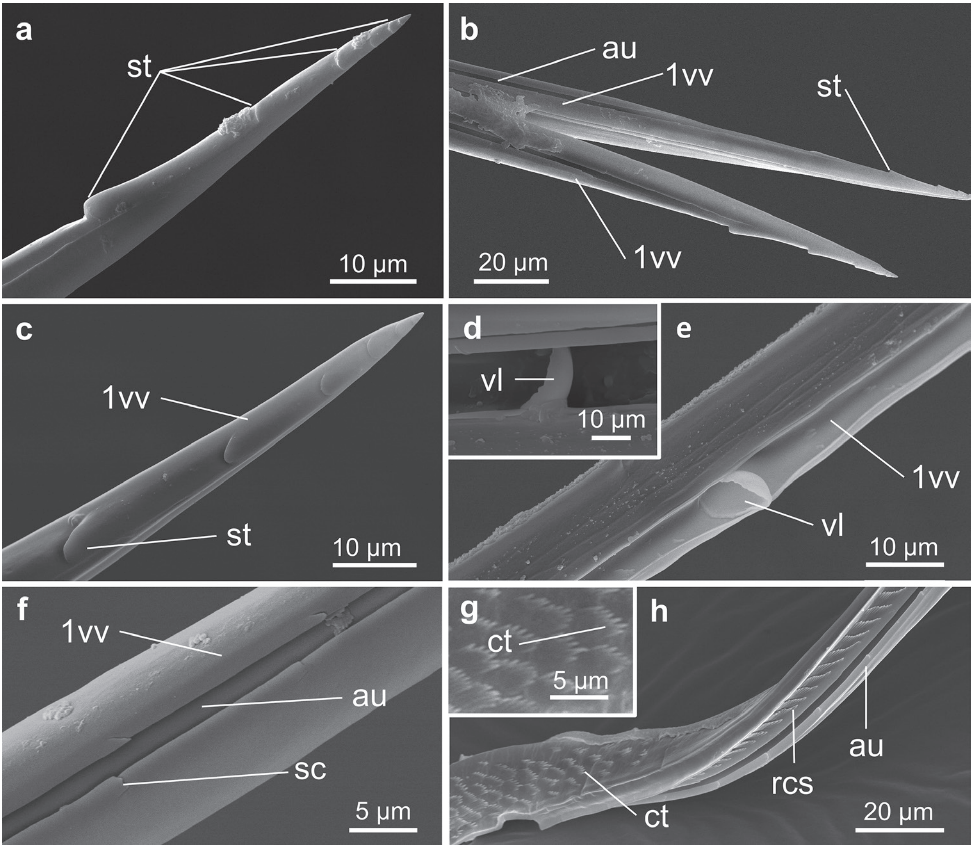

Figure 4. SEM images of the 1st valvulae of *Habrobracon hebetor* **a–c** apex of 1st valvula with sawteeth (**a** lateral aspect **b–c** dorsal aspect). The aulaces are visible (**b**) **d–e** valvillus of 1st valvula (distal is right) **f** distally oriented scale-like structures on the lateral walls of the aulax **g** leaf-like ctenidia on the medial side of 1st valvula **h** 1st valvula with distally oriented ctenoid structures on its dorsal side (contact surface with the 2nd valvula) and ctenidia on its medial side (contact surface with the opposing 1st valvula building the egg canal in the distal part of the terebra). Abbreviations: 1vv = 1st valvula; au = aulax; ct = ctenidium; rcs = row of ctenoid structures; sc = scales; st = sawtooth; vl = valvillus.

1943; Pampel 1914), where it ends at the base of the egg canal (Quicke 1997). Distally, the egg canal is largely defined by the 1st valvulae, but with the dorsal side being formed by the 2nd valvula. The diameter of the terebra decreases from proximal to distal, whereas the diameter of the egg canal remains constant for a long distance from proximal until the valvillus (see subsection '1st valvulae').

1st valvulae

The paired 1st valvulae of *H. hebetor* form the ventral half of the terebra (1vv; Figs 1c, 2a–i, 3, 7a). The proximal end of each 1st valvula is continuous with its dorsal ramus (dr1; Figs 1c, 7c, h), which is fused with the anterodorsal corner of the 1st valvifer (Figs 7a, c, e, 8).

At their apices, the 1st valvulae of *H. hebetor* possess several sawteeth, which decrease in size apically (st; Fig. 4a, b, c) (cf. Dweck et al. 2008). They probably serve to penetrate the substrate and the host's skin and tissue. Distally pointing ctenoid structures (rcs; Fig. 4h) arranged in rows can be found on the dorsal surfaces of the 1st valvulae, which are in close contact with the ventral surface of the 2nd valvula (orange line; Fig. 2e, f). These ctenoid structures potentially reduce friction forces by minimizing the contact surface between the 1st and the 2nd valvula. The aulaces do not extend all the way to the apex of the 1st valvulae but end just before the lateral sawteeth occur (au; Fig. 4b). Both 1st valvulae are separated for the most of their length. However, mediodorsally at their very apex, the two 1st valvulae become interlocked dorsally by a mechanism similar to that of the olistheter (Fig. 2h1; also see fig. 4a of Dweck et al. 2008). Such a mechanism has previously been observed in other braconids (*Zaglyptogastra* (Quicke 1991), *Aleiodes*, *Ligulibracon* and *Odontobracon* (Quicke et al. 1994), and *D. longicaudata* (van Meer et al. 2020)) and is suggested to be an adaptation to the injection of venom into the host while laying the egg externally (Dweck et al. 2008). In addition, this mechanism might also increase the stability of the apex of the terebra when the host cuticle is pierced (Quicke 2015).

A single valvillus situated on the inner surface of each 1st valvulae protrudes inside the egg canal (vl; Figs 2g, 4d, e; cf. Dweck et al. 2008). The valvillus is a bilaterally concave structure lying in the distal third of the terebra and occupies the whole diameter of the egg canal. Valvilli can be found in the Ichneumonoidea and in various families of the Apocrita (Snodgrass 1933; Quicke et al. 1992; Rahman et al. 1998). They are postulated to serve as a stop and release mechanism for the egg by maintaining the egg in position within the terebra and blocking the egg canal in Ichneumonoidea (Rogers 1972; Rahman et al. 1998; Boring et al. 2009), or for venom pumping in Apocrita (Quicke et al. 1992). However, in the ectoparasitoid *H. hebetor*, the eggs are observed to advance and even partially emerge ventrally at the base of the terebra, i.e. in between the 1st valvulae and near the genital opening (Prozell et al. 2006; Wührer et al. 2009, see also Shaw 2017). Further distally, the valvilli seem to divert the egg ventrally between the 1st valvulae and to press it out completely, since the egg does not emerge at the tip of the terebra but rather ventrally in between the 1st valvulae approximately at the region at which the valvilli are located (Prozell et al. 2006; Wührer et al. 2009). We therefore suggest that the valvilli guide the relatively large egg ventrally out in between the 1st valvulae. The latter are capable of being widely spread in this region because of the olistheter mechanism (Shaw 2017). In cross sections further apically to the valvilli, an egg canal is rarely visible or is absent (Fig. 2h, i), which suggests that at that point the egg has already left the terebra. In addition, the apical interlocking in between the two 1st valvulae (red arrow; Fig. 2h1), which is similar to that of the olistheter, prevents the canal from expanding at the very apex. Proximal to the valvillus, the walls of the egg canal carry leaf-like ctenidia (ct; Fig. 4g, h), which are arranged in rows and are directed towards the distal end of the terebra. These rows of ctenidia point distally in

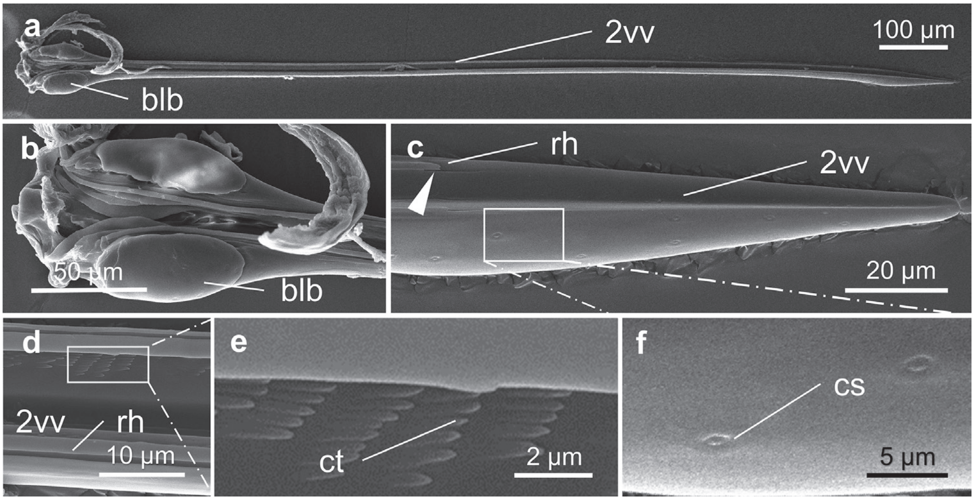

Figure 5. SEM images of the 2nd valvula of *Habrobracon hebetor* **a** overview of the 2nd valvula (ventral aspect with the interlocked 1st valvulae removed) **b** proximal part of 2nd valvula featuring the bulbs **c** apex of 2nd valvula with the ending of the rhachises (arrow) and campaniform sensillae (medioventral aspect) **d–e** middle part of the 2nd valvula showing the rhachises and distally oriented ctenidia **f** sensilla at the apex of the 2nd valvula (detail image of **c**). Abbreviations: 2vv = 2nd valvula; blb = bulb; cs = campaniform sensilla; ct = ctenidia; rh = rhachis.

the direction of egg movement and presumably prevent the regression of the egg during the oviposition process (Austin and Browning 1981). Setiform structures (= subctenidial setae *sensu* Rahman et al. 1998) are also found at the inner walls of the 1st valvulae lying distally to the valvilli. They are arranged in distinct rows.

Each 1st valvula contains a lumen (l1, Fig. 2a–i) whose cuticular walls differ along its length. Proximally, the cuticle is thin but becomes thicker towards the middle and diminishes again apical to the valvillus (Fig. 2a–i). In cross section, the shape of the 1st valvula differs between the basal region and the rest of the terebra. In the basal part, it is triangular in shape (1vv; Fig. 2a), whereas further distally, it appears more oval (1vv; Fig. 2b–i). A longitudinal flap extends along the mediodorsal edge for most of the length of the 1st valvulae and is clearly recognizable in cross sections (fl1; Fig. 2a–f). This flap is highly prominent in the proximal part of the terebra but vanishes further apically (fl1; Fig. 2g–i). It might seal the egg canal to prevent the leaking of venom, since the pressure of the venom has been suggested to squeeze the two flaps together and therefore to seal the gap (Quicke et al. 1994; Shaw 2017). It has been observed in almost all the examined braconid species (Quicke and van Achterberg 1990; Quicke et al. 1994).

2nd valvula

In *H. hebetor*, the 2nd valvula (2vv; Figs 1c, 2a–i, 3, 5a, 7a) form the dorsal half of the terebra, and its proximal bulbous end (blb; Figs 1c, 2b, 3, 5b, 7e, h; called the bulbs in the following) is connected with the 2nd valvifer via the basal articulation (ba; Figs 1c, 7h).

The apex of the 2nd valvula is not serrated but is slightly enlarged before it narrows towards the tip (Figs 5a, c, 7a). In contrast to many ichneumonid and other braconid species (cf. Boring et al. 2009; Shah et al. 2012; Eggs et al. 2018), the 2nd valvula of *H. hebetor* does not feature a prominent apical notch. Campaniform sensilla can be found in this area (cs; Fig. 5f) (for a discussion of the sensillary equipment of the terebra of *H. hebetor*, see Dweck et al. 2008). Similar to the aulaces on the 1st valvulae, the rhachises (rh; Fig. 5c, d) do not extend all the way to the apex but end at about the same distance away from the apex as seen for the aulaces (arrow; Fig. 5c). The apical half of the ventral side of the 2nd valvula forms the dorsal wall of the egg canal and is, similar to the 1st valvulae, covered by rows of ctenidia directed distally (ct; Fig. 5e). As previously discussed for the 1st valvulae, these structures might prevent the regression of the egg during oviposition (cf. Rahman et al. 1998). Medioproximally, the bulbs feature ligaments (lg; Figs 2a, 3a, b, d) that connect the 2nd valvula with the anterior section of the 2nd valvifer. The ligament marks the region at which parts of the 2nd valvifer merge into the anterior part of the 2nd valvula. The bulbs also contain a lumen (lb; Fig. 2b). The proximal end of the 2nd valvula bears the processus articularis (pa; Figs 3b, 7h) laterally and the processus musculares (pm; Figs 3b, 7h) at the anterior peak-like structure of the 2nd valvula (red arrow; Fig. 3a, b). However, the medial 2nd valvifer-2nd valvula muscle (M-2vfl-2vlv) that might stabilize the 2nd valvifer and that was newly described in the braconid *D. longicaudata* by Meer et al. (2020) was absent in our serial sections. There are two openings (black arrows; Fig. 3a, c) at the proximal side of the bulbs. The duct of the venom gland enters the dorsoproximal area of the bulbs on the left side only (vd; Figs 2a, b, 3, Suppl. material 2) (cf. Bender 1943, who investigated the anatomy and histology of the female reproductive organs of the closely related *Habrobracon juglandis* (Ashmead, 1889)). Further distally, the closed duct of the venom gland seems to disappear and to merge with the egg canal formed by the valvulae (Suppl. material 2). In this area, the venom presumably flows into the egg channel that is formed by both the 1st and 2nd valvulae with the longitudinal flaps of the 1st valvulae acting as a seal (fl1; Fig. 2a–f).

Proximally, the 2nd valvula features a distinct longitudinal crack at the ventral side along the middle, which is clearly visible in cross-section (cr; Fig. 2c–g), presumably indicating the paired origin of the 2nd valvulae. At the basal part of the 2nd valvula, fine cuticular structures (arrow; Fig. 2c) arise from it dorsal and ventral parts and define the two lumina (l2; Fig. 2c–g) that run almost the entire length of the 2nd valvula and that fuse at the apex (Fig. 2h, i). Proximally, the ventral part of the 2nd valvula gradually changes shape and forms a U-shaped structure that extends distally into the egg canal (Suppl. material 2). This internal structure (igs; Fig. 2c–e) presumably helps in guiding the egg by forming a temporary egg canal. Without this internal guiding structure, the diameter of the egg canal would be large in this proximal region; this might lead to a lowered internal pressure and thus to problems when the egg is pushed further distally.

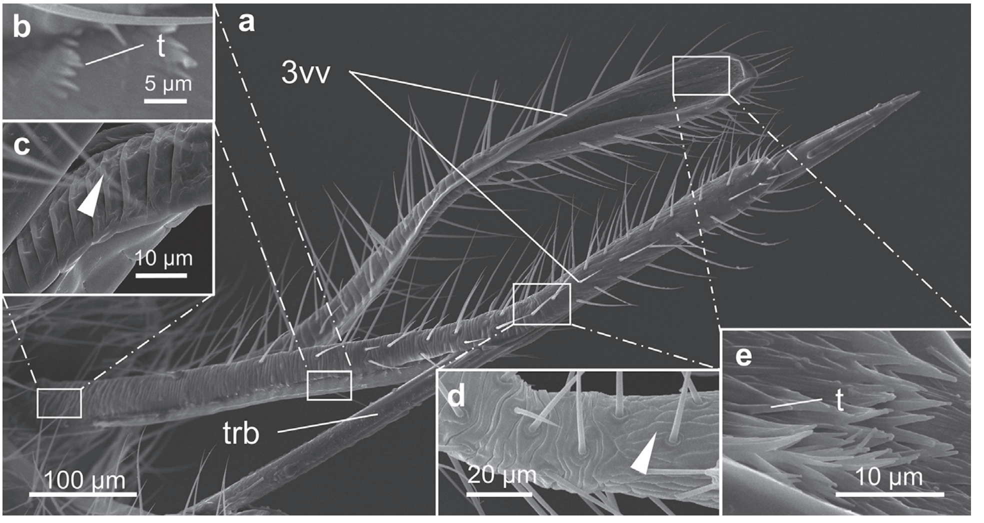

Figure 6. SEM images of 3rd valvulae of *Habrobracon hebetor* **a** the terebra is partially embraced by the 3rd valvulae **b** inner proximal surface of the 3rd valvulae with fine trichomes distally **c** outer surface of the 3rd valvulae, proximally exhibiting annulation caused by fine transverse furrows (arrow) **d** outer surface of the 3rd valvulae at the transition zone (arrow) between the distal longitudinal ridge to the proximal vertically folded surface at the region in which the 3rd valvulae expand **e** inner surface of the apex of a 3rd valvula covered by trichomes. Abbreviations: 3vv = 3rd valvula; trb = terebra; t = trichome.

3rd valvulae

The paired 3rd valvulae of *H. hebetor* originate at the distal end of the 2nd valvifers and extend far beyond the posterior tip of the metasoma towards the tip of the terebra (Figs 1b,c, 7a, e). Each is U-shaped in cross-section (3vv; Figs 2g'–i', 6a) and they completely ensheath and protect the terebra in the resting position (3vv, trb; Figs 2g'–i', 6a) (cf. Bender 1943; Dweck et al. 2008). The distal third of the 3rd valvulae is enlarged (Figs 6a, 7a), and their lateral surfaces differ over the course of their length: proximally, the 3rd valvulae are annulated by fine transverse furrows (arrow; Fig. 6c; cf. Vilhelmsen 2003; Eggs et al. 2018), whereas the enlarged distal part lacks these structures (arrow; Fig. 6d). Trichomes, which Dweck et al. (2008) have described as trichoid sensilla, cover most of the external surface of the 3rd valvulae (Fig. 6a). The density of the trichomes varies along the length of the 3rd valvulae and is highest at the apex (Fig. 6a).

The inner surface of the 3rd valvulae facing the terebra is densely covered by trichomes (t; Fig. 6b, e), particularly at the distal enlarged part (Fig. 6a, e). These structures might be involved in cleaning the terebra sensilla between oviposition episodes (Quicke et al. 1999; Vilhelmsen 2003). Observations have shown that the 3rd valvulae also play a role in stabilizing the terebra during oviposition (Prozell et al. 2006; Wührer et al. 2009; Vilhelmsen 2003; Cerkvenik et al. 2017; Eggs et al. 2018; van Meer et al. 2020).

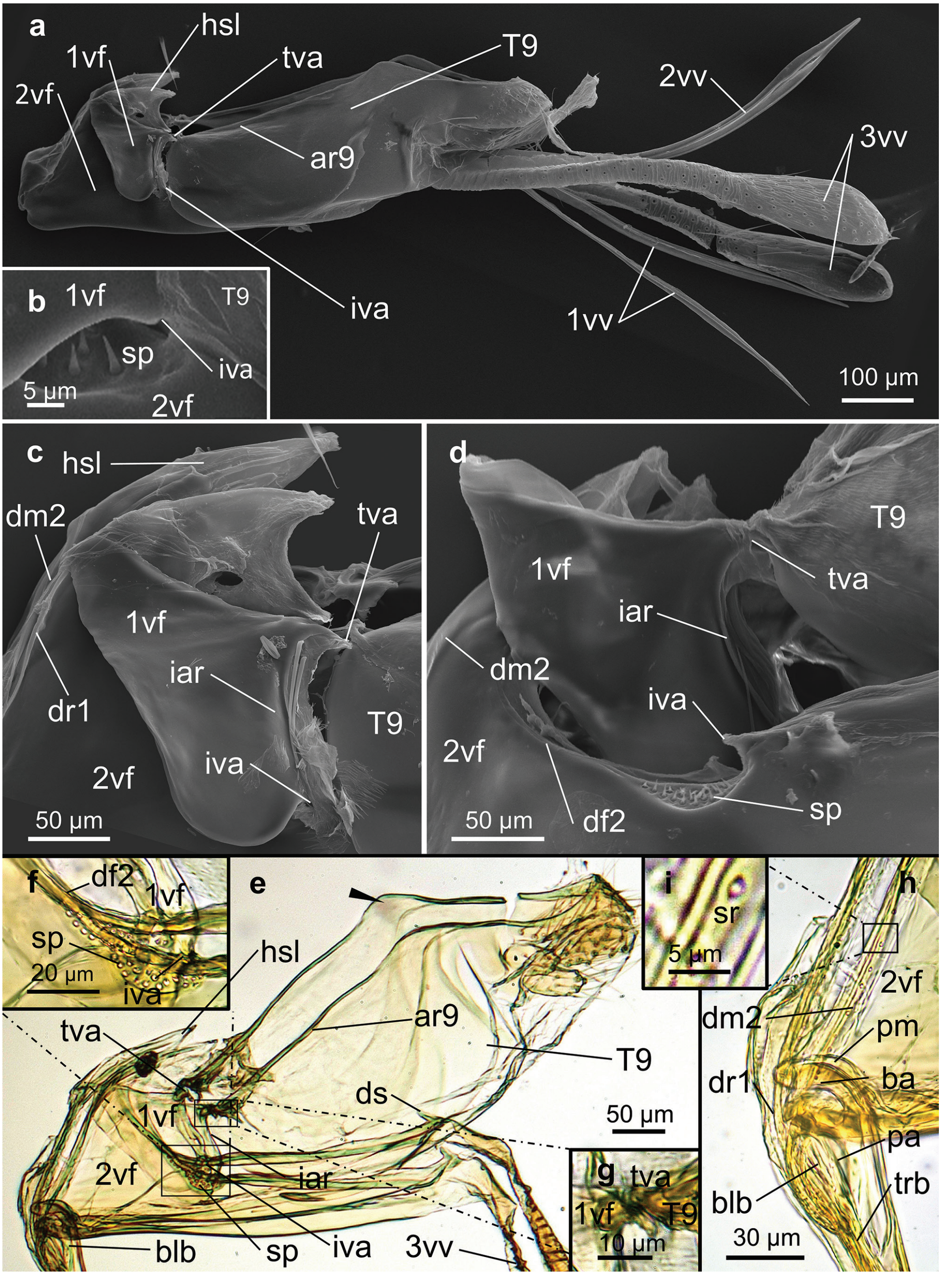

a
hsl
1vf
2vf
tva
T9
2vv
3vv
ar9
iva
1vv
100 µm
b
1vf
T9
sp
iva
5 µm
2vf
c
hsl
dm2
tva
1vf
iar
dr1
T9
iva
2vf
50 µm
d
T9
1vf
tva
iar
dm2
iva
2vf
50 µm
df2
sp
f
df2
1vf
sp
20 µm
iva
e
hsl
tva
ar9
T9
ds
1vf
2vf
iar
blb
sp
iva
3vv
50 µm
g
tva
1vf
T9
10 µm
i
sr
5 µm
h
2vf
dm2
pm
dr1
ba
pa
blb
trb
30 µm

1st valvifer

In lateral view, the paired 1st valvifers of *H. hebetor* have a compact triangular shape with rounded edges (1vf; Figs 1c, 7a, c–e, 8). The intervalvifer articulation (iva; Figs 1c, 7a, c–f), a rotational joint, is located at the rounded posteroventral side and connects the 1st valvifer to the 2nd valvifer. The ventral edge of the 1st valvifer is placed laterally of the 2nd valvifer and seems to be in contact with a sensillar patch (sp; Figs 1c, 7b, d–f) that extends dorsally at the anterior beginning of the the dorsal flange of the 2nd valvifer (df2; Fig. 7d, f). The tergo-valvifer articulation (tva; Fig. 7a, c–e, g) connects the 1st valvifer to the female T9. A ridge, called the interarticular ridge of the 1st valvifer (iar; Figs 1c, 7c–e, 8), extends in between the two articulations. This ridge might mechanically stabilize the 1st valvifer and prevent it from extensive deformation. At its anterodorsal corner (arrow; Fig. 8), the 1st valvifer is fused with the dorsal ramus of the 1st valvula (dr1; Figs 1c, 7c, h, 8), which is continuous with the 1st valvula.

2nd valvifer

The paired 2nd valvifers of *H. hebetor* are elongated in the longitudinal axis (2vf; Figs 1c, 7a, e). The anteromedial socket-like part of the 2nd valvifer is connected to the laterally placed bulbs of the 2nd valvula (blb; Figs 1c, 3, 7e, h) via the ball-and-socket-like basal articulation (ba; Figs 1c, 7h). The posterior ends of both the 2nd valvifers are connected to the 3rd valvulae (3vv; Figs 1c, 7a, e). At their posterodorsal ends, the two 2nd valvifers are connected by a median bridge (mb2; suggested position indicated in Fig. 1c). A massive dorsal spike (ds; Fig. 7e), a structure that has not as yet been described in other parasitoid wasps, is present at the posterior end of the 2nd valvifer and potentially serves as an apodeme. In addition, a flexible cuticular area, a conjunctiva called the genital membrane (gm; Fig. 2d'), connects the ventral margins of the 2nd valvifers arching above the 2nd valvula.

Figure 7. (previous page) SEM (**a–d**) and light microscopic (**e–i**) images of the ovipositor of *Habrobracon hebetor* **a** overview of the ovipositor (lateral aspect; visible pore-like structures are presumably artefacts of detached trichomes) **c** 1st valvifer exhibiting the interarticular ridge and the hook-shaped lobe of the 2nd valvifer. The 1st valvifer is continuous with the dorsal rami of the 1st valvula and is articulated with the 2nd valvifer and the female T9 via the intervalvifer articulation and the tergo-valvifer articulation, respectively **d** sensillar patch of the 2nd valvifer (made visible by partly removal of the 1st valvifer) **b, f** sensillar patch of the 2nd valvifer **e** overview of the 2nd valvifer and female T9. The arrow shows the dorsal hump of the T9 **g** tergo-valfiver articulation between the 1st valvifer and female T9 **h** detail image of e. The laterally placed bulbs of the most proximal part of the 2nd valvula are articulated with the paired 2nd valvifers via the basal articulation **i** sensilla in a row at the dorsal margin of the 2nd valvifer. Abbreviations: 1vf =1st valvifer; 1vv = 1st valvula; 2vf = 2nd valvifer; 2vv = 2nd valvula; 3vv = 3rd valvula; ar9 = anterior ridge of T9; ba = basal articulation; blb = bulb; df2 = dorsal flange of 2nd valvifer; dm2 = dorsal margin of the 2nd valvifer; dr1 = dorsal ramus of the 1st valvula; ds = dorsal spike of the 2nd valvifer; hsl = hook-shaped lobe of the 2nd valvifer; iar = interarticular ridge of the 1st valvifer; iva = intervalvifer articulation; sp = sensillar patch of the 2nd valvifer; sr = sensillar row of the 2nd valvifer; pa = processus articularis; pm = processus musculares; T9 = female T9; trb = terebra; tva = tergo-valvifer articulation.

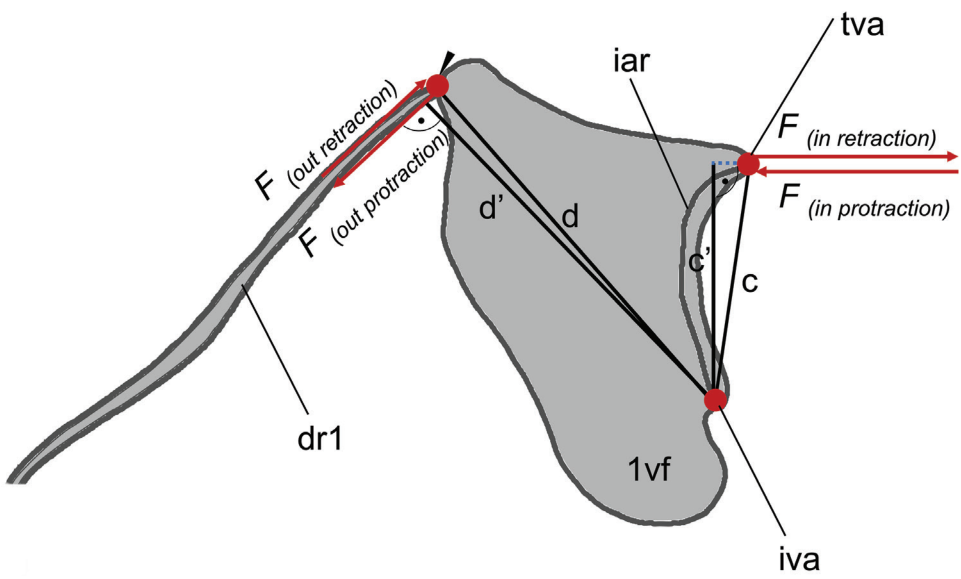

Figure 8. Functional lever model of 1st valvifer with both articulations and the beginning of the dorsal ramus of the 1st valvula (arrow) with the intervalvifer articulation acting as pivot point. c = anatomical inlever ; c' = effective (= mechanical) inlever; d = anatomic outlever; d` = effective (= mechanical) outlever; $F_{(in\ protraction)}$, $F_{(in\ retraction)}$ = Force input at the 1st valvifer; $F_{(out\ protraction)}$, $F_{(out\ retraction)}$ = Force output at the 1st valvifer that is transferred to the dorsal ramus of the 1st valvula. $c' \cdot F_{(in)} = d' \cdot F_{(out)}$. Abbreviations: 1vf = 1st valvifer; dr1 = dorsal ramus of the 1st valvula; iar = interarticular ridge of the 1st valvifer; iva = intervalvifer articulationtva = tergo-valvifer articulation.

At its anterodorsal corner, the 2nd valvifer extends upwards in a hook-shaped lobe (hsl; Fig. 7a, c, e; *sensu* Snodgrass 1933), and features the elongated anterodorsal ridge of the 2nd valvifer, the so called dorsal margin of the 2nd valvifer (dm2; Fig. 7c, d, h). The dorsal projection of the 2nd valvifer, a tongue-like structure situated on the dorsal margin of the 2nd valvifer, is continuous with the olistheter. The corresponding groove is located on the dorsal side of the dorsal ramus of the 1st valvula (dr1; Fig. 7c, h; cf. fig. 4h1 of Eggs et al. 2018) and enables its back and forth movement. This hook-shaped lobe might guide and stabilize the 1st valvifer during its posterior pivoting but might also allow for a larger arc of movement of the 1st valvifer and therefore a greater retraction distance of the 1st valvulae (cf. Eggs et al. 2018).

Two main ridges are found on the 2nd valvifer, i.e. (1) the dorsal flange of the 2nd valvifer (df2; Fig. 7d, f), which expands from the sensillar patch in the direction of the hook-shaped lobe and posteriorly from the sensillar patch to the origin of the 3rd valvulae (Fig. 7e), and (2) the dorsal margin of the 2nd valvifer (dm2; Fig. 7c, d, h). The two cuticular ridges might have a stabilizing function to prevent deformation. The 2nd valvifer of *H. hebetor* does not feature a basal line (e.g. in contrast to the ichneumonid *Venturia canescens* (Gravenhorst, 1829), see fig. 4e of Eggs et al. 2018), a ridge that extends from the pars articularis to the dorsal flange of the 2nd valvifer.

Clusters of sensillae ("styloconic sensillae" according to Dweck et al. 2008) occur in two regions. The first cluster, called the sensillar patch (sp; Figs 1c, 7b, d–f), is situated ventrally of the intervalvifer articulation and is covered by the 1st valvifer laterally. The second cluster occurs at the dorsal margin of the 2nd valvifer (sr; Figs 1c, 7h, i). These sensilla are arranged in a row and are in contact with the dorsal ramus of the 1st valvula. The two sensilla clusters presumably monitor the pro- and retraction movements of the 1st valvifers and the attached 1st valvulae, respectively. The density of sensilla in the patch is much higher than that on the dorsal margin of the 2nd valvifer.

Female T9

The female T9 is unpaired and elongated (T9; Figs 1c, 7a, c, d, e). At its anterodorsal corner, it is connected to the 1st valvifer via the tergo-valvifer articulation (tva; Figs 1c, 7a, c–e, g). Dorsally, it features the anterior ridge almost throughout its length (ar9; Fig. 7e), and posteriorly, it bears a hump-shaped structure (arrow; Fig. 7e). The female T9 mostly lies inside the abdomen, and only the posterolateral part that faces the outside is covered with hairs.

Mode of function of the ovipositor

Functional models of the actuation and movement mechanisms based on thorough analyses of the musculoskeletal system of an ichneumonid and a braconid wasp have recently been described (Eggs et al. 2020, van Meer et al. 2020) and are summarized in the following. Although, in our study, we have not considered the muscles of the system, we have basically found the same arrangement of cuticular elements in the ovipositor system of *H. hebetor* as described in both of the above-mentioned studies. Hence, we assume analogous functional morphological conditions, although we point out any possible *H. hebetor*-specific modifications.

The ovipositor movements are mainly actuated by two pairs of antagonistically working muscles (further described below), i.e. (1) the depression (i.e. downward rotation to the active position) and elevation (i.e. upward rotation back to the resting position) of the terebra, and (2) the pro- and retraction of the 1st valvulae. Smaller muscles, i.e. the 1st valvifer-genital membrane muscle or the posterior T9-2nd valvifer muscle, might predominantly serve to stabilize the ovipositor system during oviposition.

(1) Depression and elevation of the terebra: The basal articulation is composed of the processus articularis (pa; Figs 3b, 7h) at the 2nd valvulae and the pars articularis at the 2nd valvifer. The pars articularis is a small area of anteroventral corners of the 2nd valvifer, whereas the processus articularis is the respective structure of the bulb. The posterior 2nd valvifer-2nd valvula muscle depresses the terebra, i.e. rotates it downwards to the active position from its resting position between the paired 3rd valvulae. The tendon of this muscle inserts at the processus musculares (pm; Figs 3b, 7h), which is situated at the peak-like posterior part of the 2nd valvula (arrow; Fig. 3a, b) and thus

increases the moment arm. However, the moment arm most probably changes over the range of motion of the terebra. In *H. hebetor*, we assume that the virtual line that can be drawn perpendicularly to the length axis of the terebra through the ligaments (lg; Figs 2a, 3a, b, d) lying anterolaterally on the bulbs (blb; Figs 2b, 5a, b, 7e, h) most likely forms the rotation axis (= joint axis, pivot point or fulcrum; black circle; Fig. 3b), since the ligaments form the connections of the 2nd valvula with the anterior parts of the 2nd valvifers and can only stretch to a limited extent. Van Meer et al. (2020) postulate that, in the braconid *D. longicaudata*, the rotation axis lies directly anterior to the bulbs. In addition, these authors have observed that, during terebra depression (towards an active probing position), the lateral bulbs are pulled out of the socket-like anterior parts of the 2nd valvifers, which are pushed slightly apart. The ball-and-socket-like connection is therefore assumed mainly to stabilize the terebra in its resting position. The antagonistically acting anterior 2nd valvifer-2nd valvula muscle inserts at the processus musculares and elevates the terebra, i.e. rotates it back upwards towards the resting position.

(2) Pro- and retraction of the 1st valvulae: The 1st valvifer, 2nd valvifer, and the female T9 form a mechanical cluster of functionally interconnected elements (for detailed functional models see fig. 5 of Eggs et al. 2018 and fig. 8 of van Meer et al. 2020). The dorsal and the antagonistically acting ventral T9-2nd valvifer muscle change the relative position of the 2nd valvifer and the female T9. Both of these structures are connected with the 1st valvifer via the intervalvifer and the tergo-valvifer articulation (Fig. 7c), respectively. Moreover, both are rotational joints that allow rotation in the sagittal plane only. The 1st valvifer acts as a lever (Fig. 8) that transfers its movements to the dorsal ramus of the 1st valvula (dr1; Figs 7c, h, 8). Contraction of the dorsal T9-2nd valvifer muscle leads to an anterior rotation of the 1st valvifer around the intervalvifer articulation. The 1st valvifer acts as a lever that transfers these movements to the dorsal ramus of the 1st valvula, thus causing the 1st valvula to slide distally relative to the 2nd valvula, i.e. to protract. *Vice versa*, contraction of the antagonistic ventral T9-2nd valvifer muscle leads to a posterior rotation of the 1st valvifer, causing the 1st valvula to slide proximally to the 2nd valvula, i.e. to retract (Eggs et al. 2018; van Meer et al. 2020). The hook-shaped lobe of the 2nd valvifer (hsl; Fig. 7a, c, e) might allow a larger arc of movement of the 1st valvifer and therefore a larger retraction distance of the 1st valvulae. During the retraction of the 1st valvula, the dorsal ramus of the 1st valvula (dr1; Fig. 7c, h) can slide along the dorsal projection of the 2nd valvifer almost until the posterior end of the hook-shaped lobe (hsl; Fig. 7a, c, e).

In the context of the described movements, the 1st valvifer acts as a one-armed class 3 lever (force arm smaller than load arm). In our lever model (Fig. 8), we use the 2nd valvifer (2vf; Fig. 1c) as a frame of reference. However, in reality, all involved cuticular elements can move relative to each other. The anatomical inlever (c; Fig. 8) equals the distance between the intervalvifer articulation and the tergo-valvifer articulation (where the input force is applied; $F_{(\text{in protraction})}$, $F_{(\text{in retraction})}$; Fig. 8). The distance between the intervalvifer articulation and the beginning of the dorsal ramus of the 1st valvula at the anterodorsal end of the 1st valvifer equals the anatomical outlever (d; Fig. 8). The ratio of effective outlever (d'; Fig. 8) and the effective inlever (c'; Fig. 8) are indicative for the potential maximum velocity, the mechanical deflection, and the amount of force transmission to the 1st valvula. An increase of the d':c' ratio results in an increase of the potential maximum velocity and mechanical deflection but entails a smaller force output ($F_{(\text{out protraction})}$, $F_{(\text{out retraction})}$; Fig. 8) of the 1st valvulae. In resting position, the anatomical in- and outlever are both very similar to their respective effective levers, thereby creating high torques at the intervalvifer articulation and ensuring an optimal force transmission when pro- or retracting the 1st valvulae. During oviposition, the left and the right 1st valvulae slide back and forth alternately at a high frequency. These valvula movements are crucial for drilling and precise egg laying (Vilhelmsen 2000; Cerkvenik et al. 2017; van Meer et al. 2020).

The shape of the 1st valvifer varies between the various hymenopteran superfamilies (Oeser 1961). Ichneumonoid species such as the braconid *H. hebetor* in the present study possess a 1st valvifer with a rounded compact shape (Snodgrass 1933; Eggs et al. 2018), in contrast to the elongated and bow-shaped 1st valvifers of members of the superfamily Chalcidoidea (Copland and King 1972a, 1972b, 1972c, 1973), the triangularly shaped 1st valvifers of *Apis mellifera* (Linnaeus, 1758) and other aculeate species (Snodgrass 1933; Oeser 1961; Matushkina 2011; Matushkina and Stetsun 2016; Stetsun and Matushkina 2020; Graf et al. 2021), and the highly diverse 1st valvifers of basal hymenopterans (e.g. the robust-appearing 1st valvifers of Tentredinidae (Snodgrass 1933; Vilhelmsen 2000) or the triangular 1st valvifers in some Xyelidae (Vilhelmsen 2000). The ecomorphological consequences of these morphological differences remain to be explored in future systematic comparative analyses with respect to the parasitization of other hosts in different substrates and habitats.

The two sensilla clusters found on the 2nd valvifer of *H. hebetor* (sp, sr; Fig. 7b, d–f, i). probably play an important role in monitoring the pro- and retraction of the 1st valvulae, since their accurate actuation is of major importance for successful egg deposition (van Meer et al. 2020). Unlike in *H. hebetor* or *V. canescens* (Eggs et al. 2018), the sensilla patch at the intervalvifer articulation of other parasitoid wasps can be extremely reduced, e.g. in Pteromalidae (Chalcidoidea) with only three single sensilla (Copland and King 1972b). The question remains as to whether both the density and number of sensilla are linked to the importance of the control of the movements involved in oviposition, and whether this correlates with the shape of the 1st valvifer.

Conclusion

All the cuticular elements of the ovipositor of *Habrobracon hebetor* play a crucial role for successful oviposition. The 2nd valvifer and the female T9 exhibit many muscle insertions, the 1st valvifer acts as a lever that transmits movements to the 1st valvulae, and the terebra serves as a device for precise venom injection, host assessment, and accurate egg laying. All the cuticular elements feature many distinct structures in addition to the microsculpture that is crucial for the performance of these tasks. Our work also has shown that a 3D reconstruction based on a histological section series preserves useful information about the exact morphology and position of inherent structures thereby enabling us to draw conclusions about their function. Future comparative examination of the inherent ovipositor elements, their morphological structure, and the underlying mechanical and functional aspects has the potential to increase our understanding of a putative key feature in the evolution of parasitoid hymenopterans, a feature that probably has significantly impacted the evolutionary success of braconid wasps (more than 18,000 described (Quicke 2015) and about 43,000 estimated species (Jones et al. 2009)) and of parasitoid hymenopterans in general (115,000 described and 680,000 estimated species (Heraty 2009)).

Acknowledgements

We thank Paavo Bergmann for valuable hints regarding histological techniques, Monika Meinert for assistance with SEM, Verena Pietzsch and James H. Nebelsick with the Keyence digital microscope, Theresa Jones for linguistic corrections of the manuscript, and Lars Vilhelmsen and Donald L. J. Quicke for their useful comments.

This work was funded by the German Research Foundation (DFG) as part of the Transregional Collaborative Research Centre (SFB-TRR) 141 'Biological design and integrative structures' (project A03 'Inspired by plants and animals: actively actuated rod-shaped structures exhibiting adaptive stiffness and joint-free kinematics'). The article processing charge was covered by the DFG and the Open Access Publishing Fund of the University of Tübingen.

References

Alam SM (1953) The skeleto-muscular mechanism of *Stenobracon deesae* Cameron (Braconidae, Hymenoptera) – An ectoparasite of sugarcane and juar borers of India. Part II. Abdomen and internal anatomy. Aligarh Muslim University Publications (Zoology Series) 3: 1–75

Austin AD, Browning TO (1981) A mechanism for movement of eggs along insect ovipositors. International Journal of Insect Morphology and Embryology 10: 93–108. https://doi.org/10.1016/S0020-7322(81)80015-3

Barbosa DN, Vilhelmsen L, Azevedo CO (2021) Morphology of sting apparatus of Chrysidoidea (Hymenoptera, Aculeata). Arthropod Structure & Development 60: 100999. https://doi.org/10.1016/j.asd.2020.100999

Bender JC (1943) Anatomy and histology of the female reproductive organs of *Habrobracon juglandis* (Ashmead) (Hymenoptera, Braconidae). Annals of the Entomological Society of America 36: 537–545. https://doi.org/10.1093/aesa/36.3.537

Boring CA, Sharkey M, Nychka J (2009) Structure and functional morphology of the ovipositor of *Homolobus truncator* (Hymenoptera: Ichneumonoidea: Braconidae). Journal of Hymenoptera Research 18: 1–24.

Cardona A, Saalfeld S, Schindelin J, Arganda-Carreras I, Preibisch S, Longair M, Tomancak P, Hartenstein V, Douglas RJ (2012) TrakEM2 software for neural circuit reconstruction. PLoS ONE 7: e38011. https://doi.org/10.1371/journal.pone.0038011

Cerkvenik U, van de Straat B, Gussekloo SWs, van Leeuwen JL (2017) Mechanisms of ovipositor insertion and steering of a parasitic wasp. Proceedings of the National Academy of Sciences of the United States of America 114: E7822–E7831. https://doi.org/10.1073/pnas.1706162114

del Cerro M, Cogen J, del Cerro C (1980) Stevenel's blue: an excellent stain for optical microscopical study of plastic embedded tissues. Microscopica Acta 83: 117–121.

Copland MJW (1976) Female reproductive system of the Aphelinidae (Hymenoptera: Chalcidoidea). International Journal of Insect Morphology and Embryology 5: 151–166. https://doi.org/10.1016/0020-7322(76)90001-5

Copland MJW, King PE (1972a) The structure of the female reproductive system in the Eurytomidae (Chalcidoidea: Hymenoptera). Journal of Zoology 166: 185–212. https://doi.org/10.1111/j.1469-7998.1972.tb04085.x

Copland MJW, King PE (1972b) The structure of the female reproductive system in the Pteromalidae (Chalcidoidea: Hymenoptera). The Entomologist 105: 77–96.

Copland MJW, King PE (1972c) The structure of the female reproductive system in the Torymidae (Hymenoptera: Chalcidoidea). Transactions of the Royal Entomological Society of London 124: 191–212. https://doi.org/10.1111/j.1365-2311.1972.tb00363.x

Copland MJW, King PE (1973) The structure of the female reproductive system in the Agaonidae (Chalcidoidea, Hymenoptera). Journal of Entomology Series A, General Entomology 48: 25–35. https://doi.org/10.1111/j.1365-3032.1973.tb00029.x

Dweck HKM, Gadallah NS, Darwish E (2008) Structure and sensory equipment of the ovipositor of *Habrobracon hebetor* (Say) (Hymenoptera: Braconidae). Micron 39: 1255–1261. https://doi.org/10.1016/j.micron.2008.03.012

Eggs B, Birkhold AI, Röhrle O, Betz O (2018) Structure and function of the musculoskeletal ovipositor system of an ichneumonid wasp. BMC Zoology 3: 12. https://doi.org/10.1186/s40850-018-0037-2

Ernst AF, Mikó I, Deans AR (2013) Morphology and function of the ovipositor mechanism in Ceraphronoidea (Hymenoptera, Apocrita). Journal of Hymenoptera Research 33: 25–61. https://doi.org/10.3897/jhr.33.5204

Fergusson NDM (1988) A comparative study of the structures of phylogenetic importance of female genitalia of the Cynipoidea (Hymenoptera). Systematic Entomology 13: 13–30. https://doi.org/10.1111/j.1365-3113.1988.tb00225.x

Field SA, Austin AD (1994) Anatomy and mechanics of the telescopic ovipositor system of *Scelio latreille* (Hymenoptera: Scelionidae) and related genera. International Journal of Insect Morphology and Embryology 23: 135–158. https://doi.org/10.1016/0020-7322(94)90007-8

Frühauf E (1924) Legeapparat und Eiablage bei Gallwespen (Cynipidae). Zeitschrift für Wissenschaftliche Zoologie 121: 656–723.

Gauld I, Bolton B (Eds) (1988) The Hymenoptera. Oxford University Press, Oxford, 332 pp.

Graf S, Willsch M, Ohl M (2021) Comparative morphology of the musculature of the sting apparatus in *Ampulex compressa* (Hymenoptera, Ampulicidae) and *Sceliphron destillatorium* (Hymenoptera, Sphecidae). Deutsche Entomologische Zeitschrift 68: 21–32. https://doi.org/10.3897/dez.68.58217

Hanna AD (1934) The male and female genitalia and the biology of *Euchalcidia aryobori* Hanna (Hymenoptera, Chalcidinae). Transactions of the Royal Entomological Society of London 82: 107–136. https://doi.org/10.1111/j.1365-2311.1934.tb00030.x

Heraty J (2009) Parasitoid biodiversity and insect pest management. In: Foottit RG, Adler PH (Eds) Insect Biodiversity: Science and Society. Wiley-Blackwell, Oxford, 445–462. https://doi.org/10.1002/9781444308211.ch19

Hymenoptera Anatomy Consortium (2021) Hymenoptera Anatomy Ontology. [Accessed 12 January 2021]

Jones OR, Purvis A, Baumgart E, Quicke DLJ (2009) Using taxonomic revision data to estimate the geographic and taxonomic distribution of undescribed species richness in the Braconidae (Hymenoptera: Ichneumonoidea). Insect Conservation and Diversity 2: 204–212. https://doi.org/10.1111/j.1752-4598.2009.00057.x

King PE (1962) The muscular structure of the ovipositor and its mode of function in *Nasonia vitripennis* (Walker) (Hymenoptera: Pteromalidae). Proceedings of the Royal Entomological Society of London. Series A, General Entomology 37: 121–128. https://doi.org/10.1111/j.1365-3032.1962.tb00002.x

King PE, Copland MJW (1969) The structure of the female reproductive system in the Mymaridae (Chalcidoidea: Hymenoptera). Journal of Natural History 3: 349–365. https://doi.org/10.1080/00222936900770311

Kumpanenko AS, Gladun DV (2018) Functional morphology of the sting apparatus of the spider wasp *Cryptocheilus versicolor* (Scopoli, 1763) (Hymenoptera: Pompilidae). Entomological Science 21: 124–132. https://doi.org/10.1111/ens.12288

LeRalec A, Rabasse JM, Wajnberg E (1996) Comparative morphology of the ovipositor of some parasitic Hymenoptera in relation to characteristics of their hosts. Canadian Entomologist 128: 413–433. https://doi.org/10.4039/Ent128413-3

Lösel PD, van de Kamp T, Jayme A, Ershov A, Faragó T, Pichler O, Tan Jerome N, Aadepu N, Bremer S, Chilingaryan SA, Heethoff M, Kopmann A, Odar J, Schmelzle S, Zuber M, Wittbrodt J, Baumbach T, Heuveline V (2020) Introducing Biomedisa as an open-source online platform for biomedical image segmentation. Nature Communications 11: 5577. https://doi.org/10.1038/s41467-020-19303-w

Matushkina NA (2011) Sting microsculpture in the digger wasp *Bembix rostrata* (Hymenoptera, Crabronidae). Journal of Hymenoptera Research 21: 41–52. https://doi.org/10.3897/jhr.21.873

Matushkina NA, Stetsun HA (2016) Morphology of the sting apparatus of the digger wasp *Oxybelus uniglumis* (Linnaeus, 1758) (Hymenoptera, Crabronidae), with emphasis on intraspecific variability and behavioural plasticity. Insect Systematics & Evolution 47: 347–362. https://doi.org/10.1163/1876312X-47032146

Mbata GN, Shapiro-Ilan DI (2010) Compatibility of *Heterorhabditis indica* (Rhabditida: Heterorhabditidae) and *Habrobracon hebetor* (Hymenoptera: Braconidae) for biological control of *Plodia interpunctella* (Lepidoptera: Pyralidae). Biological Control 54: 75–82. https://doi.org/10.1016/j.biocontrol.2010.04.009

Oeser R (1961) Vergleichend-morphologische Untersuchungen über den Ovipositor der Hymenopteren. Mitteilungen aus dem Zoologischen Museum in Berlin 37: 3–119. https://doi.org/10.1002/mmnz.19610370102

Pampel W (1914) Die weiblichen Geschlechtsorgane der Ichneumoniden. Zeitschrift für wissenschaftliche Zoologie 108: 290–357.

Paust A, Reichmuth C, Büttner C, Prozell S, Adler CS, Schöller M (2006) Spatial effects on competition between the larval parasitoids *Habrobracon hebetor* (Say) (Hymenoptera: Braconidae) and *Venturia canescens* (Gravenhorst) (Hymenoptera: Ichneumonidae) parasitising the Mediterranean flour moth, *Ephestia kuehniella* Zeller. Proceedings of the 9th International Working Conference on Stored Product Protection, PS7-17-6189: 797–803.

Peters RS, Krogmann L, Mayer C, Donath A, Gunkel S, Meusemann K, Kozlov A, Podsiadlowski L, Petersen M, Lanfear R, Diez PA, Heraty J, Kjer KM, Klopfstein S, Meier R, Polidori C, Schmitt T, Liu S, Zhou X, Wappler T, Rust J, Misof B, Niehuis O (2017) Evolutionary history of the Hymenoptera. Current Biology 27: 1013–1018. https://doi.org/10.1016/j.cub.2017.01.027

Prozell S, Schöller M, Wyss U (2006) Die Mehlmotte *Ephestia kuehniella* und ihr natürlicher Feind, die Mehlmottenschlupfwespe *Habrobracon hebetor*. Entofilm (Kiel).

Quicke DLJ (1991) Ovipositor mechanics of the braconine wasp genus *Zaglyptogastra* and the ichneumonid genus *Pristomerus*. Journal of Natural History 25: 971–977. https://doi.org/10.1080/00222939100770631

Quicke DLJ (1997) Parasitic Wasps. Chapman & Hall Ltd, London, 470 pp.

Quicke DLJ (2015) The Braconid and Ichneumonid Parasitoid Wasps: Biology, Systematics, Evolution and Eclogy. Wiley-Blackwell, Chichester, 681 pp.

Quicke DLJ, van Achterberg C (1990) Phylogeny of the subfamilies of the family Braconidae (Hymenoptera: Ichneumonoidea). Zoologische Verhandelingen 258: 3–95.

Quicke DLJ, Fitton MG, Ingram S (1992) Phylogenetic implications of the structure and distribution of ovipositor valvilli in the Hymenoptera (Insecta). Journal of Natural History 26: 587–608. https://doi.org/10.1080/00222939200770361

Quicke DLJ, LeRalec A, Vilhelmsen L (1999) Ovipositor structure and function in the parasitic Hymenoptera with an exploration of new hypotheses. Rendiconti 47: 197–239.

Quicke DLJ, Fitton MG, Tunstead JR, Ingram SN, Gaitens PV (1994) Ovipositor structure and relationships within the Hymenoptera, with special reference to the Ichneumonoidea. Journal of Natural History 28: 635–682. https://doi.org/10.1080/00222939400770301

Rahman MH, Fitton MG, Quicke DLJ (1998) Ovipositor internal microsculpture and other features in doryctine wasps (Insecta, Hymenoptera, Braconidae). Zoologica Scripta 27: 333–343. https://doi.org/10.1111/j.1463-6409.1998.tb00465.x

Rogers D (1972) The ichneumon wasp *Venturia canescens*: oviposition and avoidance of superparasitism. Entomologia Experimentalis et Applicata 15: 190–194. https://doi.org/10.1111/j.1570-7458.1972.tb00195.x

Saalfeld S, Fetter R, Cardona A, Tomancak P (2012) Elastic volume reconstruction from series of ultra-thin microscopy sections. Nature Methods 9: 717–720. https://doi.org/10.1038/nmeth.2072

Sanower W, Mbata GN, Payton ME (2018) Improvement of reproductive performance of *Habrobracon hebetor*: Consideration of diapausing and non-diapausing larvae of *Plodia interpunctella*. Biological Control 118: 32–36. https://doi.org/10.1016/j.biocontrol.2017.12.003

Schindelin J, Arganda-Carreras I, Frise E, Kaynig V, Longair M, Pietzsch T, Preibisch S, Rueden C, Saalfeld S, Schmid B, Tinevez J-Y, White DJ, Hartenstein V, Eliceiri K, Tomancak

P, Cardona A (2012) Fiji: an open-source platform for biological-image analysis. Nature Methods 9: 676–682. https://doi.org/10.1038/nmeth.2019

Shah ZA, Blackwell A, Hubbard SF (2012) Ultramorphology of the ovipositor of *Venturia canescens* (Gravenhorst) and possible mechanisms for oviposition. International Journal of Agriculture and Biology 14: 908–914.

Shaw MR (2017) Further notes on the biology of *Pseudavga flavicoxa* Tobias, 1964 (Hymenoptera, Braconidae, Rhysipolinae). Journal of Hymenoptera Research 54: 113–128. https://doi.org/10.3897/jhr.54.10789

Smith EL (1970) Evolutionary morphology of the external insect genitalia. 2. Hymenoptera. Annals of The Entomological Society of America 63: 1–27. https://doi.org/10.1093/aesa/63.1.1

Smith EL (1972) Biosystematics and morphology of Symphyta–III External genitalia of *Euura* (Hymenoptera: Tenthredinidae): sclerites, sensilla, musculature, development and oviposition behavior. International Journal of Insect Morphology and Embryology 1: 321–365. https://doi.org/10.1016/0020-7322(72)90016-5

Snodgrass RE (1933) Morphology of the insect abdomen. Part II. The genital ducts and the ovipositor. Smithsonian Miscellaneous Collections 89: 1–148.

Stetsun H, Matushkina NA (2020) Sting morphology of the European hornet, *Vespa crabro* L., (Hymenoptera: Vespidae) re-examined. Entomological Science 23: 416–429. https://doi.org/10.1111/ens.12438

Stetsun H, Rajabi H, Matushkina N, Gorb SN (2019) Functional morphology of the sting in two digger wasps (Hymenoptera: Crabronidae) with different types of prey transport. Arthropod Structure & Development 52: 100882. https://doi.org/10.1016/j.asd.2019.100882

van Meer NMME, Cerkvenik U, Schlepütz CM, van Leeuwen JL, Gussekloo SWS (2020) The ovipositor actuation mechanism of a parasitic wasp and its functional implications. Journal of Anatomy 237: 689–703. https://doi.org/10.1111/joa.13216

Venkatraman TV, Subba Rao BR (1954) The mechanisms of oviposition in *Stenobracon deesae* (Cam.) (Hymenoptera: Braconidae). Proceedings of the Royal Society of London. Series A, General Entomology 29: 1–8. https://doi.org/10.1111/j.1365-3032.1954.tb01178.x

Vilhelmsen L (2000) The ovipositor apparatus of basal Hymenoptera (Insecta): phylogenetic implications and functional morphology. Zoologica Scripta 29: 319–345. https://doi.org/10.1046/j.1463-6409.2000.00046.x

Vilhelmsen L (2003) Flexible ovipositor sheaths in parasitoid Hymenoptera (Insecta). Arthropod Structure & Development 32: 277–287. https://doi.org/10.1016/S1467-8039(03)00045-8

Vilhelmsen L, Isidore N, Romani R, Basibuyuk HH, Quicke DLJ (2001) Host location and oviposition in a basal group of parasitic wasps: the subgenual organ, ovipositor apparatus and associated structures in the Orussidae (Hymenoptera, Insecta). Zoomorphology 121: 63–84. https://doi.org/10.1007/s004350100046

Wührer B, Zimmermann O, Wyss U (2009) Lebensweise und Entwicklung des Parasitoiden *Bracon brevicornis*. Entofim (Kiel).

Yoder MJ, Miko I, Seltmann KC, Bertone MA, Deans AR (2010) A gross anatomy ontology for Hymenoptera. PloS ONE 5: e159991. https://doi.org/10.1371/journal.pone.0015991

Appendix 1

Table A1. Morphological terms relevant to the hymenopteran ovipositor system. The terms (abbreviations used in this article in brackets) are used and defined according to the Hymenoptera Anatomy Ontology Portal (HAO) (Yoder et al. 2010; Hymenoptera Anatomy Consortium 2021) and the according Uniform Resource Identifiers (URI) are listed.

Anatomical term (abbreviation)	definition / concept	URI
1st valvifer (1vf)	The area of the 1st valvifer-1st valvulae complex that is proximal to the aulax, bears the 9th tergal condyle of the 1st valvifer and the 2nd valviferal condyle of the 1st valvifer and is connected to the genital membrane by muscle.	http://purl.obolibrary.org/obo/HAO_0000338
1st valvifer-genital membrane muscle	The ovipositor muscle that arises from the posterior part of the 1st valvifer and inserts anteriorly on the genital membrane anterior to the T9-genital membrane muscle.	http://purl.obolibrary.org/obo/HAO_0001746
1st valvula, 1st valvulae (1vv)	The area of the 1st valvifer-1st valvulae complex that is delimited by the proximal margin of the aulax.	http://purl.obolibrary.org/obo/HAO_0000339
2nd valvifer (2vf)	The area of the 2nd valvifer-2nd valvulae-3rd valvulae complex that is proximal to the basal articulation and to the processus musculares and articulates with the female T9.	http://purl.obolibrary.org/obo/HAO_0000927
2nd valvula (2vv)	The area of the 2nd valvifer-2nd valvulae-3rd valvulae complex that is distal to the basal articulation and to the processus musculares and is limited medially by the median body axis.	http://purl.obolibrary.org/obo/HAO_0000928
3rd valvula, 3rd valvulae (3vv)	The area of the 2nd valvifer-3rdvalvulae complex that is posterior to the distal vertical conjunctiva of the 2nd valvifer-3rd valvulae complex.	http://purl.obolibrary.org/obo/HAO_0001012
anterior 2nd valvifer-2nd valvula muscle	The ovipositor muscle that arises from the anterodorsal part of the 2nd valvifer and inserts subapically on the processus articularis.	http://purl.obolibrary.org/obo/HAO_0001166
anterior ridge of T9 (ar9)	The ridge that extends along the anterior margin of female T9 and receives the site of origin of the ventral and the dorsal T9-2nd valvifer muscles.	http://purl.obolibrary.org/obo/HAO_0002182
anterior section of dorsal flange of 2nd valvifer	The area of the dorsal flange of the 2nd valvifer that is anterior to the site of origin of the basal line.	http://purl.obolibrary.org/obo/HAO_0002173
apodeme	The process that is internal.	http://purl.obolibrary.org/obo/HAO_0000142
aulax (au)	The impression that is on the 1st valvifer-1st valvula complex accommodates the rhachis.	http://purl.obolibrary.org/obo/HAO_0000152
basal articulation (ba)	The articulation that is part of the 2nd valvifer-2nd valvula-3rd valvula complex and adjacent to the rhachis.	http://purl.obolibrary.org/obo/HAO_0001177
basal line of the 2nd valvifer	The line on the 2nd valvifer that extends between the pars articularis and the dorsal flange of 2nd valvifer.	http://purl.obolibrary.org/obo/HAO_0002171
bulb (blb)	The anterior area of the dorsal valve [composite structure of the fused 2nd valvulae] that is bulbous.	http://purl.obolibrary.org/obo/HAO_0002177
conjunctiva	The area of the cuticle that is more flexible than adjacent sclerites.	http://purl.obolibrary.org/obo/HAO_0000221
distal notch of the dorsal valve (no)	The notch that is distal on the dorsal valve [composite structure of the fused 2nd valvulae].	http://purl.obolibrary.org/obo/HAO_0002179
dorsal flange of the 2nd valvifer (df2)	The flange that extends on the dorsal margin of the 2nd valvifer. Part of the ventral T9-2nd valvifer muscle attaches to the flange.	http://purl.obolibrary.org/obo/HAO_0001577
dorsal projection of the 2nd valvifer (dp2)	The projection that is located on the 2nd valvifer and corresponds to the proximal end of the rhachis.	http://purl.obolibrary.org/obo/HAO_0002172
dorsal ramus of the 1st valvula (dr1)	The region that extends along the dorsal margin of the 1st valvula and bears the aulax.	http://purl.obolibrary.org/obo/HAO_0001579
dorsal T9-2nd valvifer muscle	The ovipositor muscle that arises along the posterodorsal part of the anterior margin of female T9 and inserts on the anterior section of the dorsal flanges of the 2nd valvifer.	http://purl.obolibrary.org/obo/HAO_0001569
egg canal (ec)	The anatomical space that is between the left and right olistheters.	http://purl.obolibrary.org/obo/HAO_0002191
female T9 (T9)	The tergite that is articulated with the 1st valvifer and is connected to the 2nd valvifer via muscles.	http://purl.obolibrary.org/obo/HAO_0000075
flange	The projection that is lamella-like and is located on a rim, carina, apodeme or edge.	http://purl.obolibrary.org/obo/HAO_0000344
genital membrane (gm)	The conjunctiva that connects the ventral margins of the 2nd valvifers arching above the 2nd valvula.	http://purl.obolibrary.org/obo/HAO_0001757

Anatomical term (abbreviation)	definition / concept	URI
interarticular ridge of the 1st valvifer (iar)	The ridge that extends along the posterior margin of the 1st valvifer between the intervalvifer and tergo-valvifer articulations.	http://purl.obolibrary.org/obo/HAO_0001562
intervalvifer articulation (iva)	The articulation between the 1st valvifer and 2nd valvifer.	http://purl.obolibrary.org/obo/HAO_0001558
median bridge of the 2nd valvifers (mb2)	The area that connects posterodorsally the 2nd valvifers and is the site of attachment for the posterior T9-2nd valvifer muscle.	http://purl.obolibrary.org/obo/HAO_0001780
notal membrane	The conjunctiva that connects the medial margins of the 2nd valvulae.	http://purl.obolibrary.org/obo/HAO_0001733
notch	The part of the margin of a sclerite that is concave.	http://purl.obolibrary.org/obo/HAO_0000648
olistheter (oth)	The anatomical cluster that is composed of the rhachis of the 2nd valvula and the aulax of the 1st valvula.	http://purl.obolibrary.org/obo/HAO_0001103
ovipositor	The anatomical cluster that is composed of the 1st valvulae, 2nd valvulae, 3rd valvulae, 1st valvifers, 2nd valvifers and female T9.	http://purl.obolibrary.org/obo/HAO_0000679
ovipositor apparatus	The anatomical cluster that is composed of the ovipositor, abdominal terga 8-10, abdominal sternum 7 and muscles connecting them.	http://purl.obolibrary.org/obo/HAO_0001600
ovipositor muscle	The abdominal muscle that inserts on the ovipositor.	http://purl.obolibrary.org/obo/HAO_0001290
pars articularis / pars articulares	The articular surface that is situated anteriorly on the ventral margin of the 2nd valvifer and forms the lateral part of the basal articulation.	http://purl.obolibrary.org/obo/HAO_0001606
posterior 2nd valvifer-2nd valvula muscle	The ovipositor muscle that arises posteroventrally from the 2nd valvifer and inserts on the processus musculares of the 2nd valvula.	http://purl.obolibrary.org/obo/HAO_0001815
processus articularis / processus articulares	The process that extends laterally from the proximal part of the 2nd valvula and forms the median part of the basal articulation, and corresponds to the site of attachment for the anterior 2nd valvifer-2nd valvula muscle. The processus articularis is part of the sclerite.	http://purl.obolibrary.org/obo/HAO_0001704
processus musculares / processus muscularis	The apodeme that extends dorsally from the proximal part of the 2nd valvula to the genital membrane and receives the site of attachment of the posterior 2nd valvifer-2nd valvula muscle.	http://purl.obolibrary.org/obo/HAO_0001703
rhachis (rh)	The ridge that extends along the ventral surface of the 2nd valvula that is partially enclosed by the aulax.	http://purl.obolibrary.org/obo/HAO_0000898
ridge	The apodeme that is elongate.	http://purl.obolibrary.org/obo/HAO_0000899
sawtooth (st)	The process that is located along the ventral margin of the 1st valvula of the dorsal margin of the 2nd valvula.	http://purl.obolibrary.org/obo/HAO_0001681
sclerite	The area of the cuticle that is less flexible than adjacent conjunctivae.	http://purl.obolibrary.org/obo/HAO_0000909
sensillar patch of the 2nd valvifer (sp)	The patch that is composed of placoid sensilla adjacent to the intervalvifer articulation.	http://purl.obolibrary.org/obo/HAO_0001671
sensillum	A sense organ embedded in the integument and consisting of one or a cluster of sensory neurons and associated sensory structures, support cells and glial cells forming a single organized unit with a largely bona fide boundary.	http://purl.obolibrary.org/obo/HAO_0000933
terebra (trb)	The anatomical cluster that is composed of the 1st and 2nd valulae.	http://purl.obolibrary.org/obo/HAO_0001004
tergite	The sclerite that is located on the tergum.	http://purl.obolibrary.org/obo/HAO_0001005
tergo-valvifer articulation (tva)	The articulation that is located between the female T9 and the 1st valvifer and is composed of the 9th tergal condyle of the 1st valvifer and the 1st valviferal fossa of the 9th tergite.	http://purl.obolibrary.org/obo/HAO_0001636
valvillus (vlv)	The sclerite that articulates on the 1st valvula and projects into the egg/poison canal.	http://purl.obolibrary.org/obo/HAO_0001619
venom gland reservoir of the 2nd valvifer (vd)	The gland reservoir that is between the 2nd valvifers.	http://purl.obolibrary.org/obo/HAO_0002176
ventral ramus of the 2nd valvula	The area of the 2nd valvifer-2nd valvula-3rd valvula complex that bears the rhachis.	http://purl.obolibrary.org/obo/HAO_0001107
ventral T9-2nd valvifer muscle	The ovipositor muscle that arises from the lateral region of female T9 and inserts along the posterior part of the dorsal flange of the 2nd valvifer.	http://purl.obolibrary.org/obo/HAO_0001616

Supplementary material 1

Video S1

Authors: Michael Csader, Karin Mayer, Oliver Betz, Stefan Fischer, Benjamin Eggs

Data type: Video file (mp4)

Explanation note: Animation of the rotated segmented 3D reconstruction of the terebra of *Habrobracon hebetor*.

Link: https://doi.org/10.3897/jhr.83.64018.suppl1

Supplementary material 2

Video S2

Authors: Michael Csader, Karin Mayer, Oliver Betz, Stefan Fischer, Benjamin Eggs

Data type: Video file (mp4)

Explanation note: Animation of the rotated segmented 3D reconstruction of the proximal region of the terebra of *Habrobracon hebetor* (cf. Fig. 3), highlighting the 1st and 2nd valvulae, the ligaments, and the duct of the venom gland.

Link: https://doi.org/10.3897/jhr.83.64018.suppl2

JHR 83: 101–124 (2021)
doi: 10.3897/jhr.83.66829
https://jhr.pensoft.net

RESEARCH ARTICLE

JOURNAL OF Hymenoptera RESEARCH
A peer-reviewed open-access journal
The International Society of Hymenopterists

Strumigenys perplexa (Smith, 1876) (Formicidae, Myrmicinae) a new exotic ant to Europe with establishment in Guernsey, Channel Islands

Matthew T. Hamer[1], Andy D. Marquis[2], Benoit Guénard[1]

1 *School of Biological Sciences, The University of Hong Kong, Kadoorie Biological Sciences Building, Pok Fu Lam Road, Hong Kong SAR, China* **2** *Official Recorder: Guernsey Biological Records Centre, Raymond Falla House, Longue Rue St. Martin, GY4 6HG, St. Martin, UK*

Corresponding author: Matthew T. Hamer (matt.hamer@hotmail.co.uk)

Academic editor: Jack Neff | Received 2 April 2021 | Accepted 27 May 2021 | Published 28 June 2021

http://zoobank.org/F6FB8086-014D-4EDE-840C-6CEF8842ECD7

Citation: Hamer MT, Marquis AD, Guénard B (2021) *Strumigenys perplexa* (Smith, 1876) (Formicidae, Myrmicinae) a new exotic ant to Europe with establishment in Guernsey, Channel Islands. Journal of Hymenoptera Research 83: 101–124. https://doi.org/10.3897/jhr.83.66829

Abstract
Ants are continually introduced into regions outside of their natural biogeographic ranges via global trade. The genus *Strumigenys* Smith 1860 (Formicidae: Myrmicinae) are minute predators with a growing history of global introductions, although tropical introductions into temperate zones are rarely able to establish outside of heated infrastructures. We report the first record of the Australasian *Strumigenys perplexa* (Smith 1876) to Europe and the British Isles from four sites on Guernsey, Channel Islands. This novel discovery is likely attributable to the species wide climatic and habitat tolerances, enabling the species to establish away from its natural range in Australasia and from heated-infrastructure. A key to the West Palaearctic *Strumigenys* species is provided alongside a preliminary and critical checklist of ant species recorded from the Channel Island archipelago, listing 32 species.

Keywords
Biological invasions, checklist, Dacetini, species introduction, taxonomic key

Introduction

Ants (Hymenoptera: Formicidae) are among the most successful group of biological invaders, particularly within insular systems (Moser et al. 2018). Their small size, relative inconspicuous nature, and social structure allow them to be frequently overlooked and transported via globally-facilitated human trade (McGlynn 1999). As a result, numerous ant species have been spread outside of their native ranges (McGlynn 1999). Compared to warmer zones, many introductions into temperate regions remain, however, limited to climate-controlled buildings (e.g. greenhouses) which provide shelter from unfavourable conditions (e.g. Donisthorpe 1915; Blatrix et al. 2018). Therefore, fewer successful introductions result in established viable outdoor populations (Dawson et al. 2017).

The ant genus *Strumigenys* (Formicidae: Myrmicinae) is increasingly emerging as a successful invader, with a recent review listing 24 species introduced outside their native range (Tang et al. 2019). *Strumigenys* is also the third most diverse ant genus, currently including 853 described species and is characterized by small size, cryptobiotic habits and specialized predatory behaviour (Bolton 2000; Bolton 2021). Most species forage and nest within the leaf litter, soil, and rotting wood, where many species are predators of small soft-bodied arthropods, such as Collembola (Masuko 1984). Many species within the genus have evolved a specialised kinetic trap-jaw mandibular mechanism with which to subdue prey (Gronenberg 1996; Booher et al. 2021). In some *Strumigneys* species groups the distinctive mandibular adaptations make the genus easily recognisable, particularly among the European ant fauna. Other distinctive morphological-characters, such as spongiform tissue on the metasoma, dorso-ventrally flattened head and a diverse range of specialised pilosity as well as a reduction in antennomere count can be found in both short and long mandibular forms.

Strumigenys is mainly and widely distributed within the tropical and subtropical regions, with a peak of diversity observed in Borneo with 97 recorded species (Bolton 2000; Janicki et al. 2016). Temperate species are relatively common and diverse in temperate North America and Asia, but in contrast records of this genus in Europe are scant with just four native species reported: *S. argiola* Emery, 1869, *S. baudueri* Emery, 1875, *S. tenuipilis* Emery, 1915 and *S. tenuissima* Brown, 1953 (Janicki et al. 2016; Seifert 2018). In addition, four introduced species have been recorded within Europe: *S. lewisi* Cameron, 1886 (but see discussion below), *S. membranifera* Emery, 1869, *S. rogeri* Emery, 1890 and *S. silvestrii* Emery, 1906. *Strumigenys rogeri* is only known from indoor and interception records, while *S. membranifera* and *S. silvestrii* are known to have established populations outdoors, but mainly limited to the more Mediterranean regions of Europe, characterized by warmer temperatures (Wetterer 2011; MacGown et al. 2012; Scupola 2019). Here we report a fifth introduced *Strumigenys* species from the Channel Islands, the Australian species *S. perplexa* Smith, 1876, which also represents the northernmost record for an outdoor population of the genus within Europe.

The Channel Islands are an archipelago of British Crown dependencies encompassing eight inhabited and several uninhabited islands located 15 to 50 kilometres off the northern French coast of Normandy within the English Channel (Fig. 1A, B). An updated list of both native and introduced ant species and their distribution across the whole archipelago is included, alongside an updated dichotomous key to the Western Palaearctic *Strumigenys* fauna.

Methods

Photographs taken by the second author (ADM) of individuals extracted via leaf litter sifting at Les Cotils Wood were initially posted onto the 'UK Bees, Wasps and Ants' Facebook group page on 25 Jan 2020, which were subsequently identified as *Strumigenys* by the first author (MTH). Sampling methods involved the collection of 5 litres of litter and soil and subsequent sieving using a 5 mm sieve onto a white tray. Morphological characters were examined using Bolton (2000) key to Australian *Strumigenys*. Determinations lead to unsatisfactory identifications in all other regional keys within Bolton (2000). Specimens were sent to Barry Bolton, for confirmation on MTH's determinations, as well as Mike Fox of the Bees, Wasps and Ants Recording Society (**BWARS**).

Microscopic examination and measurements were conducted using a Brunel BMDZ stereo-microscope, a Wild 5 with 2× objective and a Leica M205 C dissecting microscope by MTH, B. Bolton and BG respectively. Morphometric measurements were compared to Bolton's (2000) metric diagnoses of *S. perplexa* including: Total length (TL), Head length (HL), Head width (HW), Cephalic index (CI), Mandible length (ML), Mandible index (MI), Scape length (SL), Scape index (SI), Pronotal width (PW), Alitrunk (=mesosoma) length (AL = Weber's Length). All measurements are given in millimetres. Worker specimens measured include MTHENT1432, ANTWEB1013915, ANTWEB1013916, MTHENT1434 and two specimens in Barry Bolton collection (no codes). Queen specimens measured include ANTWEB1013917. Morphological characters were compared to AntWeb images of syntype specimens CASENT0900905, CASENT0909317 and CASENT0909318 as well as specimen images of CASENT0172367 and CASENT0178872.

A number of specimens which had not been collected, but were only photographed in-situ were also included in our examination of specimens. The lack of congeneric species within the study area (Channel Islands) and the distinct morphological characters of the study species make in-situ photographs reliable records. In addition, and following the same approach, a predated springtail (Collembola) was identified using Hopkin (2007).

Photographs & distribution map

Specimen photographs (Figs 3, 4) were taken using a Leica DFC450 camera mounted on a Leica M205 C dissecting microscope and stacked in Leica Application Suite V. 4.5. In-situ photos were captured using a Canon EOS 5 DSR with Canon MP-E65 lens connected to an extension tube alongside a Canon MT-26 EX-RT twin flash system. Habitat shots were taken using an Olympus EM1-X with Olympus 12–40 mm

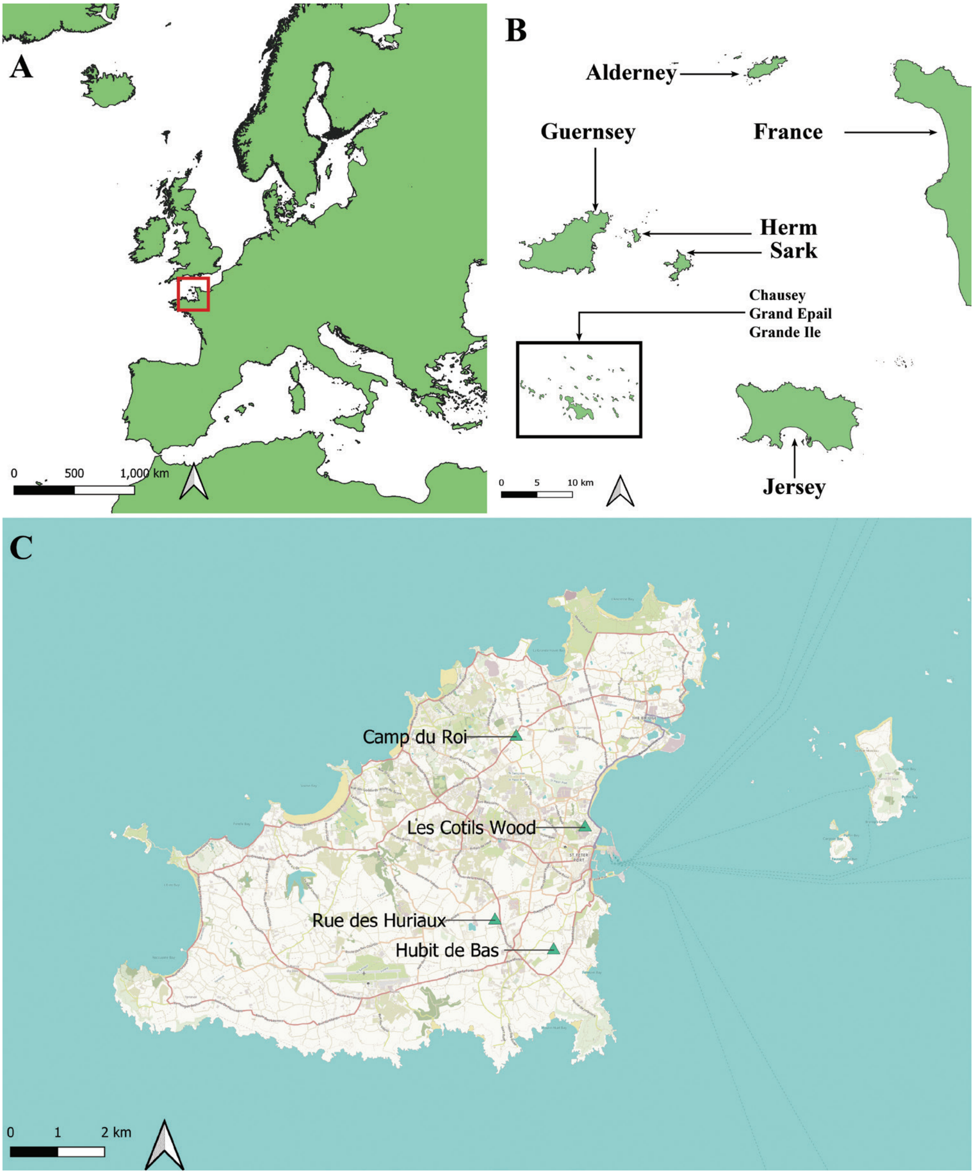

Figure 1. Study focus area in the Channel Islands **A** map of Western Europe with the location of the Channel Island indicated by the red square **B** the Channel Islands. Chausey, Grand Epail and Grande Ile (magnified black square) are a small set of islands located south of Jersey **C** distribution of *S. perplexa* sites on the island of Guernsey, Channel Islands. Base map and data from OpenStreetMap and OpenStreetMap Foundation.

PRO lens. Maps of Europe and the Channel Islands were generated in QGIS (v. Hanover 3.18.0) using OpenStreetMap Humanitarian Tiles and land polygons derived from OpenStreetMaps.

Figure 2. *Strumigneys perplexa* collection sites **A** let Cotils Wood in which specimens of *Strumigenys perplexa* were initially collected via litter sifting **B** the general habitat of Rus des Huriaux where specimens of *S. perplexa* were found through litter sifting. Photos by Andy Marquis.

Channel island checklist

Native ant species and introduced species recorded from the Channel Islands were obtained from the Global Ant Biodiversity Informatics (**GABI**) (Guénard et al. 2017) and the Bees, Wasps and Ants Recording Society (BWARS) database from across the archipelago. Records for both GABI and BWARS are validated by experts before incorporation into respective databases. Species distribution for each island is here presented, island names or particular locality information (e.g. city names, georeferenced) allowing the identification of the island for each record were used to develop the list of species found on each island. However, in a few cases, only the mention of Channel Islands without further geographic mentions was available. Species belonging to a species complex in which specimens have yet to be determined in light of modern taxonomic changes are included and discussed.

Results

The ants were determined to be *Strumigenys perplexa* (Smith, 1876), a member of the Austral *signeae*-complex within the *Strumigenys godeffroyi*-group. Determinations were confirmed by B. Bolton via morphological characters within Bolton (2000) key to Australian *Strumigenys*. In addition, morphometrics taken by B. Bolton, MTH and Benoit Guénard fell within the metric ranges given in Bolton (2000) for *S. perplexa*. Records are deposited with BWARS, Guernsey Biological Records Centre and the UK Non-Native Species Secretariat. Specimens are deposited in the personal collections of MTH (MTHENT1434), B. Bolton and M. Fox (BWARS) as well as BMHN (MTHENT1432) and the Insect Biodiversity and Biogeography Laboratory (The University of Hong Kong, ANTWEB1013915, ANTWEB1013916, ANTWEB1013917).

Taxonomic treatment

Strumigenys perplexa (Smith 1876)

Figs 3–5

Orectognathus perplexa Smith, F., 1876: 491 (w. q.) New Zealand. Australasia
Synonyms: *Strumigenys antarctica* Emery, 1924: 321: *Strumigenys leae*: Brown, 1958: 38
See Bolton (2000) for full synonymy data.

Diagnosis. Worker diagnosis (adapted from Bolton (2000)): Mandibles long and subtly convex in dorsal view with apical fork and preapical tooth within the apical quarter. Apical fork of right mandible with intercalary tooth. Hairs on the leading edge of scape spatulate and curved apically; secondary hairs shorter, distinguishable from the former. Apicoscrobal hair simple, short and weakly curved. Cephalic dorsum with sharp reticulopunctate ; 4–6 standing hairs on occipital margin. Eye with 7–10 ommatidia. Pronotal humeral hair simple, straight to weakly curved; pronotal dorsum and mesonotum each with 1–3 pairs stiff, erect, simple hairs. Alitrunk dorsum with fine and dense reticulation and punctation. Pronotum from reticulate-punctate to smooth; metapleuron is reticulate-punctate to entirely smooth, most common with smooth patches extending to the anterior portion of metapleuron and ventral sides portions of propodeum. Propodeum with pair of denticles formed of spongiform tissue. Petiole dorsum entirely reticulate-punctate; ventrally with curtain of spongiform tissue. Postpetiole dorsum smooth with sculpture consigned to the periphery; ventrally, laterally and encircling the disc with spongiform tissue. Gastral tergites with short, apically blunt hairs; often distributed evenly over sclerites. Basigastral costulae shorter than disc of postpetiole.

Queen: As worker but with usual queen modifications including larger eyes, mesosoma and metasoma, presence of three ocelli. Lamella of spongiform tissue on propodeal declivity is also discontinuous on the queen specimen but continuous on workers.

Measurements. Morphometrics were gathered by B. Bolton from two workers collected from Rue des Huriaux, by BG from two workers and a queen from Rue des Huriaux and by MTH from two workers collected from Les Cotils Wood and Rue Des Huriaux. Worker results were compared to Bolton (2000). See supplementary information (Suppl. material 1: Table S1) for more details. There are no measurements for a queen in Bolton (2000) or elsewhere, we have supplied the first here. Measurements are in millimetres (mm).

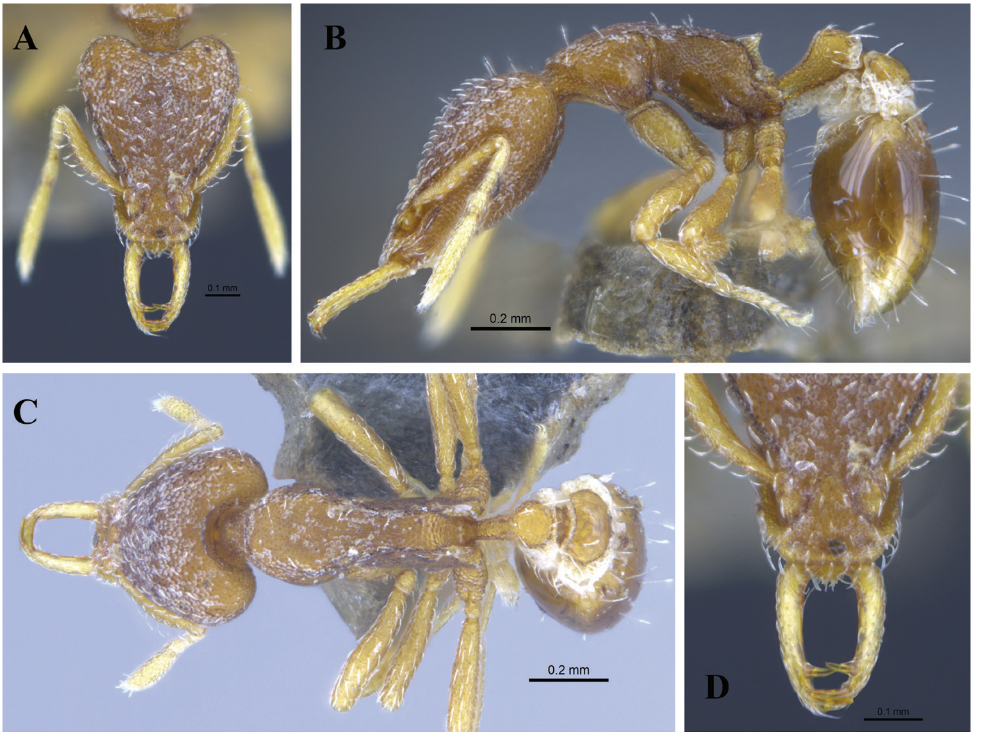

Figure 3. *Strumigenys perplexa* worker (ANTWEB1013915) **A** head view **B** profile view **C** dorsal view **D** mandibles view. Images by Benoit Guénard.

Worker morphometrics (n = 6): TL = 2.16–2.54, HL = 0.58–0.63, HW = 0.44–0.48, CI = 74–78, ML = 0.25–0.28, MI = 41–49, SL = 0.31–0.33, SI = 68–71, PW = 0.24–0.28, AL = 0.54–0.63.

Bolton (2000) worker (n = 35): TL = 2.0–2.6, HL = 0.53–0.65, HW = 0.42–0.49, CI = 69–79, ML = 0.21–0.30, MI = 34–48, SL = 0.29–0.36, SI = 68–78, PW = 0.25–0.30, AL = 0.53–0.68.

Queen morphometrics (n = 1): TL = 3.07, HL = 0.70, HW = 0.54, CI = 77, ML = 0.33, MI = 48, SL = 0.37, SI = 71, PW = 0.28, AL = 0.73

Material examined. Specimens examined: UK, 5 Workers, *Guernsey*, Rue des Huriaux, 49.444811, -2.563510, 03 May 2020, Det. M. Hamer 2020, Coll. A. D Marquis, Litter Sifting, M. Hamer Collection MTHENT1432, B. Bolton Collection, IBBL collection ANTWEB1013915, ANTWEB1013916, • UK, 1 Queen, *Guernsey*, Rue des Huriaux, 49.444811, -2.563510, 03 May 2020, Det. M. Hamer 2020, Coll. A. D Marquis, Litter Sifting, M. Hamer Collection, IBBL collection ANTWEB1013917, • UK, 1 Worker, *Guernsey*, Les Cotils Wood, 49.462479, -2.5371520, 25 Jan 2020, Det. M. Hamer 2020, Coll. A.D Marquis, Litter Sifting, M. Hamer Collection MTHENT1434

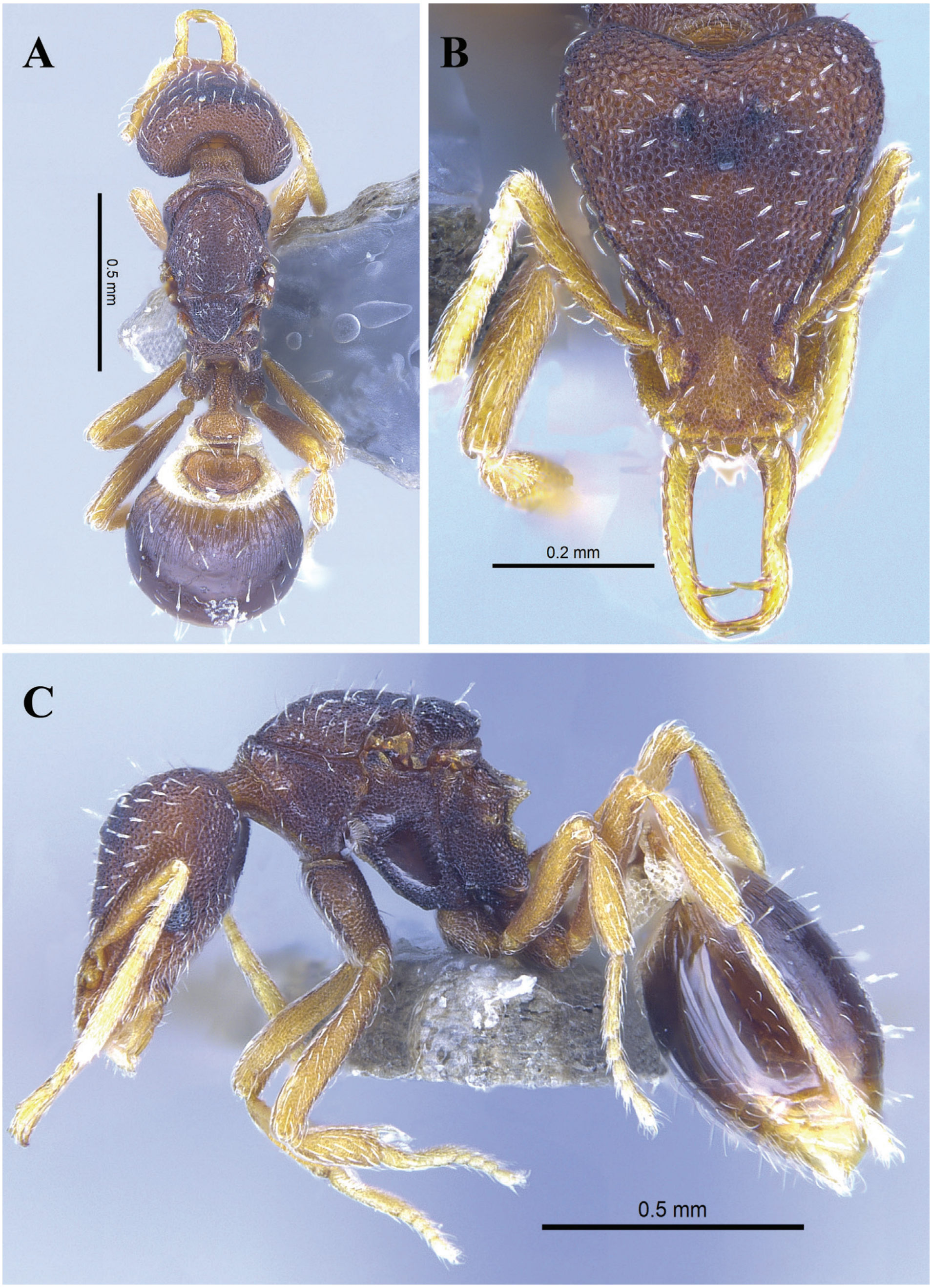

Figure 4. *Strumigenys perplexa* queen (ANTWEB1013917) **A** dorsal view **B** head view **C** profile view. Images by Benoit Guénard.

Determined to be *S. perplexa* from ADM photographs. UK, 19 Workers, *Guernsey*, Camp du Roi, 49.479724, -2.557311, 01 Nov 2020, Det. M. Hamer 2020, Coll. A. D Marquis, Litter Sifting, Fig. 5B • UK, 5 Workers, *Guernsey*, Les Hubit de

Figure 5. In-situ photo records in which specimens were not collected **A** *Strumigenys perplexa* worker carrying prey *Entomobrya intermedia* (Collembola: Entomobryidae) at Les Hubit de Bas **B** *S. perplexa* worker under wood from Camp du Roi. Photos by Andy Marquis.

Bas, 49.43915, -2.54637, 26 July 2020, Det. M. Hamer 2020, Coll. A.D Marquis, Under rotten log, Fig. 5A.

Distribution, ecology and behaviour. Specimens have been collected from four sites on the island of Guernsey, all outdoors. Collection sites are inland, ranging from deciduous forest (Les Cotils Wood. Fig. 2A) to semi-urban conurbations such as household gardens and on roadside verges (Rue des Huriaux Fig. 2B). It should be noted that Rue des Huriaux (Figs 1C, 2B) is an access track within 200 meters of a former garden centre. All specimens have been collected or photographed from within typical *Strumigenys* habitat i.e. soil, leaf litter, decomposing detritus or underneath logs. Workers were observed to be slow and deliberate in their movements and have been noted to prey upon *Entomobrya intermedia* Brooks, 1993 (Collembola: Entomobryidae) (Fig. 5A).

Key to West Palaearctic *Strumigenys* species (workers)

[Adapted from Bolton, 2000: 285. with permission]

Note: there is also a single record of a *Strumigenys* species from Malta, identified as *S. lewisi* Cameron, by Schembri & Collingwood, 1995: 154, which is almost certainly a misidentification. Because Schembri & Collingwood gave no description or illustration of the Maltese species, and because no material from this collection is available for study, it is omitted here. Within Europe, a second mention of *S. lewisi* is found in Georgia, near the city of Batumi, (Arakelian and Dlussky 1991), however, following the examination of the drawings illustrating this species, we consider this record uncertain, as the preapical teeth seem rather short, the angle between the apical and preapical teeth more open, and the anterior margin of the clypeus strongly convex.

These specimens should be re-examined. *Strumigenys lewisi* is not the tramp species it was once thought to be, and its identity, entangled with several other species of the *S. godeffroyi* Mayr species group, was frequently misinterpreted and considerably confused (Bolton pers. comm.).

Taxonomic key of the native and introduced *Strumigenys* species known from Europe

1 Mandibles elongate and narrow, MI 34–58, linear or sublinear. At full closure elongate mandibles interlock only at their apices. Tooth at dorsal apex of mandible long and spiniform, strongly crossing over the tooth from the opposite mandible when closed. Inner margin of mandible with 1–4 teeth or denticles (Fig. 6 A–D)..**2**

– Mandibles short and triangular, MI 15–20. At full closure mandibles engage throughout their visible length, without an open space between them. Tooth at apex of mandible small and inconspicuous, not spiniform, not strongly crossing over the tooth from the opposite mandible when closed. Inner margin of mandible with 12–14 teeth and denticles, some of which may be minute (Fig. 6E–H) **5**

2 Dorsum of mesosoma without standing hairs (Fig. 7A), these different from background pilosity i.e. not erect. Pronotal humeral hair absent. Cephalic dorsum with small orbicular setae. Mandibles each with 3–4 preapical denticles. When mandibles fully closed, the labral lobes are visible between them as a pair of elongate narrow triangles (Fig. 7B). (Austria, Azerbaijan, Bulgaria, Croatia, Czech Republic, France (southern mainland & Corsica), Georgia, Germany, Greece, Hungary, Israel, Italy (mainland, Sardinia & Sicily), Malta, Morocco, Russia (Caucasus), Serbia, Spain, Switzerland, Tunisia, Turkey)...........***argiola***

– Dorsum of mesosoma with at least one pair of standing hairs (Fig. 7C, E). Pronotal humeral hair present (Fig. 7C) (can be abraded). Cephalic dorsum without orbicular setae. Mandibles each with 1–2 preapical teeth. When mandibles fully closed the labral lobes are not visible or at most appear between them as a pair of minute points basally (Fig. 7D, F) **3**

3 Ventrolateral margin of head interrupted by a deep, strongly incised preocular notch; in dorsal view anterior portion of eye is detached from side of head (Fig. 8A, B). With head in ventral view the preocular notch forms the apex of a transverse impression in the ventral surface of the head capsule that extends toward the midline, well behind the postbuccal impression. First gastral sternite without a basal spongiform pad. Apicoscrobal hair absent. Pronotal humeral hair flagellate (Fig. 7C). Mandibles each with 2 short preapical teeth, located close to the apicodorsal tooth, and the proximal preapical tooth longer than the distal (Fig. 6B) (Cosmopolitan tramp species)........... ***rogeri***

– Ventrolateral margin of head uninterrupted to anterior margin of eye; in dorsal view anterior portion of eye is not detached from side of head (Fig. 8C, D). With head in ventral view without a transverse impression in the ventral surface of the head capsule posterior to the postbuccal impression. First gastral sternite with a basal spongiform pad. Apicoscrobal hair present. Pronotal humeral hair straight and simple. Mandibles either with 1 spiniform preapical tooth, located close to the apicodorsal tooth, or also with a denticle close to the midlength which is much shorter than the spiniform preapical tooth (Fig. 6C, D)..**4**

4 Leading edge of scape with all hairs curved toward the apex of the scape (Fig. 9B). Ventral surface of petiole with a conspicuous strip or curtain of spongiform material (Fig. 9A). Mandible with a single spiniform preapical tooth, located close to the apicodorsal tooth, without an additional denticle close to the midlength (Fig. 9B). Dorsum of mesosoma obviously with more than one pair of standing hairs, on pronotum and mesonotum. Mandibles relatively slightly shorter, MI 34–48. (Guernsey [British Channel Islands])... ....***perplexa***

– Leading edge of scape with 2 or more hairs curved toward the base of the scape (Fig. 9D). Ventral surface of petiole entirely lacks spongiform material (Fig. 9C). Mandible with a single spiniform preapical tooth, located close to the apicodorsal tooth, and also with an additional denticle close to the midlength (Fig. 9D). Dorsum of mesosoma with only a single pair of standing hairs, on the mesonotum. Mandibles relatively slightly longer, MI 50–57 (Madeira, southern Atlantic Islands. Portugal, Leiria district).......... ***silvestrii***

5 Pronotal humerus without a projecting hair; pronotum dorso-laterally with sharp raised margination (Fig. 10A). Dorsal mesosoma and first gastral tergite without standing hairs (Fig. 10A). Leading edge of scape with 1–2 hairs near the subbasal bend that are distinctly curved toward the scape base (Fig. 10B). Dorsal surface of mandible basally with a very distinct transverse sharp edge or rim that extends across its width, parallel to and in front of the anterior clypeal margin (Fig. 10B). CI 84–90, SI 51–57. (Cosmopolitan tramp species).................... ***membranifera***

– Pronotal humerus with a projecting simple hair; pronotum dorso-laterally without sharp raised margination (Fig. 10C). Dorsal mesosoma and first gastral tergite with standing hairs (Fig. 10C). Leading edge of scape with all hairs curved or inclined toward the scape apex (Fig. 10D). Dorsal surface of mandible basally without a transverse sharp edge or rim running across its width (Fig. 10D). CI 66–72, SI 69–76..**6**

6 Dorsum of clypeus in full-face view densely clothed with conspicuous broadly spatulate to spoon-shaped hairs; in profile these hairs parallel with the surface from which they arise and closely applied (Fig. 11A). Medially curved ground-pilosity bordering the upper scrobe margins distinctly spatulate. (Algeria, Armenia, Bulgaria, Croatia, France (southern mainland & Corsica), Greece, Hungary, Italy (mainland, Sardinia & Sicily), Macedonia, Malta, Montenegro, Morocco, Romania, Russia, Serbia, Spain, Switzerland, Tunisia, Turkey)..***baudueri***

– Dorsum of clypeus in full-face view clothed with slender hairs that are very narrowly spatulate or simple and cylindrical; in profile these hairs markedly elevated and either arched or inclined anteriorly (Fig. 11B). Medially curved ground-pilosity bordering the upper scrobe margins fine and simple...........7

7 Hairs on clypeal dorsum narrowly spatulate; in profile the hairs distinctly anteriorly curved or anteriorly arched (Fig. 12A). (Bulgaria, France (mainland & Corsica), Greece, Italy, Spain, Turkey) ....***tenuipilis***

– Hairs on clypeal dorsum simple, fine and cylindrical throughout their length and tapered or truncated apically; in profile the hairs mostly straight, inclined anteriorly (Fig. 12B). (France (Corsica), Greece)..........................***tenuissima***

Channel Island checklist

A total of four ant subfamilies, 16 genera and 32 species (including species complexes), plus *Strumigenys perplexa*, are currently recorded from the Channel Islands (Table 1). Guernsey and Jersey hold the largest number of species, with 27 and 17 species respectively. *Temnothorax unifasciatus* (Latreille, 1798) is most widespread across the archipelago recorded from all islands except Grand Epail. In addition to *S. perplexa*,

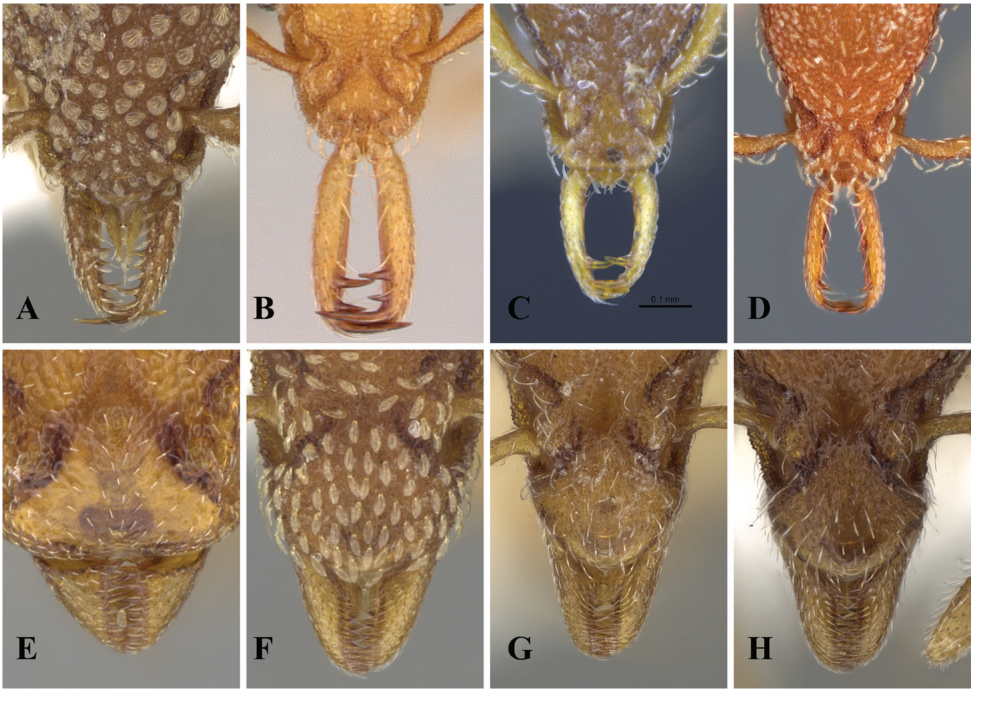

Figure 6. Mandible morphology of European *Strumigenys* species **A** *Strumigenys argiola* (CASENT0280693, Estella Ortega) **B** *S. rogeri* (CASENT0179508, Erin Prado) **C** *S. perplexa* (ANTWEB1013915, Benoit Guénard) **D** *S. silvestrii* (FMNHINS0000078527, Gracen Brilmyer) **E** *S. membranifera* (CASENT0023769, Michele Esposito) **F** *S. baudueri* (CASENT0280694, Estella Ortega) **G** *S. tenuipilis* (CASENT0280695, Estella Ortega) **H** *S. tenuissima* (CASENT0280696, Estella Ortega). Pictures available from www.antweb.org.

Table 1. List of ant species recorded in the Channel Islands. [E] showing introduced species with established outdoor populations and [I] introduced species not established outdoors. Species records indicated with a '?' require further identification work to resolve ambiguity.

Species names	Alderney	Chausey	Grand Epail	Grande Ile	Guernsey	Herm	Jersey	Sark	Channel Islands*
DOLICHODERINAE									
Linepithema humile[I] (Mayr, 1868)					X				
Tapinoma erraticum (Latreille, 1798)					X				
Tapinoma sp. *erraticum* complex							?		
FORMICINAE									
Formica cunicularia Latreille, 1798	X	X			X	X	X	X	
Formica fusca Linnaeus, 1758	X	X			X	X	X	X	
Formica pratensis Retzius, 1783					X		X		
Lasius alienus (Foerster, 1850)	X	X			X	X	X	X	
Lasius emarginatus (Olivier, 1792)	X	X	X		X	X	X		
Lasius flavus (Fabricius, 1782)	X				X	X	X	X	
Lasius fuliginosus (Latreille, 1798)					X	X	X	X	
Lasius mixtus (Nylander, 1846)									X
Lasius myops Forel, 1894		X							
Lasius niger (Linnaeus, 1758)	X				X	X	X	X	
Lasius psammophilus Seifert, 1992					X	X	X		
Lasius umbratus (Nylander, 1846)					X				
Plagiolepis pallescens Forrel, 1889	X				X	X		X	
MYRMICINAE									
Aphaenogaster subterranea (Latreille, 1798)	X				X				
Monomorium pharaonis[I] (Linnaeus, 1758)	X				X				
Myrmecina graminicola (Latreille, 1802)	X				X	X	X	X	
Myrmica ruginodis Nylander, 1846		X			X		X		
Myrmica sabuleti Meinert, 1861	X	X			X	X	X	X	
Myrmica scabrinodis Nylander, 1846	X	X			X	X	X	X	
Solenopsis fugax (Latreille, 1798)		X			X		X	X	
Stenamma westwoodii Westwood, 1839					X				
Stenamma sp. *westwoodii* complex							?	?	
Stenamma debile (Foerster, 1850)					X				
Strumigenys perplexa[E] (Smith, 1876)					X				
Temnothorax albipennis (Curtis, 1854)	X				X	X	X	X	
Temnothorax unifasciatus (Latreille, 1798)	X	X		X	X	X	X	X	
Tetramorium atratulum (Schenck, 1852)									
Tetramorium caespitum (Linnaeus, 1758)	X	X			X	X	X	X	X
Tetramorium impurum (Foerster, 1850)					X				
PONERINAE									
Ponera sp. *coarctata* complex					?	?	?		
Hypoponera sp. *punctatissima*[E] complex							?		
Total, not including complexes	15	11	1	1	27	15	17	14	

* No further mention.

two species and one species complex of exotic origin have been recorded, *Linepithema humile* (Mayr, 1868), *Monomorium pharaonis* (Linnaeus, 1758) and the *Hypoponera punctatissima* species complex. Four species complex groups are here recognized, including records for *Ponera coarctata*, *Hypoponera punctatissima*, *Tapinoma erraticum* and *Stenamma westwoodii* will require further taxonomic work on the basis of existing or new specimens collected.

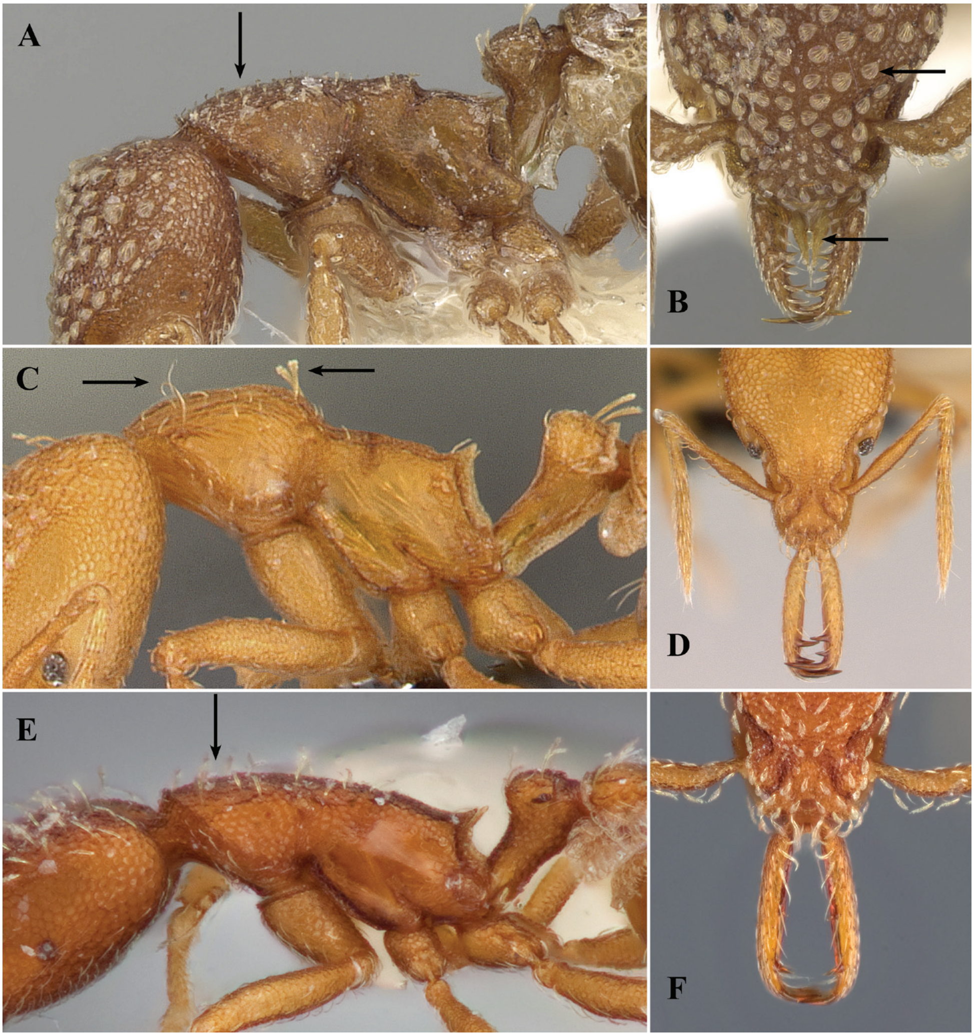

Figure 7. Distinguishing *Strumigenys argiola* from other long mandibular *Strumigenys* species **A** *S. argiola* with arrow showing the lack of standing hairs on mesosoma and pronotal humeral hair (CASENT0280693, Estella Ortega) **B** *S. argiola***,** full face view with labral lobes and orbicular hairs indicated (CASENT0280693, Estella Ortega) **C** *S. rogeri* mesosoma profile, humeral hairs and standing mesoma hairs indicated (CASENT0179508, Erin Prado) **D** *S. rogeri* full face view showing lack of orbicular hairs and visible labral lobes (CASENT0179508, Erin Prado) **E** *S. silvestrii* mesosoma profile with standing hairs on mesosoma arrowed (FMNHINS0000078527, Gracen Brilmyer) **F** *S. silvestrii* in full face view with labral lobes not visible (FMNHINS0000078527, Gracen Brilmyer). Pictures available from www.antweb.org.

Discussion

The discovery of *S. perplexa* within the Channel Islands is remarkable not only because it represents the first record of this species in Europe but also the northernmost record of an outdoor population of any *Strumigenys* species for the continent. It also marks

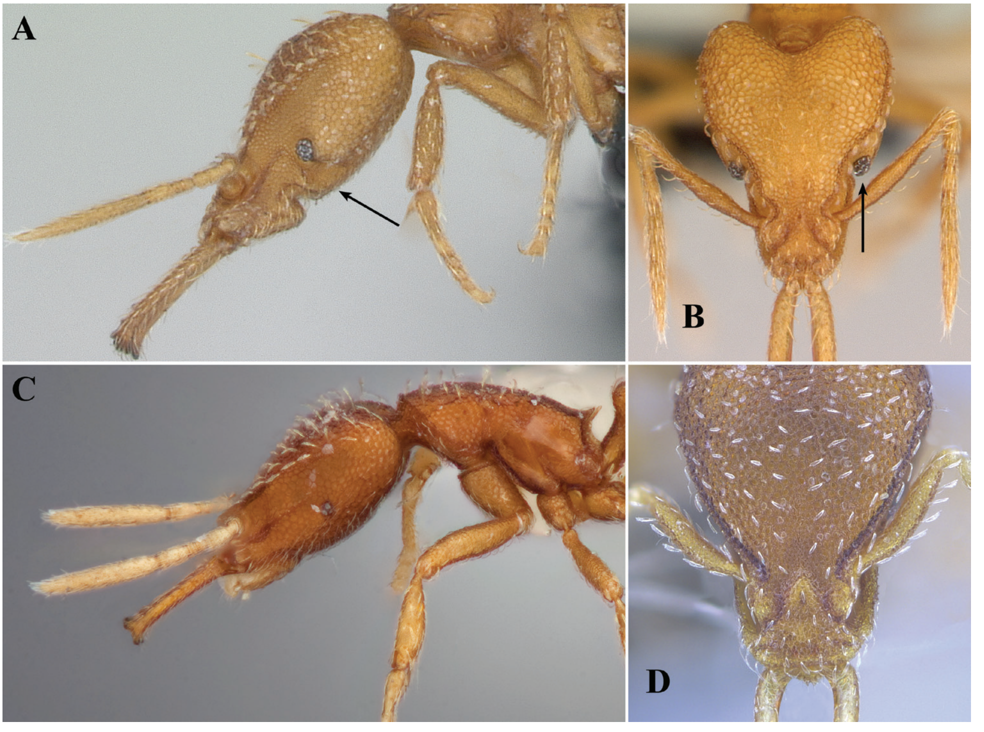

Figure 8. Separating *Strumigenys rogeri* from *S. silvestrii* and *S. perplexa* **A** *S. rogeri* head in profile indicating preocular notch (CASENT0135259, April Noble) **B** *S. rogeri* with anterior portion of eye detached from head (CASENT0179508, Erin Prado) **C** *S. silvestrii* displaying lack of preocular notch (FMNHINS0000078527, Gracen Brilmyer) **D** *S. perplexa*, lacking detached anterior portion of eye (ANTWEB1013916, Benoit Guénard). Pictures available from www.antweb.org.

the first finding of a member of this genus established outside of climate-controlled environments in the British Isles. The United Kingdom has continuously been the recipient of exotic ant species both historically and contemporarily (Donisthorpe 1927; Hamer and Cocks 2020). By 1925, 49 exotic species had been recorded, within the Royal Botanical Gardens, Kew, London, comprising a substantial 38 exotic ant records, which was undoubtedly driven by the trade and movement of horticultural material (Donisthorpe 1915; Donisthorpe 1927; Brangham 1938). Of the 49 records, *S. rogeri* represents the only previous member of *Strumigenys* recorded from the United Kingdom. *Strumigenys rogeri* is known to be a cosmopolitan species with a worldwide distribution facilitated by human commerce (Wetterer 2012a), and records in the United Kingdom originate from the "propagating pits" of both Kew Gardens, London (Donisthorpe 1915; Brangham 1938) and Edinburgh Botanical Gardens (Donisthorpe 1915). In recent years, a number of newly introduced ant species have been recorded in the UK including *Linepithema iniquum* (Mayr, 1870) and the highly invasive Argentine ant, *L. humile* (Fox and Wang 2016; Hamer and Cocks 2020). It is crucial for such findings to be appropriately recorded, particularly for those species of conservation or economical concerns (Notton and Norman 2017).

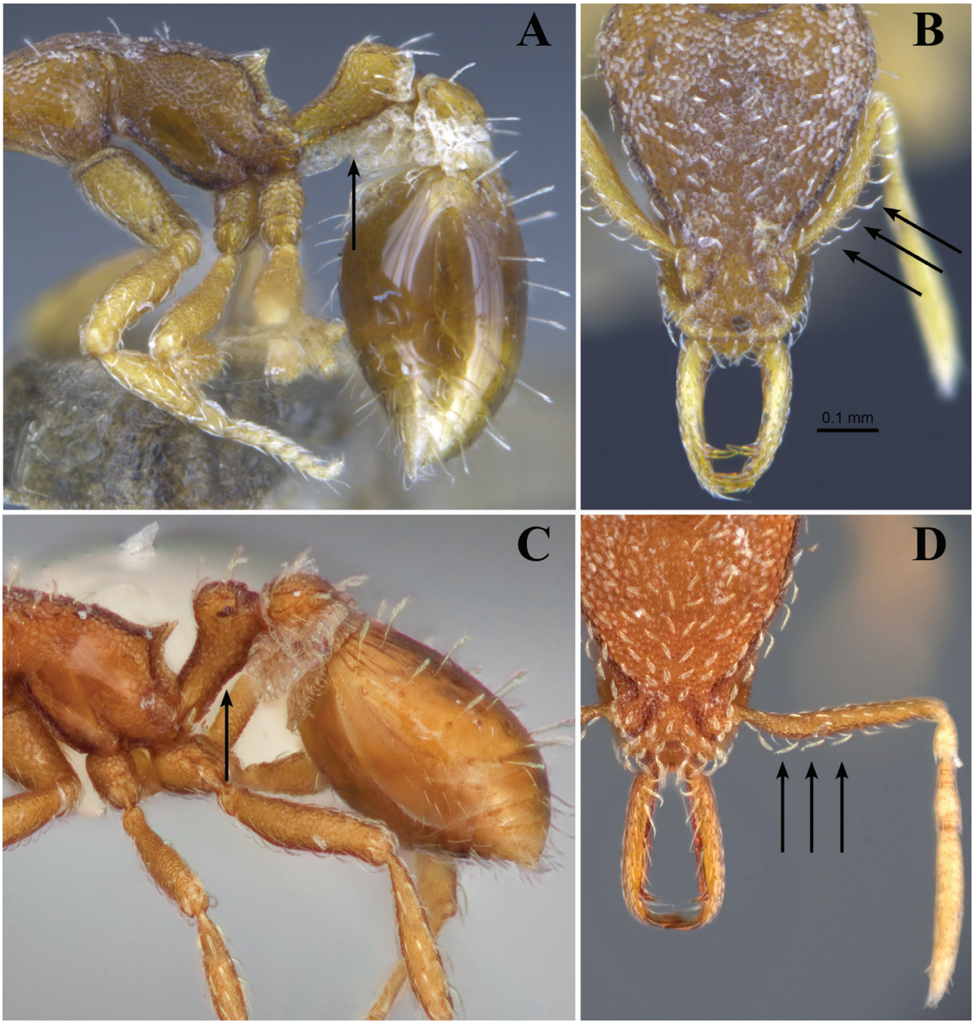

Figure 9. Separating *Strumigneys perplexa* and *S. silvestrii* **A** *Strumigenys perplexa* with ventral petiole spongiform strip indicated (ANTWEB1013915, Benoit Guénard) **B** *S. perplexa* showing all scape hairs curved toward apex (ANTWEB1013915, Benoit Guénard) **C** *S. silvestrii* indicating lack of ventral petiole spongiform tissue (FMNHINS0000078527, Gracen Brilmyer) **D** *S. silvestrii* with 2 or more hairs directed toward scape base (FMNHINS0000078527, Gracen Brilmyer). Pictures available from www.antweb.org.

Strumigenys perplexa was first described from New Zealand by Smith (1876) as *Orectognathus perplexus*. Specimens that were actually *S. perplexa* were subsequently collected and erroneously described as new species from elsewhere in Australasia resulting in the junior synonyms *S. leae* Forel (1913) and *S. antarctica* (Forel, 1892). Bolton (2000) synonymised *S. leae* and *S. antarctica* into *S. perplexa*. In Australia it seems *S. perplexa* is widely distributed (antmaps.org, Janicki et al. 2016) and tolerant of a broad range of habitats with nests located in dry, open woodland, to 'moist fern gullies'

Figure 10. Separating *Strumigenys membranifera* from other short mandibular *Strumigenys* **A** *S. membranifera* in profile view with pronotal margination and lack of standing hairs on mesosoma and first tergite shown (CASENT0023769, Michele Esposito) **B** *S. membranifera* in full face view showing sharp transverse edge across width of mandible anterior to the clypeal margin, and hairs on subbasal bend that are directed toward scape base (CASENT0023769, Michele Esposito) **C** *S. baudueri* in profile with hairs on mesosoma and first gasteral tergite indicated (CASENT0280694, Estella Ortega) **D** *S. baudueri* full face face lacking hairs that direct toward scape base (CASENT0280694, Estella Ortega). Pictures available from www.antweb.org.

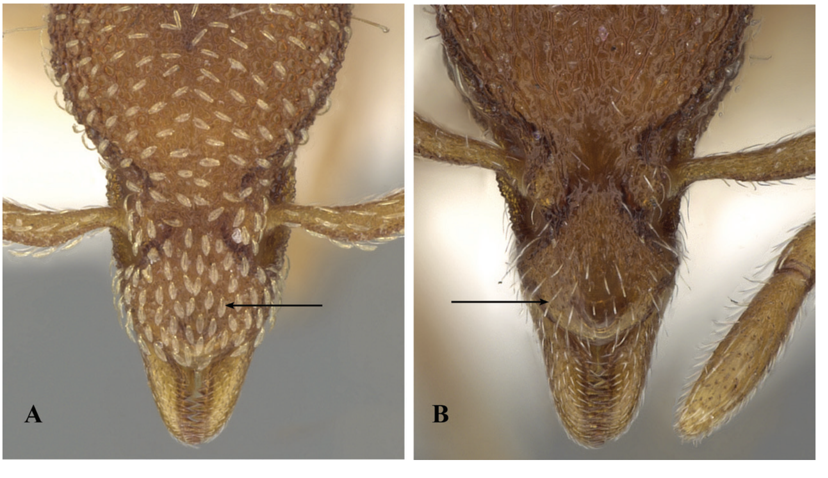

Figure 11. Separating *Strumigneys bauderi* from *S. tenuissima* and *S. tenuipilis* **A** *Strumigenys bauderi* in full face view with dense broadly spatulated hairs indicated (CASENT0280694, Estella Ortega) **B** *S. tenuissima* lacking dense spatulate hairs, hairs structurally different (CASENT0280696, Estella Ortega). Pictures available from www.antweb.org.

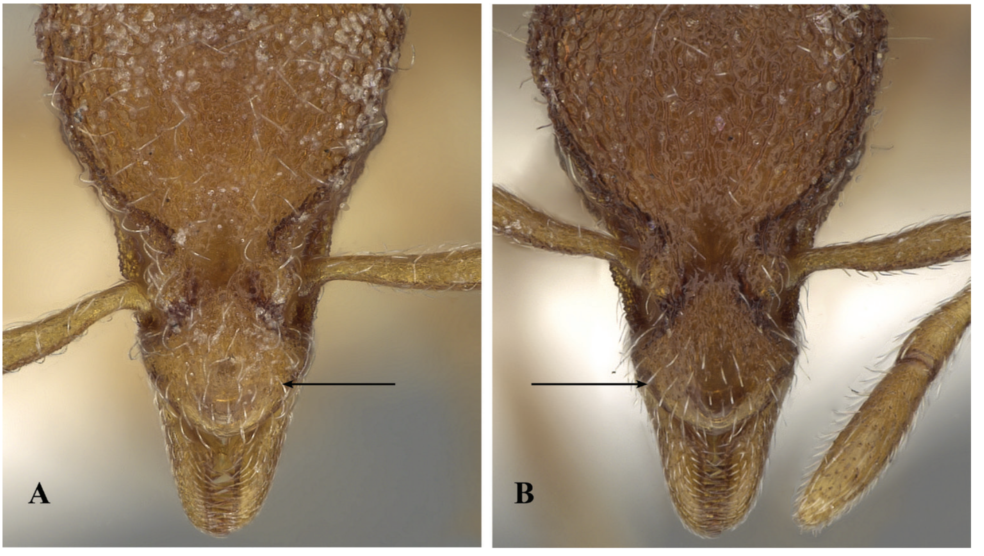

Figure 12. Distinguishing *Strumigenys tenuipilis* from *S. tenuissima* **A** *S. tenuipilis* in full face view with narrowly spatulate hairs indicated (CASENT0280695, Estella Ortega) **B** *S. tenuissima* in full face view with simple hairs shown (CASENT0280696, Estella Ortega). Pictures available from www.antweb.org.

(Brown 1957, 1958). Taylor (1968) however, notes that the temperate rainforests of Australia provide 'optimum' conditions for *S. perplexa*. On New Zealand, where it has been introduced, *S. perplexa* has been collected widely across the North Island (Brown 1958; Cumber 1959; Taylor 1987; Don 2007) and has been successful in native forests on the island (Taylor 1968). Populations on New Zealand as well as Lord Howe and Norfolk Islands are thought to be historical introductions from Australia (Wheeler 1927; Brown 1958). Considering the distance between the Channel Islands and Australia or New Zealand, these findings mark a substantial biogeographic 'leap' from the southern hemisphere, to the north west realm. Our results indicate that other temperate regions around the world should thus include *S. perplexa* into their list of potential successful exotic species able to establish populations outdoor, even at relatively high latitude and under cooler climate. Another Australian *Strumigenys* species, *S. emmae* (Emery, 1890), is also an emerging invader (Wetterer 2012b) but is currently restricted to tropical and sub-tropical climates.

Considering the tolerance of a wide range of climatic and habitat conditions in Australasia, it is of no surprise for *S. perplexa* to be able of establishing on Guernsey. Although Australia and Guernsey do not share overly similar climates, parts of New Zealand and Guernsey certainly do. Both landmasses have a maritime climate of mild winters and warm summers. In addition, numerous other organisms from New Zealand have established themselves in the United Kingdom, including the New Zealand flat worm (*Arthurdendyus triangulates* (Dendy 1896)) (Cannon et al. 1999), and several *Acanthoxyla* Uvarov, 1944 phasmid species (Brock et al. 2018), alongside various plants such as the neckless vine (*Muehlenbeckia complexa* Cunn (Polygonaceae)). Thus, demonstrating the transferability of temperate climate tolerant species from Australasia to the Western Palaearctic.

It is currently unclear whether the seemingly wide distribution of records from Guernsey (Fig. 1C) originates from a single source or from multiple. Speculative entry points include escapes from traded greenhouse plants, or the widespread use of the New Zealand broadleaf (*Griselinia littoralis* Cunn (Griseliniaceae)) hedging. Brown (1958) notes that individuals were collected from Melbourne suburban garden and suggested this to be a likely introductory route to New Zealand. Winged reproductives have not been collected, and so it is unclear whether the population is reproducing, although it could be assumed from the wide distribution recorded here (Fig. 1C). It is likely that the introduction and spread of this species is relatively recent, with impromptu sampling by amateur entomologists and previous surveys of the island not finding the species (Donisthorpe 1947). However, the small size (2–3 mm) and deliberate, slow nature of the species could be a possible reason for the lack of previous records. Colonies are also small with between 40–200 workers and polygynous (Brown 1958). There is currently no evidence to suggest introduced *Strumigenys* fauna have detrimental effects on native fauna, however few studies have examined this topic (Deyrup and Deyrup 1999).

The population of *S. perplexa* should be monitored in order to fully ascertain their distribution and long-term survival on Guernsey. Considering the species' distinctive morphological characteristics relative to indigenous ant species and the lack of congeneric species, monitoring and recording can be completed with relative ease. However, close attention should be made to female reproductives for the workerless inquiline ant *Strumigneys xenos* Brown, 1955 which parasitises *S. perplexa* colonies. Individuals have distinctively smaller mandibles and overall length, amongst other characters (Brown 1955). Introduced populations of *S. xenos* have been recorded in populations of *S. perplexa* in both New Zealand and Lord Howe Island (Brown 1955; Taylor 1968; Hoffmann et al. 2017). The species could potentially have followed *S. perplexa* in a similar fashion or will follow in the future if introductory routes remain open. Similar patterns of introduced social parasites tracking the newly established range of their host is not uncommon and has been recorded in *Tetramorium atratulum* (Creighton, 1934) and *Vollenhovia nipponica* Kinomura & Yamauchi, 1992 which parasite *T. immigrans* Santschi, 1927 and *V. emeryi* Wheeler, 1906 respectively (Wetterer et al. 2015).

Channel Islands checklist

We recorded 32 species across the whole Channel Islands, providing a more comprehensive and updated checklist for the archipelago (Donisthorpe 1947). The ant fauna is typical of West Palaearctic with a dominance in both Formicinae and Myrmicinae. Interestingly, several species which are abundant and frequently recorded in both northern France and southern Great Britain have yet to be recorded, namely *Myrmica rubra* (Linnaeus, 1758), *Leptothorax acervorum* (Fabricius, 1793), *Temnothorax nylanderi* (Foerster, 1850) and *Lasius playthorax* Seifert, 1991. Such species are highly likely to be present and should be looked for in future surveys. Relative to the fauna of Great Britain, of which the islands are British Crown dependencies, the archipelago has several species that are unique, including; *Aphaenogaster subterranea* (Latreille, 1798), *Plagiolepis pallescens* Forel, 1889, *Tetramorium impurum* (Foerster, 1850) and the newly recorded *Strumigenys perplexa*. Moreover, the islands are home to rare species such as *Formica pratensis* Retzius, 1783, thought to be extinct in Great Britain, and *Temnothorax unifasciatus* which is absent from the mainland Great Britain except from an isolated record, likely imported, from West London.

Our checklist includes four complex species groups that are yet to be identified using current taxonomic concepts. Several complex are members of the Ponerinae subfamily including *Ponera coarcata* (Latreille, 1802), a complex split into *P. coarcata* and *P. testacea* Emery, 1895 by Csösz and Seifert (2003), recorded from Jersey, Herm and Guernsey, alongside a second complex group for *Hypoponera punctatissima*, recorded from Jersey. The *Hypoponera punctatissima* complex comprises two species, *Hypoponera punctatissima* (Roger, 1859) and *H. ergatandria* (Forel, 1893) (Seifert 2013, though see Bolton and Fisher 2011). Both are considered widespread tramp species with records of *H. punctatissima* known from outdoor xerothermic habitats (Seifert 2013). *Tapinoma erraticum* complex (Dolichoderinae) includes *T. erraticum* (Latreille, 1798) and *T. subboreale* Seifert, 2012, both of which are recorded from mainland Britain and France (Seifert 2012). *Tapinoma erraticum* has been confirmed from Guernsey and is potentially more widespread with the *Tapinoma erraticum* complex recorded from Jersey, while for now *T. subboreale* appears to have a more oriental distribution within Europe. The *Stenamma westwoodii* complex (Myrmicinae) comprises two species, *S. debile* (Foerster, 1850) and *S. westwoodii* Westwood, 1839 (DuBois 1993), both recorded from Guernsey. Other records of the *S. westwoodii* complex from Jersey and Sark Islands should be confirmed. Future investigations and surveys, using contemporary taxonomic concepts identification tools and comphrensive collecting protocols will clarify these ambiguous records.

Conclusions

Overall, ant diversity known from the Channel Islands is relatively low, and more comprehensive surveys should determine if this relatively low richness is the result of incomplete sampling or of a biogeographic phenomenon resulting from the recent isolation of these islands following the Last Glacial Maximum period and the limited colonization process by native species. Our results also highlight the importance of anthropogenic introductions on these temperate islands, with four introduced species recorded thus far, including the new and notable outdoor presence of *S. perplexa* populations. This discovery represents not only the first record of *Strumigenys* away from heated infrastructure in Northern Europe, but also of surprising biogeographic novelty and major human-driven dispersal jump. Now that *S. perplexa* is seemingly well-established on Guernsey, additional survey work on the other Channel Islands, southern England or nearby European nations may provide further records of this species.

Acknowledgements

We would like to thank Barry Bolton for the key and measurements of several workers, alongside his thoughts and critiques of the manuscript. The authors would also like to thank Mike Fox for access to the BWARs Channel Island ant records, as well as all recorders who have contributed ant records.

References

Arakelian GR, Dlussky GM (1991) Dacetine ants (Hymenoptera: Formicidae) of the USSR [in Russian]. Zoologicheskii Zhurnal 70: 149–152.

Attewell PJ, Wagner HC (2019) *Tetramorium impurum* Foerster (Hymenoptera: Formicidae), first record for Guernsey and the Channel Islands. British Journal of Entomology and Natural History 32: 287–295.

Blatrix R, Colin T, Wegnez P, Galkowski C, Geniez P (2018) Introduced ants (Hymenoptera: Formicidae) of mainland France and Belgium, with a focus on greenhouses. Annales de la Societe Entomologique de France. Taylor & Francis 54(4): 293–308. https://doi.org/10.1080/00379271.2018.1490927

Boieiro M, Espadaler M, Azedo AR, Collingwood CA, Serrano ARM (2009) One Genus and Three Ant species new to Portugal (Hymenoptera, Formicidae). Boletin Sociedad Entomologica Aragonesa 45: 2007–2009.

Bolton B (2000) The ant tribe Dacetini. Memoirs of the American Entomological Institute 65: 1–1028.

Bolton B, Fisher BL (2011) Taxonomy of Afrotropical and West Palaearctic ants of the ponerine genus *Hypoponera* Santschi (Hymenoptera: Formicidae). Zootaxa 2843: 1–118. https://doi.org/10.11646/zootaxa.2843.1.1

Bolton B (2021) An Online Catalog of the Ants of the World. http://antcat.org [2021-01-20]

Booher DB, Gibson JC, Liu C, Longino JT, Fisher BL, Janda M, Narula N, Toulkeridou E, Mikheyev S, Suarez AV, Economo EP (2021) Functional innovation promotes diversification of form in the evolution of an ultrafast trap-jaw mechanism in ants. PLoS Biology 19(3): 1–22. https://doi.org/10.1371/journal.pbio.3001031

Brock PD, Lee M, Morgan-Richards M, Trewick SA (2018) Missing Stickman Found: The First Male of the Parthenogenetic New Zealand Phasmid Genus *Acanthoxyla* Uvarov, 1944 Discovered in the United Kingdom. Atropos 60: 16–23.

Brown WL (1955) The first social parasite in the ant tribe dacetini. Insectes Sociaux 2: 181–186. https://doi.org/10.1007/BF02224379

Brown WL (1957) A preliminary report on dacetine ant studies in Australia. Annals Entomological Society of America 46: 465–471. https://doi.org/10.1093/aesa/46.4.465

Brown WL (1958) A Review of the Ants of New Zealand (Hymenoptera). Acta Hymenopterologica 1(1): 1–50.

Cannon RJC, Baker RHA, Taylor MC, Moore JP (1999) A review of the status of the New Zealand flatworm in the UK. Annals of Applied Biology 135(3): 597–614. https://doi.org/10.1111/j.1744-7348.1999.tb00892.x

Creighton W (1934) Description of three new North American ants with certain ecological observations on previously described forms. Psyche 41(4): 185–200. https://doi.org/10.1155/1934/26532

Csösz S, Seifert B (2003) *Ponera testacea* Emery, 1895 stat. n. – A sister species of *P. coarctata* (Latreille, 1802) (Hymenoptera, Formicidae). Acta Zoologica Academiae Scientiarum Hungaricae 49(3): 201–214.

Cumber RA (1959) Distributional and Biological Notes on Sixteen North Island Species of Formicidae (Hymenoptera). New Zealand Entomologist 2(4): 10–14. https://doi.org/10.1080/00779962.1959.9722774

Dawson W, Moser D, van Kleunen M, Kreft H, Pergl J, Pysek P, Weigelt P,Winter M, Lenzner B, Blackburn TM, Dyer EE, Cassey P, Scrivens SL, Economo EP, Guénard B, Capinha C, Seebens H, Garcia-Diaz P, Nentwig W, Garcia-Berthou E, Casal C, Mandrak NE, Fuller P, Meyer C, Essl F (2017) Global hotspots and correlates of alien species richness across taxonomic groups. Nature Ecology & Evolution 1: e0186. https://doi.org/10.1038/s41559-017-0186

Deyrup M, Deyrup S (1999) Notes on the introduced ant *Quadristruma emmae* (Hymenoptera: Formicidae) in Florida. Entomological News 110: 13–21.

Don W (2007) Ants of New Zealand. Otago University Press, Dunedin, 138–141.

Donisthorpe H (1915) British ants, their life-history and classification. Plymouth. W. Brendon and Son, Limited, 341–342.

Donisthorpe H (1947) The Formicidae of the Channel Islands. The Entomologist 80: 180–182.

DuBois M (1993) What's in a name? A Clarification of *Stenamma westwoodi*, *S. debile* and *S. lippulum* (Hymenoptera: Formicidae: Myrmicinae). Sociobiology 21(3): 299–334.

Else GR, Bolton B, Broad GR (2016) Checklist of British and Irish Hymenoptera – Aculeates (Apoidea, Chrysidoidea and Vespoidea). Biodiversity Data Journal 4(1): e8050.

Fox M, Wang C (2016) Colony of the Argentine ant, *Linepithema humile* (Hymenoptera: Formicidae), in Fulham, West London. British Journal of Entomology and Natural History 29: 193–195.

Gronenberg W (1996) The trap-jaw mechanism in the dacetine ants *Daceton armigerum* and *Strumigenys* sp. The Journal of Experimental Biology 199(9): 2021–2033. https://doi.org/10.1242/jeb.199.9.2021

Guénard B, Weiser MD, Gomez K, Narula N, Economo EP (2017) The Global Ant Biodiversity Informatics (GABI) database: synthesizing data on ant species geographic distribution. Myrmecological News 24: 83–89.

Hamer MT, Cocks LR (2020) *Linepithema iniquum* (Mayr) (Hymenoptera: Formicidae) found at the National Botanic Garden of Wales. British Journal of Entomology and Natural History 33: 71–75.

Hoffmann BD, Graham R, Smith D (2017) Ant species accumulation on Lord Howe Island highlights the increasing need for effective biosecurity on islands. NeoBiota 34: 41–52. https://doi.org/10.3897/neobiota.34.10291

Hölldobler B, Wilson EO (1990) The Ants, Harvard University Press, 732 pp. https://doi.org/10.1007/978-3-662-10306-7

Hopkin SP (2007) A Key to the Collembola (Springtails) of Britain and Ireland. FSC Publications, 247 pp.

Janicki J, Narula N, Ziegler M, Guénard B, Economo PE (2016) Visualizing and interacting with large-volume biodiversity data using client-server web-mapping applications: The design and implementation of antmaps.org. Ecological Informatics 32: 185–193. https://doi.org/10.1016/j.ecoinf.2016.02.006

Livory A (2003) Les fourmis de la Manche – Premier catalogue. Argiope 39: 25–49.

MacGown JA, Wetterer JK, Hill JG (2012) Geographic spread of *Strumigenys silvestrii* (Hymenoptera: Formicidae: Dacetini). Terrestrial Arthropod Reviews 5: 213–222. https://doi.org/10.1163/18749836-05031051

Masuka K (1984) Studies on the predatory biology of oriental dacetine ants (Hymenoptera: Formicidae) I. Some Japanese species of *Strumigenys*, *Pentastruma*, and *Epitritus*, and a Malaysian *Labidogenys*, with special reference to hunting tactics in short-mandibulate forms. Insectes Sociaux 31(4): 429–451. https://doi.org/10.1007/BF02223658

McGlynn TP (1999) The worldwide transfer of ants: Geographical distribution and ecological invasions. Journal of Biogeography 26(3): 535–548. https://doi.org/10.1046/j.1365-2699.1999.00310.x

Moser D, Lenzner B, Weigelt P, Dawson W, Kreft H, Pergl J, Pyšek P, van Kleunen M, Winter M, Capinha C, Cassey P, Dullinger S, Economo EP, García-Diaz P, Guénard B, Hofhansl F, Mang T, Seebens H, Essl F (2018) Remoteness promotes biological invasions on islands worldwide. Proceedings of the National Academy of Sciences 115: 9270–9275. https://doi.org/10.1073/pnas.1804179115

Notton DG, Norman H (2017) Hawk's-Beard Nomad Bee, *Nomada facilis*, New to Britain (Hymenoptera: Apidae). British Journal of Entomology and Natural History 30: 201–214.

Schembri S, Collingwood CA (1995) The Myrmecofauna of the Maltese Islands. Remarks and Additions. Bollettino della Società Entomologica Italian 127(2): 153–158.

Seifert B (2012) Clarifying naming and identification of the outdoor species of the ant genus *Tapinoma* Förster, 1850 (Hymenoptera: Formicidae) in Europe north of the Mediterranean region with description of a new species. Myrmecological News 16: 139–147.

Seifert B (2013) *Hypoponera ergatandria* (Forel, 1893) – a cosmopolitan tramp species different from *H. punctatissima* (Roger, 1859) (Hymenoptera: Formicidae). Soil Organisms 85: 189–201.

Seifert B (2018) The Ants of Central and North Europe. Lutra, 152–153.

Smith F (1876) Descriptions of three new species of Hymenoptera (Formicidae) from New Zealand. Transactions of the Entomological Society of London 4: 489–492. https://doi.org/10.1111/j.1365-2311.1876.tb01923.x

Tang KL, Pierce MP, Guénard B (2019) Review of the genus *Strumigenys* (Hymenoptera, Formicidae, Myrmicinae) in Hong Kong with the description of three new species and the addition of five native and four introduced species records. ZooKeys 831: 1–48. https://doi.org/10.3897/zookeys.831.31515

Taylor RW (1968) The Australian workerless inquiline ant *Strumigenys xenos* Brown (Hymenoptera: Formicidae) Recorded from New Zealand. New Zealand Entomologist 4(1): 47–49. https://doi.org/10.1080/00779962.1968.9722888

Taylor RW (1987) A Checklist of the Ants of Australia, New Caledonia and New Zealand (Hymenoptera: Formicidae). Division of Entomology Report. Commonwealth Scientific and Industrial Research Organisation, Australia 41: 1–92.

Wetterer JK (2011) Worldwide spread of the membraniferous dacetine ant, *Strumigenys membranifera* (Hymenoptera: Formicidae). Myrmecological News 14: 129–135.

Wetterer JK (2012a) Worldwide spread of Roger's dacetine ant, *Strumigenys rogeri* (Hymenoptera: Formicidae). Myrmecological News 16: 1–6.

Wetterer JK (2012b) Worldwide spread of Emma's dacetine ant, *Strumigenys emmae* (Hymenoptera: Formicidae). Myrmecological News 16: 69–74.

Wetterer JK (2015) Geographic spread of *Vollenhovia emeryi* (Hymenoptera: Formicidae). Asian Myrmecology 7(1): 105–112.

Wheeler WM (1927) The Ants of Lord Howe Island and Norfolk Island. Proceedings of the American Academy of Arts and Sciences 62: 121–153. https://doi.org/10.2307/25130110

Supplementary material 1

Table S1. Morphological measurements descriptions based on Bolton (2000, p. 5).

Authors: Matthew T. Hamer, Andy D. Marquis, Benoit Guénard

Data type: measurements

Link: https://doi.org/10.3897/jhr.83.66829.suppl1

JHR 83: 125–137 (2021)
doi: 10.3897/jhr.83.64380
https://jhr.pensoft.net

RESEARCH ARTICLE

JOURNAL OF Hymenoptera RESEARCH
A peer-reviewed open-access journal
The International Society of Hymenopterists

A key to all species of *Fagineura* Vikberg & Zinovjev (Hymenoptera, Tenthredinidae) worldwide with the descriptions of two new Chinese species

Meng-Meng Liu[1], Ze-Jian Li[2], Mei-Cai Wei[3]

1 *College of Ecology, Lishui University, Lishui, Zhejiang 323000, China* **2** *Postdoctoral Work Station, Scientific Research and Management Center of East China Pharmaceutical Botanical Garden, Lishui Ecological Forestry Development Center, Lishui, Zhejiang 323000, China* **3** *College of Life Science, Jiangxi Normal University, Nanchang, Jiangxi, 330022, China*

Corresponding authors: Ze-Jian Li (lizejian2006@163.com), Mei-Cai Wei (weimc@126.com)

Academic editor: Marko Prous | Received 13 February 2021 | Accepted 25 May 2021 | Published 28 June 2021

http://zoobank.org/AF006ACB-0692-4CF0-985F-3898A044BE68

Citation: Liu M-M, Li Z-J, Wei M-C (2021) A key to all species of *Fagineura* Vikberg & Zinovjev (Hymenoptera, Tenthredinidae) worldwide with the descriptions of two new Chinese species. Journal of Hymenoptera Research 83: 125–137. https://doi.org/10.3897/jhr.83.64380

Abstract
Fagineura was established by Vikberg & Zinovjev in Shinohara et al. (2000). In this paper, two new species of *Fagineura* are described and illustrated, *F. brevicornis* **sp. nov.** collected in Hubei Province and *F. longitangia* **sp. nov.** collected in Hunan Province from China. A key to all species of *Fagineura* worldwide is provided, now including six species.

Keywords
China, key, Nematinae, sawfly, taxonomy, Tenthredinoidea

Introduction

Fagineura Vikberg & Zinovjev, 2000 (Shinohara et al. 2000) is a small genus of the subfamily Nematinae (Tenthredinidae). Until now, only four species have been known worldwide (Taeger et al. 2010; Liu et al. 2019), namely *F. crenativora* Vikberg & Zinovjev, 2000 and *F. quercivora* Togashi, 2006, distributed in Japan; and *F. flactoserrula* Liu, Li & Wei, 2019 and *F. xanthosoma* Liu, Li & Wei, 2019, distributed in China. In the course of studying Nematinae from China, two specimens of *Fagineura* were found that are different from the four known species, and they are described here as new species. The two species are described and illustrated, and a key to the known species of *Fagineura* worldwide is provided.

Materials and methods

Imaging, terminology, deposition of material

The specimens were examined with a Motic-SMZ-171 stereomicroscope. Images of the imagines were taken with a Nikon D700 digital camera and a Leica Z16APO separately. The genitalia were examined with a Motic BA410E microscope, and images of the genitalia were taken with Motic Moticam Pro 285A. The series of images produced were focus-stacked using Helicon Focus (HeliconSoft, Kharkiv, Ukraine) and further processed with Adobe Photoshop CS 11.0.

The terminology of genitalia follows Ross (1945) and that of general morphology follows Viitasaari (2002). For a few terms, including middle fovea, lateral fovea, and lateral walls, we follow Takeuchi (1952).

Specimens examined in this study are deposited in the Asian Sawfly Museum, Nanchang, China (**ASMN**), including holotypes of the two new species, 2 specimens of *F. flactoserrula* Liu, Li & Wei, 2019 and 16 specimens of *F. xanthosoma* Liu, Li & Wei, 2019.

Abbreviations used in the text and illustrations are as follows:

OCL The distance between a lateral ocellus and the occipital carina, or the hind margin of the head where this carina would be if it were developed (Benson 1954);
OOL The distance between an eye and a lateral ocellus;
POL The distance between the mesal margins of the 2 lateral ocelli.

Results

Taxonomy

Fagineura Vikberg & Zinovjev, 2000

Figures 1, 2

Type species. *Fagineura crenativora* Vikberg & Zinovjev, 2000.

Diagnosis. Compared with the diagnosis of Liu et al. (2019), we present the following changes: Medium-sized; clypeus and labrum yellowish white to yellow; clypeus with broad and moderately deep (0.3–0.5) emargination apically; mandibles symmetrical; malar space shorter than diameter of median ocellus, and in most species not exceeding 0.5 × of diameter of median ocellus; postocellar area more than 2.0 × as wide as long;

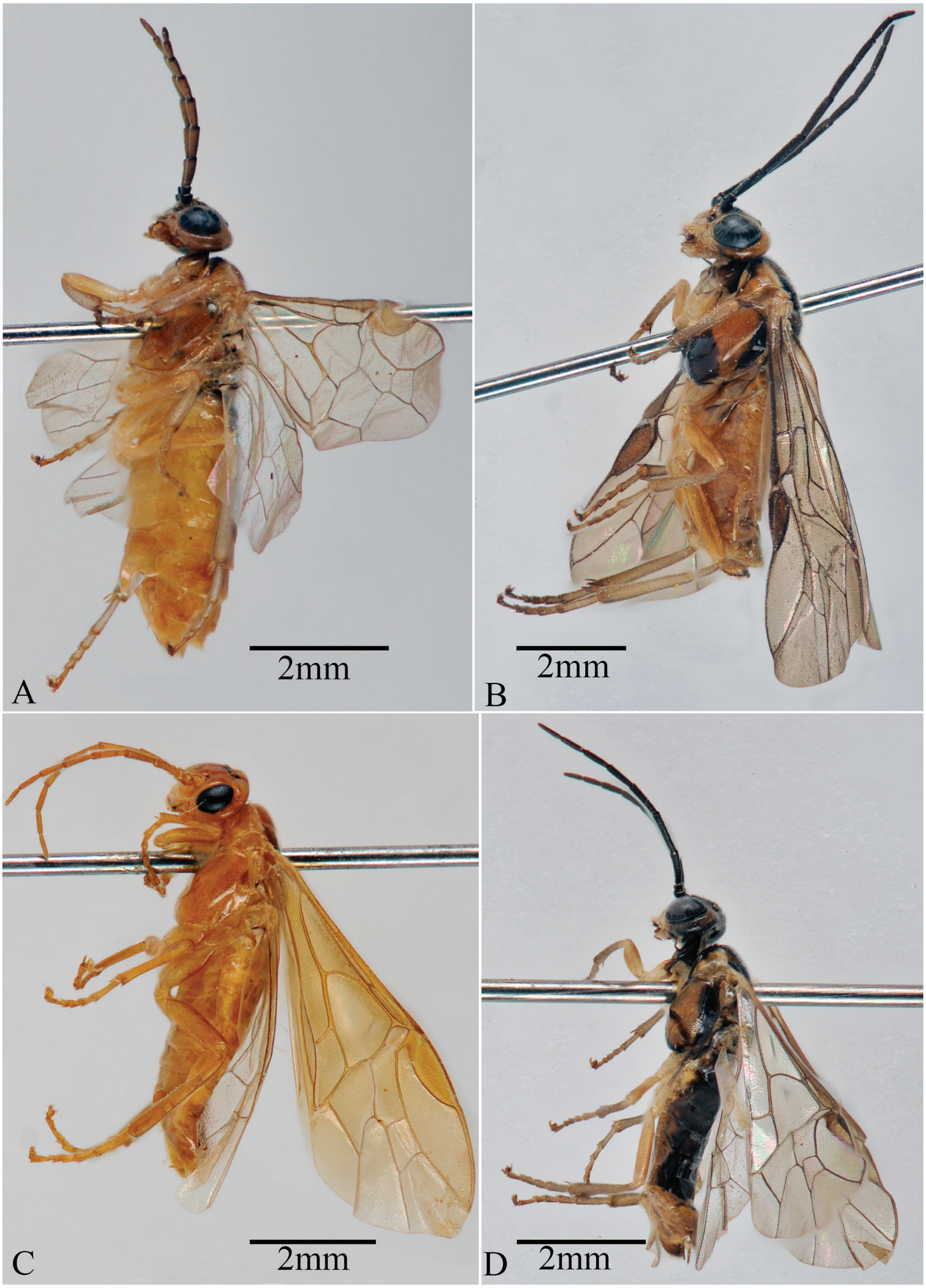

Figure 1. Whole body in lateral view of *Fagineura* species, female **A, B, D** holotype **C** paratype **A** *F. brevicornis* sp. nov. **B** *F. longitangia* sp. nov. **C** *F. xanthosoma* Liu, Li & Wei, 2019 **D** *F. flactoserrula* Liu, Li & Wei, 2019.

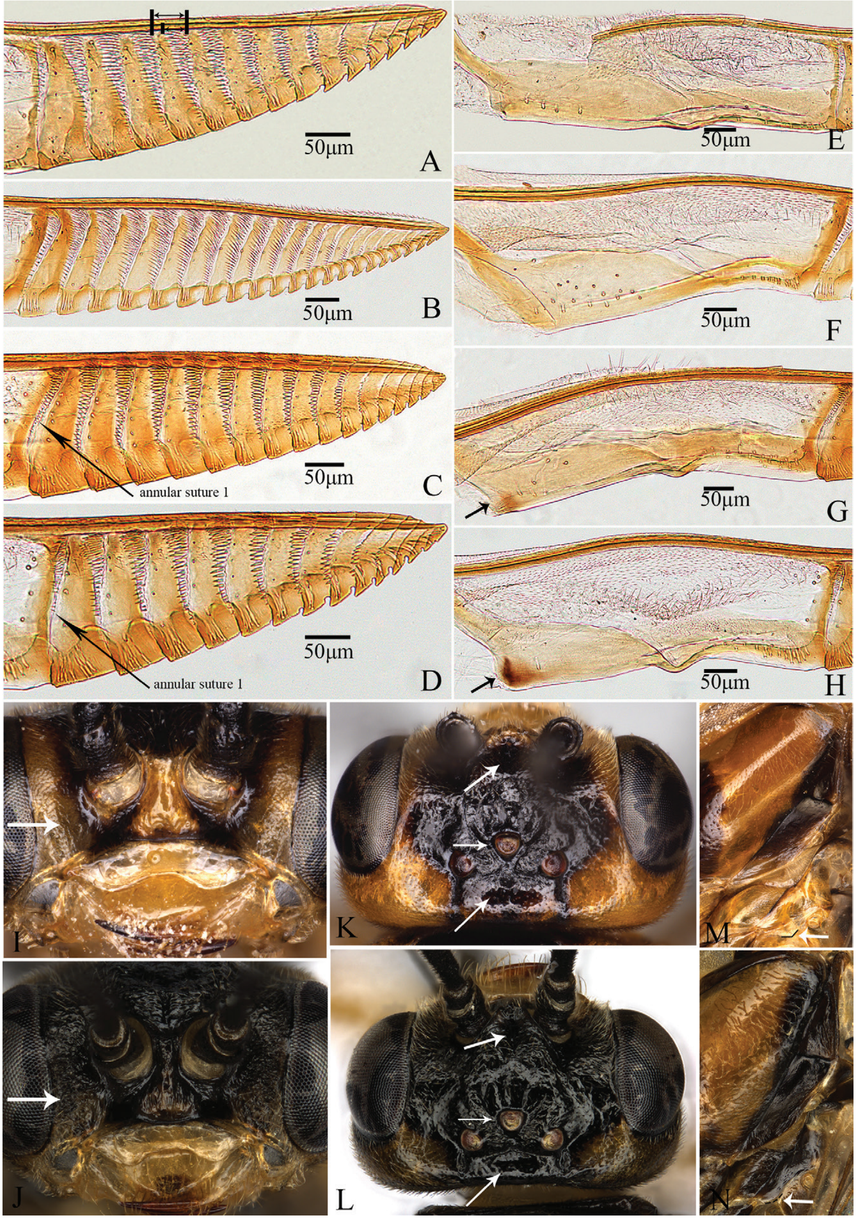

Figure 2. Characters used to identify *Fagineura* species **A** *F. brevicornis*, lamnium (the short double arrow denotes the longest setae band, the long double arrow denotes the length of the annulus) **B** *F. xanthosoma*, lamnium **C** *F. longitangia*, lamnium **D** *F. flactoserrula*, lamnium **E** *F. brevicornis*, tangium **F** *F. xanthosoma*, tangium **G** *F. longitangia*, tangium (arrow denotes the posterior corner not swollen) **H** *F. flactoserrula*, tangium (arrow denotes the posterior corner swollen) **I** *F. longitangia* (arrow denotes inner orbit of head) **J** *F. flactoserrula* (arrow denotes inner orbit of head) **K** *F. longitangia* (arrows from top to bottom denote middle fovea, circumocellar furrow and postocellar area) **L** *F. flactoserrula* (arrow denotes inner orbit of head) **K** *F. longitangia* (arrows from top to bottom denote middle fovea, circumocellar furrow and postocellar area) **M** *F. longitangia* (arrow denotes posterodorsal corner of metepimeron) **N** *F. flactoserrula* (arrow denotes posterodorsal corner of metepimeron).

antenna usually shorter than thorax and abdomen together; posterior part of mesopleural katepimeron covered with hairs; distance between cenchri as long as or shorter than breadth of a cenchrus; forewing without radial cross-vein; the costa of forewing less dilated than in *Pristiphora*; petiole of anal cell of hindwing of *F. quercivora* Togashi, 2006 short than cu-a, and the other 5 species longer than cu-a; claws bifid, inner tooth large; sawsheath short; annular suture 1 with setae band; the longest setae bands of lancet is at least 0.5 × length of annulus; cypsella of basal serrulae absent, apically short and with emargination; tangium of lancet with campaniform sensilla in most species; except for *F. quercivora* Togashi, 2006 we unknown, the radix of *F. xanthosoma* Liu, Li & Wei, 2019 shorter than lamnium, and the other 4 species longer than or as long as lamnium.

Remarks. Shinohara et al. (2000) provided the differences between *Fagineura* and *Nematus*, but based on all species of *Fagineura*, it differs from *Nematus* in annular suture 1 of lancet with setae band; less derived shape of the mandibles; malar space narrower than the diameter of the median ocellus; katepimeron of the mesopleuron with hairs; having campaniform sensilla on the tangium except for *F. flactoserrula* only one or none; the apically emarginate sawsheath except for *F. xanthosoma*.

Key to all species of *Fagineura* worldwide

1 Mesepisternum, all coxae and ovipositor sheath black; inner tooth of tarsal claw longer than outer tooth. Japan (Honshu)....***F. quercivora* Togashi, 2006**

– Mesepisternum mostly or entirely yellow or yellowish brown (Fig. 1A–D); all coxae yellowish white or yellow, or only basal margin black; ovipositor sheath yellow or yellowish brown, or apical margin of valvula 3 black; inner tooth of tarsal claw shorter than outer tooth...**2**

2 Frontal area mostly yellow or yellowish brown; mesonotum mostly yellowish brown; wing veins mostly pale yellow **3**

– Frontal area entirely black; mesonotum mostly black; wing veins mostly black-brown...**4**

3 Area surrounding anterior tentorial pit and subantennal groove black; malar space 0.4 × as long as diameter of median ocellus; middle fovea sub-circular (Fig. 3B, C); sheath 2.3 × as long as metatarsomere 1, valvula 3 almost as long as valvifer 2 (Fig. 3G); lancet with 15 serrulae, sutures 1–12 with setae bands, longest setae band about 0.7 × length of annulus (Fig. 2A); cypsellae of serrulae 1–7 absent, tangium with 4 campaniform sensilla, radix 1.1 × as long as lamnium (Figs 2E, 3H–J). China (Hubei) ....***F. brevicornis* sp. nov.**

– Area surrounding anterior tentorial pit and subantennal groove yellow; malar space 0.8 × as long as diameter of median ocellus; middle fovea long, groove-like; sheath 1.8 × as long as metatarsomere 1, valvula 3 1.3 × as long as valvifer 2; lancet with 21 serrulae, sutures 1–13 with setae bands, longest setae band about 0.9 × length of annulus (Fig. 2B); cypsellae of serrulae 1–2 nearly absent, tangium with more than 10 campaniform sensilla (Fig. 2F), radix 0.6 × as long as lamnium. China (Hubei, Hunan) ..... ***F. xanthosoma* Liu, Li & Wei, 2019**

4 Mesopleuron entirely pale yellowish browm; ovipositor sheath short, 1.6 × as long as metatarsomere 1, with shallow emargination apically; annular suture 1 of lancet straight, and with 3 marginal sensilla below. Japan (Hokkaido, Honshu, Kyushu, Shikoku) ....***F. crenativora*** **Vikberg & Zinovjev, 2000**

– Mesopleuron with distinct black spots; ovipositor sheath relatively long, 1.9 or 2.0 × as long as metatarsomere 1, tapering toward apex; annular suture 1 of lancet oblique to the apex of lancet, and with 7 or 9 marginal sensilla below........ **5**

5 Supraclypeal area and inner orbit black, and with wrinkles (Fig. 2J); metapleuron and abdominal terga mostly black; posterodorsal corner of metepimeron rounded (Fig. 2N); middle fovea long and groove-like; circumocellar furrow indistinct; postocellar area 3.0 × as wide as long (Fig. 2L); lancet with 14 serrulae, each middle serrula with 10–13 distal teeth; annular suture 1 slightly curved, sutures 1–10 with setae bands, longest setae band about 0.7 × length of annulus; cypsella of serrulae 1–4 absent (Fig. 2D); tangium with 1 campaniform sensillum, and basoventral corner swollen (Fig. 2H). China (Hubei)..***F. flactoserrula*** **Liu, Li & Wei, 2019**

– Most of supraclypeal area, inner orbit, metapleuron, most of abdominal terga yellowish brown (Fig. 4C, E); posterodorsal corner of metepimeron squared (Fig. 2M); middle fovea sub-circular; circumocellar furrow distinct; postocellar area 2.5 × as wide as long (Fig. 2K); lancet with 16 serrulae, each middle serrula with 13–16 distal teeth; annular suture 1 distinctly curved, sutures 1–11 with setae bands, longest setae band about 0.6 × length of annulus; cypsella 1–9 absent (Fig. 2C); tangium with 6 campaniform sensilla, and basoventral corner not swollen (Figs 2G, 4H, I). China (Hunan).............***F. longitangia*** **sp. nov.**

Fagineura brevicornis **Liu, Li & Wei, sp. nov.**

http://zoobank.org/6543B58F-779E-48AA-A4B8-FD290B16CA8D

Figure 3

Material examined. ***Holotype*****,** female, China: Hubei Province, Yichang City, Shengnongjia Mountain, Guitouwan, 31°28.44'N, 110°08.87'E, 2150 m, 19 May 2012, leg. Ze-Jian Li, ASMN.

Diagnosis. *F. brevicornis* is most similar to *F. xanthosoma* in having both the mesepisternum, head and wing veins mainly yellow or yellow-brown; ovipositor sheath entirely yellow or yellowish brown; but *F. brevicornis* can be differentiated from the latter by the black subantennal groove and area surrounding anterior tentorial pit (in *F. xanthosoma* these are yellow); malar space 0.4 × as long as diameter of median ocellus; middle fovea sub-circular (Fig. 3B, C); sheath 2.3 × as long as metatarsomere 1, valvula 3 almost as long as valvifer 2 (Fig. 3G); lancet with 15 serrulae, sutures 1–12 with setae bands, longest setae band about 0.7 × length of annulus (Fig. 2A); cypsellae of serrulae 1–7 absent, tangium with 4 campaniform sensilla, radix 1.1 × as long as lamnium (Figs 2E, 3H–J).

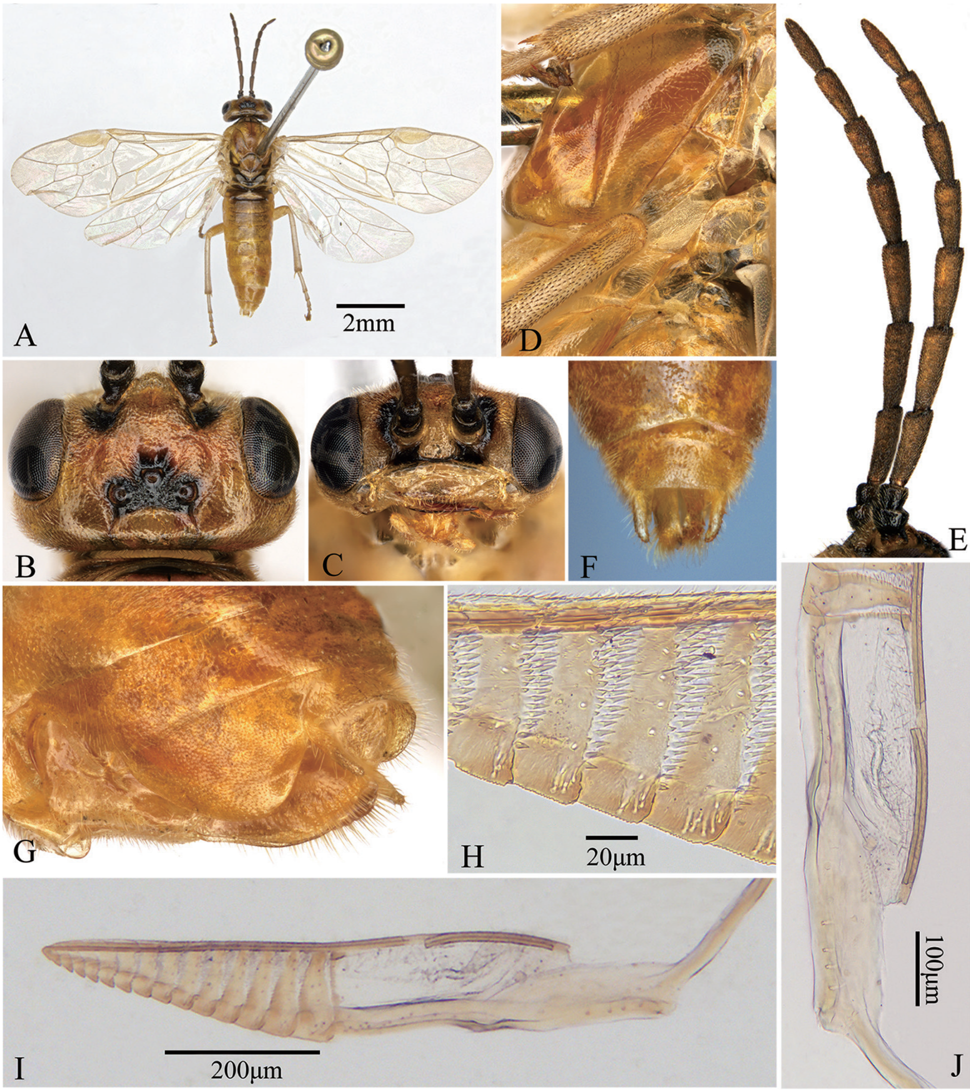

Figure 3. *Fagineura brevicornis* sp. nov., female, holotype **A** dorsal view **B** head, dorsal view **C** head, anterior view **D** mesopleuron and metapleuron **E** antenna, lateral view **F** ovipositor sheath, dorsal view **G** ovipositor sheath, lateral view **H** middle serrulae **I** lancet **J** tangium.

Description. Holotype, female. Body length approximately 7.0 mm (Fig. 3A).

Color. Body yellowish brown. Areas surrounding ocelli, antennal sockets, subantennal groove, anterior tentorial pit, scape and pedicel of antenna, triangular spot on the upper side of mesepisternum, anterior edge on the upper side of median mesoscutal lobe, spot of median metascutellum, tergum 1 except triangular spot, anterior edge of tergum 2 black; cenchrus yellowish white. Wings hyaline, without smoky macula, stigma and most parts of veins pale yellow.

Head. Base of labrum elevated, apex rounded; base of clypeus strongly elevated, anterior margin of clypeus arcuate and incised to 0.5 × length of clypeus, lateral corners slightly rounded; labrum and clypeus shiny, basally without punctures or microsculpture, apically with sparse and small punctures, without microsculpture. Malar space 0.4 × as long as diameter of median ocellus. Inner margins of eyes slightly convergent downward in frontal view, distance between eyes 2.0 × as long as height of eyes (Fig. 3C). In dorsal view, inner margins of eyes subparallel; middle fovea sub-circular, slightly deep, with a longitudinal groove at bottom. Frontal area elevated, slightly shiny, punctures small and somewhat sparse, with weak microsculpture; anterior wall slightly elevated, notched medially, lateral walls low and blunt, lateral furrows of frontal area slightly narrow and shallow. The top surface of ocelli higher than the top surface of eye clearly in lateral view; interocellar furrow broad and shallow, postocellar furrow somewhat narrow and shallow; circumocellar furrow indistinct; POL : OOL : OCL = 0.9 : 1.0 : 0.8 (Fig. 3B). Vertex and postocellar area shiny, punctures faint and very sparse, without microsculpture; postocellar area slightly convex, middle furrow of postocellar area faint, approx. 2.2 × as wide as long, lateral postocellar furrows narrow and slightly deep, divergent backward clearly (Fig. 3B). Antenna filamentous, shorter than thorax and abdomen together, antennomeres 3–8 slightly compressed; antennomere 2 1.2 × as wide as long, relative length of antennomere 3 : antennomere 4 : antennomere 5 = 1.0 : 1.1 : 1.0 (Fig. 3E).

Thorax. Mesonotum slightly shiny, with fine and somewhat dense punctures, without microsculpture; median mesoscutal groove shallow and thin; mesoscutellum shiny, with faint and sparse punctures, without microsculpture, and flat, without middle ridge, about 0.8 × as long as wide; mesoscutellar appendage shiny, with small and sparse punctures, microsculpture indistinct, about 0.3 × length of scutellum, middle ridge very low and blunt. Distance between cenchri as long as breadth of a cenchrus. Mesepisternum shiny, without microsculpture, with fine setigerous punctures; anepimeron of mesepimeron shiny, with few punctures and microsculpture; katepimeron smooth and shiny, posterior part with distinct microsculpture and covered with setae, punctures indistinct; metapleuron shiny and smooth, punctures and microsculpture indistinct (Fig. 3D). Vein Sc almost interstitial with origin of vein M from R, and vein M shorter than vein R+M; forewings with cross-vein cu-a joining cell 1M at basal 0.6, cell 2Rs 1.5 × as long as wide, petiole of anal cell of hindwing 1.7 × as long as cu-a.

Abdomen. All abdominal terga slightly shiny, with small and very sparse setigerous punctures, microsculpture fine and dense. Ovipositor sheath slightly shiny, punctures on valvula 3 fine and sparse, microsculpture indistinct; sheath 2.3 × as long as metatarsomere 1 and 1.4 × as long as front tibia, valvula 3 almost as long as valvifer 2; in lateral view, sheath tapering toward apex (Fig. 3G); in dorsal view, apex of cercus hardly protruding beyond valvula 3, angle between most lateral setae of valvula 3 about 40°. Lancet with 15 serrulae (Fig. 3I); each middle serrula with 14–16 distal teeth (Fig. 3H); annular suture 1 approximately straight, sutures 1–12 with setae bands, longest setae band about 0.7 × length of annulus; cypsellae of serrulae 1–7, 14–15 absent, cypsellae of serrulae 8–13 short; tangium slender and 5.5 × as long as annulus 1, with 4 campaniform sensilla (Fig. 3J), radix 1.1 × as long as lamnium.

Legs. Protarsomere 1 shorter than combined length of tarsomeres 2–4; inner apical spur of hind tibia 0.4 × as long as metatarsomere 1, metatarsomere 1 0.6 × as long as combined length of metatarsomeres 2–5; tarsal claw with inner tooth long, 0.8 × as long as outer tooth.

Male. Unknown.

Distribution. China (Hubei).

Remarks. The new species can be easily distinguished from the other *Fagineura* species in body color and antenna (antennomeres 3–8 slightly compressed and looks more stubby than other *Fagineura* species).

Etymology. The specific name "*brevicornis*" is refers to the short antenna.

Fagineura longitangia Liu, Li & Wei, sp. nov.

http://zoobank.org/606EF4B7-2DC2-4A55-BFB2-DB9B05720128
Figure 4

Material examined. ***Holotype*,** female, China: Hunan Province, Yizhang County, Mang Mountain, Datangkeng, 24°59.02'N, 112°48.14'E, 1090 m, 11 April 2007, leg. Mei-Cai Wei, ASMN.

Diagnosis. *F. longitangia* is most similar to *F. flactoserrula* in having both the frontal area entirely black; mesonotum mostly black; wing veins mostly black-brown; margin of valvula 3 black; but *F. longitangia* can be differentiated from the latter by most of supraclypeal area, inner orbit, metapleuron, most of abdominal terga yellowish brown (Fig. 4C, E); posterodorsal corner of metepimeron squared (Fig. 2M); middle fovea sub-circular; circumocellar furrow distinct; postocellar area 2.5 × as wide as long (Fig. 2K); lancet with 16 serrulae, each middle serrula with 13–16 distal teeth; annular suture 1 distinctly curved, sutures 1–11 with setae bands, longest setae band about 0.6 × length of annulus; cypsella 1–9 absent (Fig. 2C); tangium with 6 campaniform sensilla, and basoventral corner not swollen (Figs 2G, 4H–I).

Description. Holotype, female. Body length approximately 7.5 mm (Fig. 4A).

Color. Body yellowish brown. Area surrounding subantennal groove and anterior tentorial pit, antenna, most of frontal aspect of head, anterior margin of pronotum, mesonotum except triangular spot of median mesoscutal lobe, metanotum, ventral third and posterior margin of mesepisternum, most of mesepimeron, median spot and lateral margin of tergum 1, margin of valvula 3 black; cenchrus yellowish white. Wings hyaline, without smoky macula, stigma and veins black brown.

Head. Base of labrum elevated weakly, apex rounded; base of clypeus elevated, anterior margin of clypeus and incised to 0.3 × length of clypeus, lateral corners rounded; labrum smooth and shiny, without punctures and microsculpture, clypeus smooth and shiny, with few fine punctures, without microsculpture. Malar space 0.3 × as long as diameter of median ocellus. Inner margins of eyes convergent downward in frontal view, distance between eyes 1.6 × as long as height of eye (Fig. 4C). In dorsal view, inner margins of eyes subparallel; middle fovea sub-circular, deep, with a longitudinal

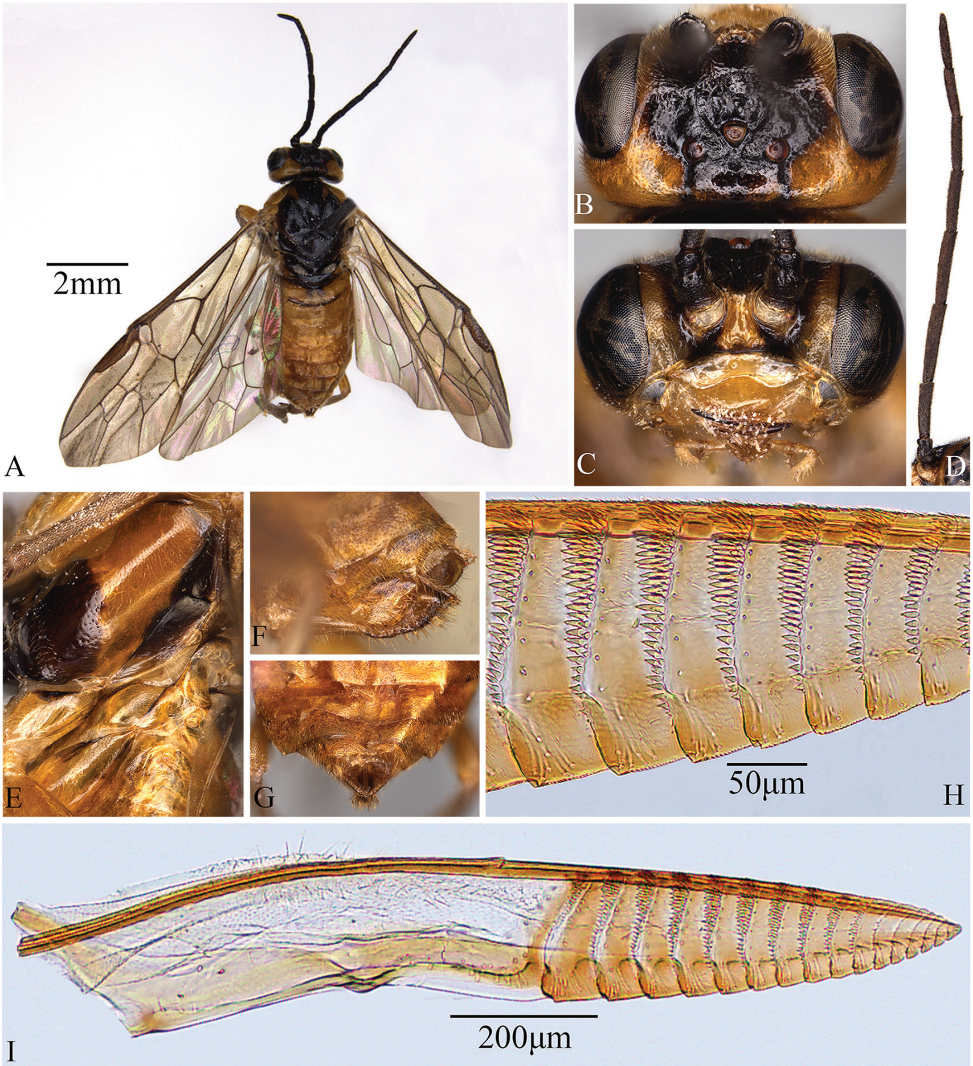

Figure 4. *Fagineura longitangia* sp. nov., female, paratype **A** dorsal view **B** head, dorsal view **C** head, anterior view **D** antenna, lateral view **E** mesopleuron and metapleuron **F** ovipositor sheath, lateral view **G** ovipositor sheath, dorsal view **H** middle serrulae **I** lancet.

groove at bottom. Frontal area hardly elevated, weakly shiny, with some hair warts and wrinkles, punctures small and sparse; anterior wall elevated and curved, notched medially, lateral walls slightly low and blunt, lateral furrows of frontal area broad and shallow. The top surface of ocelli higher than the top surface of eye in lateral view; interocellar furrow broad and deep, postocellar furrow slightly narrow and shallow; circumocellar furrow distinct; POL : OOL : OCL = 1.0 : 1.0 : 0.7 (Fig. 4B). Vertex and postocellar area smooth and shiny, punctures faint and sparse, without microsculpture; postocellar area convex, middle furrow of postocellar area narrow and shallow, 2.5 × as wide as long, lateral postocellar furrows broad and shallow, subparallel backward (Fig. 4B). Antenna filiform, slightly shorter than thorax and abdomen together, relative length of antennomere 3 : antennomere 4 : antennomere 5 = 1.0 : 1.4 : 1.2 (Fig. 4D).

Thorax. Mesonotum shiny, with minute and slightly sparse punctures, microsculpture indistinct; median mesoscutal groove very shallow and narrow; mesoscutellum and mesoscutellar appendage shiny, with minute and slightly dense punctures, microsculpture indistinct, mesoscutellum 0.7 × as long as wide; mesoscutellar appendage approximately 0.3 × as long as scutellum, middle ridge low and blunt. Distance between cenchri 0.9 × as long as breadth of cenchrus. Mesepisternum smooth and shiny, setigerous punctures fine and very sparse, without microsculpture; mesepimeron smooth and shiny, with some microsculpture on margins, punctures indistinct, posterior part of katepimeron covered with setae; metapleuron shiny and smooth, posterior of metepisternum with some setigerous punctures, without microsculpture (Fig. 4E). Vein Sc little basad of origin of vein M from R, vein M slightly shorter than vein R+M; forewings with cross-vein cu-a joining cell 1M at basal 0.5, cell 2Rs 1.5 × as long as wide, petiole of anal cell of hindwing 1.4 × as long as cu-a.

Abdomen. All abdominal terga slightly shiny, with weak and sparse setigerous punctures, microsculpture fine and dense. Ovipositor sheath shiny, punctures on valvula 3 small and very sparse, microsculpture indistinct; ovipositor sheath 1.9 × as long as metatarsomere 1 and 1.2 × as long as front tibia, valvula 3 1.2 × as long as valvifer 2; in lateral view, sheath tapering toward apex (Fig. 4F); in dorsal view, apex of cercus slightly protruding beyond valvula 3, angle between most lateral setae of valvula 3 about 70° (Fig. 4G). Lancet with 16 serrulae (Fig. 4I); each middle serrula always with 13–16 distal teeth (Fig. 4H); annular suture 1 oblique and curved, sutures 1–11 with setae bands, longest setae band approx. 0.6 × length of annulus; cypsellae 1–9 absent; tangium 4.1 × as long as annulus 1, with 6 campaniform sensilla, radix approximately as long as lamnium (Fig. 4I).

Legs. Protarsomere 1 approximately as long as combined length of tarsomeres 2–4; inner apical spur of hind tibia 0.5 × as long as metatarsomere 1, hind tibia 1.3 × as long as hind tarsus, metatarsomere 1 0.7 × as long as combined length of metatarsomeres 2–5; tarsal claw with inner tooth 0.7 × as long as outer tooth.

Male. Unknown.

Distribution. China (Hunan).

Remarks. The new species is very similar to *F. flactoserrula* Liu, Li & Wei, 2019, having similar body color, clypeus, antenna and so on, but *F. longitangia* can be distinguished from the latter using the above diagnosis and key to species. While we recognize that some of these differences are quite small, we found the characters of *F. flactoserrula* described Liu et al. (2019) to be relatively steady across the two specimens we examined. Furthermore, we argue that the holotype of *F. longitangia* differs in too many respects for these differences to be attributable to intraspecific variability of *F. flactoserrula*, and that it therefore represents a distinct species.

Etymology. The specific name "*longitangia*" is refers to the long tangium of the lancet.

Discussion

In this paper, two new species of *Fagineura* are described and illustrated. The morphological characters of the two new species conform to the generic characters of *Fagineura* proposed by Shinohara et al. (2000), Prous et al. (2014) and Liu et al. (2019), such as: malar space shorter than diameter of median ocellus, and in most species not exceeding 0.5 × of diameter of median ocellus; postocellar area short, more than 2.0 × as wide as long; posterior part of mesopleural katepimeron covered with hairs; annular suture 1 with setae band; tangium of lancet with campaniform sensilla; and others. Also the two new species can be distinguished easily from the four known species using the key to all species of *Fagineura* worldwide above. Only one specimen of the new species and we think they can be distinguished from the known species by morphological characters, there is no sequence data in this paper.

Acknowledgements

The authors are deeply grateful to the anonymous referees for valuable comments and suggestions. The research was supported by the National Natural Science Foundation of China (grant No. 31970447 and 31672344) and GDAS Special Project of Science and Technology Development (2020GDASYL-20200102021, 2020GDASYL-20200301003).

Reference

Benson RB (1954) Some sawflies of the European Alps and the Mediterranean region (Hymenoptera: Symphyta). Bulletin of the British Museum (Natural History). Entomology series 3(7): 267–295. https://doi.org/10.5962/bhl.part.1054

Liu MM, Li ZJ, Wei MC (2019) First record of the genus *Fagineura* Vikberg & Zinovjev (Hymenoptera, Tenthredinidae) with descriptions of two new species from China. Zookeys 829: 29–42. https://doi.org/10.3897/zookeys.829.30086

Prous M, Blank SM, Goulet H, Heibo E, Liston A, Malm T, Nyman T, Schmidt S, Smith DR, Vardal H, Viitasaari M, Vikberg V, Taeger A (2014) The genera of Nematinae (Hymenoptera,Tenthredinidae). Journal of Hymenoptera Research 40: 1–69. https://doi.org/10.3897/JHR.40.7442

Ross HH (1945) Sawfly genitalia: terminology and study techniques. Entomological News 61(10): 261–268.

Shinohara A, Vikberg V, Zinovjev AG, Yamagami A (2000) *Fagineura crenativora*, a New Genus and Species of Sawflies (Hymenoptera, Tenthredinidae, Nematinae) Injurious to Beech Trees in Japan. Bulletin of the National Science Museum, Series A, Zoology 26(3): 113–124.

Taeger A, Blank SM, Liston AD (2010) World Catalog of Symphyta (Hymenoptera). Zootaxa 2580: 1–1064. https://doi.org/10.11646/zootaxa.2580.1.1

Takeuchi K (1952) A Generic Classification of the Japanese Tenthredinidae (Hymenoptera: Symphyta). Published by the authors' friends, Kyoto, 90 pp.

Togashi I (2006) A new sawfly, *Fagineura quercivora* (Hymenoptera: Tenthredinidae) feeding on *Quercus serrata* and *Q. mongolica crispula* in Honshu, Japan. Proceedings of the Entomological Society of Washington 108(1): 169–173.

Viitasaari M (2002) The suborder Symphyta of the Hymenoptera. In: Viitasaari M (Ed.) Sawflies (Hymenoptera, Symphyta) I. A review of the suborder, the Western Palaearctic taxa of Xyeloidea and Pamphilioidea. Tremex, Helsinki, 11–174.